R-05-06

Description of climate, surface hydrology, and near-surface hydrogeology

Preliminary site description Forsmark area – version 1.2

Per-Olof Johansson, Artesia Grundvattenkonsult AB

Kent Werner, Golder Associates AB

Emma Bosson, Sten Berglund
Svensk Kärnbränslehantering AB

John Juston, DBE Sweden

June 2005

Svensk Kärnbränslehantering AB
Swedish Nuclear Fuel
and Waste Management Co
Box 5864
SE-102 40 Stockholm Sweden
Tel 08-459 84 00
+46 8 459 84 00
Fax 08-661 57 19
+46 8 661 57 19

ISSN 1402-3091
SKB Rapport R-05-06

Description of climate, surface hydrology, and near-surface hydrogeology

Preliminary site description Forsmark area – version 1.2

Per-Olof Johansson, Artesia Grundvattenkonsult AB

Kent Werner, Golder Associates AB

Emma Bosson, Sten Berglund
Svensk Kärnbränslehantering AB

John Juston, DBE Sweden

June 2005

Summary

The Swedish Nuclear Fuel and Waste Management Company (SKB) is conducting site investigations at two different locations, the Forsmark and Simpevarp areas, with the objective of siting a geological repository for spent nuclear fuel. The results from the investigations at the sites are used as a basic input to the development of Site Descriptive Models (SDM). The SDM shall summarise the current state of knowledge of the site, and provide parameters and models to be used in further analyses within Safety Assessment, Repository Design and Environmental Impact Assessment. The present report is a background report describing the meteorological conditions and the modelling of surface hydrology and near-surface hydrogeology in support of the Forsmark version 1.2 SDM based on the data available in the Forsmark 1.2 "data freeze" (July 31, 2004).

The area covered in the conceptual and descriptive modelling is characterised by a low relief and a small-scale topography. Almost the whole area is located below 20 m a s l (metres above sea level). The corrected mean annual precipitation is 600–650 mm and the mean annual evapotranspiration can be estimated to a little more than 400 mm, leaving approximately 200 $mm \cdot year^{-1}$ for runoff. In total, 25 "lake-centered" catchments, ranging in size from 0.03 to 8.67 km^2, have been delineated and described within the model area. The 25 mapped lakes range in size from 0.006 to 0.752 km^2. The lakes are very shallow with maximum depths ranging from 0.4 m to 2.0 m. No major water courses flow through the model area. Wetlands are frequent and cover 10–20% of the areas of the three major catchments, and up to 25–35% of some sub-catchments.

Till is the dominating Quaternary deposit covering approximately 75% of the area. In most of the area, the till is sandy. Bedrock outcrops are frequent but cover only approximately 5% of the area. The till is relatively shallow, usually with a thickness of less than 5 m. Based on site-specific and generic data, a three-layer model is proposed for the hydraulic properties of the dominating till. The uppermost layer is assigned relatively high hydraulic conductivity ($1.5 \cdot 10^{-5}$ $m \cdot s^{-1}$) and porosity (total: 35%, effective: 15%) values due to the impact of soil forming processes. The middle layer is given lower values of both conductivity ($1.5 \cdot 10^{-7}$–$1.5 \cdot 10^{-6}$ $m \cdot s^{-1}$) and porosity (total: 25%, effective: 3-5%), in agreement with both site-specific and generic data. The bottom layer, resting on the bedrock, is in accordance with site-specific data assigned a higher conductivity value ($1.5 \cdot 10^{-5}$ $m \cdot s^{-1}$) than the middle layer.

Direct groundwater recharge from precipitation is the dominant source of groundwater recharge. The groundwater is very shallow, with groundwater levels within one meter below ground as an annual mean for almost all groundwater monitoring wells. Also, the annual groundwater level amplitude is less than 1.5 m for most wells. The shallow groundwater levels mean that there is a strong interaction between evapotranspiration, soil moisture and groundwater. In the modelling, surface water and near-surface groundwater divides are assumed to coincide. The small-scale topography implies that many local, shallow groundwater flow systems are formed in the Quaternary deposits, overlaying more large-scale flow systems associated with groundwater flows at greater depths.

Groundwater level time series from wells in till and bedrock within the same areas show a considerably higher groundwater level in the till than in the bedrock. The observed differences in levels are not fully consistent with the good hydraulic contact between overburden and bedrock indicated by the hydraulic tests in the Quaternary deposits.

However, the relatively lower groundwater levels in the bedrock may be caused by the horizontal to sub-horizontal highly conductive zones shown to exist in the upper bedrock.

The sediment stratigraphy of lakes and wetlands is crucial for their function as discharge areas for groundwater. Low-permeable sediments will restrict the discharge and result in a relocation of the discharge to areas where such sediments are missing. Concerning the interactions between surface water and groundwater, it may also be noted that comparisons between measured lake water levels and groundwater levels below and around lakes indicate that the lakes in some cases may act as sources of groundwater recharge. Specifically, observations from Lake Bolundsfjärden and Lake Eckarfjärden show that such conditions were at hand during the dry summer of 2003. However, whether the observed water level relations correspond to significant water fluxes depends also on the hydrogeological properties of the lake sediments and the underlying Quaternary deposits.

"Old" water with high chloride content has been found below Lake Bolundsfjärden, Lake Eckarfjärden and Lake Gällsboträsket. These observations can either be interpreted as the result of a continuous discharge of deep water, or as evidence of more or less stagnant water below the lakes. Furthermore, the relations between the sea water level and the water levels in Lake Norra Bassängen, Lake Bolundsfjärden and Lake Lillfjärden show that inflow of sea water can occur during periods of high sea water levels.

The results from the hydrological GIS modelling support the assumptions and conclusions in the descriptive model. The flow model is highly sensitive to the topography, as this is the only parameter determining the flow pattern. Consequently, the simulated locations of recharge and discharge areas are strongly influenced by the local topography. In addition, the flat topography implies that small errors in the topographical model (the Digital Elevation Model, DEM) may have large effects on the modelled flow pattern. Ditches, diverted water courses and other human impacts on the system are important in some parts of the model area. These and other types of "man-made structures" are not fully considered in the DEM.

The water balance for the Forsmark area, as calculated with the MIKE SHE modelling tool, agrees with the presented conceptual and descriptive models of the flow system. The transient model simulations for the selected reference year (1988) result in an annual total runoff of 226 mm and a total actual evapotranspiration of 441 mm. These values, which are average values for the considered model area, are considered to be reasonable for the Forsmark area. At present, however, they cannot be tested against site-specific measurements. The MIKE SHE model produces a shallow groundwater table, which approximately agrees with the groundwater level measurements within the area, and with the overall conceptualisation of the system. However, no detailed model calibration has been performed.

The modelling results show that most of the groundwater flow occurs in the Quaternary deposits. During dry summer periods, the evapotranspiration has a strong influence on the groundwater flow. The groundwater flow is dominated by its vertical component. The horizontal groundwater flow paths are short, indicating small-scale local flow systems. Similar to the GIS modelling, the process-based modelling with the MIKE SHE model shows that the locations of recharge and discharge areas are strongly influenced by the local topography.

The results also illustrate the importance of the fracture zones for the groundwater recharge to, or discharge from, the bedrock (the model includes the bedrock to a depth of 150 m, based on the Forsmark 1.1 description of the hydraulic properties of the rock). The groundwater flow in the bedrock between the fracture zones is very small. There is a small

exchange of groundwater across the bottom boundary of the model (at 150 m depth); the flow direction and magnitude is consistent with the results obtained with the corresponding Forsmark version 1.1 DarcyTools groundwater flow model, i.e. average inflows (upward flows) of 1.3 (MIKE SHE) and 2.3 (DarcyTools) mm·year^{-1}, respectively.

Also the results from the particle tracking simulations show that the groundwater flow is dominated by its vertical component. The dominant transport of particles in the rock occurs in the fracture zones. Therefore, the shortest travel times are observed for the registration/ observation zones underlain by large fracture zones. However, it should be noted that the present particle tracking results are based on the Forsmark 1.1 hydrogeological model of the rock, and that changes in the spatial patterns of particle release areas can be expected when the present model is updated in accordance with the Forsmark 1.2 hydrogeological model of the rock.

A relatively large amount of new data has been available for the Forsmark version 1.2 modelling of surface hydrology and near-surface hydrogeology. Specifically, the evaluation of time series of local meteorological data and surface water and groundwater levels, enabling comparisons between different processes and hydrological sub-systems, has lead to an improved understanding of the site that supports some of the fundamental aspects of the descriptive model. However, significant uncertainties still exist regarding the interactions between different sub-systems and the spatial and temporal variability of model parameters. In particular, the site-specific basis for setting boundary conditions in hydrological models (i.e. meteorological data) and for evaluating calculated water balances and surface water discharges (i.e. discharge measurements) is still quite weak.

The available local meteorological time series are very short and longer time series are needed to get reliable correlations to nearby regional SMHI-stations. Local continuous discharge measurements were not available for the Forsmark 1.2 modelling. Future time series from such measurements will be most valuable for the derivation of a more accurate total water balance.

The groundwater levels in the area are very shallow. However, there is a bias towards local topographical minima in the location of the monitoring wells. Some additional wells should be located to typical local topographical maxima (recharge areas).The evident difference in groundwater levels between the Quaternary deposits and the upper bedrock observed at some of the core-drill sites should be further investigated for a better understanding of the hydraulic contact between the Quaternary deposits and the rock. The locations of recharge and discharge areas at different scales are crucial for the understanding of the groundwater flow system. A combination of complementary field investigations, including hydrogeological and hydrogeochemical methods, and modelling exercises using models based on morphological parameters as well as hydrogeological modelling is recommended. The model results should be compared with, e.g. the vegetation map, the soil type map and the Quaternary deposits map.

Sammanfattning

Svensk Kärnbränslehantering AB genomför platsundersökningar på två platser, i Forsmarks- och Simpevarpsområdena, med avsikten att lokalisera ett djupförvar för använt kärnbränsle. Resultaten från platsundersökningarna används som underlag för platsbeskrivande modellering. Platsmodelleringarna sammanfattar den aktuella kunskapen om områdena och tillhandahåller parametrar och modeller som används i de vidare analyserna inom säkerhetsanalys, förvarsdesign och miljökonsekvensbeskrivning. Föreliggande rapport är en bakgrundsrapport som beskriver de meteorologiska förhållandena och modelleringen av ythydrologi och ytnära hydrogeologi som underlag till platsmodell version 1.2 för Forsmark.

Det område som omfattas av den konceptuella och beskrivande modelleringen är flackt och karakteriseras av en småskalig topografi. Nästan hela området ligger lägre än 20 m över havet. Den genomsnittliga korrigerade årliga nederbörden är 600–650 mm och evapotranspirationen kan uppskattas vara drygt 400 mm per år, vilket ger en årlig avrinning av ca 200 mm. Totalt har 25 ”sjö-centrerade” avrinningsområden avgränsats, varierande i storlek från 0,03 till 8,67 km^2. De 25 karterade sjöarna varierar i storlek från 0,006 till 0,752 km^2. Sjöarna är grunda med maximidjup varierande mellan 0,4 och 2,0 m. Det finns inga större vattendrag i området. Våtmarker förekommer frekvent och täcker 10–20 % av ytan i de tre största avrinningsområdena och upp till 25–35 % av vissa delavrinningsområden.

Morän dominerar de kvartära avlagringarna och täcker ca 75 % av modellområdet. Moränen är vanligen sandig. Berget går i dagen på många ställen men utgör endast ca 5 % av ytan. Moränavlagringarna är relativt tunna, mestadels mindre än 5 m tjocka. Baserat på platsdata och generiska data har en trelagermodell för moränens hydrauliska egenskaper föreslagits. Det översta lagret har tilldelats en relativt hög hydraulisk konduktivitet ($1{,}5 \cdot 10^{-5}$ $m \cdot s^{-1}$) och porositet (total: 35 %, effektiv: 15 %). Mellanlagret har, i enlighet med platsdata och generiska data, givits lägre värden både på hydraulisk konduktivitet ($1{,}5 \cdot 10^{-7}$–$1{,}5 \cdot 10^{-6}$ $m \cdot s^{-1}$) och porositet (total: 25 %, effektiv: 3–5 %). Lagret närmast berget har på basis av platsdata tilldelats ett högre värde på hydraulisk konduktivitet än det mellersta lagret ($1{,}5 \cdot 10^{-5}$ $m \cdot s^{-1}$).

Direkt grundvattenbildning från nederbörd dominerar. Grundvattnet ligger ytligt i området med grundvattennivån mindre än en meter under markytan som årsmedelvärde i de flesta mätpunkter. Den årliga variationen i grundvattennivån är i allmänhet mindre än 1,5 m. Det ytliga grundvattnet innebär att det är en nära interaktion mellan evapotranspiration, markvatten och grundvatten. Grundvattendelarna för det ytliga grundvattnet har antagits sammanfalla med ytvattendelarna. Den småskaliga topografin innebär att många lokala, ytliga grundvattensystem bildas i de kvartära avlagringarna, vilka överlagrar mer storskaliga system associerade med det djupare grundvattnet.

Tidsserier för grundvattennivåerna i morän och berg från samma platser visar på en betydligt högre grundvattennivå i morän än i berg. Dessa observationer stämmer inte överens med de indikationer på en god hydraulisk kontakt mellan jord och berg som erhållits vid de hydrauliska testerna i jordlagren. En möjlig förklaring till de lägre grundvattennivåerna i bergborrhålen är de högkonduktiva horisontella och subhorisontella zonerna som påvisats i bergets ytligare delar.

Jordlagerföljden under sjöar och våtmarker är avgörande för deras funktion som utströmningsområden. Lågpermeabla sediment försvårar utströmningen och styr den till områden där denna typ av sediment saknas. Beträffande interaktionen mellan grund- och ytvatten kan också noteras att jämförelser mellan uppmätta sjövattennivåer och grundvattennivåer under och kring sjöarna i några fall indikerar att sjöarna kan fungera som inströmningsområden för grundvatten. Sådana observationer har gjorts i data från Bolundsfjärden och Eckarfjärden från den torra sommaren 2003. Huruvida dessa observerade nivåförhållanden också motsvaras av betydande grundvattenbildning beror dock även av de hydrauliska egenskaperna hos sjösedimenten och de underliggande kvartära avlagringarna.

”Gammalt” vatten med höga kloridhalter har hittats under Bolundsfjärden, Eckarfjärden och Gällsboträsket. Dessa resultat kan antingen förklaras av ett kontinuerligt utflöde av djupare grundvatten eller ses som ett tecken på ett mer eller mindre stagnant grundvatten under sjöarna. Jämförelser mellan uppmätta vattennivåer i havet och i sjöarna Norra bassängen, Bolundsfjärden och Lillfjärden visar att inflöde av havsvatten till sjöarna kan förekomma under perioder av höga vattenstånd i havet.

Resultaten från den hydrologiska GIS-modelleringen stöder antagandena och slutsatserna i den beskrivande modellen. Flödesmodellen är mycket känslig för topografin eftersom detta är den enda parameter som bestämmer flödesmönstret. Följaktligen är läget av de simulerade in- och utströmningsområdena starkt kopplade till den lokala topografin. Den flacka topografin innebär att små fel i den topografiska modellen kan ha stora effekter på det modellerade flödesmönstret. Dränering och annan mänsklig påverkan förekommer i delar av området. I den topografiska modellen har inte full hänsyn kunnat tas till denna påverkan.

Den vattenbalans som beräknats för Forsmarksområdet med MIKE SHE-modellen stämmer väl med den konceptuella och beskrivande modellen av området. De transienta modelleringarna för det utvalda representativa året (1988) gav en årlig avrinning av 226 mm och en total årlig evapotranspiration av 441 mm. Dessa värden förefaller rimliga för området, men har inte kunnat valideras med platsspecifika data. MIKE SHE-modellen ger ytliga grundvattennivåer, vilket överensstämmer med den generella bilden från grundvattennivåmätningarna i området. Någon detaljerad modellkalibrering har dock inte genomförts, främst beroende på att grundvattennivådata härrör från en annan tidsperiod än det modellerade representativa året.

Modelleringarna visar att det dominerande grundvattenflödet sker i de kvartära avlagringarna. Under torra sommarförhållanden påverkas grundvattenflödet starkt av evapotranspirationen. Grundvattenflödet domineras av dess vertikala komponent och de horisontella flödesvägarna är korta, vilket indikerar småskaliga lokala flödessystem. Liksom GIS-modelleringen visar den processbaserade modelleringen med MIKE SHE att lägena för in- och utströmningsområdena starkt påverkas av den lokala topografin.

Modellresultaten illustrerar också betydelsen av bergets sprickzoner för grundvatten-bildning till eller utströmning från berget (modellen inkluderar berget ner till ett djup av 150 m baserat på beskrivningen av bergets hydrauliska egenskaper i Forsmark SDM version 1.1). Grundvattenflödet i berget mellan sprickzonerna är mycket litet. Där är ett litet grundvattenflöde över modellens undre rand (på 150 m djup). Flödesriktning och flödets storlek överensstämmer väl med de flöden som simulerades med grund-vattenflödesmodellen DarcyTools i Forsmark SDM version 1.1; som medelvärden beräknades inflöden (uppåtriktade flöden) på motsvarande 1,3 (MIKE SHE) respektive 2,3 (DarcyTools) mm per år.

Även simuleringarna av partikeltransport indikerar att grundvattenflödets vertikala komponent dominerar. Den dominerande partikeltransporten i berget sker i sprickzonerna. De kortaste transporttiderna erhålls för de områden som underlagras av stora sprickzoner. Det bör emellertid noteras att dessa resultat baseras på 1.1-versionen av den hydrogeologiska modellen av berget och att stora förändringar gjorts av denna i version 1.2. Därför kan stora skillnader i partikelbanor och transporttider förväntas vid en uppdatering av modellen med data från version 1.2 av den hydrogeologiska beskrivningen av berget.

Relativt mycket ny platsspecifik data har varit tillgänglig för version 1.2-modelleringen. Särskilt har utvärderingen av tidsserier för meteorologiska data och yt- och grundvattennivådata möjliggjort jämförelser av processer i olika delsystem, vilket har lett till en bättre förståelse av platsen och vissa grundläggande aspekter av den konceptuella och beskrivande modellen. Fortfarande kvarstår dock betydande osäkerheter när det gäller sambanden mellan olika delsystem och den rumsliga och tidsmässiga variationen av viktiga modellparametrar. I synnerhet är det platsspecifika underlaget för randvillkoren i de hydrologiska modellerna, framförallt med avseende på meteorologiska data, och för validering av simulerade vattenbalanser, särskilt beträffande avrinningen, fortfarande otillfredsställande.

De platsspecifika meteorologiska tidsserier som presenteras i denna modellversion är mycket korta och längre tidsserier krävs för att erhålla tillförlitliga korrelationer med närliggande SMHI-stationer. Vidare saknades kontinuerliga avrinningsmätningar i underlaget för modellversion 1.2. Sådana tidsserier kommer att vara mycket värdefulla vid framtagandet av en mer detaljerad vattenbalans för området.

Grundvattennivåerna i området ligger mycket nära markytan. Det kan dock konstateras att det föreligger en viss överrepresentation av lokala lågpunkter i placeringarna av de nuvarande grundvattenrören. Några kompletterande grundvattenrör bör lokaliseras till topografiska höjdlägen (typiska inströmningsområden). Den observerade skillnaden i grundvattennivå i närbelägna jordrör och bergborrhål bör undersökas ytterligare för att skapa en bättre förståelse av den hydrauliska kontakten mellan jord och berg.

Lägena för inströmnings- och utströmningsområden i olika skalor är av avgörande betydelse för förståelsen av grundvattenflödessystemen. En kombination av kompletterande fältundersökningar, inkluderande hydrogeologiska och hydrokemiska metoder, och simuleringar med modeller baserade på geomorfologiska parametrar och processbaserade modeller rekommenderas. Modellsimuleringarna bör jämföras med exempelvis vegetations-, jordmåns- och jordartskartorna.

Contents

1 Introduction

1.1 Background

The Swedish Nuclear Fuel and Waste Management Company (SKB) is conducting site investigations at two different locations, the Forsmark and Simpevarp areas, with the objective of siting a geological repository for spent nuclear fuel. The investigations are divided into an initial site investigation phase and a complete site investigation phase /SKB, 2001/. The results of the presently on-going initial investigation phase will be used as a basis for deciding on the subsequent complete investigation phase, which, in turn, will provide the basis for the application for a licence to build and operate the repository.

The results from the investigations at the sites are used as a basic input to the site descriptive modelling. A Site Descriptive Model (SDM) is an integrated description of the site and its regional setting, covering the current state of the geosphere and the biosphere as well as ongoing natural processes of importance for long-term safety. The SDM shall summarise the current state of knowledge of the site, and provide parameters and models to be used in further analyses within Safety Assessment, Repository Design and Environmental Impact Assessment.

The first steps of the site descriptive modelling have been taken with the version 1.1 models of the Forsmark /SKB, 2004a/ and Simpevarp /SKB, 2004b/ areas. It can also be noted that the Forsmark 1.1 SDM was used as a basis for the work presented in the Safety Assessment "SR-Can Interim report" /SKB, 2004c/, including some examples of how the surface systems will be handled in forthcoming safety assessments. The present report is produced as a part of the version 1.2 modelling of the Forsmark area. The version 1.2 models are the final models that will be presented in the initial site investigation stage, which implies that they, among other things, should provide the information necessary for focusing the repository-related parts of the investigations to more limited areas within the presently considered candidate areas.

Models are developed on a regional scale (hundreds of square kilometres) and on a local scale (tens of square kilometres). These model areas include the candidate area, within which most of the deep rock boreholes are located. The Forsmark regional model area and candidate area are shown in Figure 1-1. Also shown in the figure is the surface water divide, that constitutes the main upstream boundary in the conceptual and quantitative modelling of surface hydrology and near-surface hydrogeology described in the present report.

As indicated above, the continued investigations will be focused on a specific subarea within the candidate area. Note, however, that this focusing has different implications for different types of investigations and modelling, as determined by the different "end users". For surface hydrology and near-surface hydrogeology, which are strongly related to biosphere modelling in Safety Assessment and to Environmental Impact Assessment, also forthcoming models versions will to large extent deal with the regional model area. Furthermore, the modelling should consider subareas of specific interest for, e.g. radionuclide release from the planned repository, which likely to some extent will be located outside the subarea prioritised for geological investigations for the repository.

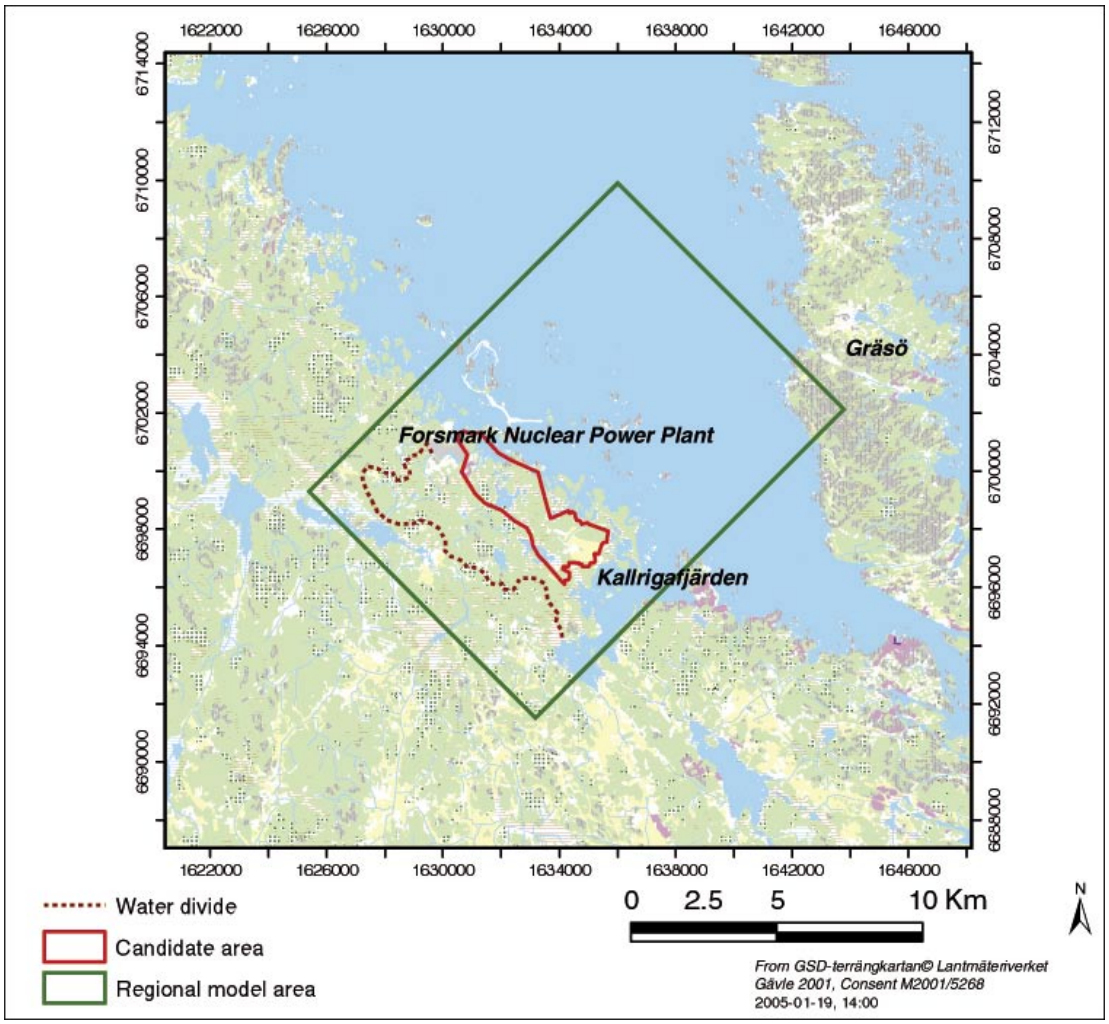

Figure 1-1. *Overview of the Forsmark area and identification of the regional model area, the candidate area, and the water divide bounding the model area considered in the present report.*

1.2 Objectives and scope

The general objectives of the site descriptive modelling of the Forsmark area and the specific objectives of the Forsmark 1.2 modelling are presented in the Forsmark 1.2 SDM report /SKB, 2005a/. The present report is a background report describing the meteorological conditions and the modelling of surface hydrology and near-surface hydrogeology in support of the Forsmark 1.2 SDM. Concerning these disciplines, it may be noted that they were not covered by background reports in the version 1.1 modelling. However, the available datasets were analysed and the results were integrated and described in the version 1.1 SDM report /SKB, 2004a/.

The objectives of the modelling reported in this document are to:

- analyse and present the data available in the Forsmark 1.2 dataset,
- update the descriptive model presented in the previous model version /SKB, 2004a/,
- present the results of the initial flow modelling performed in order to support the site description and to provide input data to the ecological systems modelling,
- summarise and present the results in the form of an updated site description.

As further described below, the database available at the time for the Forsmark 1.2 "data freeze" (July 31, 2004) contains a relatively large amount of data, including time series of meteorological parameters and surface water and groundwater levels for a 15-month period, and hydraulic parameters from about 50 field tests. Furthermore, the descriptions of, e.g. catchment areas and Quaternary deposits have been further developed in the version 1.2 modelling, which has enabled improvements of the surface hydrology and near-surface hydrogeology description. In particular, the present model includes results from quantitative flow modelling (no flow modelling was performed in version 1.1).

Since a lot of new data have become available, the version 1.2 modelling effort has to large extent been focused on the presentation and evaluation of site-specific data. Thus, the present knowledge of the site is mainly inferred directly from observations in measurement results. The work conducted to evaluate and generalise these results by use of flow modelling has been limited, especially in terms of the testing against site investigation data. It is anticipated that quantitative flow modelling will become a more important component of the modelling work when local discharge measurements and longer time series from local meteorological measurements become available.

Thus, it should be emphasised that although significant steps have been taken in the descriptive modelling, there are still substantial uncertainties in the model description. The main reasons for these uncertainties are the limited amount of local meteorological and discharge data (short time series), and that time has been insufficient for carrying out supporting exploratory analyses and flow modelling exercises. Furthermore, spatial variability, especially the variability in the hydraulic properties of the various Quaternary deposits, remains a potentially important source to uncertainty.

1.3 Setting

The Forsmark area is located in northern Uppland within the municipality of Östhammar, about 150 km north of Stockholm. The regional model area indicated in Figure 1-1 covers approximately 165 km^2, extending from the island Gräsö in the east to a boundary southwest of and parallel with the Forsmarksån water course. The depth of the model volume is 2,200 m, from 100 m above present sea-level to 2,100 m below sea-level. The local model area, covering some 31.5 km^2, is a slightly extended idealisation of the candidate area /SKB, 2004a/. It is not used explicitly in the present context, and is therefore not further discussed in the present report.

The candidate area is situated in the immediately vicinity of the Forsmark nuclear power plant and the underground repository for low- and medium-active radionuclear waste, SFR, see Figure 1-2. It is located along the shoreline of Öresundsgrepen and extends from the nuclear power plant and the access road to the SFR facility in the northwest to Kallrigafjärden in the southeast. The candidate area is approximately 6 km long and 2 km wide.

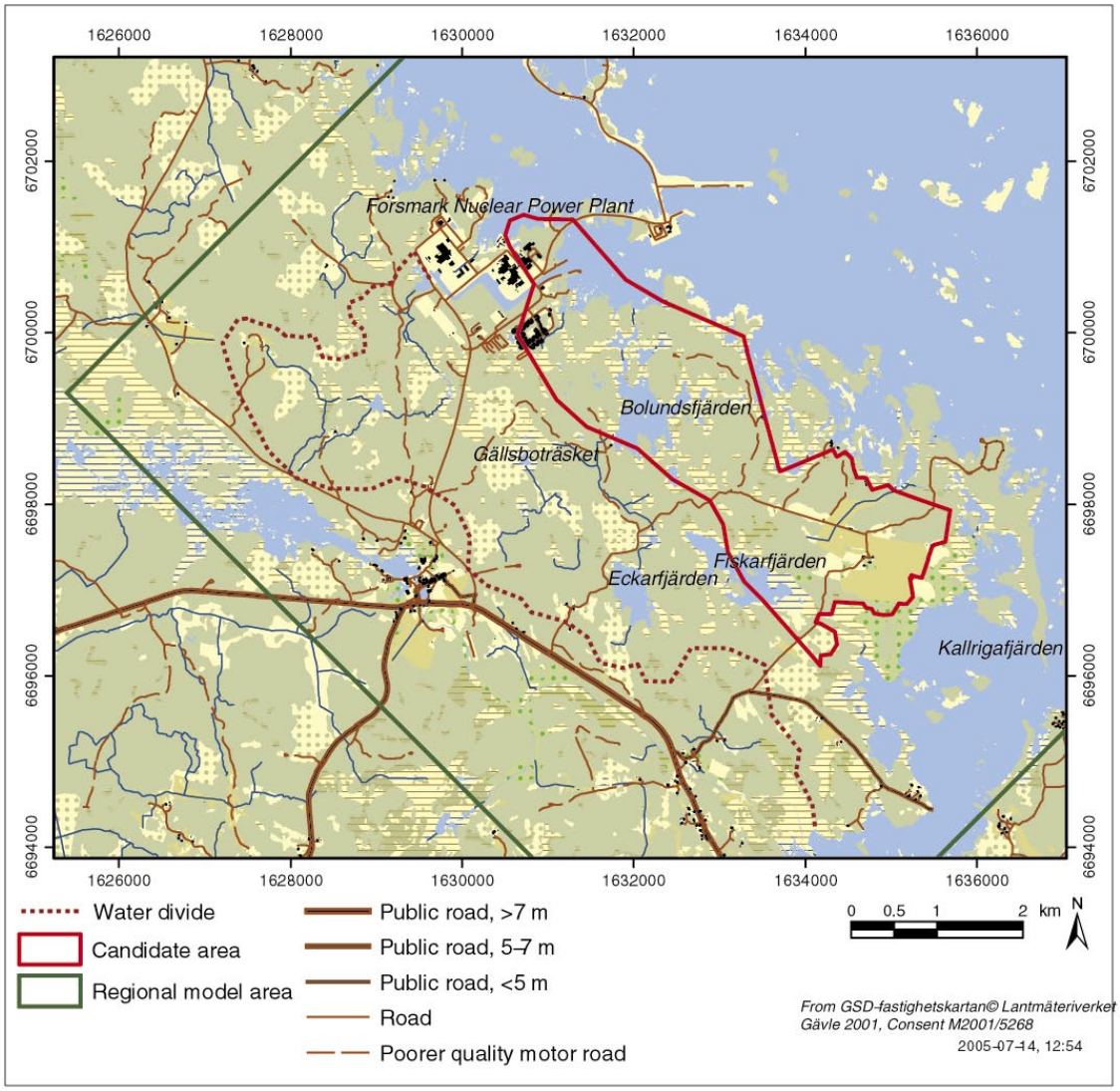

Figure 1-2. *Detailed map of the candidate area and some objects of particular interest for the hydrological modelling.*

1.4 Methodology and organisation of work

1.4.1 Methodology

The methodology for the conceptual and descriptive modelling of surface water hydrology and hydrogeology in the overburden was presented in the modelling strategy report for hydrogeology /Rhén et al. 2003/. The strategy report describes the input data, the modelling process and the resulting descriptive model, based on a systems approach in which the descriptive model of the surface and near-surface system is presented as a set of Hydraulic Soil Domains (HSD). The HSDs are to be specified in terms of geometry and hydrogeological parameters, as described in the strategy report.

The description based on HSDs provides a suitable framework for conveying the site modellers' interpretation of the site conditions, especially if the result is to be used as a basis for a groundwater flow model. However, other users may be interested in other aspects of the site descriptive modelling. In particular, the biosphere modelling within Safety Assessment uses "box models", which require input data on the water turnover in the various "biosphere objects" that are modelled. As input to these models, the site descriptive modelling should provide spatial distributions of, e.g. the total runoff or other specific components of the water balance, such that water turnover times can be calculated for arbitrary spatial objects. Furthermore, a descriptive model organised in terms of "hydrological elements" such as sub-catchments with associated parameters, may be more relevant for some applications. This type of data is also presented in this report.

The methodology employed in the version 1.2 modelling is illustrated in Figure 1-3. The data evaluation and modelling activities are carried out in a number of steps. In the first step, simply termed "Data evaluation" in the figure, each data type is evaluated and presented separately. The second step, "Surface hydrology integration" consists of an integration of the different types of hydrological data available. For example, correlations between time series of groundwater levels and precipitation, and between groundwater and surface water levels, have been studied.

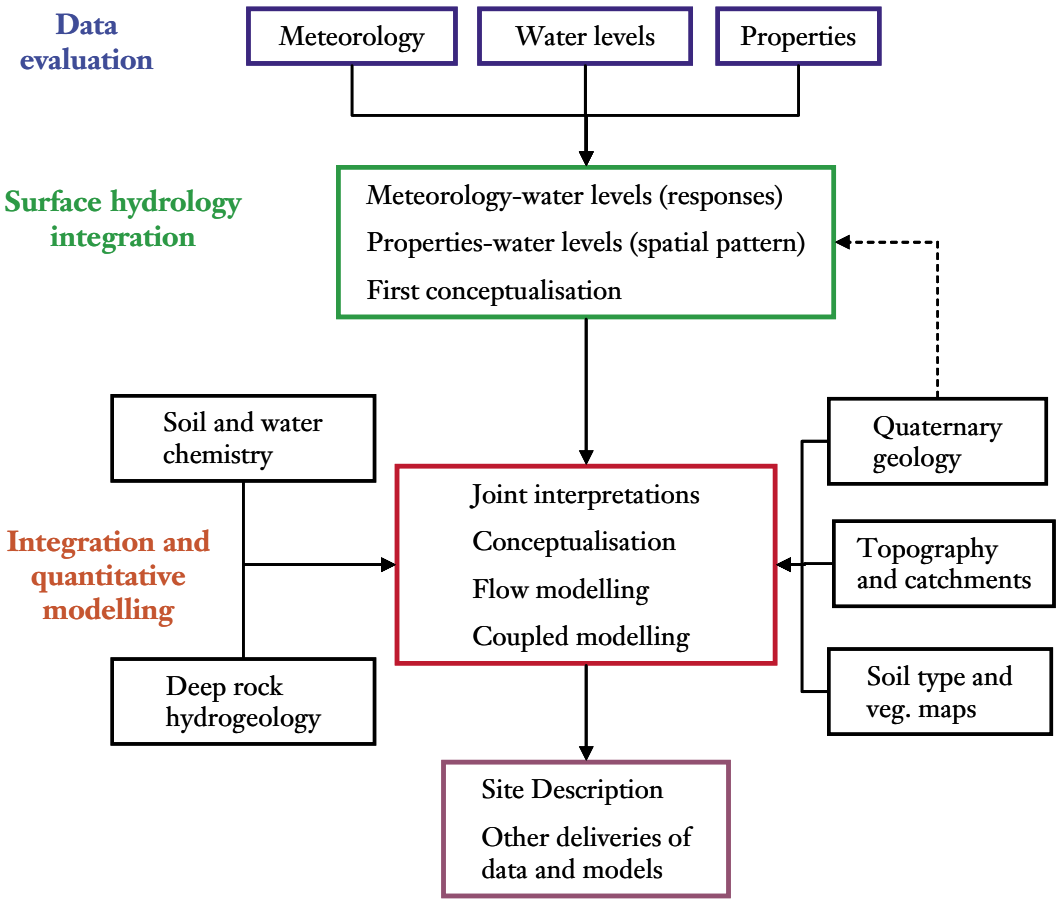

Figure 1-3. *Overview of the modelling process.*

In the "Integration and quantitative modelling" step, data and models from other modelling disciplines are introduced into the modelling. These inputs and integrations are required in order to develop descriptive models and quantitative flow models of the site. It should be noted that flow models and coupled models (i.e. models in which flow is coupled to other physical and/or chemical processes) are developed also by other modelling disciplines. Specifically, the surface system is part of the model domains considered in the modelling of groundwater flow in the deep rock. Furthermore, coupled hydrogeological and hydrogeochemical modelling is performed within the framework of the hydrogeochemical modelling /SKB, 2005b/. In these cases, the interactions could imply deliveries of surface hydro(geo)logical data to the modellers, and feedback in the form of "import" of some of the results to the surface system description.

It should be noted that whereas the interactions indicated in Figure 1-3 indeed have taken place in the form of inputs to the numerical flow modelling presented herein, feedbacks from the present modelling to those providing the inputs have been quite limited. Interactions (iterations) regarding, for instance, the hydraulic interface between rock and overburden, need to be further developed in future model versions. Data and models that could be used to support the modelling of surface hydrology and near-surface hydrogeology are further discussed in Chapter 4.

1.4.2 Terminology

/Rhén et al. 2003/ establish the terminology to be used within the site descriptive hydrogeological modelling. Since the term "hydrology" often refers to all aspects of the hydrological cycle, i.e. atmospheric, surface and subsurface processes and parameters, it should be noted that the following distinction is made between "hydrology" and "hydrogeology" in the data handling within SKB's site investigation programme:

- *Hydrology* refers to the surface water system only; hydrological data include water levels and flow rates in water courses and lakes, and surface water divides and the associated catchments and sub-catchments.
- *Hydrogeology* refers to the subsurface system, i.e. the water below the ground surface, including the unsaturated and saturated parts of the subsurface; hydrogeological data include groundwater levels and hydraulic parameters for unsaturated and saturated flow.

Thus, the terminology is clear as far as the input data are concerned; hydrological data are obtained on the ground surface and in surface waters, and hydrogeological data from the subsurface, primarily from drillings and observation wells (sampling for analysis of hydraulic properties has also been made in pits and trenches).

The above distinction is made also within the site descriptive modelling /Rhén et al. 2003/. However, in some cases additional qualifiers are used; "surface hydrology" clarifies that the modelling is dealing with the surface part of the hydrological cycle, whereas "near-surface hydrogeology" or "hydrogeology in overburden/Quaternary deposits" is used when there is a need to distinguish the modelling from that dealing with the deep rock. Obviously, there is an overlap between "near-surface" and "deep rock" hydrogeological models, since they must incorporate components of each other in order to achieve an appropriate parameterisation and identification of boundary conditions.

1.4.3 Organisation of work

The modelling of hydrology and hydrogeology within and related to the surface system has been performed as part of the SurfaceNet project. This project incorporates all site descriptive modelling of the surface system, i.e. both abiotic aspects such as hydrology and hydrogeology, and models of the biotic parts of the system. A project group with representatives for all the surface system modelling disciplines has been formed. Most disciplines have additional modellers associated with the project group.

The interactions with related modelling disciplines, primarily the hydrogeological and hydrogeochemical modelling of the deep rock, have taken place both by informal contacts and discussions and by participation in project meetings with the HydroNet and HAG teams. As indicated above, the actual results of these contacts in the models presented are limited; the aim, given the recent initiation of SurfaceNet and the limited time and data available, has been to divide the responsibilities and develop a basis for future co-operation.

The SurfaceNet modelling for Forsmark 1.2 is reported in /Lindborg (ed), 2005/, which provides input to the Forsmark 1.2 SDM report /SKB, 2005a/. Thus, the contents of the present background report are used as a basis for the corresponding parts of the SurfaceNet report, which are then summarised in the SDM report.

1.5 This report

The disposition of this report follows the overall disposition of the SDM reports: first, data presentation and evaluation, followed by conceptual, descriptive and quantitative flow modelling, and then the resulting description. Specifically, Chapter 2 summarises the available primary data and provides an overview of their usage, whereas Chapter 3 contains a presentation of the actual data in the form of figures and tables. The conceptual and descriptive model is described in Chapter 4, and the quantitative flow modelling in Chapter 5. Finally, the resulting description is presented in Chapter 6.

2 Investigations and available data

2.1 Previous investigations

Two site descriptive models (SDM) of the Forsmark area have been presented before the present version: version 0 (F0) /SKB, 2002/ and version 1.1 (F1.1) /SKB, 2004a/. F0 was developed before the start of the site investigations and was mainly based on data compiled for the Östhammar feasibility study /SKB, 2000/ and related background reports. This model was developed at a regional scale and covered a rectangular area, 15 km by 11 km, surrounding the area identified in the feasibility study as favourable for further study. This area was called the Forsmark regional model area.

The information that provided the basis for the F0 model was mainly 2D in nature (surface data) and general and regional, rather than site specific, in character. However, 3D (depth) information was available from boreholes, shafts and tunnels from the construction of the Forsmark nuclear power plant and the underground low to medium active radioactive waste storage facility, SFR.

Meteorological and hydrogeological data were compiled from nearby stations operated by the Swedish Meteorological and Hydrological Institute (SMHI) /Lindell et al. 2000/, whereas data on catchments were obtained from /SMHI, 1985/ and /Brunberg and Blomqvist, 1998/. The description of the Quaternary deposits (QD) in the feasibility study /SKB, 2000/ formed the basis for the conceptualisation of the hydrogeology of the QD. However, no data on hydraulic properties or groundwater levels in the QD were presented in F0.

At the time for the F1.1 “data freeze”, i.e. April 30, 2003, the site investigations in terms of surface hydrology and near-surface hydrogeology included:

- delineation of catchment areas in the field in the central parts of the model area,
- manual discharge measurements at 8 locations,
- installation of surface water level gauges, drilling of boreholes and excavation of pits in QD,
- installation of groundwater monitoring wells in QD,
- hydraulic tests (slug tests) in these groundwater monitoring wells.

Local meteorological and hydrological stations were not established before the F1.1 data freeze, and there was no time to collect time series of surface water and groundwater levels. The still very limited amount of site specific data implied that also F1.1 was mainly based on generic and/or regional data regarding climate, hydrology and near-surface hydrogeology.

2.2 Meteorological, hydrological and near-surface hydrogeological investigations

Between the F1.1 (April 30, 2003) and F1.2 (Forsmark 1.2; July 31, 2004) data freezes, the meteorological, surface hydrological and near-surface hydrogeological investigations have comprised the following major components:

- Establishment of two meteorological stations and collection of meteorological data.
- Establishment of one hydrological station and collection of hydrological data.
- Survey of lake thresholds, and brook gradients and cross-sections.
- Simple manual discharge measurements in brooks.
- Installation of additional surface water level gauges.
- Installation of additional groundwater monitoring wells in QD.
- Supplementary slug tests in groundwater monitoring wells.
- Collection of surface water level and groundwater level data.
- Installation of BAT-type filter tips.
- Installation of two pumping wells in QD.
- Pumping tests in the two installed pumping wells.

2.3 Other investigations contributing to the modelling

In addition to the investigations listed in Section 2.2, the modelling is based on data from the SKB databases SICADA and SKB-GIS on:

- topographical and other geometrical conditions,
- surface-based geological investigations of QD and soil type mapping,
- composition and stratigraphy from boreholes and pits in QD,
- hydrogeological properties of the bedrock,
- soil and water chemistry.

2.4 Summary of available data

Table 2-1 gives references to site investigation reports and other sources that have provided the meteorological, hydrological and near-surface hydrogeological data used in the F1.2 modelling. Table 2-2 lists the corresponding information with respect to other disciplines and types of investigations. Table 2-3 specifies the references to SKB reports referred to in Table 2-1 and 2-2.

In general, the site investigation data are available in SKB's SICADA and GIS databases. However, due to technical problems the time series data from SKB's meteorological stations, surface water level gauges, and groundwater wells were not available in SICADA when the final version of the present report was produced (May, 2005). Instead, quality assured data from SKB's HMS (Hydro Monitoring System) database were used in the presentations and analyses of time series data in this report.

Table 2-1. Available meteorological, hydrological and near-surface hydrogeological data and their handling in F1.2 (HMS = SKB's Hydro Monitoring System database, see text).

Available site data Data specification	Ref	Usage in F1.2 Analysis/modelling	Cf Section	Not utilised in F1.2 Arguments/comments
Meteorological data				
Regional data				
Summary of precipitation, temperature, wind, humidity and global radiation up to 2003	R-99-70 TR-02-02	Basis for general description and quantitative modelling of ground-water and surface water flow	3.1.1	
Site Investigation data				
Precipitation, temperature, wind, humidity, global radiation and potential evapotranspiration June 2003 – July 2004 from the meteorological stations at Högmasten and Storskäret	HMS	Comparison with regional meteorological data	3.1.2	
Snow depth, ground frost and ice cover	P-03-117 P-04-137	Validation of snow routine in quantitative modelling	3.3.3 App 3	
Hydrological data				
Regional data				
Regional discharge data	R-99-70 TR-02-02	Specific discharge in conceptual and quantitative modelling	3.2.6 Ch 4, 5	
Site Investigation data				
Geometric data on catchment areas, lakes and water courses	SKB GIS P-04-25	Delineation and description of catchment areas and lakes	3.2.1	
Automatic discharge measurements	HMS			Only < 3 months time series from one station available
Manual discharge measure-ments in water courses	SICADA P-03-27 P-04-146	General description of temporal variability in surface water discharge	3.2.6	
Installation of surface water level gauges	P-03-64 P-04-139	Basis for surface water level measurements	3.2.5	
Level measurements in lakes and the sea	P-04-313 HMS	Surface water-groundwater level relations, conceptual modelling and test of quantitative modelling with MIKE SHE	3.2.5 Ch 4, 5	
Hydrogeological data				
Inventory of private wells and water prospecting wells	R-02-17	Description of available hydrogeological information	3.3.4	No attempt made to infer hydraulic parameters from these data
Data on installed groundwater monitoring wells, abstraction wells and BAT filter tips	P-03-64 P-04-136 P-04-138 P-04-139	Description of QD type and depth to bedrock, basis for groundwater level measurements and hydraulic tests	3.3.1	
Hydraulic conductivity of QD	P-03-65 P-04-136 P-04-138 P-04-140 P-04-142	Basis for assigning hydraulic conductivity of QD in conceptual and quantitativel models	3.3.2	
Groundwater levels in QD	P-04-313 HMS	General description, conceptual and quantitative modelling	3.3.3 Ch 4, 5	

Table 2-2. Input data from other disciplines and their handling in F1.2.

Available site data Data specification	Ref	Usage in F1.2 Analysis/modelling	Cf Section	Not utilised in F1.2 Arguments/comments
Topographcal data				
Digital Elevation Model (DEM)	SKB GIS P-04-03	Conceptual and quantitative modelling (GIS and MIKE SHE)	3.3.1, 3.3.3 Ch 4, 5	
Vegetation and land use data				
Vegetation map	SKB GIS P-03-83	Conceptual and quantitative modelling (GIS/PCRaster-POLFLOW, MIKE SHE)	3.2.3 Ch 4, 5	
Surface-based geological data				
Soil type map	SKB GIS R-04-08	Conceptual modelling and quantitative modelling with MIKE SHE	Ch 4, 5	
Geological map of QD	SKB GIS P-03-11 P-03-14 R-04-39	Basis for the conceptual hydrogeological model of QD and for the quantitative modelling (GIS/PCRaster-POLFLOW, MIKE SHE)	4.3.4 Ch 5	
Geophysical data	P-04-78 P-04-99 P-04-156	Conceptual and quantitative modelling with MIKE SHE	Ch 4, 5	
Geological data from boreholes and pits				
Stratigraphical data of QD	P-03-24 P-04-34 P-04-86 P-04-111 P-04-127 P-04-148	Basis for the conceptual hydrogeological model of QD and for the quantitative modelling (MIKE SHE)	4.3.4 Ch 5	
Hydrochemical data				
Surface water	P-03-27 P-04-146	Conceptual modelling (in part)	4.6	Limited use, mainly due to time constraints
Shallow groundwater	SICADA	Conceptual modelling	4.6	
Hydrogeological properties of the rock				
Modelled hydraulic conductivity and pressure distributions in the upper part of the rock – results of DarcyTools modelling for Forsmark 1.1	R-04-15	Quantitative modelling (MIKE SHE) – parametrisation and identification of boundary conditions	Ch 5	

Table 2-3. Reports in the SKB P, R and TR-series referred to in Tables 2-1 and 2-2.

P-03-11	**Sohlenius G, Rudmark L, Hedenström A.** Mapping of unconsolidated Quaternary deposits. Field data 2002.
P-03-14	**Sohlenius G, Rudmark L**. Mapping of unconsolidated Quaternary deposits. Stratigraphical and analytical data.
P-03-24	**Hedenström A.** Investigation of marine and lacustrine sediments in lakes. Field data 2003.
P-03-27	**Nilsson A-C, Karlsson S, Borgiel M.** Sampling and analyses of surface waters. Results from sampling in the Forsmark area, March 2002 to March 2003.
P-03-64	**Johansson P-O.** Drilling and sampling in soil. Installation of groundwater monitoring wells and surface level gauges.
P-03-65	**Werner K, Johansson P-O.** Slug tests in groundwater monitoring wells in soil.
P-03-83	**Boresjö Bronge L, Wester K**. Vegetation mapping with satellite data of the Forsmark, Tierp and Oskarshamn regions.
P-03-117	**Aquilonius K, Karlsson S.** Snow depth, frost in ground and ice cover during the winter 2002/2003.
P-04-03	**Brydsten L.** A method for construction of digital elevation models for site investigation program in Forsmark and Simpevarp.
P-04-25	**Brunberg A-K, Carlsson T, Blomqvist P, Brydsten L, Strömgren M.** Identification of catchments, lake-related drainage parameters and lake habitats.
P-04-34	**Sundh M, Sohlenius G, Hedenström A.** Stratigraphical investigation of till in machine cut trenches.
P-04-78	**Marek R.** Ground penetration radar survey 2003.
P-04-86	**Hedenström A.** Investigation of marine and lacustrine sediments in lakes. Stratigraphical and analytical data.
P-04-99	**Bergman B, Palm H, Juhlin C.** Estimate of bedrock topography using seismic tomography along reflection seismic profiles.
P-04-111	**Hedenström A, Sohlenius G, Albrecht J.** Stratigraphical and analytical data from auger drillings and pits.
P-04-127	**Fredriksson D.** Peatland investigation Forsmark.
P-04-136	**Johansson P-O.** Undisturbed pore water sampling and permeability measurements with BAT filter tips. Soil sampling for pore water analyses.
P-04-137	**Heneryd N.** Snow depth, ground frost and ice cover during the winter 2003/2004.
P-04-138	**Werner K, Lundholm L, Johansson P-O.** Drilling and pumping test of wells at Börstilåsen.
P-04-139	**Werner K, Lundholm L.** Supplementary drilling and soil sampling, installation of groundwater monitoring wells, a pumping well and surface water level gauges.
P-04-140	**Werner K.** Supplementary slug tests in groundwater monitoring wells in soil.
P-04-142	**Werner K, Lundholm L.** Pumping test in well SFM0074.
P-04-146	**Nilsson A-C, Borgiel M.** Sampling and analyses of surface waters. Results from sampling in the Forsmark area, March 2003 to March 2004.
P-04-148	**Hedenström A.** Stratigraphical and analytical data of Quaternary deposits.
P-04-156	**Marek R.** A co-ordinated interpretation of ground penetrating radar data from the Forsmark site.
P-04-313	**Nyberg G, Wass E, Askling P, Johansson P-O.** Hydromonitoring program. Report for June 2002 – July 2004.
R-99-70	**Lindell S, Ambjörn C, Juhlin B, Larsson-McCann S, Lindquist K.** Available climatological and oceanographical data for site investigation program.
R-02-17	**Ludvigsson J-E.** Brunnsinventering i Forsmark.
R-04-08	**Lundin L, Lode E, Stendahl J, Melkerud P-A, Björkvald L, Thorstensson A.** Soils and site types in the Forsmark area.
R-04-15	**SKB.** Preliminary site description. Forsmark area – version 1.1.
R-04-39	**Sohlenius G, Rudmark L, Hedenström A.** Mapping of unconsolidated Quaternary deposits 2002–2003. Map description.
R-05-07	**Vikström M, 2005.** Modelling of soil depth and lake sediments. An example from the Forsmark site.
TR-02-02	**Larsson-McCann S, Karlsson A, Nord M, Sjögren J, Johansson L, Ivarsson M, Kindell S.** Meteorological, hydrological and oceanograpical information and data for the site investigation program in the communities of Östhammar and Tierp in northern part of Uppland.

3 Evaluation and presentation of primary data

3.1 Meteorological data

The regional meteorological conditions in the Forsmark area were described in /Larsson-McCann et al. 2002/. Meteorological stations of interest for the Forsmark regional area were listed, and long-term average data for selected meteorological stations considered to be representative for estimating different meteorological parameters for the Forsmark area were presented. These data were used in F1.1 to characterise the Forsmark area in terms of climate.

In May 2003, two meteorological stations were established in the Forsmark area, and site-specific meteorological data for F1.2 are available from May 2003 to the data freeze at the end of July 2004. For the characterisation of the meteorological conditions in F1.2, mainly long-term regional data are used. Local meteorological data are presented for the period May 2003 – July 2004 and compared with nearby SMHI stations for which long-term measurements exist.

3.1.1 Long-term regional data

Before the site investigations, existing long-term regional meteorological data were compiled by /Lindell et al. 2000/ and /Larsson-McCann et al. 2002/. The locations of meteorological stations, relevant for the Forsmark area, are shown in Figure 3-1, together with relevant hydrological and oceanographical measurement stations. Information on the meteorological stations is presented in Table 3-1.

Table 3-1. Existing regional meteorological data relevant for the Forsmark area /Larsson-McCann et al. 2002/.

Station no	Station name	Co-ordinates, RT90		Period	Information
10832	Örskär	671476	164097	1881–1995	No air pressure
10832	Örskär A	671475	164099	1995–	
10815	Östhammar	668510	164176	1989–	Only prec
10811	Risinge	667533	163423	1962–	Only temp, prec
10725	Lövsta	670070	161437	1925–	Only prec
10714	Films Kyrkby	668149	161626	1982–2000	
10714	Films Kyrkby A	668156	161629	2000–	
9753	Uppsala flygplats	664306	159991	1949–	
307	Uppskedika V	668148	163416	1990–	Only in the winter
320	Dannemora V	667855	161318	1990–	Only in the winter
324	Gräsö V	670861	164362	2001–	
2994	Forsmark MAST	670029	163015	1992–1996	Raw data
2389	Forsmark biotest	670256	163118	1992–1998	Only wind, temp

Figure 3-1. *Meteorological, hydrological and oceanographical stations of interest for the Forsmark area /Larsson-McCann et al. 2002/.*

The short description below of the meteorological conditions in the Forsmark area is based on data compiled by /Lindell et al. 2000/ and /Larsson-McCann et al. 2002/. More detailed descriptions are given in these reports. The regional meteorological data are used in the F1.2 modelling, and will be important also in forthcoming modelling efforts. In particular, these data constitute a basis for "extrapolating" the relatively short time series measured at the local stations (up to 4–5 years during the site investigations) to time series statistics for longer periods. Obviously, this approach relies on the establishment of sufficiently strong correlations between the regionally and locally measured time series during the periods for which comparisons can be made.

A wind rose from the station at Örskär, which in the study by /Larsson-McCann et al. 2002/ was judged to be representative for the Forsmark area, is presented in Figure 3-2, together with a wind rose from Uppsala airport. Compared to the common pattern in southern Sweden, northerly winds are much more frequent at Örskär. In the winter, the strong northerly winds often bring heavy snowfall.

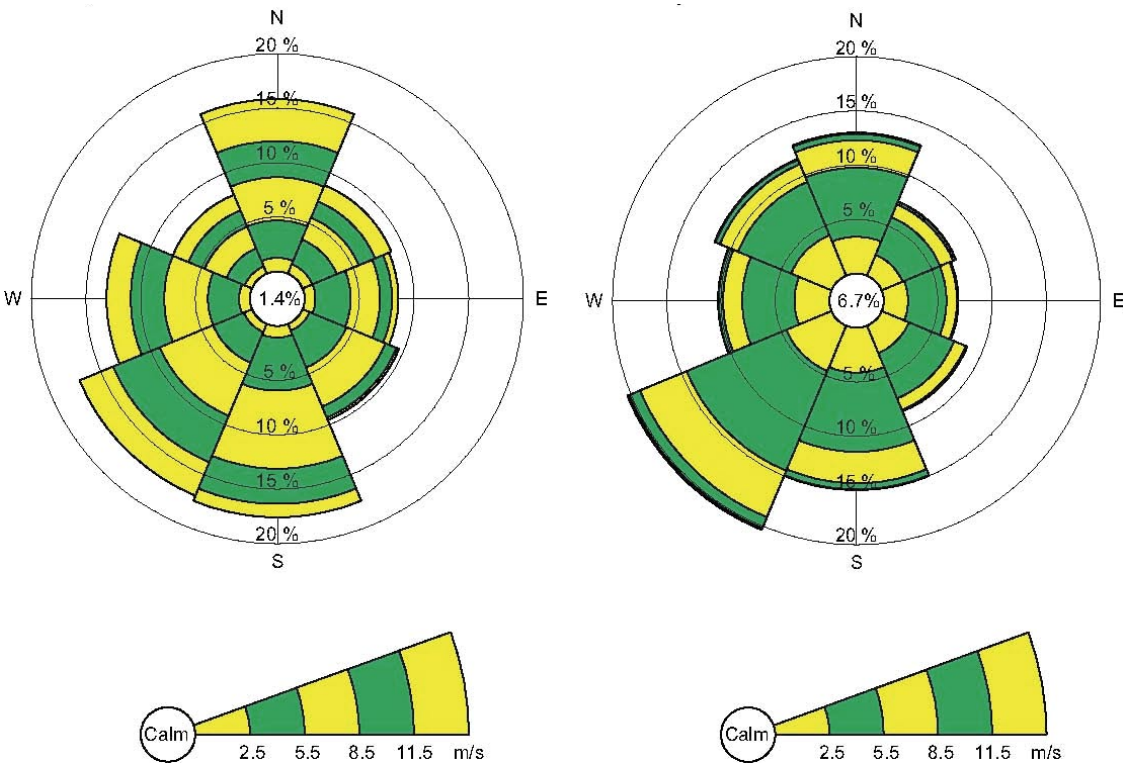

Figure 3-2. *Wind roses from the SMHI stations at Örskär and Uppsala airport /Larsson-McCann et al. 2002/.*

In north-eastern Uppland, the highest precipitation often occurs some distance inland from the coast. For example, the mean annual precipitation in Lövsta, approximately 10 km inland, is 758 mm, which can be compared with the corresponding value of 588 mm at Örskär (values corrected for wind losses etc by 15% and 21% for Lövsta and Örskär, respectively). The mean annual precipitation in the Forsmark area can be estimated to 600–650 mm. Some 25–30% of the annual precipitation falls in the form of snow. The ground is covered by snow about 120–130 days per year with an average annual maximum snow depth of approximately 50 cm.

The average monthly mean temperature varies between –4°C in January–February and +15°C in July. The winters are slightly milder at the coast than inland, and the mean annual temperature at Örskär is 5.5°C compared to 5.0°C at the more inland stations at Risinge and Films kyrkby. The vegetative period, defined as the period with daily mean temperatures exceeding 5°C, is about 180 days.

Monthly and annual mean potential evapotranspiration was calculated by /Larsson-McCann et al. 2002/ based on routine meteorological observations by use of the Penman formula according to /Eriksson, 1981/. On the average, the potential evpotranspiration at Örskär is about 100 mm per month in the summer and 500 mm·year^{-1}, whereas the values are lower at the more inland station at Films kyrkby (about 10 mm per month lower in the summer and an annual mean of approximately 400 mm·year^{-1}). The potential evapotranspiration in the Forsmark area can be estimated to be somewhere in between the values for Örskär and Films kyrkby.

The annual sunshine time is 1,700–1,800 hours on the coast of north-eastern Uppland /SKB, 2002/. Based on the synoptic observations at Örskär, the mean annual global radiation was calculated to 930 kWh/m^2, with the mean monthly values varying from 4 kWh/m^2 in December to more than 170 kWh/m^2 in June.

3.1.2 Local data

In May 2003, two local meteorological stations were established within the site investigation program; one at the northern end of the candidate area at the existing mast at the Forsmark nuclear power plant (Högmasten), and one in the southern part of the candidate area at Storskäret (Figure 3-3). The measurement programs at these two stations are specified in Table 3-2. The same measurements are performed at the two stations, with the exceptions that the global radiation and the air pressure are measured at Högmasten only.

Tabell 3-2. Meteorological measurements at Högmasten and Storskäret.

Parameter	Registration interval	Högmasten	Storskäret
Precipitation	30 min (sum)	x	x
Air temperature	30 min (mean)	x	x
Wind direction and wind speed (10 m above ground)	30 min (mean)	x	x
Humidity	30 min (mean)	x	x
Air pressure	30 min (mean)	x	–
Global radiation	30 min (mean)	x	–

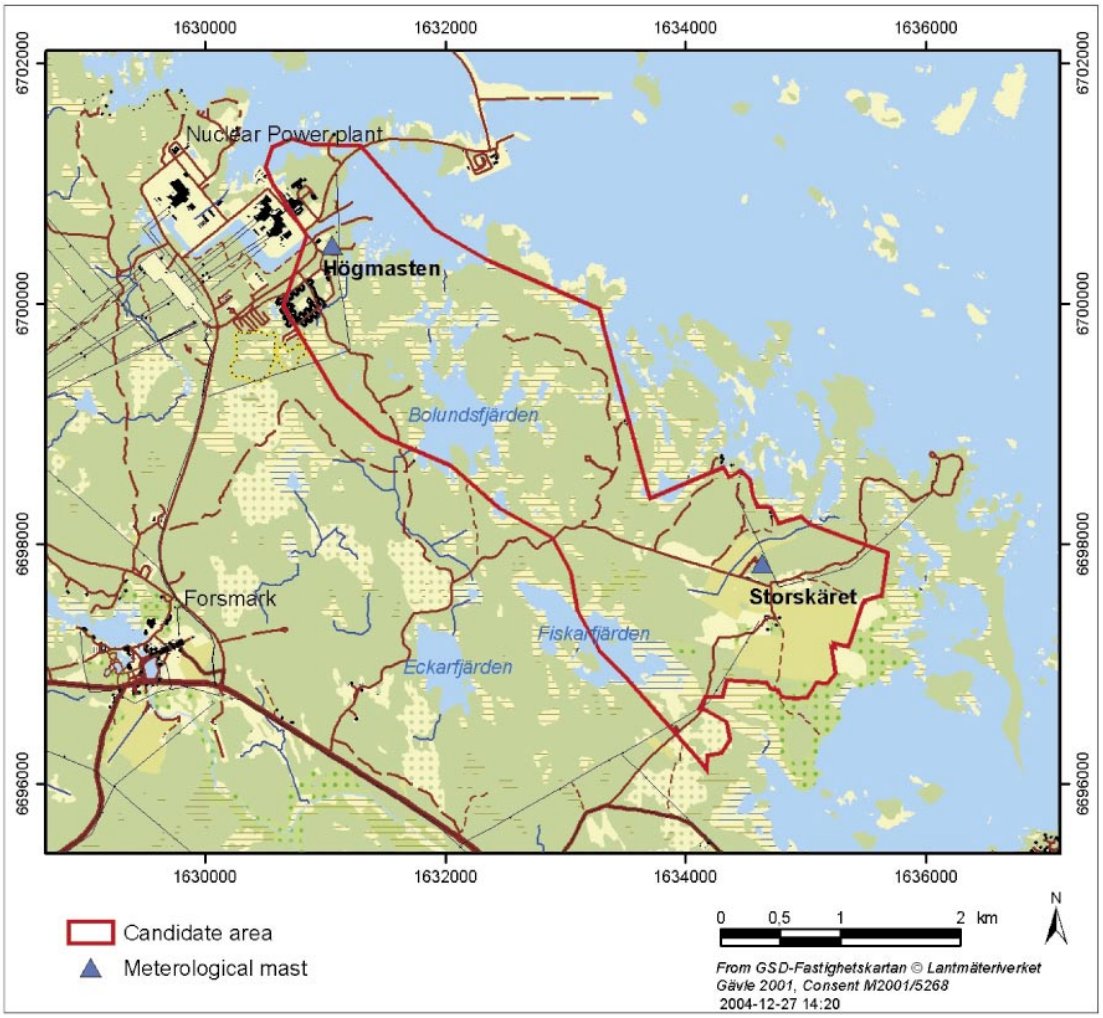

Figure 3-3. *Locations of the two new meteorological stations in the Forsmark area.*

Figure 3-4 shows a comparison of time series of daily values of corrected precipitation (P) measured at Storskäret and Högmasten during the period May 2003 – July 2004. The measured precipitation data were corrected by +10% if the temperature was < 1°C and by +6% for temperatures ≥ 1°C. There are two time intervals with missing data in the Storskäret precipitation time series: July 5–9, 2003 (during which period no rain was reported at Högmasten), and August 11–20, 2003 (when heavy rain was reported at Högmasten). In general, the time series of daily precipitation matched each other quite well, see Figure 3-5. The correlation coefficient of the two time series was calculated to $R^2 = 0.85$.

Data on locally measured precipitation events and the number of days with precipitation are summarised in Table 3-3. Precipitation was recorded in about 30% of the days during the one-year period from August 2003 to July 2004. The maximum daily precipitation was 25 mm and the maximum hourly value was 7 mm. These peak events were recorded at different stations; thus, this limited data evaluation does not indicate more pronounced peak events at the one station compared to the other.

Table 3-3. Precipitation intensity and number of days with precipitation.

August 1, 2003 – July 31, 2004	Storskäret	Högmasten
Peak one-hour event	7.4 mm	6.4 mm
Peak one-day event	17.9 mm	24.7 mm
No of days with precipitation	105	106

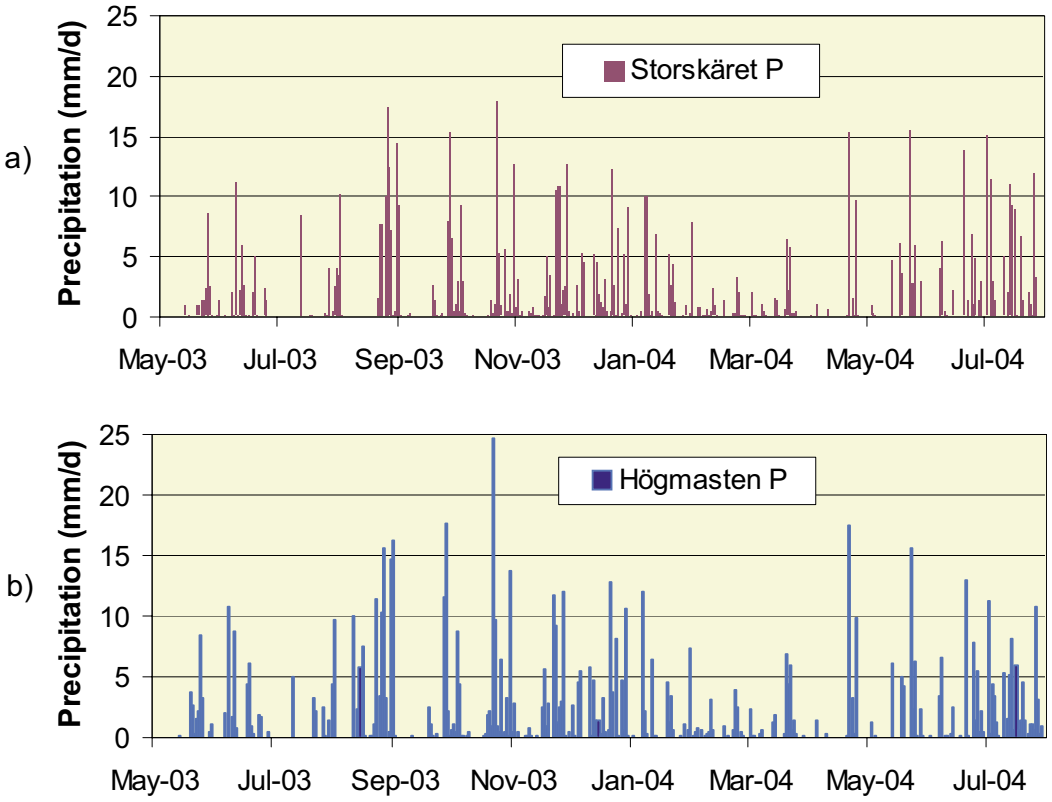

Figure 3-4. *Time series of daily corrected precipitation (P) at (a) Storskäret and (b) Högmasten.*

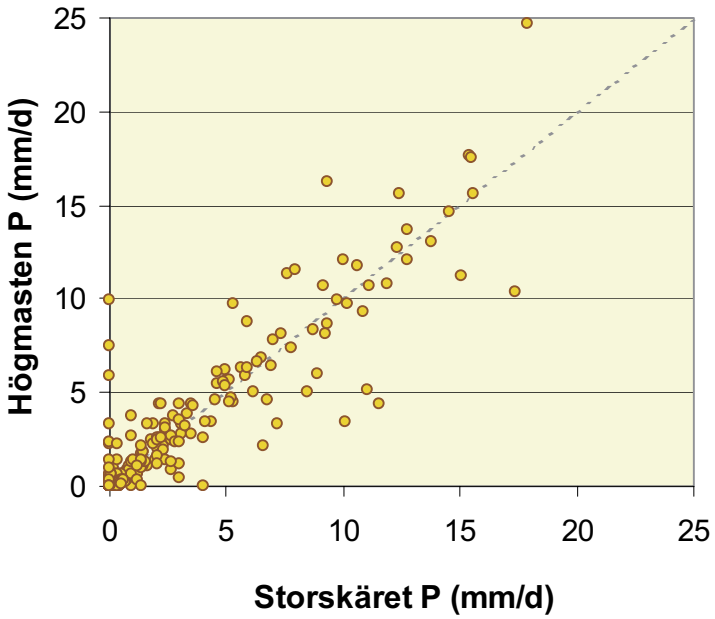

Figure 3-5. *Correlation between daily amounts of precipitation measured at Storskäret and Högmasten.*

Figure 3-6 shows a comparison of monthly total values of corrected precipitation (P) reported for Storskäret and Högmasten, and calculated monthly potential evapotranspiration (PET) based on data for Högmasten. The difference in reported P-values between the two stations during the month of August is in part explained by the missing data in the Storskäret time series during this period. The annual total corrected precipitation for the period from August 1, 2003, to July 31, 2004, was 619 and 641 mm for Storskäret and Högmasten, respectively.

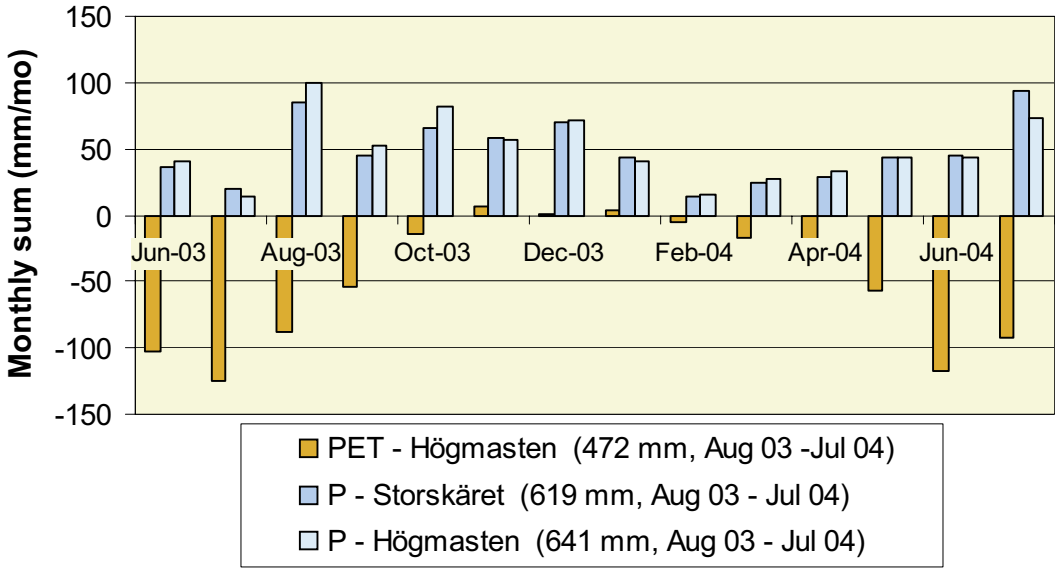

Figure 3-6. *Monthly values of corrected precipitation at Storskäret and Högmasten, and calculated potential evapotranspiration at Högmasten.*

The PET data were estimated from meteorological data measured at Högmasten using the Penman formula for a short grass crop. The annual total PET for the studied one-year period was calculated to 472 mm. Negative PET values (shown as positive values in Figure 3-6) were obtained for the winter months, essentially because the condensation exceeded the evapotranspiration. However, such low/negative values are uncertain and should be used with caution /Larsson-McCann et al. 2002/.

Figure 3-7 shows a comparison of monthly corrected precipitation values from the two SKB stations for a six-month period and regional data measured by SMHI at Lövsta and Örskär. In general, the datasets compare favorably. The SMHI data from Örskär are similar in magnitude and trend to the data from the SKB investigation area. On the other hand, the reported precipitation from the station at Lövsta is generally larger than that at the SKB stations, which would be expected due to its more inland location.

Figure 3-8 shows monthly average air temperatures measured at Storskäret and Högmasten, and the corresponding data for the SMHI stations at Örskär, Risinge and Films Kyrkby. The figure shows that the temperature (except from in August 2003) is 0.5–1°C higher at Högmasten than at Storskäret. The largest difference between the local average monthly temperature and the corresponding regional data is approximately 1.6°C (Högmasten-Örskär in June 2003, and Storskäret-Örskär in October 2003). The temperature is generally a little higher at Örskär during autumn and winter and a little lower during spring and early summer compared with the local data. This is due to the greater influence of Baltic Sea water temperatures at Örskär. However, there is no particular SHMI station for which the temperature data are consistently the most similar to the local data, and the differences are generally small (on the order of 1°C).

The daily average wind speeds measured at Storskäret and Högmasten are shown in Figure 3-9, together with the corresponding data for the SMHI station at Örskär for the year 2003. The measured wind speeds at Storskäret and Högmasten are considerably lower than at Örskär. The station at Örskär is more exposed to wind, mainly because the wind speed is measured at 39 m above ground at Örskär and at only 10 m above ground at Storskäret and Högmasten. Although the large short-term variations make trends somewhat difficult to observe, there is an apparent correlation between the wind speeds recorded at the SKB stations and those at Örskär.

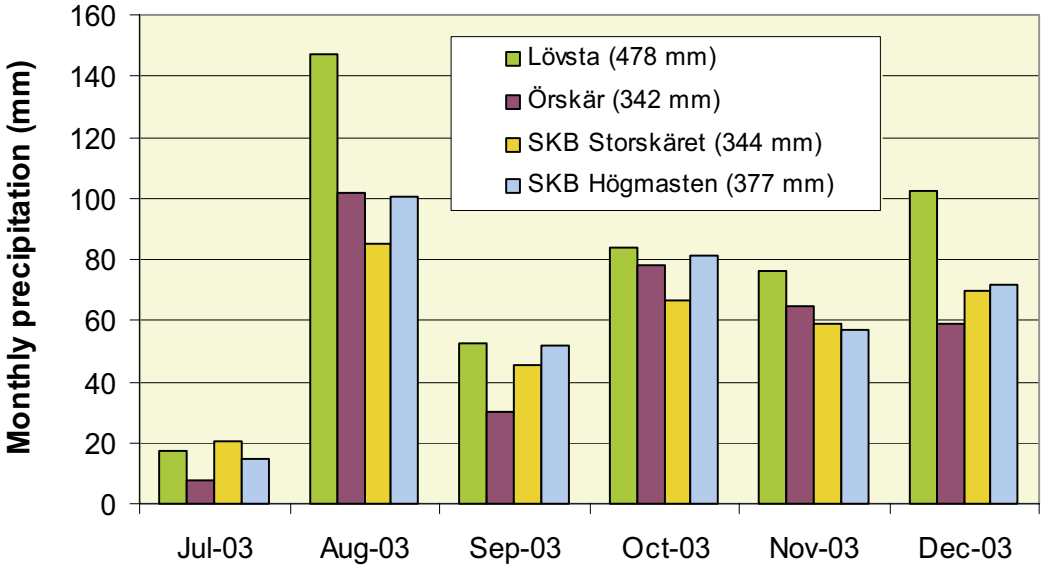

Figure 3-7. *Comparison of precipitation data from Storskäret and Högmasten and regional SMHI data from Lövsta and Örskär.*

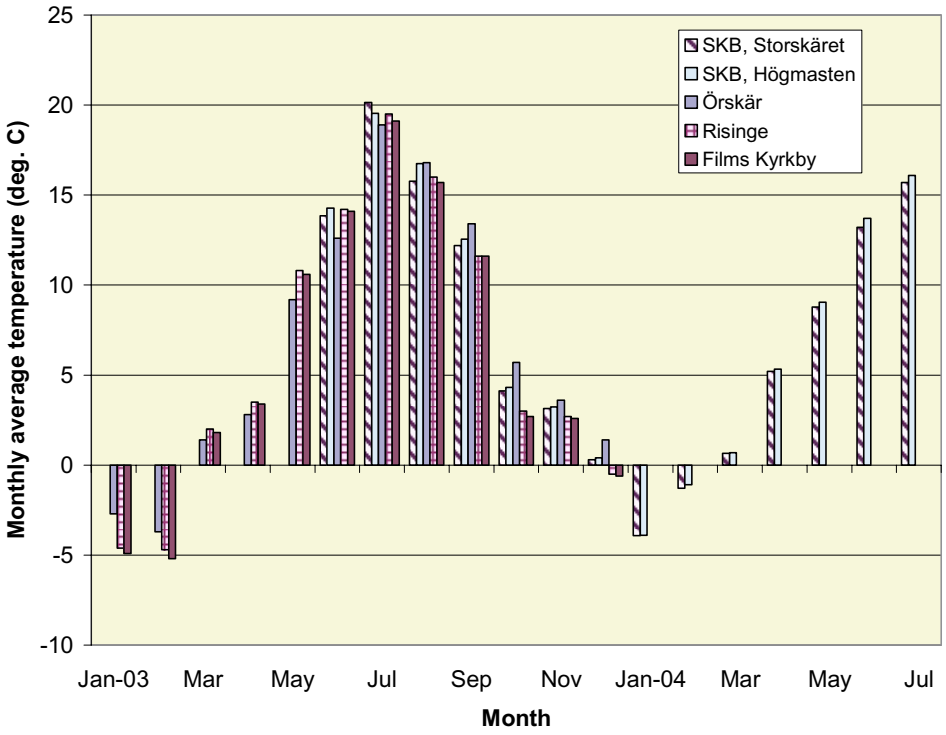

Figure 3-8. *Monthly average air temperatures at Storskäret and Högmasten compared to the SMHI stations at Örskär, Risinge and Films Kyrkby.*

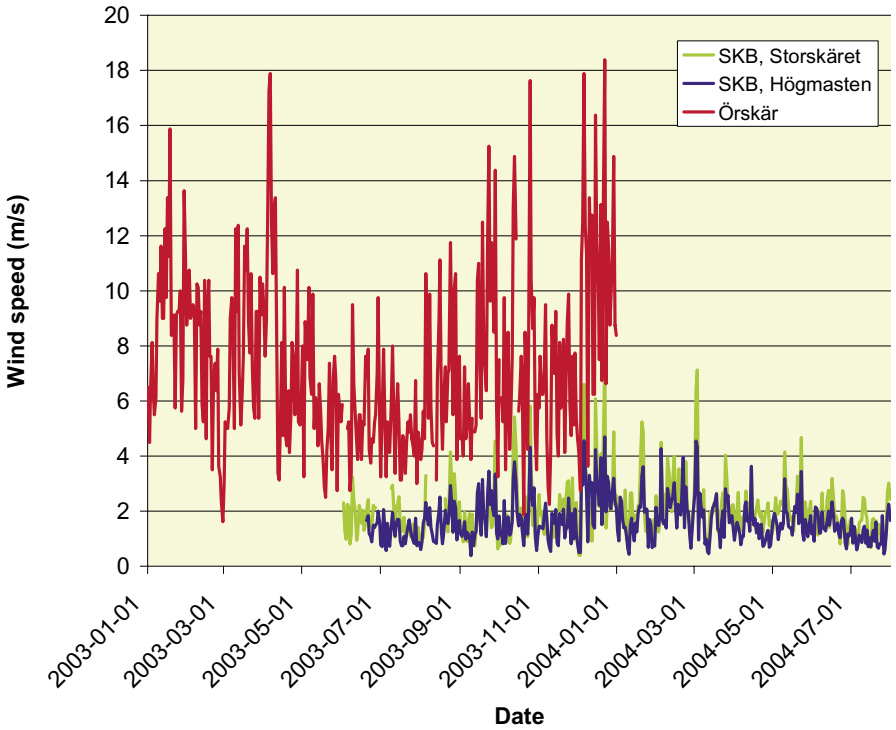

Figure 3-9. *Daily average wind speed ($m \cdot s^{-1}$) at Storskäret and Högmasten compared to the SMHI station at Örskär.*

Figure 3-10 shows the daily average relative humidity measured at Storskäret and Högmasten and the corresponding data for the SMHI station at Örskär during 2003. The figure shows that the temporal variation of the relative humidity is very similar at the three stations during the period of overlapping data (August–December, 2003). The relative humidity is generally in the interval 50–90%, with the lowest values recorded in the summer 2004 and the highest in December 2003.

Figure 3-11 shows the daily average air pressures measured at Högmasten, together with the corresponding data for the SMHI station at Örskär. As observed for the relative humidity (Figure 3-10), the temporal variations of the air pressure are very similar at the two stations. The air pressure is generally in the interval 990–1,030 mbar.

Figure 3-12 shows the monthly average global radiation measured at Högmasten. Since the global radiation is not measured at any of the nearby SMHI stations, no comparisons can be made with those. The maximum of monthly average global radiation, measured in June and July, is approximately 250 W/m^2, whereas the corresponding minimum values, observed during the period from November to January, are less than 10 W/m^2. The total global radiation during the period August 1, 2003 to July 31, 2004 is approximately 900 kWh/m^2, with monthly values ranging from 3 kWh/m^2 in December to 177 kWh/m^2 in June.

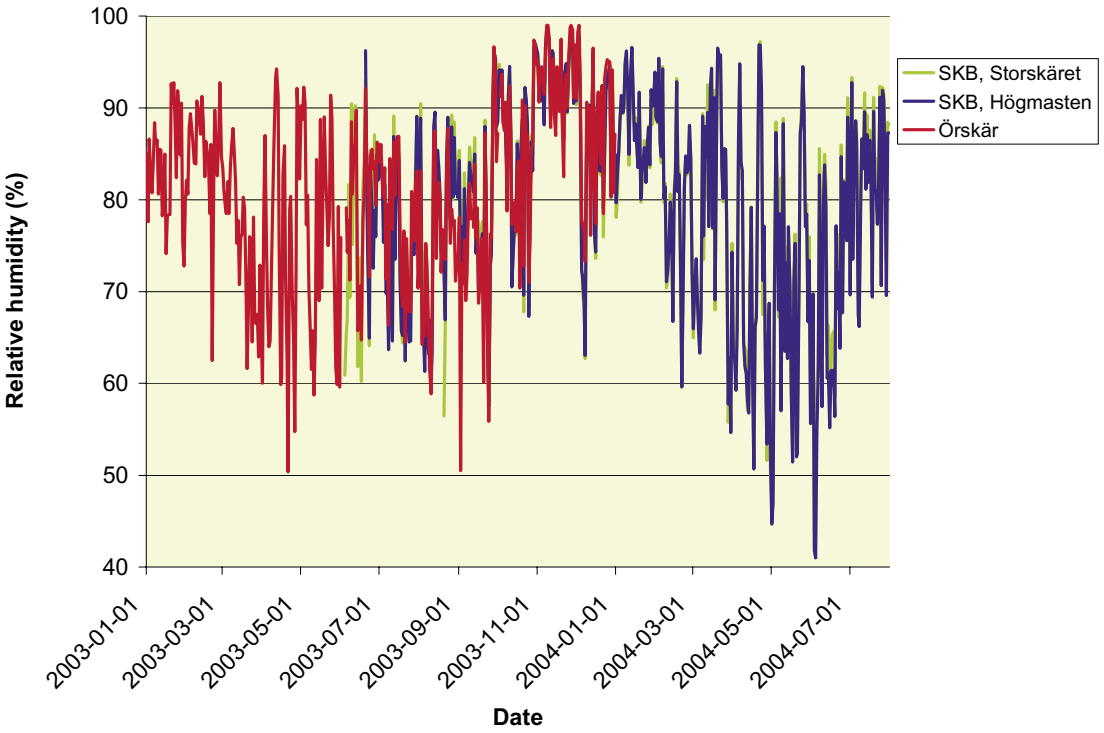

Figure 3-10. *Daily average relative humidity (%) at Storskäret and Högmasten compared to the SMHI station at Örskär.*

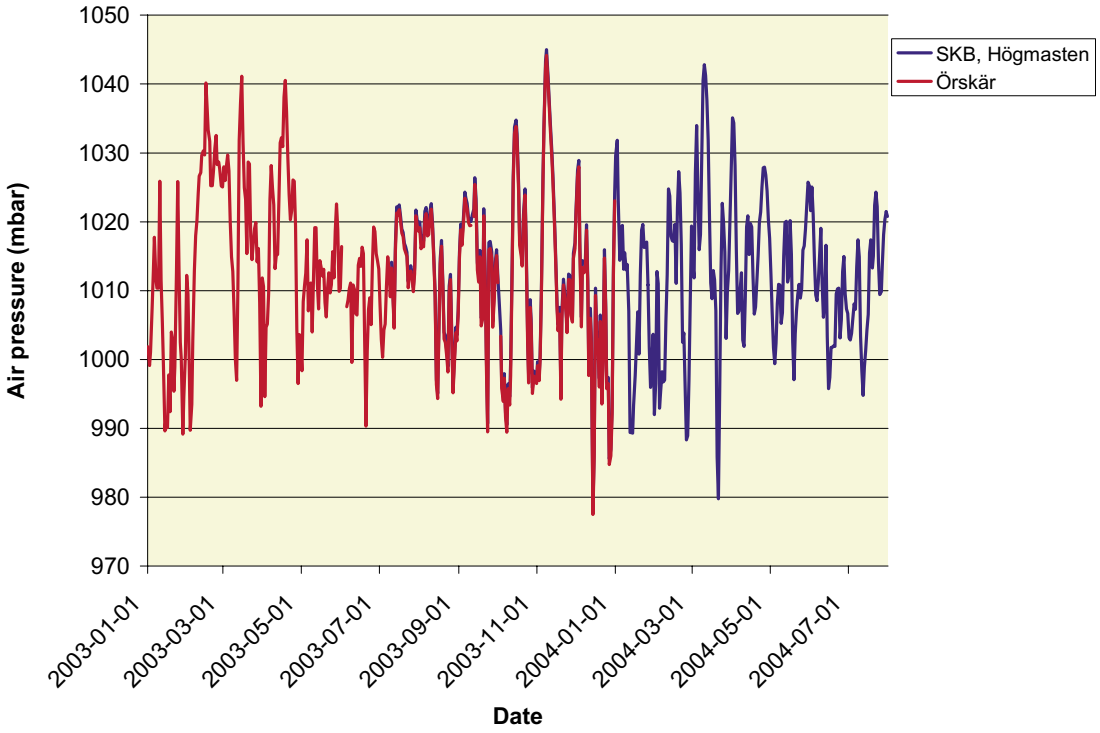

Figure 3-11. *Daily average air pressures (mbar) at Högmasten compared to the SMHI station at Örskär.*

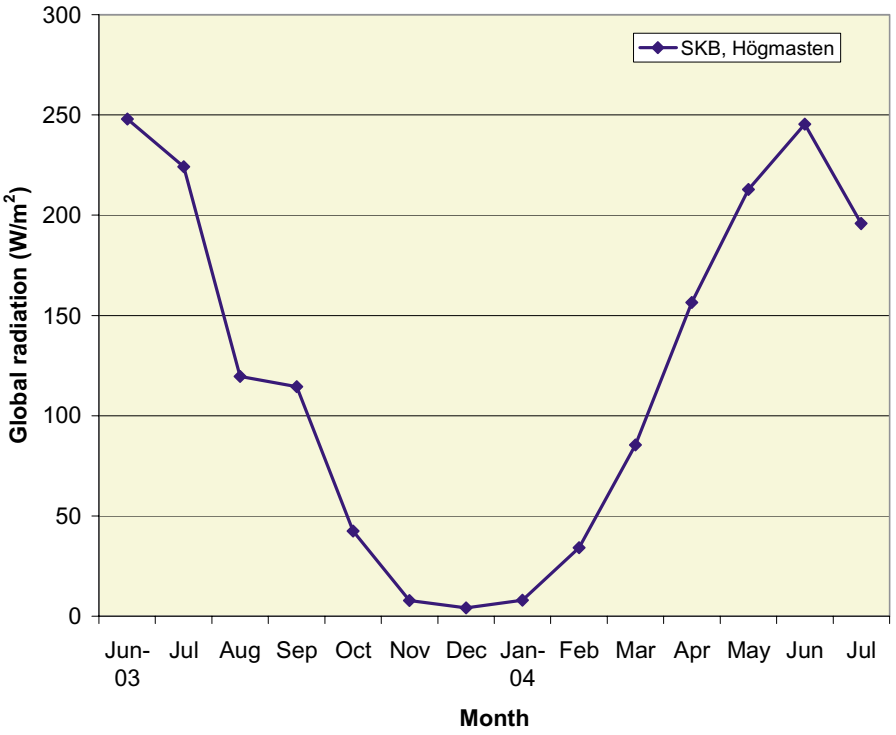

Figure 3-12. *Monthly average global radiation (W/m²) at Högmasten.*

3.2 Hydrological data

3.2.1 Catchment areas

Based on the SKB digital elevation model (10 m grid), maps, aerial photos, and field control including DGPS measurements, a detailed delineation of catchment areas was made in the central part of the regional model area /Brunberg et al. 2004/; the result is shown in Figure 3-13. In Table 3-4, data on size and land use of the catchment areas are presented. In total, 25 "lake-centred" catchment areas were delineated, ranging in size from 0.03 km^2 to 8.67 km^2. Forest is dominating and covers between 50% and 96% of the areas of the different catchments. Wetlands, both forest-covered and open, are frequent and cover more than 20% of the area in five of the catchments. Agricultural land constitutes an important part of the total area in only one of the catchment areas (5:1, Bredviken, with 27% agricultural land). A more detailed description of the catchment areas is given in /Brunberg et al. 2004/.

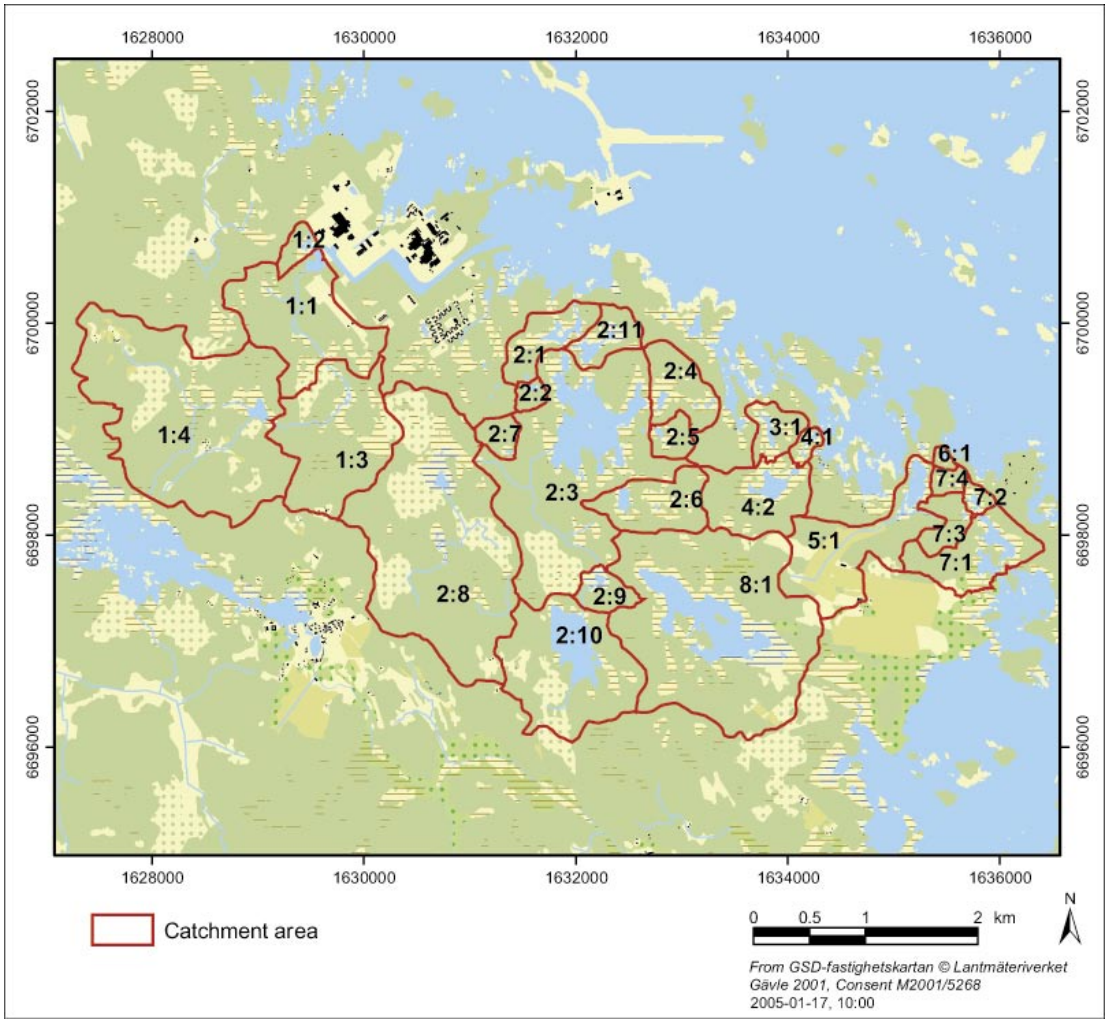

Figure 3-13. *Delineated catchment areas /Brunberg et al. 2004/.*

Table 3-4. Size and land use of delineated catchment areas.

Number in Figure 3-13	Name	Catchment area (km²)	Forest (%)	Forest wetland (%)	Clear-cut area (%)	Agric. land (%)	Open land wetland (%)	Other open land (%)	Water (%)
1:1 (incl 1:2-1:4)	Gunnarsbo-Lillfjärden (södra)	5.1202	78.1	2.1	6.7	0.8	7.7	3.2	1.3
1:2	Gunnarsbo-Lillfjärden (norra)	0.1035	70.6	5.1			10.9	2.8	10.6
1:3 (incl 1:4)	Labboträsket	3.9277	78.8	2.1	8.2	1.0	7.0	2.0	0.9
1:4	Gunnarsboträsket	2.7344	80.5	1.9	8.2	1.5	4.6	2.4	0.9
2:1 (incl 2:2-2:11)	Norra Bassängen	8.6682	67.1	0.6	10.6		11.4	1.1	9.1
2:2		0.0714	92.5					0.3	7.3
2:3 (incl 2:4-2:10)	Bolundsfjärden	8.0030	67.1	0.7	11.5		10.5	1.1	9.1
2:4	Graven	0.3917	71.7	0.6			23.9		3.8
2:5	Fräkengropen	0.1384	79.9				16.3		3.9
2:6	Vambörsfjärden	0.4837	74.5	0.7			20.0		4.8
2:7	Kungsträsket	0.1257	93.0				5.4		1.6
2:8	Gällsboträsket	2.8910	67.9	0.7	21.3		8.7	1.0	0.5
2:9 (incl 2:10)	Stocksjön	1.4720	66.4	0.1	7.7		6.7	4.1	15.0
2:10	Eckarfjärden	1.2972	65.3	0.1	8.7		5.0	4.4	16.5
2:11	Puttan	0.2488	60.2				26.6		13.2
3:1	Tallsundet	0.2154	57.9	2.8			32.0		7.4
4:1		0.6898	64.2	3.6			22.8	0.3	9.1
4:2	Lillfjärden	0.6208	66.3	4.0			21.1	0.3	8.3
5:1	Bredviken	0.9439	49.2	0.8	1.4	26.9	3.4	11.4	6.9
6:1	Simpviken	0.0346	76.4				9.3		4.3
7:1 (incl 7:1–7.4)		0.8952	70.2	1.6			15.6	1.8	10.7
7:2 (incl 7:3–7:4)	Märrbadet	0.3372	81.0	2.2			13.2	0.1	3.6
7:3		0.1918	92.2	3.8			3.1		1.0
7:4		0.0771	82.7				15.4		2.0
8:1	Fiskarfjärden	2.9259	63.7	3.2	1.4	0.7	13.5	4.1	13.4

3.2.2 Lakes

Morphometrical data for the lakes are summarised in Table 3-5; for a more detailed description of the lakes, see /Brunberg et al. 2004/. Several lakes have water levels close to the Baltic Sea level. During events of high sea levels, water from the Baltic Sea may intrude into these lakes. For example, sea water relatively frequently flows into Lake Bolundsfjärden (cf Section 3.2.5).

Table 3-5. Morphometrical data for the lakes in the Forsmark area.

No in Figure 3-13	Name	Water level (m a s l)	Area (m^2)	Max depth (m)	Mean depth (m)	Volume (m^3)
1:1	Gunnarsbo-Lillfjärden (södra)	1.60*	33,107	2.22	0.70	23,110
1:2	Gunnarsbo-Lillfjärden (norra)	1.64*	23,148	0.90	0.30	6,870
1:3	Labboträsket	3.56*	60,042	1.07	0.27	15,950
1:4	Gunnarsboträsket	5.81**	67,453	1.29	0.51	34,040
2:1	Norra Bassängen	0.56*	76,070	0.88	0.31	23,650
2:2		1.82*	9,921	0.60	0.29	2,860
2:3	Bolundsfjärden	0.64*	611,312	1.81	0.61	373,950
2:4	Graven	0.65*	50,087	0.35	0.12	5,920
2:5	Fräkengropen	1.35*	19,423	0.79	0.19	3,660
2:6	Vambörsfjärden	1.14*	49,577	0.98	0.43	20,550
2:7	Kungsträsket	2.60*	7,733	0.54	0.20	1,550
2:8	Gällsboträsket	1.91*	187,048	1.51	0.17	32,100
2:9	Stocksjön	2.92*	36,480	0.82	0.22	8,030
2:10	Eckarfjärden	5.37*	283,850	2.12	0.91	257,340
2:11	Puttan	0.63*	82,741	1.29	0.37	30,150
3:1	Tallsundet	0.13*	79,414	0.80	0.23	18,350
4:1		–0.29*	35,058	1.53	0.38	13,000
4:2	Lillfjärden	–0.07*	161,269	0.89	0.29	47,030
5:1	Bredviken	–0.12*	97,664	1.72	0.74	72,010
6:1	Simpviken	–0.29*	9,119	1.80	0.50	5,000
7:1		–0.26*	163,052	1.07	0.32	52,570
7:2	Märrbadet	0.00*	23,611	1.01	0.36	8,500
7:3		0.22*	6,393	0.70	0.25	1,620
7:4		0.38*	9,312	0.81	0.24	2,250
8:1	Fiskarfjärden	0.54**	754,303	1.86	0.37	274,450

* Water levels measured April 16–20, 2002.

** Water levels measured Oct 22–23, 2002.

3.2.3 Wetlands

Different types of wetlands occur frequently within the Forsmark investigation area. In Figure 3-14, the different wetlands types, as presented in the ground layer of the vegetation map /Boresjö Bronge and Wester, 2003/, are shown. The percentages of forested and open wetlands in each catchment are given in Table 3-4.

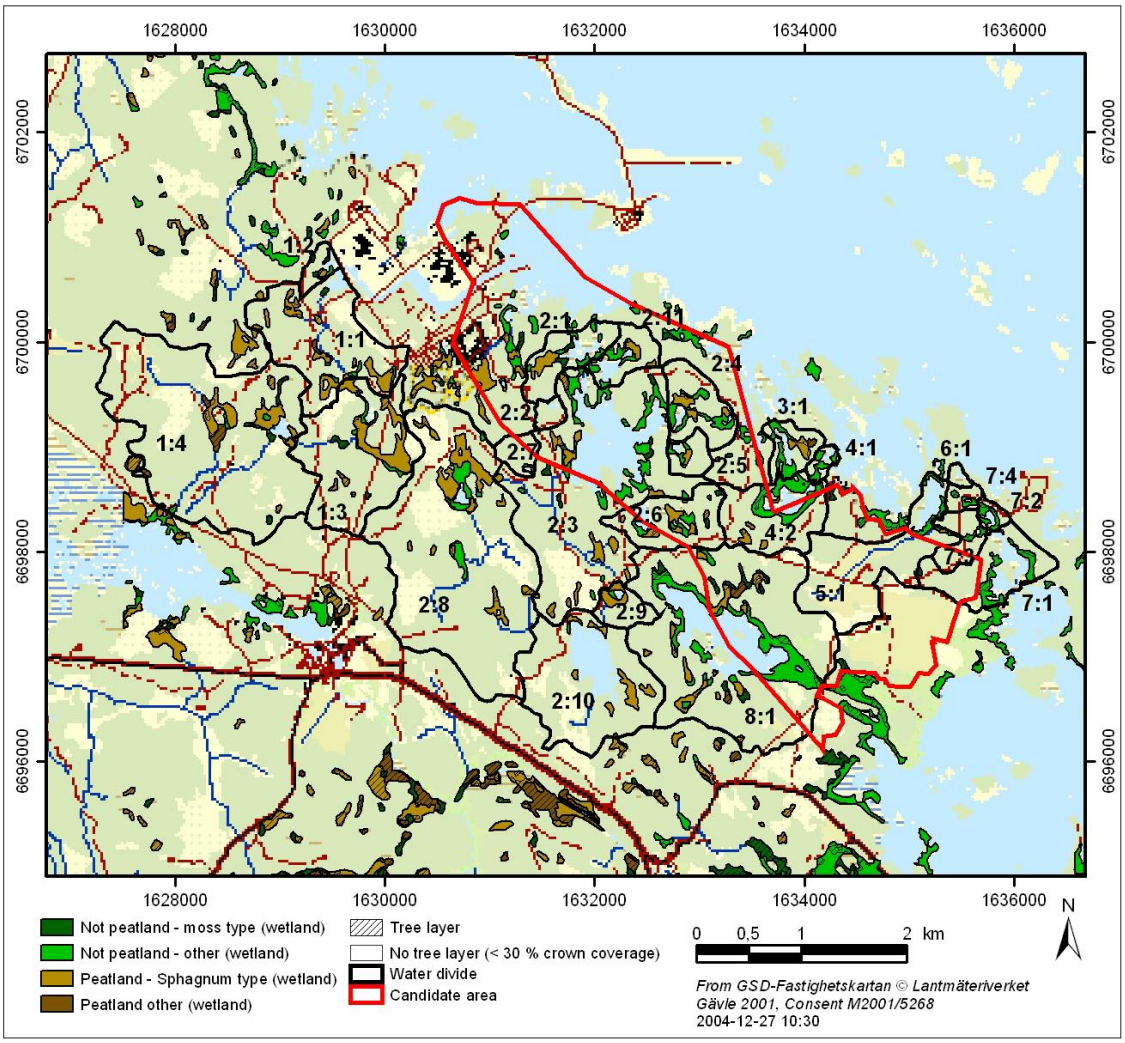

Figure 3-14. *Wetlands of different types within the Forsmark area, based on the vegetation map /Boresjö Bronge and Wester, 2003/.*

3.2.4 Water courses and lake thresholds

The existing digital elevation model (DEM), in the form of a regular grid with a resolution of 10 m, does not describe the brooks and the lake thresholds with an adequate accuracy for the quantitative surface water flow modelling. In particular, brooks have been deepened for drainage purposes, which may lead to significant differences between their bottom elevations and the surrounding topography described by the DEM. Man-made alterations of the flow system may also have changed the overall discharge directions from some sub-catchments, as compared to those inferred directly from the DEM.

In order to obtain a better description of the brooks in the area, field surveying was performed of the deepest furrows and cross-sections at regular distances along the major brooks within the central parts of the regional model area. The field work was only partly finalised at the time for the F1.2 data freeze; the brooks for which results are available in F1.2 are shown in Figure 3-15.

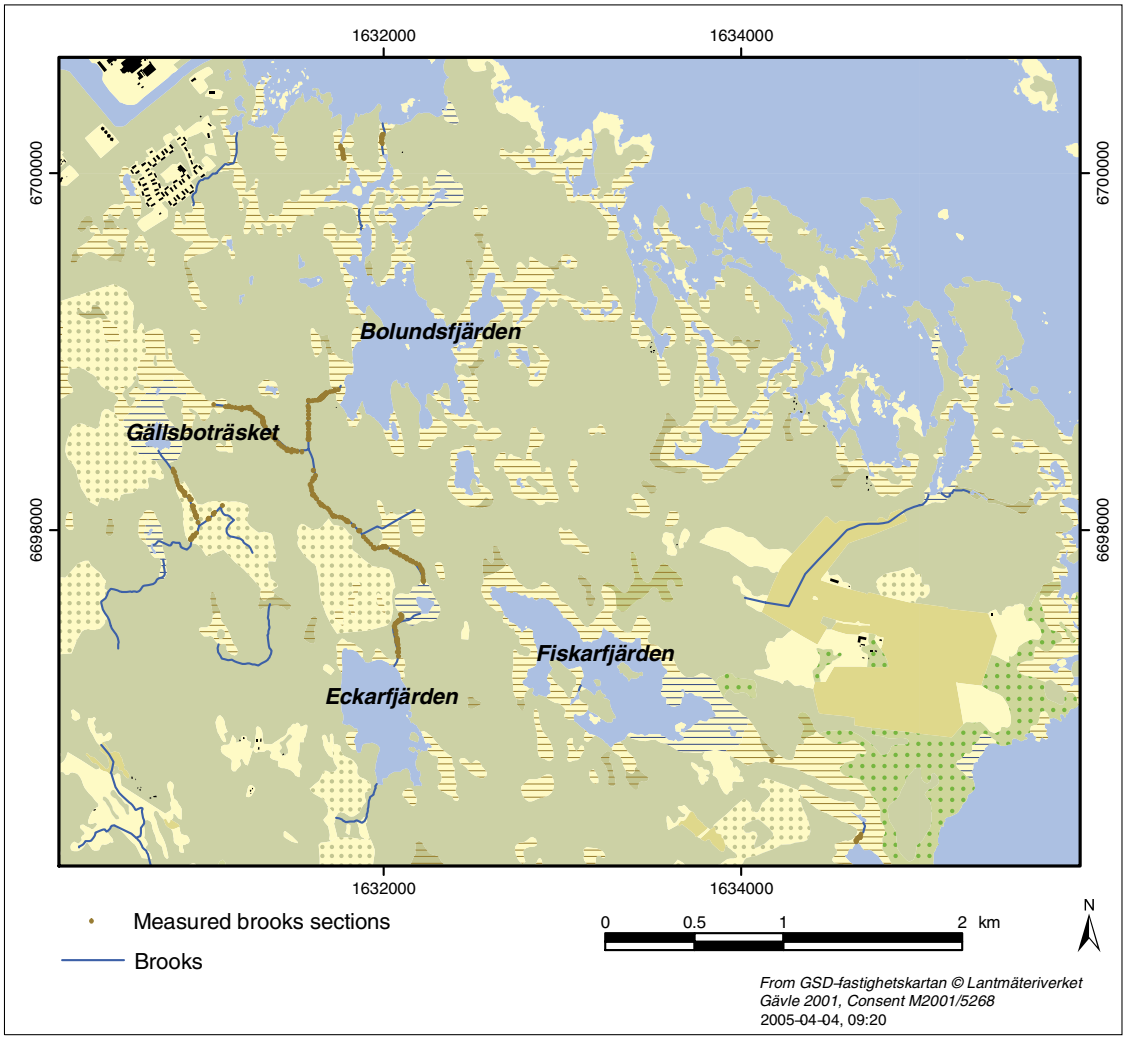

Figure 3-15. *The brook sections measured in the spring 2004 survey.*

Figures 3-16 and 3-17 show the bottom elevations along two major brooks in the central part of the investigation area, the brook from Eckarfjärden to the Baltic Sea, and that from about 400 m upstream of Gällsboträsket to the conjunction with the brook from Eckarfjärden, respectively (cf Figure 3-15). Note the large difference between the vertical and horizontal scales; the total drop in water level is actually small in both cases.

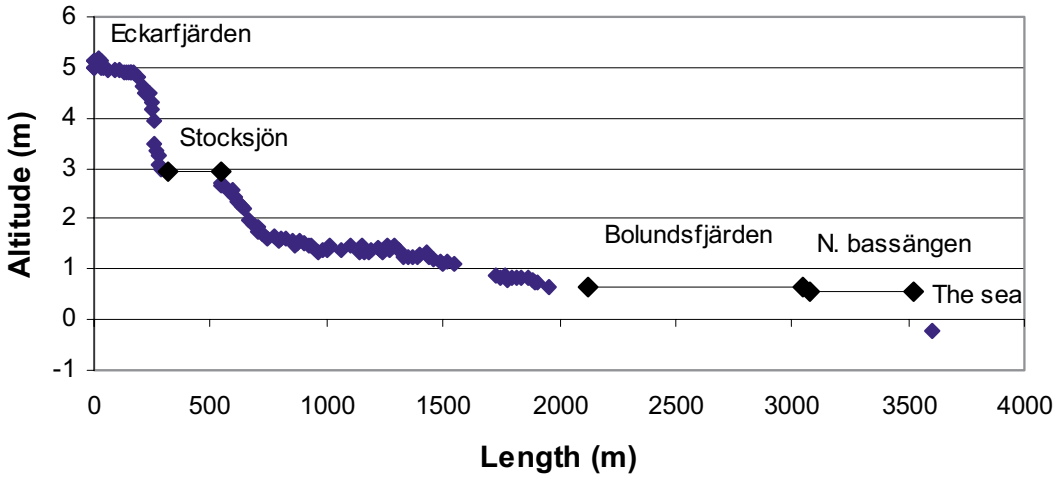

Figure 3-16. *The bottom elevation of the brook between Eckarfjärden and the Baltic Sea.*

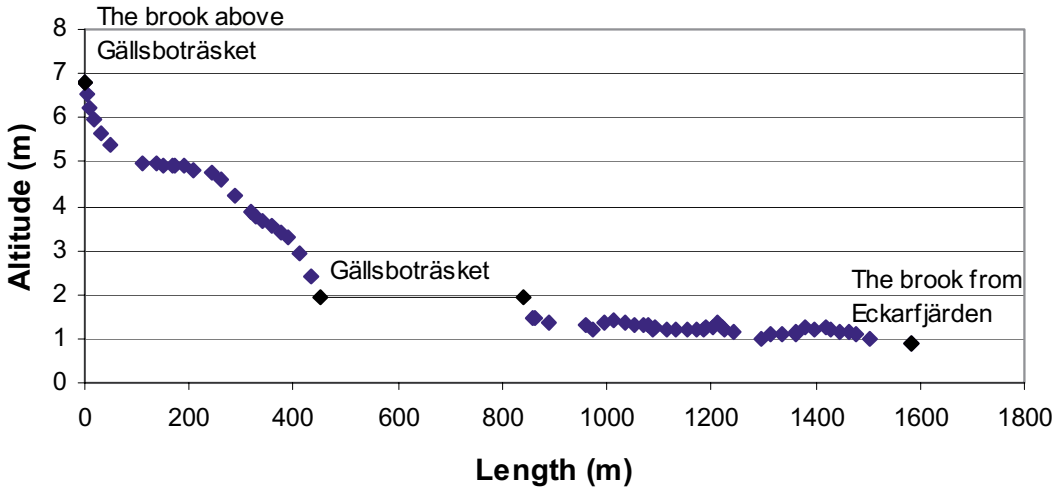

Figure 3-17. *The bottom elevation of the brook between a point 400 m upstream of Gällsboträsket and the conjunction with the brook from Eckarfjärden.*

3.2.5 Surface water levels

Surface water level gauges have been installed in six lakes (SFM0039–42, SFM0064 and SFM0066) and at two locations in the Baltic Sea, in the Forsmark harbour (SFM0038, now changed to PFM010038) and in Kallrigafjärden (SFM0043). The measurement locations are shown in Figure 3-18. SMHI also independently measures the sea level in the Forsmark harbour, in the immediate vicinity of the SKB station. Time series from the surface water level gauges are shown in Figure 3-19.

On average, the reported SMHI sea levels were about 6 cm higher than the reported SKB measurements ("SFM 38") with a range of +16 cm to –6 cm (daily mean values). The reported SKB data at Kallrigafjärden ("SFM 43") averaged about 12 cm less than the SKB data from the Forsmark harbour. At the time of writing, these differences are difficult to explain, and it is recommended that this issue is further investigated. In general, the three time series showed similar trends in sea level amplitudes, despite the differences in absolute levels.

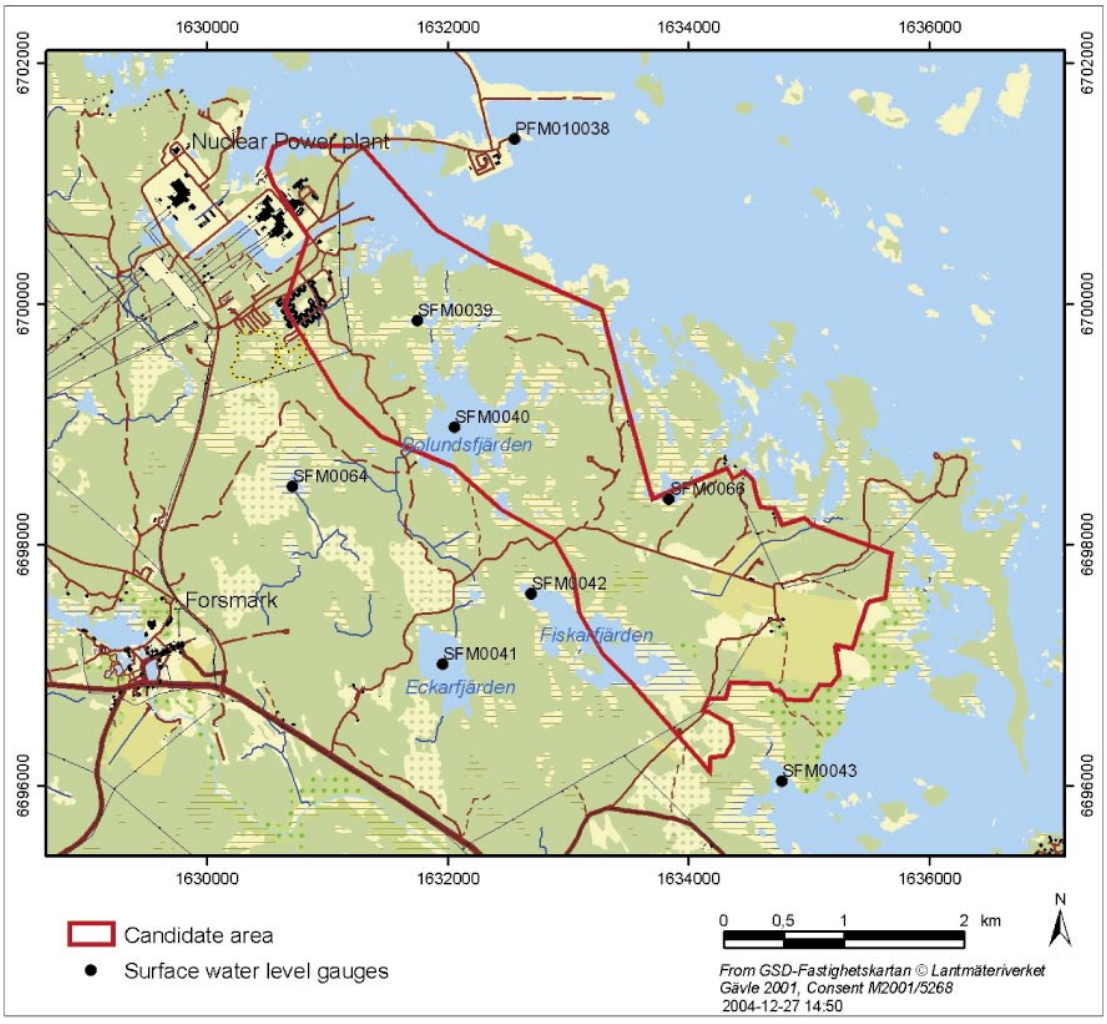

Figure 3-18. *Surface water level gauges.*

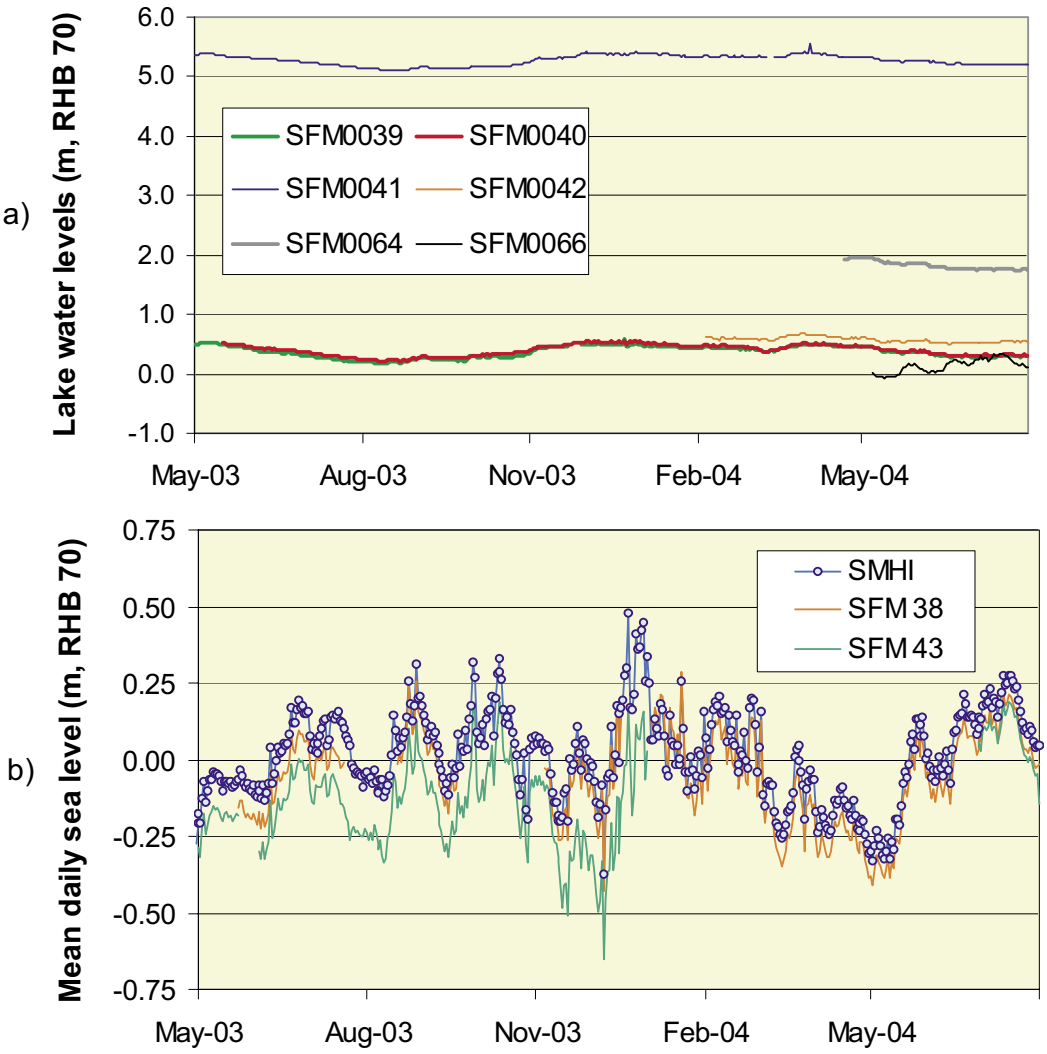

Figure 3-19. *Surface water levels in the lakes and the Baltic Sea.*

The available time series for Lake Lillfjärden (SFM0066) is very short. However, the dataset at hand indicates that the lake level is mainly determined by the sea level. The lake levels of Lake Norra Bassängen (SFM0039) and Lake Bolundsfjärden (SFM0040) are also quite low, but these levels seem to be determined mainly by the lake thresholds and the groundwater and surface water inflow from the inland. However, during the period for which level measurements were available, the sea level was higher than the water levels in Lake Norra Bassängen and Lake Bolundsfjärden at a few occasions, thus allowing for sea water intrusion into these lakes.

The level of Lake Fiskarfjärden is slightly higher than the levels of Lake Norra Bassängen and Lake Bolundsfjärden, and during the period for which level measurements were available the level of this lake is always higher than that of the sea. A detailed comparison of the levels of the Baltic Sea, Lake Lillfjärden, Lake Norra Bassängen, Lake Bolundsfjärden and Lake Fiskarfjärden is shown in Figure 3-20.

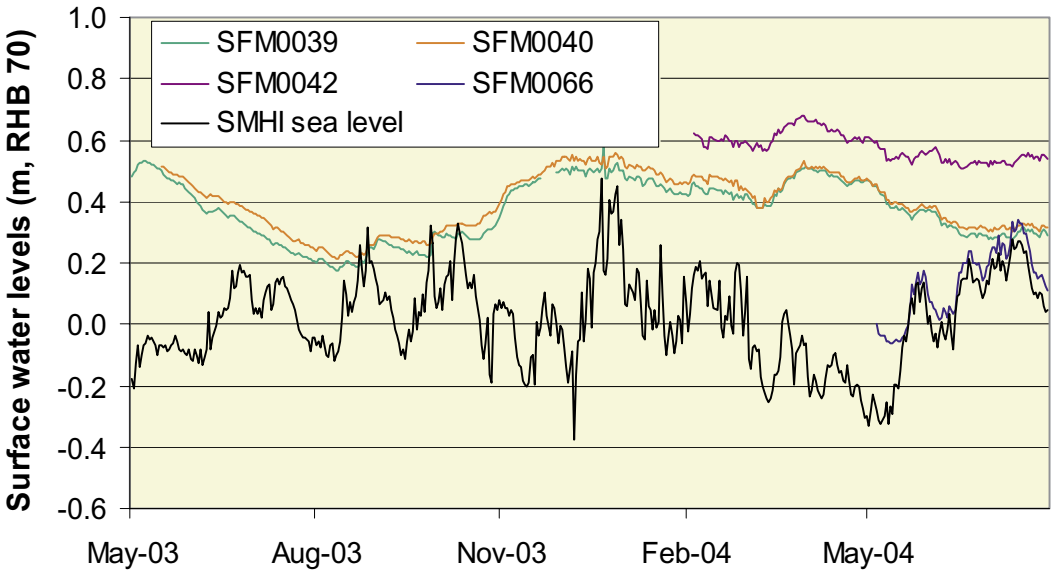

Figure 3-20. *Detailed comparison of the water levels in the Baltic Sea, Lake Norra Bassängen (SFM0039), Lake Bolundsfjärden (SFM0040), Lake Fiskarfjärden (SFM0042) and Lake Lillfjärden (SFM0066).*

3.2.6 Discharge data

Regional data

The locations of the hydrological stations in Uppland are shown in Figure 3-1, and data on the stations are presented in Table 3-6.

The station at Vattholma was chosen by /Larsson-McCann et al. 2002/ to be the main representative hydrological station for the Forsmark area. The catchment area is 294 km^2 and the mean specific discharge is 7.5 L·s^{-1}·km^{-2}. Monthly discharge values for the Vattholma Station are shown in Figure 3-21. The precipitation gradient, with lower precipitation closer to the coast, means that the specific discharge in the Forsmark area will be lower than the corresponding measured discharge at Vattholma. The specific discharge can be estimated to be approximately 6.5 L·s^{-1}·km^{-2} (approximately 200 mm·year^{-1}) /SGU, 1983/.

Table 3-6. Hydrological stations in Uppland /Larsson-McCann et al. 2002/.

Stn No	Name	River	Lake %[1)]	Area km^2	N	E	Period
50110	Vattholma	Fyrisån	5	294	665713	160736	1917–2000
910	Uvlunge	Vendelån	2.6	263	666663	160043	1917–1942
2299	Tärnsjö	Stalbobäcken	2	13.7	666859	156333	1975–2000
573	Gimo	Olandsån	3.2	587	667489	163287	1922–1932
1256	Fors	Olandsån	3.2	577	667170	163344	1931–1959
1053	Näs	Tämnarån	4.2	1,176	670862	159995	1925–1971
1260	Odensfors	Tämnarån	6.3	772	668382	158822	1930–1950
	OL1[2)]	Olandsån	1.4	880.9	669252	163452	1962–2001
	FO1[2)]	Forsmarksån	4.6	375.5	669500	163249	1962–2001

[1)] percentage of catchment area.

[2)] time series simulated by SMHI's HBV-model.

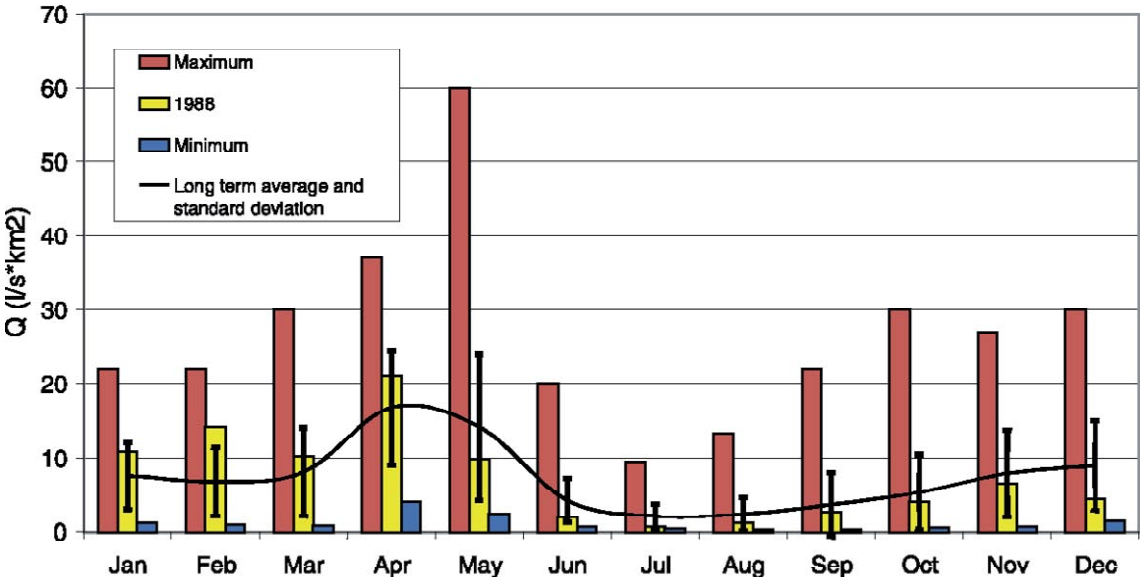

Figure 3-21. *Monthly discharge at Vattholma. Maximum and minimum daily mean, long term average and standard deviation ($L \cdot s^{-1} \cdot km^{-2}$). /Larsson-McCann et al. 2002/ selected 1988 as a representative year.*

Manual discharge measurements

Manual discharge measurements have been performed in the water courses at eight locations since March 2002 /Nilsson et al. 2003; Nilsson and Borgiel, 2004/. The locations of the measurement points are shown in Figure 3-22. The manual discharge measurements are performed 1–5 times per month, except from periods when the water courses were dry, covered with ice, or when the flow was too small to allow measurements.

The discharge measurements were performed by using a 150 mL plastic bottle, filled to 2/3 by water, as a float. The time (t) required for the bottle to float a known distance (l) between two points in the water course was measured. This procedure was repeated 5 times, and the average value of t was calculated. Based on the average width (w) and depth (d) of the water course over the measured distance, the discharge Q was estimated as

$$Q = \frac{l \cdot w \cdot d}{t}$$

where all parameters except l are average values.

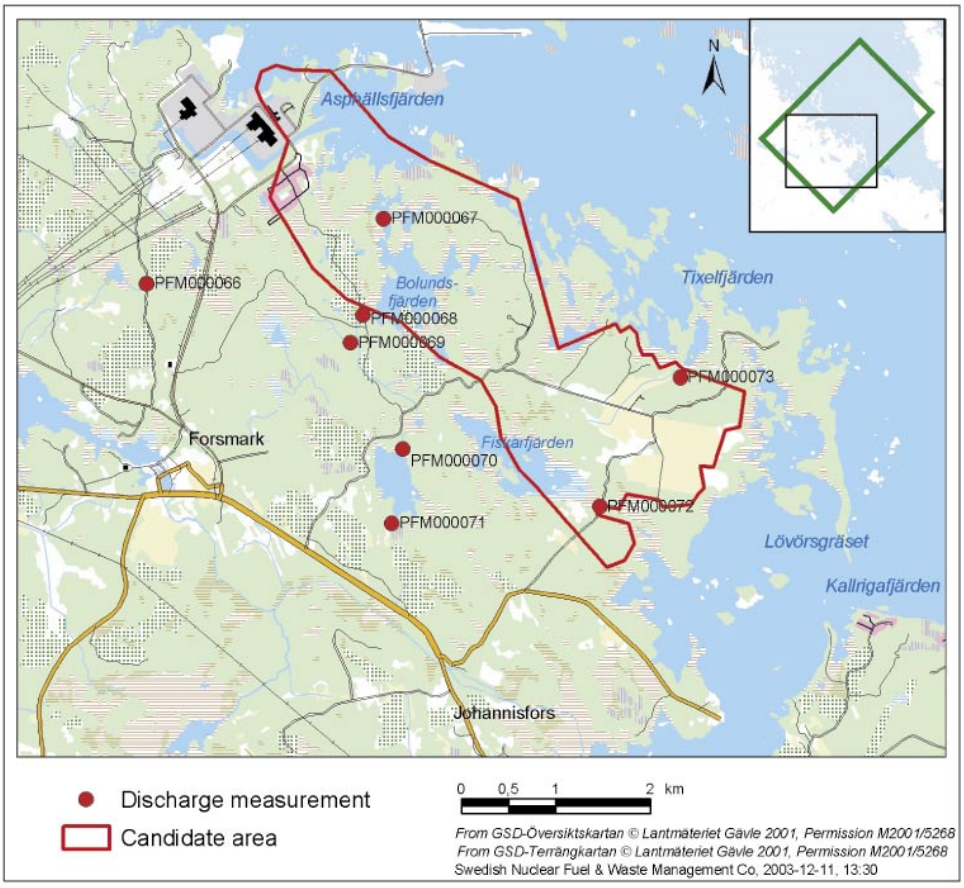

Figure 3-22. *Stations for manual discharge measurements.*

The results of the manual discharge measurements are summarised in Table 3-7 and Figures 3-23 to 3-26. In the figures, data points are connected with a solid line if the time period between consecutive measurements is two weeks (14 days) or less. It can be noted that the results generally display significant temporal variations.

Table 3-7. Summary of manual discharge measurements in water courses.

Station	Location	Measurement period (YYYY-MM-DD)	Number of measurements
PFM000066	East of Gunnarsboträsket	2002-04-15 – 2004-07-06	48
PFM000067	Lillputtsundet	2002-11-26 – 2004-06-29	40
PFM000068	Kungsträsket	2002-04-15 – 2004-10-11	47
PFM000069	Bolundsskogen	2002-04-17 – 2004-10-11	52
PFM000070	North of Eckarfjärden	2002-04-02 – 2004-08-16	40
PFM000071	South of Eckarfjärden	2002-04-16 – 2004-06-29	25
PFM000072	Flottbron	2002-04-15 – 2004-06-29	23
PFM000073	South of Bredviken	2002-04-15 – 2004-06-29	31

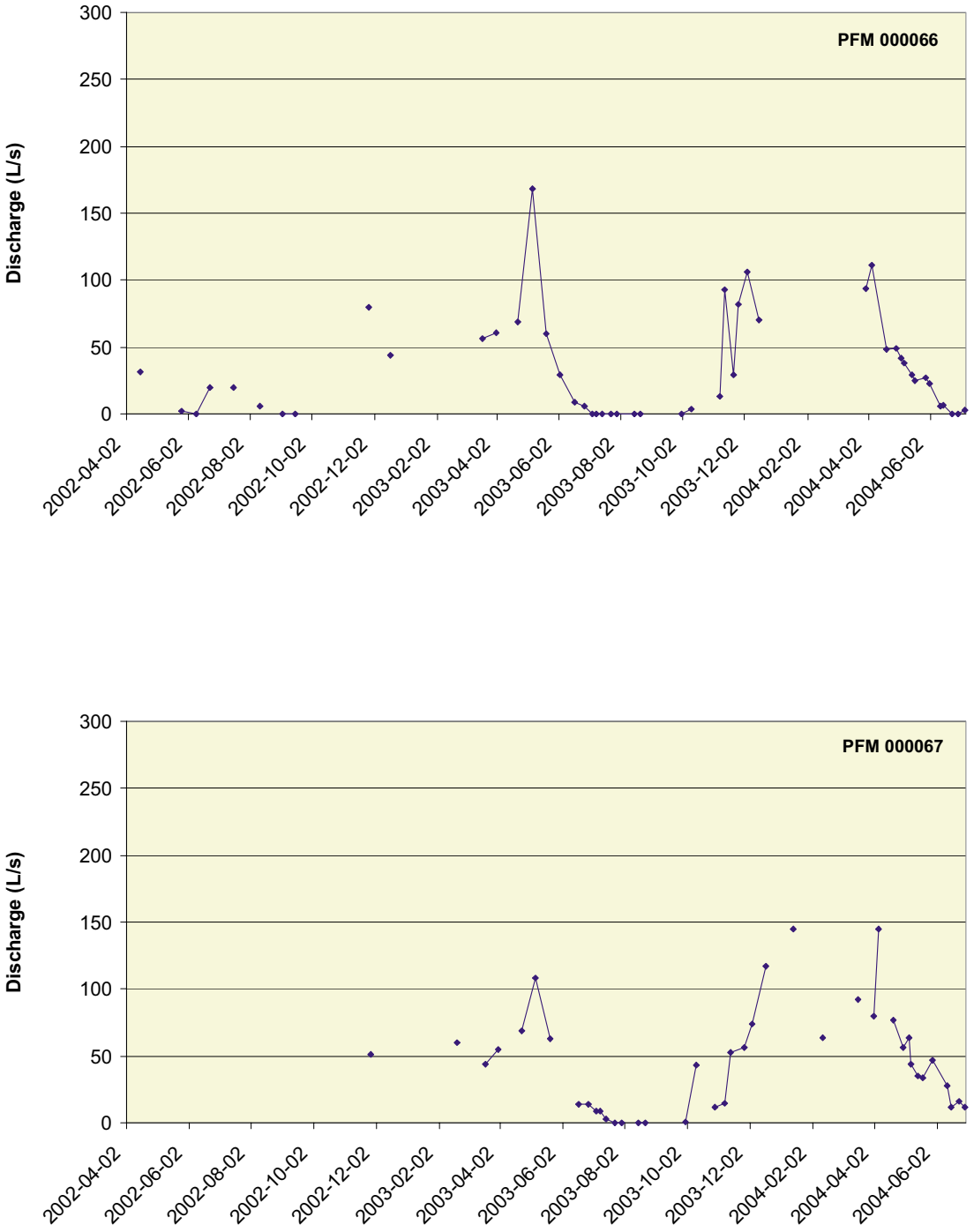

Figure 3-23. *Results of manual discharge measurements at locations PFM000066–67.*

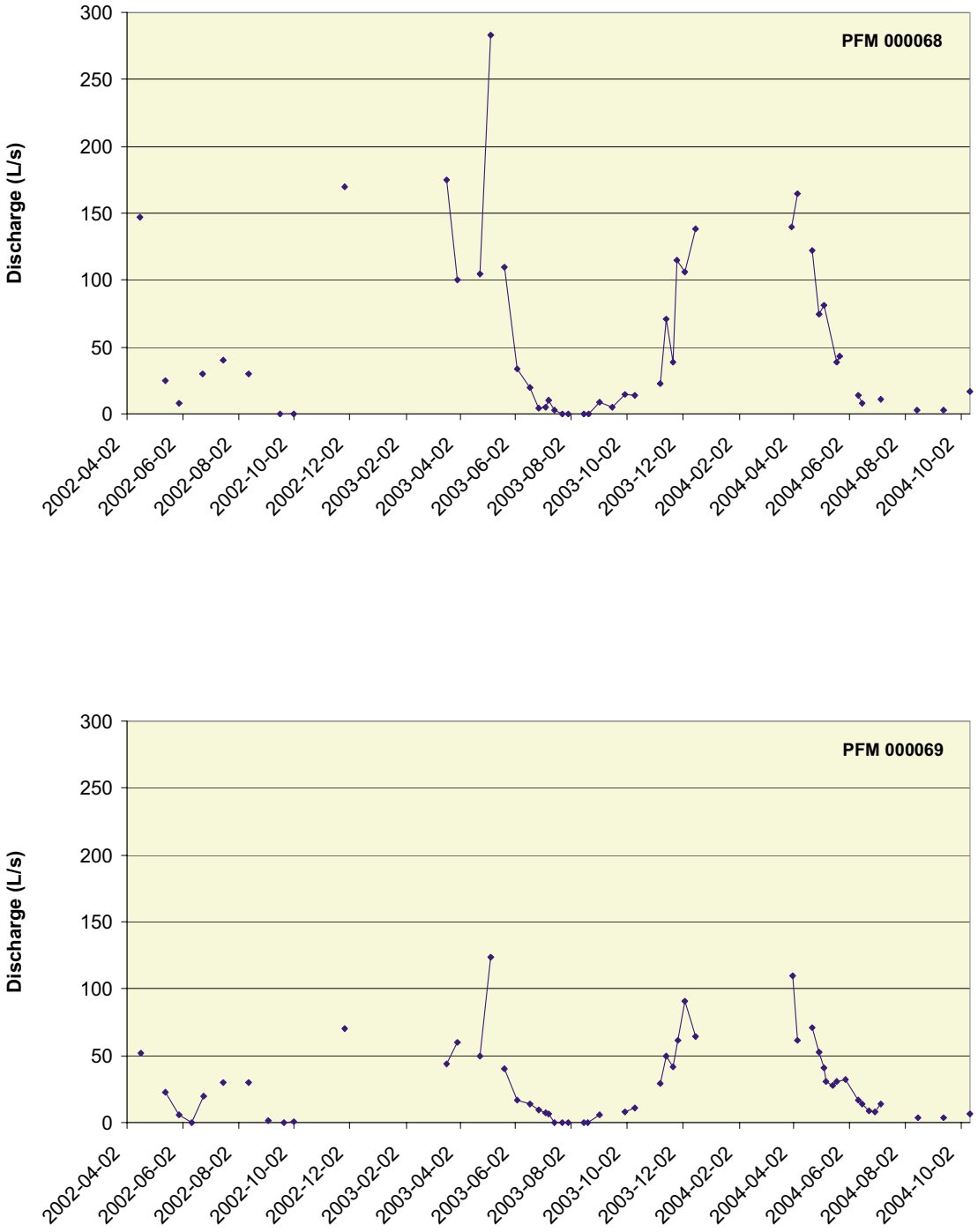

Figure 3-24. *Results of manual discharge measurements at locations PFM000068–69.*

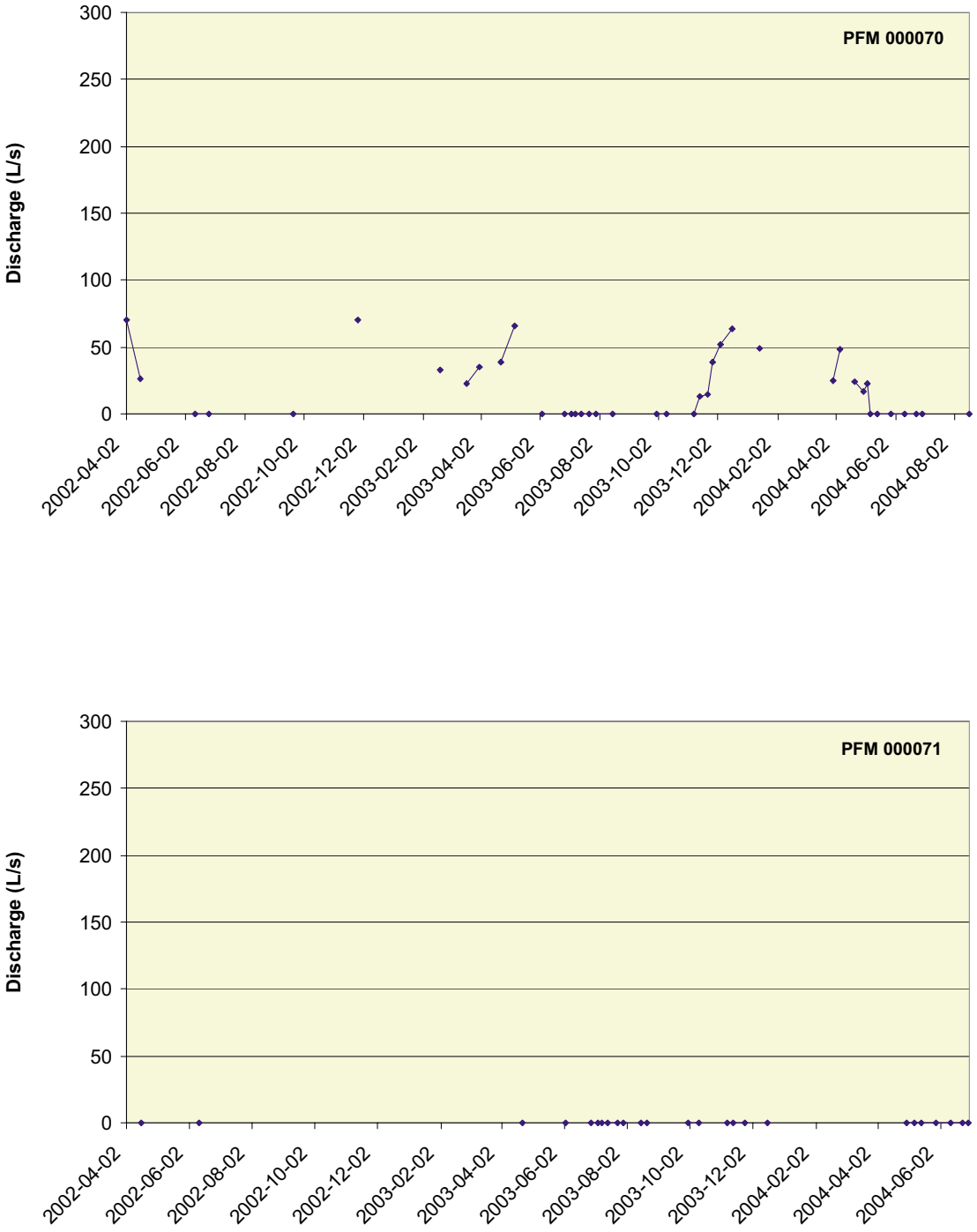

Figure 3-25. *Results of manual discharge measurements at locations PFM000070–71.*

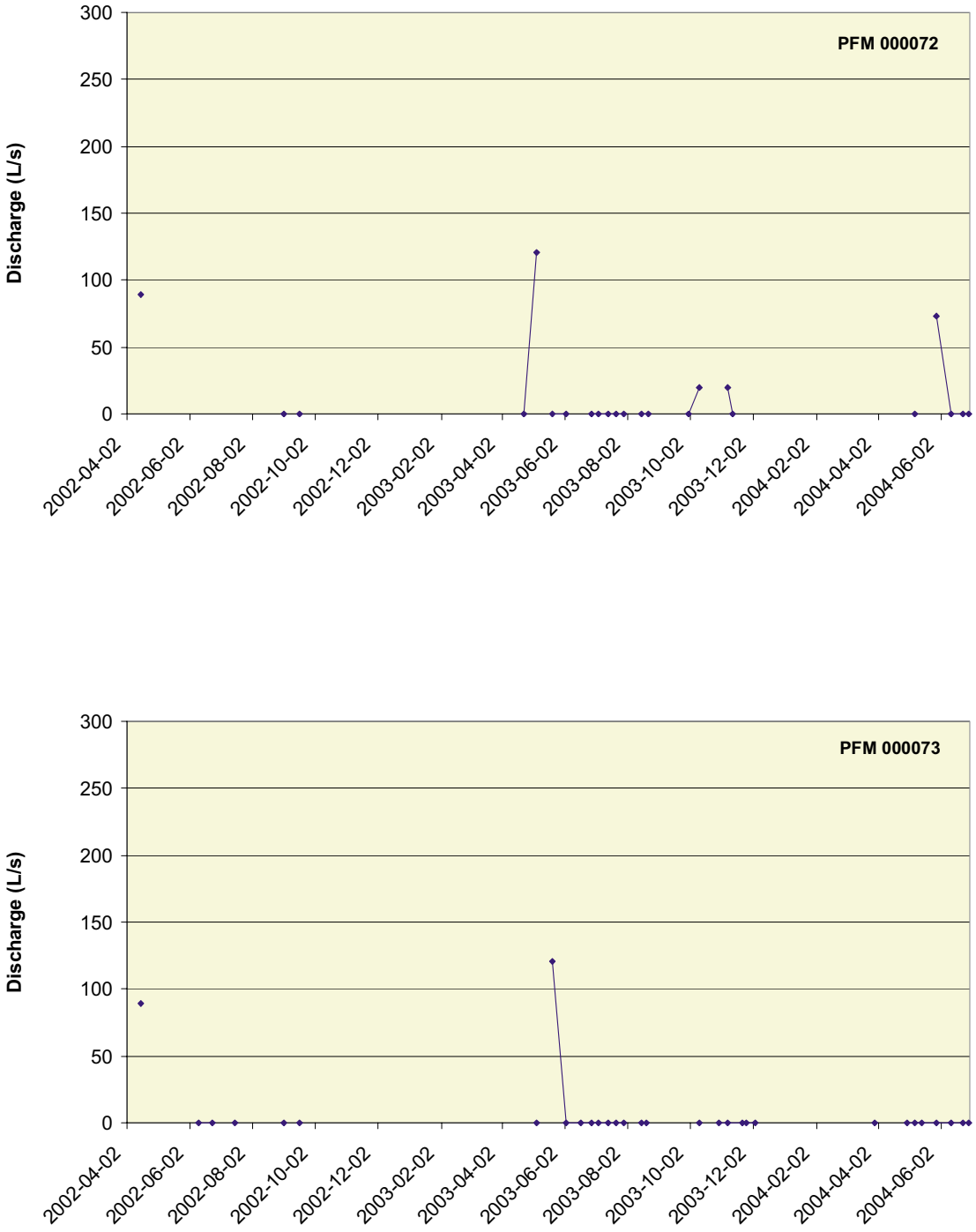

Figure 3-26. *Results of manual discharge measurements at locations PFM000072–73.*

The largest recorded discharge during the period March 2002 – October 2004 was 283 $L \cdot s^{-1}$ at PFM000068 (May 5, 2003). This discharge corresponds to a specific discharge of approximately 50 $L \cdot s^{-1} \cdot km^{-2}$. It should be emphasised that the measurements are sparse, and that even larger discharges likely would have been observed if more measurements had been performed. Several measurements were cancelled during low-flow periods and due to the presence of ice at the measurement locations.

The discharge measurements at PFM000066 and PFM000068–70 are considered to provide reasonable estimates of the site-specific discharge conditions. However, at PFM000067 it has been observed that a significant by-pass flow occurs when the discharge is large. The largest discharge measured at PFM000067 is 145 $L \cdot s^{-1}$ (January and April, 2004), but due to the by-pass flow the discharge measurements underestimate the actual discharge. Moreover, with few exceptions, zero discharge was recorded at PFM000071–73.

3.3 Hydrogeological data

3.3.1 Groundwater monitoring wells and abstraction wells

At the time of the data freeze F1.2, a total of 54 groundwater monitoring wells had been installed in the QD /Johansson, 2003; Werner and Lundholm, 2004a/. Of these wells, 12 were located in the vicinity of the core-drill sites. Nine wells were placed in till below the bottom of some of the lakes or below the Baltic Sea. Furthermore, two abstraction wells were installed to enable pumping tests /Werner et al. 2004; Werner and Lundholm, 2004b/.

After installation, during which sampling of the QD was performed, the groundwater monitoring wells were used for determination of the hydraulic properties of the QD and the QD/rock interface. Furthermore, the observation wells are used for continuous groundwater level measurements and for water sampling. The geological data collected during the drillings in the QD, and the analyses of the samples that were taken, have been used in the geological modelling of the QD, see /Lindborg (ed), 2005/ and Chapter 4–5 of the present report.

For determination of hydraulic properties and water sampling, also six BAT-type filter tips were installed /Johansson, 2004/. The BAT-type filter tips enable “undisturbed” groundwater sampling, and are particularly useful for sampling materials characterised by low hydraulic conductivities.

The locations of the groundwater level monitoring wells and abstraction wells (all referred to as just “monitoring wells”), and the BAT-type filter tips are shown in Figure 3-27. In many cases, the measurement locations are “clustered” in the vicinity of objects of particular hydrological interest (e.g. the lakes and areas of thick QD). This reflects a strategy for the well installations that aims at providing a basis for studying the hydrological/hydrogeological interactions between, e.g. groundwater and surface water, and shallow and deeper groundwater. A list of the wells and the filter tips, including also the surface water gauges, is given in Appendix 1.

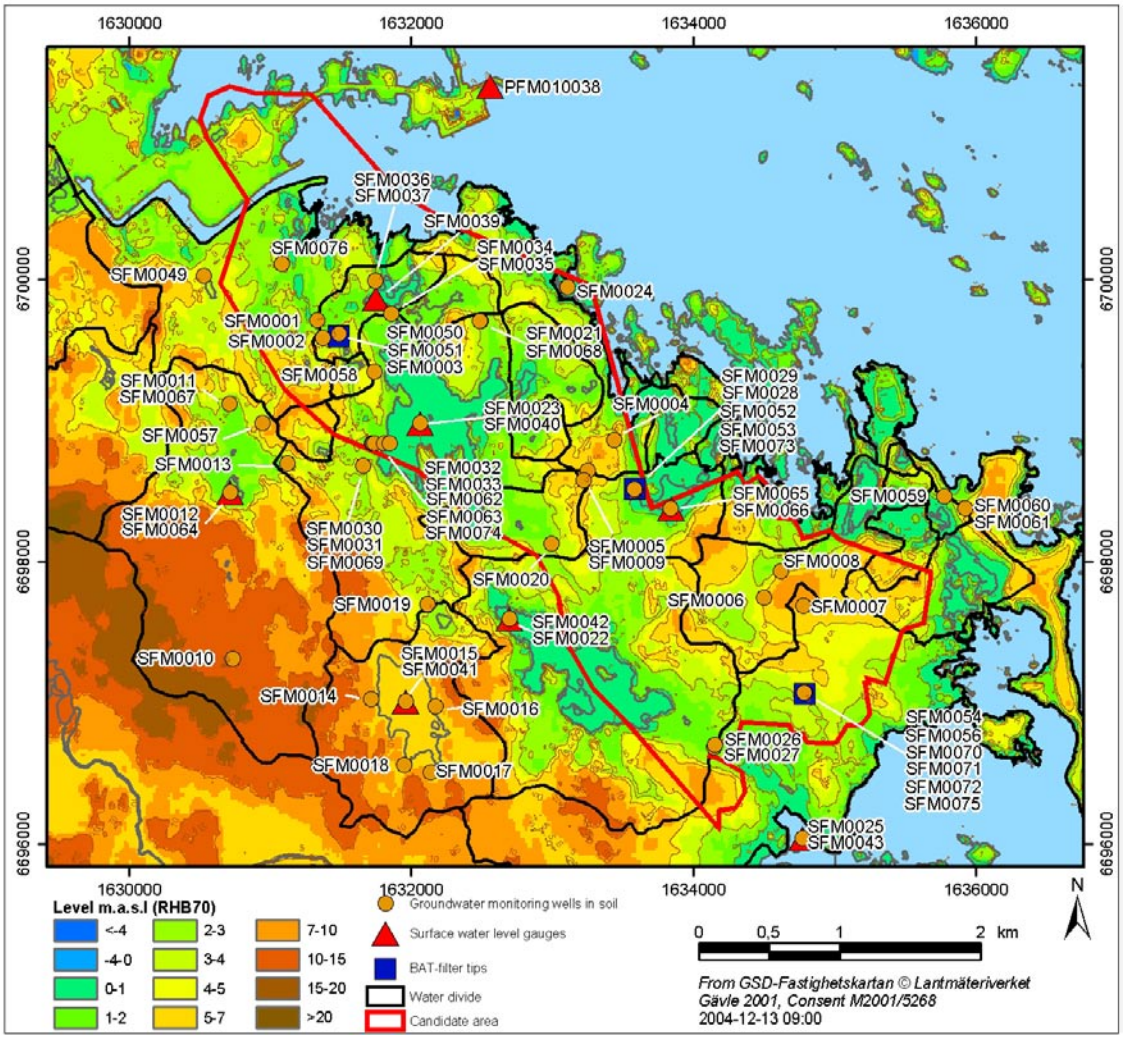

Figure 3-27. *Locations of groundwater monitoring and abstraction wells (shown as one group, referred to "monitoring wells"), BAT-type filter tips, and surface water level gauges.*

3.3.2 Hydraulic properties of Quaternary deposits

The hydraulic properties of the Quaternary deposits (QD) and/or the QD/rock interface in the Forsmark area were described in SDM F1.1, based on hydraulic conductivities from 36 slug tests. For model version F1.2, an additional 12 slug tests /Werner, 2004/ and two pumping tests /Werner and Lundholm, 2004a; Werner et al. 2004/ have been performed to determine hydraulic conductivity and storativity values.

The data from the slug tests were evaluated using three separate methods: the Cooper et al. method /Cooper et al. 1967/, the Hvorslev method, and the Bouwer & Rice method /Butler, 1998/. For most wells, a good to acceptable fit to the type curves of the Cooper et al. method was obtained when applying a fixed α (corresponding to a storativity (S) of 10^{-5}). Figure 3-28 shows the resulting values of the hydraulic conductivity. The data presented are all from the evaluation by the Cooper et al. method with a fixed α.

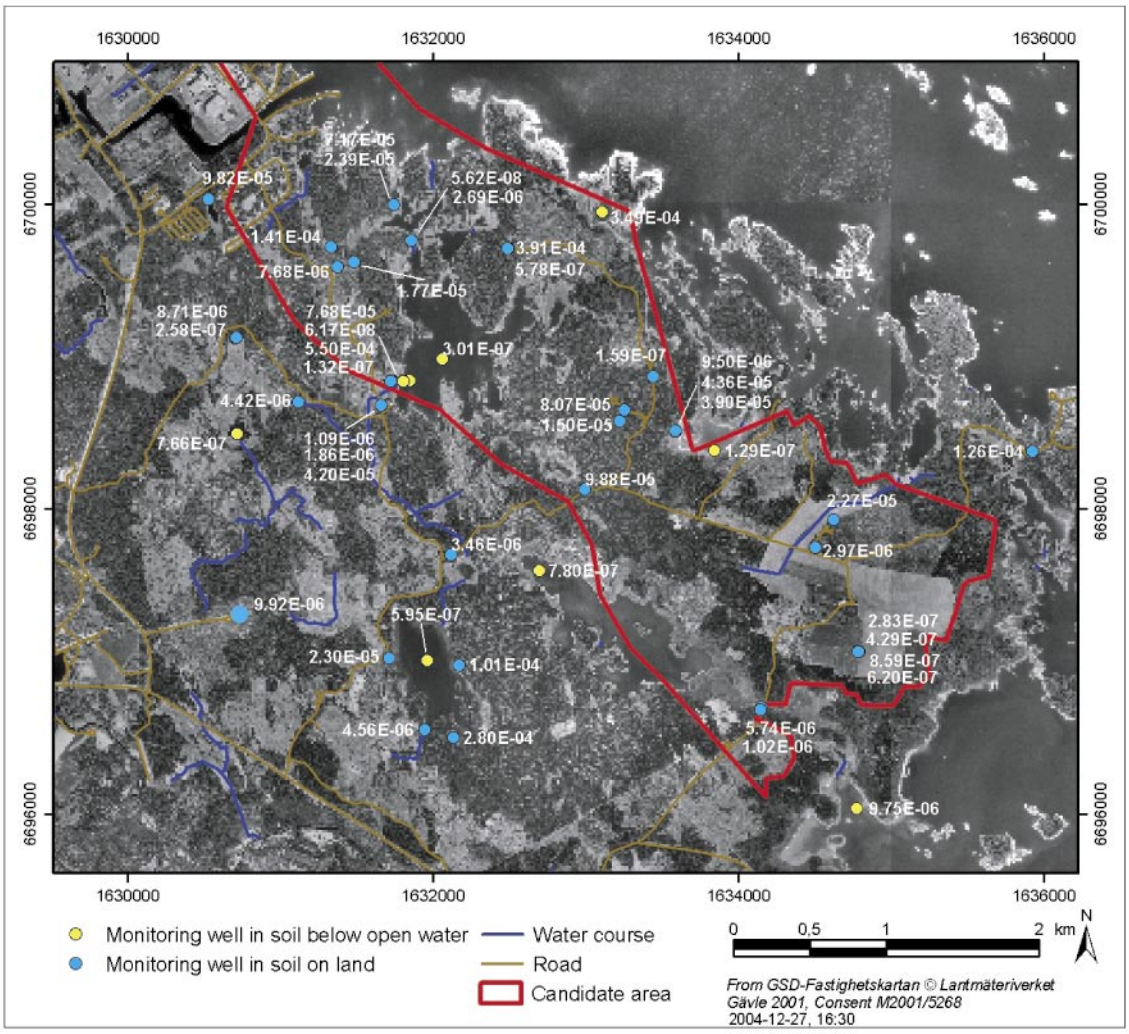

Figure 3-28. *Hydraulic conductivities obtained from slug tests evaluated by the Cooper et al. method /Cooper et al. 1967/.*

Figure 3-29 shows a histogram of the hydraulic conductivities. The histogram shows that most hydraulic conductivity values are in the range 10^{-7}–10^{-4} m·s^{-1}; the measured hydraulic conductivities vary between $5.6 \cdot 10^{-8}$ and $7.0 \cdot 10^{-4}$ m·s^{-1}. The geometric mean is $6.0 \cdot 10^{-6}$ m·s^{-1} (arithmetic mean $6.0 \cdot 10^{-5}$ m·s^{-1}, median $6.7 \cdot 0^{-6}$ m·s^{-1}) and the standard deviation of log K (base: 10) is 1.07, which corresponds to 2.46 if the natural logarithm is used. This can be regarded as a relatively high degree of spatial variability, which probably reflects the fact that the dataset includes K-values associated with different materials (primarily different types of till). Assuming a log-normal distribution, the 95% confidence interval for the mean is $3.0 \cdot 10^{-6}$–$1.2 \cdot 10^{-5}$ m·s^{-1}, and the 95% confidence interval for a new observation is $4.9 \cdot 10^{-8}$–$7.4 \cdot 10^{-4}$ m·s^{-1}.

The screens of the tested wells are placed in till, at different depths below the ground surface; in most cases, the screens are placed at or across the interface between the QD and the bedrock. In some wells, the screen is placed in QD only (i.e. not at the QD/bedrock interface). As shown in Figure 3-30 below, this allows a comparison of the evaluated hydraulic conductivity values as a function of the screen depth, also taking into consideration whether the screen is placed at the QD/bedrock interface.

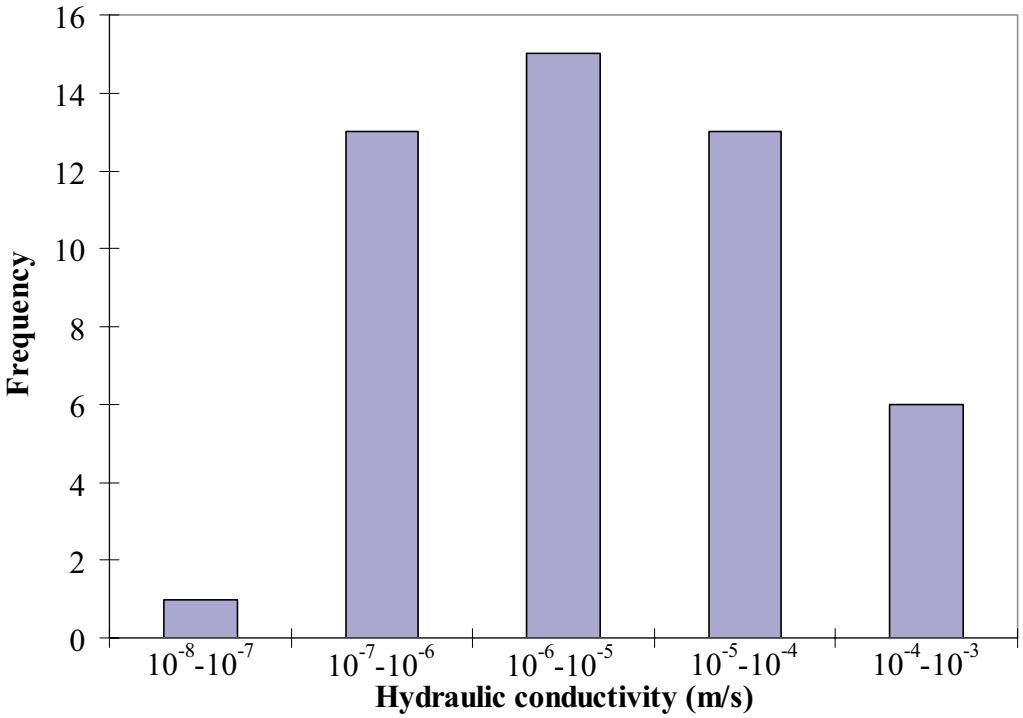

Figure 3-29. *Histogram for the hydraulic conductivities of the QD, obtained from slug tests in 48 groundwater monitoring wells /Werner and Johansson, 2003; Werner, 2004/.*

Even though there is a large spread in the data, the linear fits in Figure 3-30 agree with the conceptual model of a decreasing hydraulic conductivity with depth in the QD; the conductivity decreases by approximately half an order of magnitude over a depth interval of 8 m for wells with the screen in QD only. The separation of the data fits for the two different "classes" of wells indicates that the hydraulic conductivity on the average is larger at the QD/bedrock interface (geometric mean: $1.3 \cdot 10^{-5}$ m·s^{-1}), than in the QD (geometric mean: $1.2 \cdot 10^{-6}$ m·s^{-1}); including also wells installed below open water, the geometric mean for the wells in QD only is $1.3 \cdot 10^{-6}$ m·s^{-1}.

Another issue of interest is the potential influence of the well-installation technique on the estimations of hydraulic properties that are obtained from the hydraulic tests. In order to investigate this issue, the hydraulic conductivities obtained from slug tests in groundwater monitoring wells installed on land (air rotary-casing driver) are compared to the corresponding values obtained from wells installed below open water (hammer drilled). As mentioned above, an analysis of the conductivity data shows that the geometric mean value from slug tests in wells installed on land, not including those with their screens at or across the QD/bedrock interface, is $1.2 \cdot 10^{-6}$ m·s^{-1}, whereas the corresponding value for slug tests in wells installed below open water is $4.6 \cdot 10^{-6}$ m·s^{-1}; no well below open water is installed at the QD/bedrock interface. (The geometric mean for all wells on land is $8.0 \cdot 10^{-6}$ m·s^{-1}.) Hence, the well installation technique is not considered to have a large influence on the evaluated hydraulic parameters.

Grain-size analyses were performed on a large number of QD samples. The resulting particle-size distribution curves (PSD) were used to estimate the hydraulic conductivity using three different methods: the equations presented by Hazen and Gustafson, respectively /Andersson et al. 1984/, and the Fair-Hatch equation /Freeze and Cherry, 1979/. The results obtained with the Fair-Hatch equation are summarised in Table 3-8.

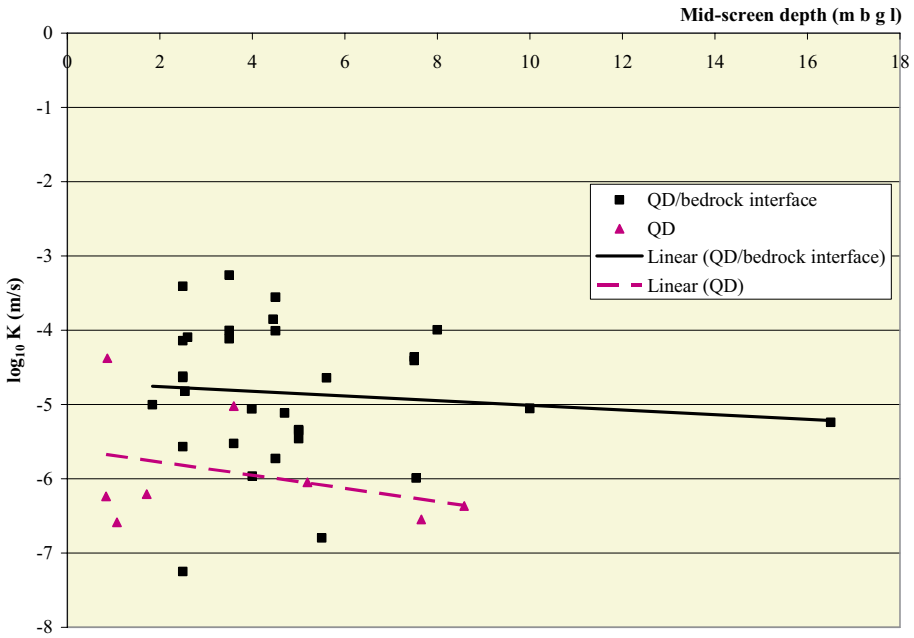

Figure 3-30. *Hydraulic conductivities (logarithmic scale) of the QD obtained from slug tests in wells installed on land (i.e. wells installed below open water are not included). The data are plotted as a function of depth (m b g l.; metres below ground level). Squares are data for wells with the screen at the QD/bedrock interface, and triangles are data for wells with the screen in QD only. The lines are linear fits to the measured data.*

Table 3-8. Statistical analysis of hydraulic conductivity K ($m \cdot s^{-1}$) obtained from evaluation of particle-size distribution curves by the Fair-Hatch equation. The available number of K-values for each QD type is shown within parentheses.

	Gravelly till, sandy till (25)	Clayey sandy-silty till, clayey sandy till, clayey gravelly till (28)	Sand, sandy gravel (2)	Till clay (3)	Silty sand (1)
Arithmetic mean of log-K	–5.91	–6.49	–4.63	–6.74	–6.05
Standard deviation of log-K	0.45	0.28	0.004	0.19	–
Geometric mean of K	$1.23 \cdot 10^{-6}$	$3.23 \cdot 10^{-7}$	$2.35 \cdot 10^{-5}$	$1.81 \cdot 10^{-7}$	$8.97 \cdot 10^{-7}$
Arithmetic mean of K	$2.14 \cdot 10^{-6}$	$4.01 \cdot 10^{-7}$	$2.35 \cdot 10^{-5}$	$1.94 \cdot 10^{-7}$	$8.97 \cdot 10^{-7}$
Median of K	$1.20 \cdot 10^{-6}$	$3.10 \cdot 10^{-7}$	$2.35 \cdot 10^{-5}$	$1.42 \cdot 10^{-7}$	$8.97 \cdot 10^{-7}$
95% confidence interval for K	$8.17 \cdot 10^{-7}$– $1.84 \cdot 10^{-6}$	$2.55 \cdot 10^{-7}$– $4.08 \cdot 10^{-7}$	–	–	–
95% confidence interval for a new measurement	$1.62 \cdot 10^{-7}$– $9.30 \cdot 10^{-6}$	$9.33 \cdot 10^{-8}$– $1.12 \cdot 10^{-6}$	–	–	–

The hydraulic conductivity of the till, as obtained from the PSDs, is on the order of 10^{-6} m·s^{-1} for the gravelly-sandy till types, and on the order of 10^{-7} m·s^{-1} for the clayey till types. Figure 3-31 shows a comparison between hydraulic conductivity values obtained from slug tests and those obtained from PSDs. The analysis includes only the PSDs that are sampled within the same depth interval as where each well screen is located; in some cases, there is only a small overlap between the sampling interval and the well screen depths for the data shown in the figure.

For those wells where the screen is located across the QD/bedrock interface, the figure shows that the hydraulic conductivities obtained from slug tests generally are higher compared to the corresponding values obtained from the PSD. The deviations are larger for those wells where the QD consists of clayey till types. On the other hand, the correlation between the two data sets is stronger for wells where the screen is located in QD only (i.e. not at or across the QD/bedrock interface).

Considering the hydraulic conductivities obtained from the slug tests where the grain size distribution is known from the QD sampling, the results show that there is no correlation between grain size distribution and hydraulic conductivity for wells where the screen is located across the QD/bedrock interface. The geometric mean of the conductivity values for slug tests in gravelly-sandy till types is $1.4 \cdot 10^{-5}$ m·s^{-1} (excluding SFM0035, which is considered an outlier with a very low conductivity), and $1.9 \cdot 10^{-5}$ m·s^{-1} for the clayey till types. Considering wells in QD only, the wells from which PSDs are available at the screen depth are too few to allow a statistical analysis.

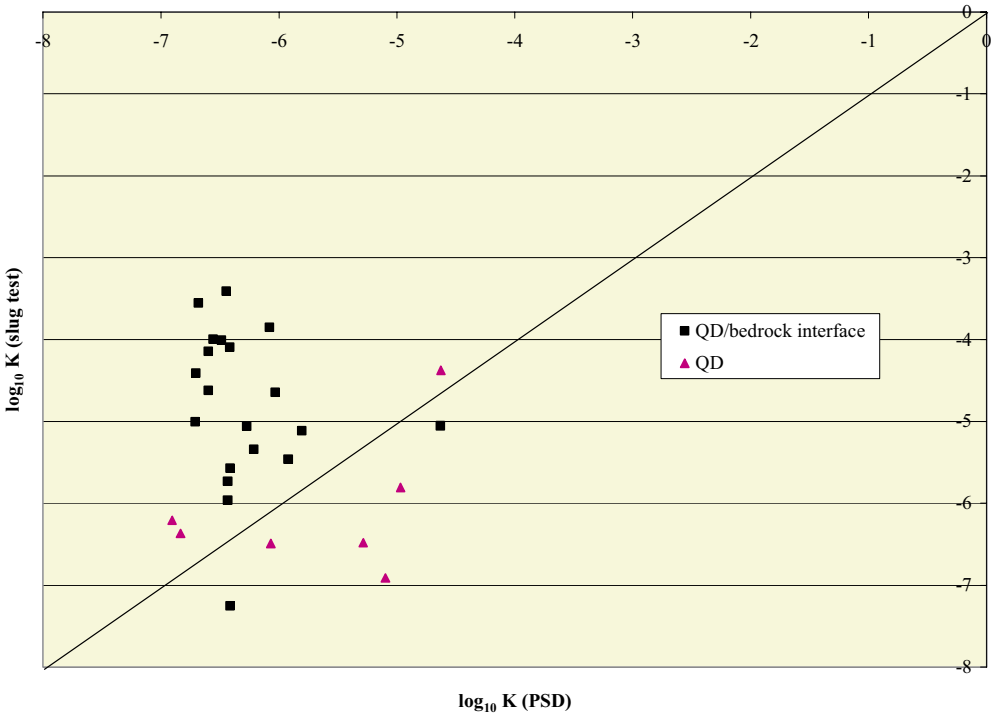

Figure 3-31. *Hydraulic conductivities (logarithmic scale) of the QD obtained from slug tests plotted versus corresponding values obtained from particle-size distribution curves (PSD). Squares are data for wells with screens at the QD/bedrock interface, and triangles are data for wells with screens in QD only. The solid line represents a perfect correlation between the two datasets.*

Pumping tests were performed in wells SFM0061 /Werner et al. 2004/ and SFM0074 /Werner and Lundholm, 2004b/. The hydraulic conductivity values evaluated from these pumping tests are presented in Table 3-9 below.

It should be noted that the wells SFM0059–61 are located in a glaciofluvial deposit, the Börstilåsen esker, and that the material consists of sand, gravel and stones. The well SFM0074 is installed across the QD/bedrock interface, whereas the observation wells for that pumping test are installed in the QD (SFM0031–32 on land and SFM0062–63 below open water). The evaluation of the pumping test in SFM0074 also included an analysis of the impact of hydraulic boundaries and lake-water leakage. The results showed that there is a limited hydraulic contact (potentially limited by low-permeable lake sediments) between Lake Bolundsfjärden and the pumped aquifer.

The hydraulic conductivities evaluated from the pumping tests, which represent larger aquifer volumes than the slug tests, are approximately 2–3 orders of magnitude larger than the corresponding values from the slug tests for wells SFM0031 and SFM0062–63, whereas the values are approximately equal for well SFM0032. Thus, the evidence of a scale effect on the hydraulic conductivity is not fully consistent.

The hydraulic conductivity has also been measured in BAT filter tips at three locations /Johansson, 2004/. The results of these measurements are shown in Table 3-10. The hydraulic conductivities obtained from the filter-tip tests concern a fine-grained till material, and can be expected to be low. However, the K-values from the BAT filter are also much lower than those from slug tests in similar geological materials. The reasons for this difference, which could be related to, e.g. scale effects or methodological differences, have not been investigated in detail.

Table 3-9. Evaluated hydraulic conductivity from pumping tests /Werner et al. 2004; Werner and Lundholm, 2004a/.

Pumping well	Observation well	Hydraulic conductivity ($m \cdot s^{-1}$)
SFM0061[1]		$2.06 \cdot 10^{-4}$
	SFM0060	$1.26 \cdot 10^{-4}$
SFM0074		$5.61 \cdot 10^{-5}$
	SFM0031	$5.61 \cdot 10^{-4}$
	SFM0032	$5.57 \cdot 10^{-5}$
	SFM0062	$5.53 \cdot 10^{-5}$
	SFM0063	$3.71 \cdot 10^{-4}$

[1] SFM0059 was also used as an observation well in the pumping test, but the drawdown data from that well were insufficient for an evaluation of the hydraulic properties.

Table 3-10. Measurements of hydraulic conductivity in BAT filter tips /Johansson, 2004/.

Station	Hydraulic conductivity ($m \cdot s^{-1}$)	Type of test
SFM0050	$(4.0–4.3) \cdot 10^{-8}$	Inflow test
SFM0052	$4.0 \cdot 10^{-9}$	Inflow test
SFM0054	$(8.5–8.8) \cdot 10^{-9}$	Outflow test

3.3.3 Groundwater levels

Data representativity

Figure 3-32 shows a comparison of the frequency distribution of ground elevations for the groundwater monitoring wells in QD to the overall topography of the study area (the area within the delineated catchments in Figure 3-13 plus areas with discharge to the Baltic Sea). The distribution for the groundwater wells was based on ground elevations from 29 of the 56 wells in the SKB database and did not include below water wells (SFM0012, 15, 22, 23, 24, 25, 62, 63, 65), or wells with no reported data (SFM0007, 27, 29, 31, 32, 35, 37, 60, 67–76).

The distribution of topographic elevations was derived from a GIS analysis of digital elevation maps. The comparison suggests that the groundwater monitoring wells generally over-represent lower ground elevations. There is only one SKB well with a ground elevation above 7 m (SFM0010), whereas 36% of the study area has ground elevations greater than 7 m.

The local topography around the groundwater monitoring wells can also be assumed to influence the depth and variations of the groundwater level. Relatively deep groundwater levels and large variations can be expected in elevated areas constituting typical groundwater recharge areas, and shallow groundwater levels with small variations in low-lying areas constituting typical groundwater discharge areas.

To investigate whether correlations between terrain characteristics and the depth to the groundwater level could be identified, a number of geomorphometrical (slope, convexity and curvature) and hydrological (flow accumulation and topographical wetness index) parameters were calculated for the areas around groundwater wells. These parameters were then analysed statistically together with groundwater level measurements. In addition, the representativity of the locations of the existing groundwater wells, in terms of terrain characteristics, was checked based on the same geomorphological and hydrological parameters.

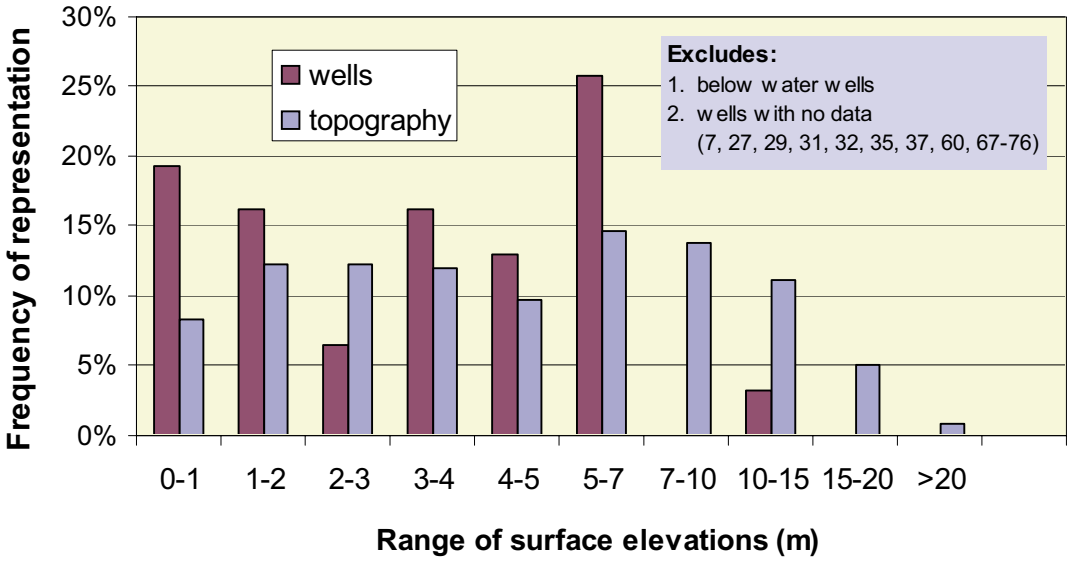

Figure 3-32. *Frequency distribution of ground elevations of groundwater monitoring wells in QD compared to the study area topography.*

The regional DEM and GIS analysis tools were used in the study, and a subset of the existing groundwater wells was selected for the analysis. When wells were located in the immediate vicinity of each other only one of the wells were used. Furthermore, wells below open water and wells with very short time series were not included in the study. Details on the methodology and results of the study are given in Appendix 4.

The best correlation with the geomorphometrical parameters was obtained for the average depth of the groundwater level. A stepwise multiple linear regression analysis resulted in a correlation coefficient (R^2) of 0.67 for a linear equation with mean and maximum curvature and slope as independent variables. For the curvatures, the best results were obtained if an area of 110 × 110 m was used in the calculations. The best equation for the amplitudes gave a considerably lower R^2 of 0.43.

The comparison of the geomorphometrical and hydrological parameters for the groundwater well sites and the randomly placed points gave very similar values for the curvatures, but somewhat wetter environments and also somewhat flatter slopes for the well sites. The geomorphometrical features ridges and channels were also somewhat underrepresented and overrepresented, respectively, for the well sites. One reason for the bias in the locations of the wells to locally low-lying areas is that the drillings used for installation of monitoring wells were made in order to also provide information on stratigraphy and depth of the QD at locations where QD of relatively large thickness could be expected.

Time series

Figure 3-33 shows a plot of daily average groundwater elevations from 36 wells in the study area, including wells below surface waters. The reported groundwater elevations range from about –1 to +13 m (RHB 70), with most recordings in the interval from sea level to +6 m. SFM0010 shows significantly higher groundwater levels than the other observation wells. This well is located in the high-altitude area west of Lake Eckarfjärden; it has the highest ground elevation among all observation wells.

Figure 3-34 shows a plot of the same data for 31 of these wells (excluding wells in surface waters), but represented as groundwater depth below surface. The majority of the wells (26 of 31) form a tight-packed cluster with reported groundwater depths in the range of

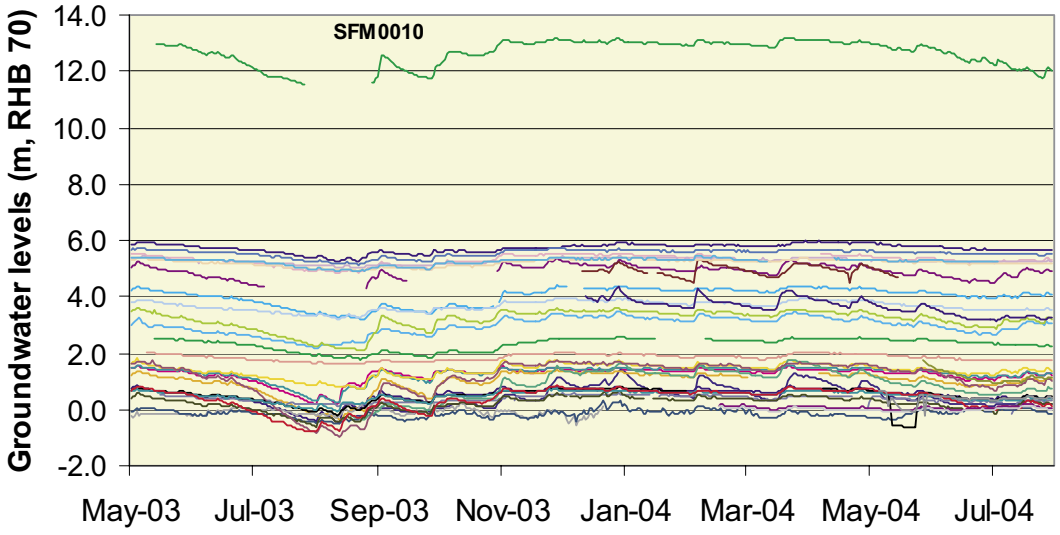

Figure 3-33. *Daily average groundwater elevations for groundwater monitoring wells in QD.*

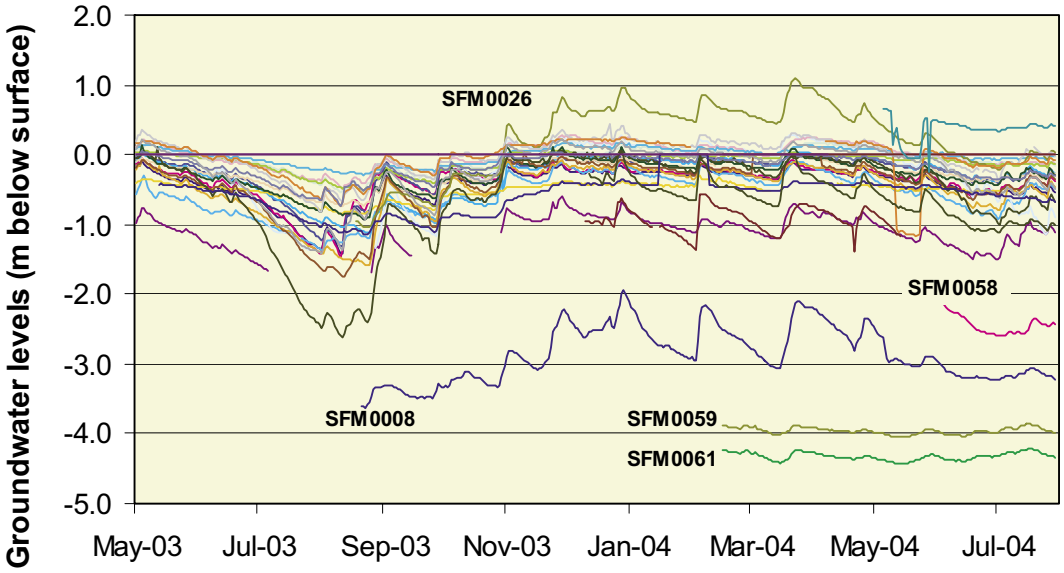

Figure 3-34. *Daily average depth below ground surface for groundwater monitoring wells in QD, excluding wells with screens below water.*

+0.2 to –1.25 m relative to the ground surface. The wells typically show a strong uniformity in their responses to the dry conditions of July and August 2003. Similarly, the wells typically show very similar groundwater level responses to recharge events following major precipitation and snow melt events.

Amplitudes

Figure 3-35 shows a summary of the range of water level amplitudes in all reported data, i.e. data from surface water level gauges and groundwater monitoring wells in QD. Note that, due the different lengths of the available time series, some of the presented values represent an amplitude range from only a limited period of available data, whereas others are representative of complete or near-complete time series for the May 1, 2003 to July 31, 2004 period. For example, the reported response amplitudes for SFM0058, 62, 64, 65 and 66 were based on less than 100 reported daily data values, whereas the SFM0006, 42, 59 and 61 time series had between 100 and 200 values. Response amplitudes for all other stations were based on more than 200 data days, with the majority being greater than 390 (maximum possible = 457 days).

As would be expected, the range of amplitudes of lake water elevations was typically smaller than the range of amplitudes of the groundwater and sea (SFM0038/PFM010038 and SFM0043) levels. Among the inland lakes, Lake Lillfjärden (SFM0066) reported the highest amplitude (in spite of its short time series) and Lake Fiskarfjärden the lowest (SFM0042). For groundwater wells with more than 200 data days, amplitudes ranged between 0.4 to 2.9 m. The highest amplitude was reported from SFM0030, located just west of Lake Bolundsfjärden, followed by SFM0026 (2.3 m).

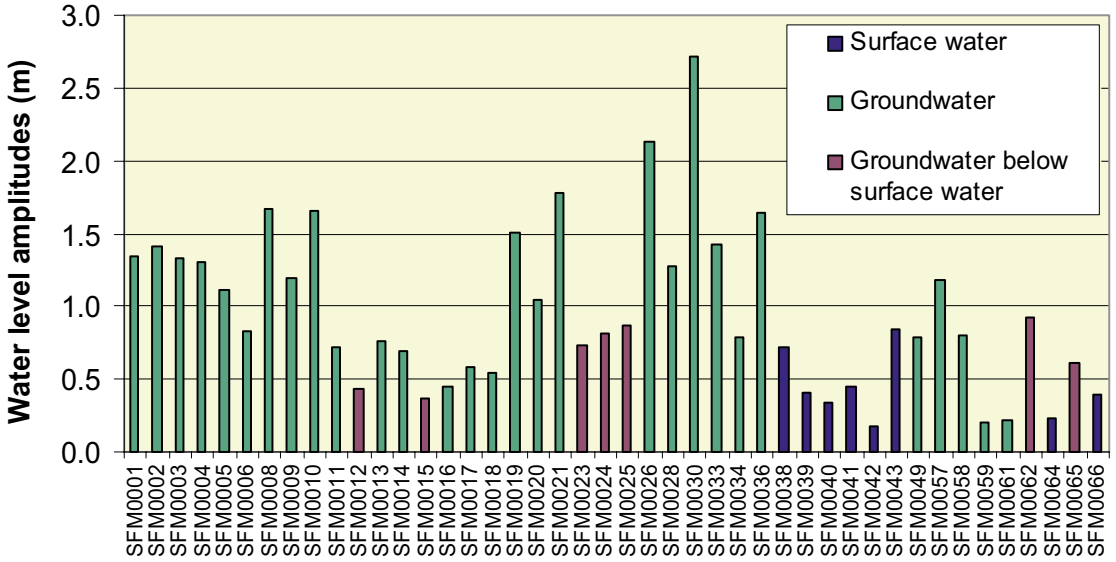

Figure 3-35. *Water level amplitudes for the surface water level gauges and the groundwater monitoring wells in QD.*

Figure 3-36 shows a duration curve of the average groundwater depth below ground surface in all wells placed in till for the period May 1, 2003 – July 31, 2004 (all available daily mean levels have been averaged for each day). Note that all time series have been used, although not all have data for the whole period. The very shallow groundwater levels in the area are clearly illustrated with the average groundwater level within 0.5 m below the ground for approximately 50% of the time. However, a reservation should be made for a probable over-representation of local topographical lows in the locations of the monitoring wells.

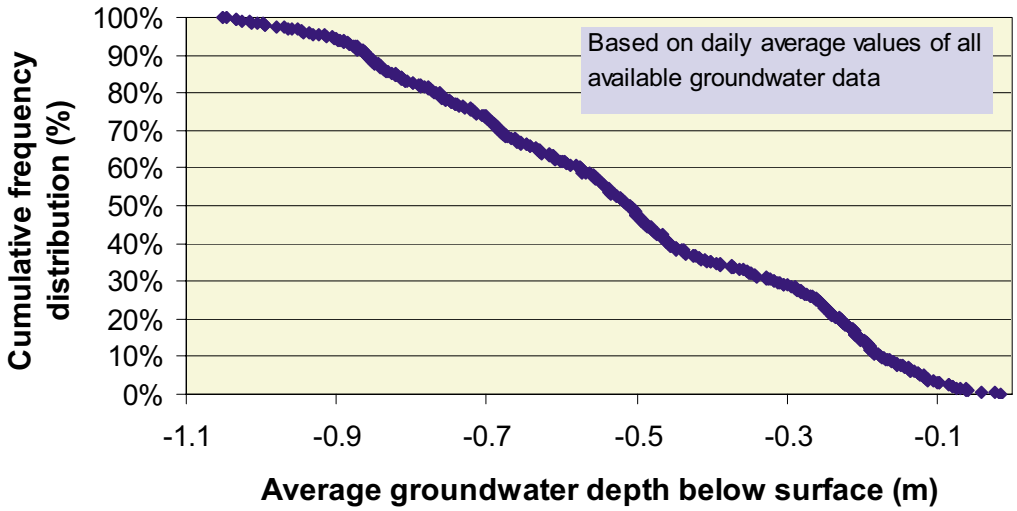

Figure 3-36. *Duration curve for the average depth below ground of the groundwater levels in all wells placed in till.*

Correlation studies

Correlation between groundwater monitoring well time series

There is a very strong correlation between the groundwater level time series from most of the groundwater monitoring wells. In the analysis, only wells with > 200 days time series have been considered. Most R^2-values are well above 0.8, and many are above 0.95, see Appendix 2 for a complete correlation matrix.

The two wells below water directly influenced by the sea water level (SFM0024 and SFM0025) are exceptions from the otherwise strong correlations between groundwater level time series. Furthermore, the two wells on the Börstil Esker, for which only shorter time series were available, also showed significantly lower R^2-values than the other wells. Also these wells can be assumed to be influenced by the sea water level.

Correlation to meteorological conditions and sea water level

To provide a deeper insight into the observed groundwater fluctuations, the covariance of the groundwater level time series data and the cumulative difference between precipitation (P) and potential evapotranspiration (PET) and the covariance of groundwater and sea level data were studied. For the precipitation, a snow routine similar to the one in SMHI's HBV model /Lindström et al. 1996/ was used to correct the effective precipitation for snow accumulation and melting during winter months.

Figure 3-37 shows groundwater depths below ground surface (the same data as in Figure 3-34), plotted together with the sea water level and the cumulative difference between precipitation and potential evapotranspiration. Visually, little correlation is evident between sea level and groundwater level variations in most time series. On the other hand,

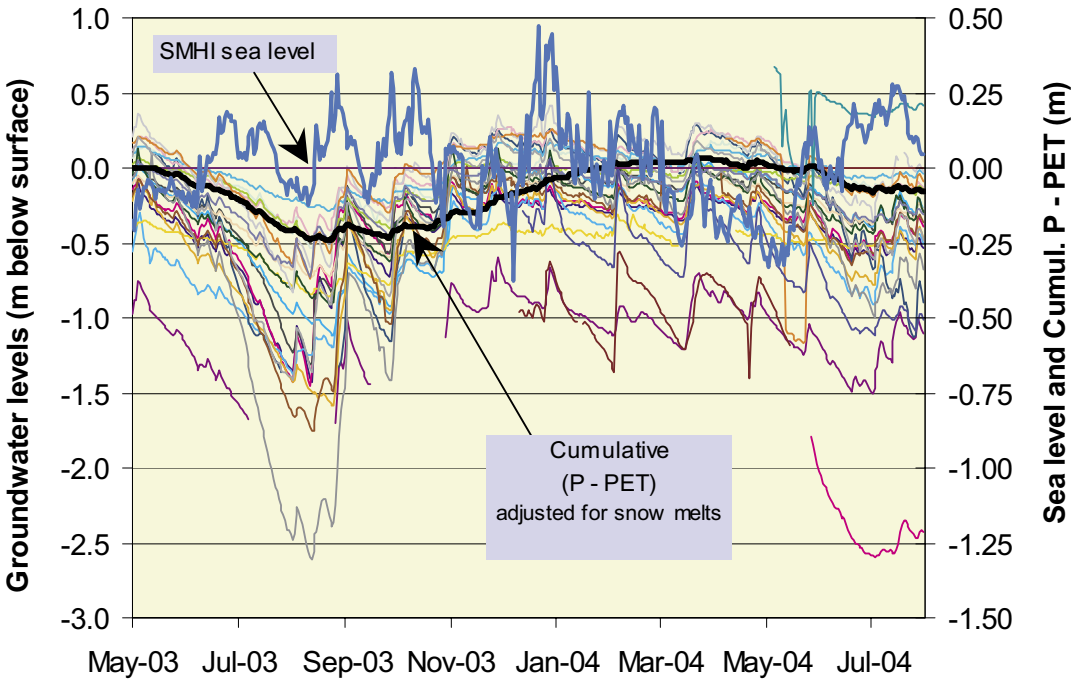

Figure 3-37. *Daily average groundwater depth below ground surface plotted together with daily average sea level and the cumulative difference between daily precipitation (adjusted with a snow routine) and potential evapotranspiration.*

the cyclic nature of the cumulative P-PET difference bears a strong resemblance to the overall cyclic variation in many groundwater level observations, although the cycles are slightly out of phase.

In order to improve the understanding of the relationships between precipitation, evapotranspiration and the observed groundwater levels, a hydrological model was calibrated on a well-by-well basis to best simulate the well time series. The model structure that was selected for this study was virtually identical to the PULS model /Carlsson et al. 1987/. The modelling is described in detail in Appendix 3.

Overall, the calibration of this relatively simple model, based on a PULS-like structure, provided consistently excellent simulations of time series of groundwater levels from the 22 wells that were considered. Correlation coefficients between measured and calculated levels ranged from a minimum of $R^2 = 0.87$ to a maximum of $R^2 = 0.98$. Examples from three wells are shown in Figure 3-38. These strong correlations suggest that the near-surface hydrogeology of the study area can be well explained as hydrogeological responses to precipitation events and evapotranspiration cycles.

However, the results of the PULS-based model analysis also indicated that there was a wide range of model parameters that provided accurate fits to each well time series. Therefore, neither a unique set of calibrated model parameters (such as estimated values of the field capacity) nor a unique set of estimated model output (e.g. actual ET and runoff rates) could be obtained at this stage. Presently, the only available data that can be used for model calibration are the groundwater level time series.

Clearly, the selected model is over-determined, i.e. contains too many parameters to uniquely calibrate to the available time series data. However, it seems highly likely that this problem could be resolved with the addition of more time series data, and with a complementary data set such as gauged stream discharge. Data of both these categories should be available after the next data freeze in July 2005.

Figure 3-39 shows the correlation coefficients (R^2) that were calculated for sea level and P-PET profiles with groundwater data for wells with time series longer than 200 data days. Only two groundwater monitoring wells showed significant correlations with the SMHI sea level data. These two wells were located below open water directly influenced by the sea level (SFM0024 and 25). On the other hand, most other wells showed some correlation with the cumulative P-PET curve, with 13 of the 36 wells demonstrating correlations greater than $R^2 = 0.50$.

The general pattern was that the groundwater time series at a particular location either showed correlation with sea level or with the cumulative P-PET curve, but typically not with both. SFM0025, located near the sea level gauge SFM0043 in the easternmost part of the area, was the only well to show some degree of correlation to both parameters. Only two wells (SFM0005 and 33) showed no significant correlation to either parameter.

Figure 3-40 shows a close-up of the December 2003 period. In the data presented, precipitation has been adjusted for snow accumulation and melting using a snow routine. There is little or no evidence of a response in groundwater levels to the 0.85 m increase in sea level, at least not in the form of a continuous increase similar to the one displayed by the sea level.

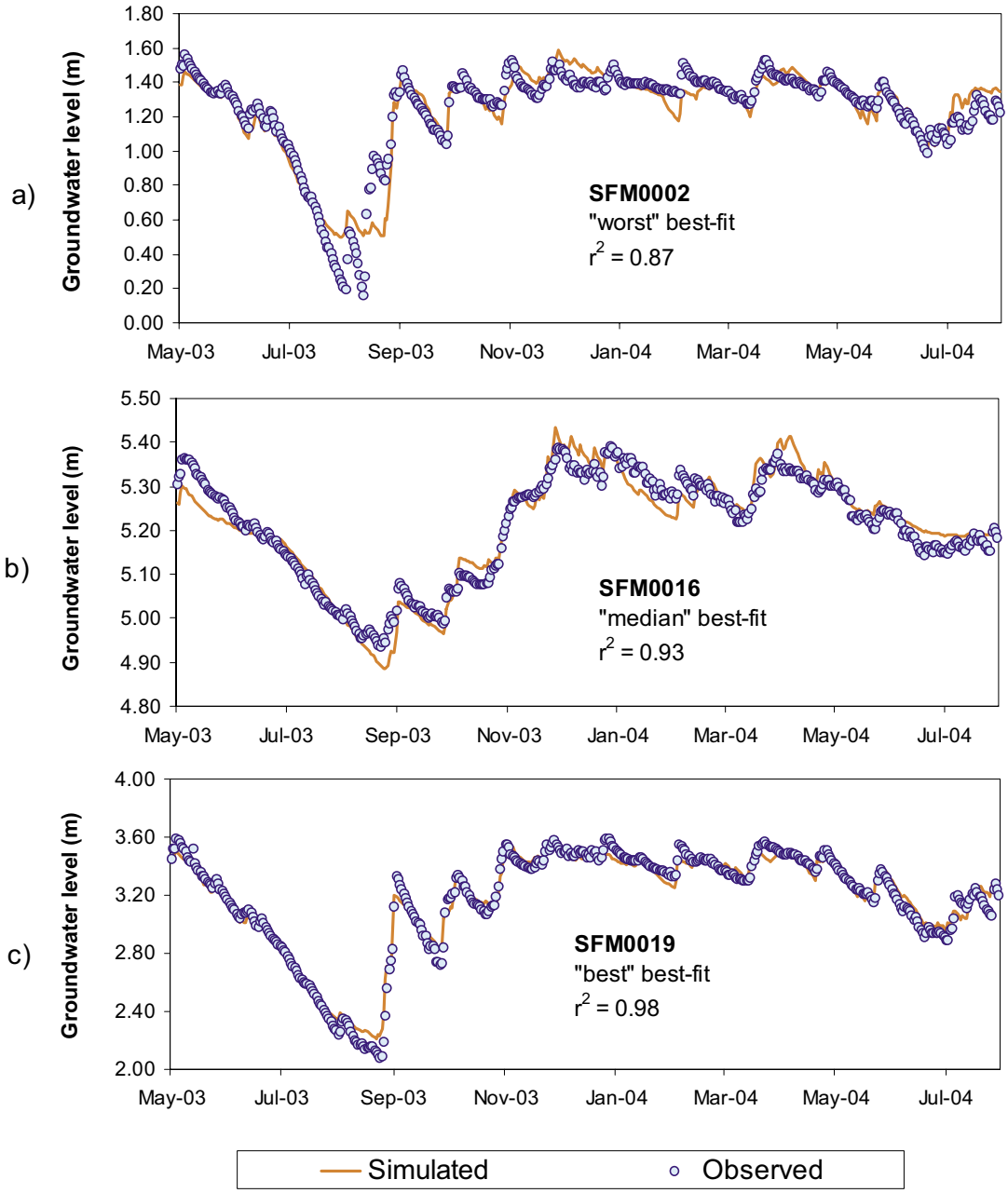

Figure 3-38. *Simulated time series compared to measured data for a) the "worst" data fit, b) the "median" data fit, and c) the "best" data fit. All groundwater levels are expressed in terms of meters above sea level (RHB 70).*

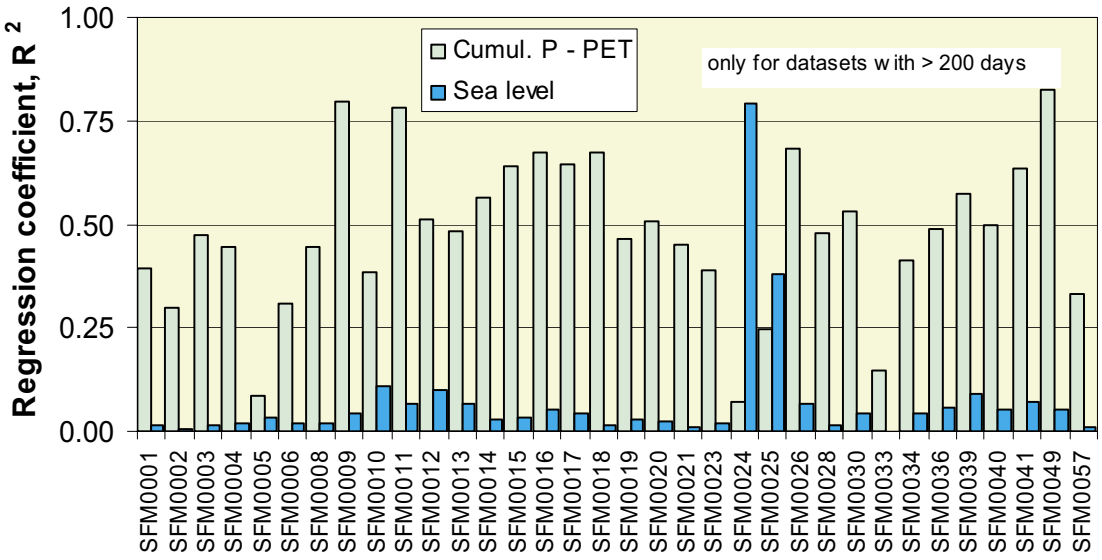

Figure 3-39. *Correlation coefficients for groundwater level data to sea level data and cumulative P-PET difference.*

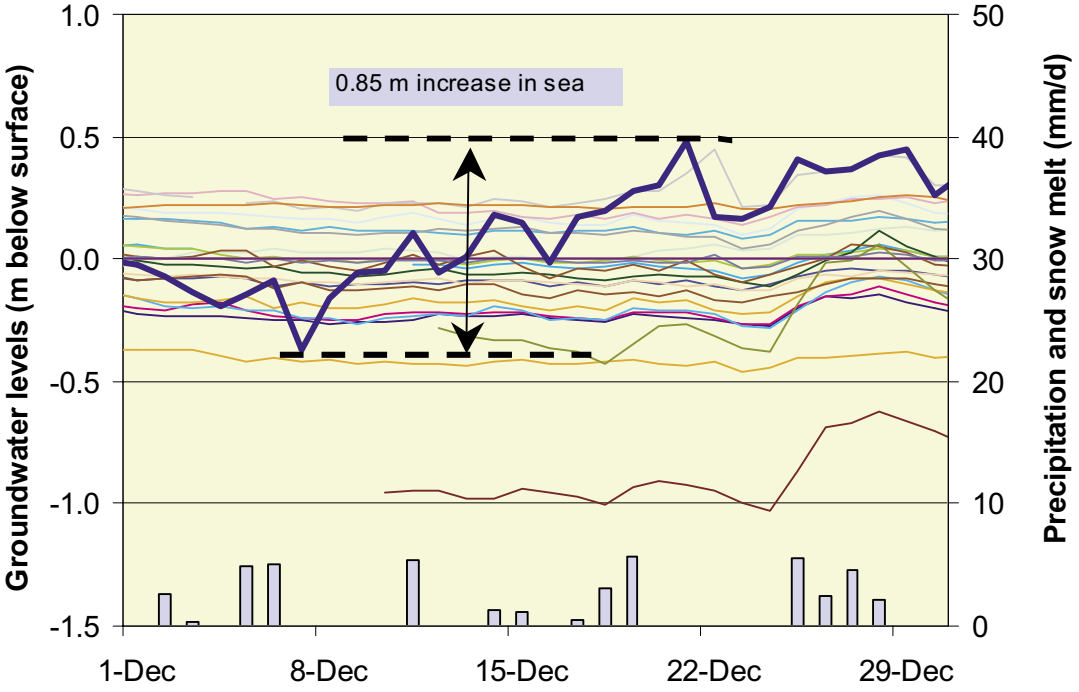

Figure 3-40. *Close-up view of groundwater levels during a one-month period (December 2003) when the sea level increased by 0.85 m.*

Wells in proximity to Lake Bolundsfjärden and Lake Eckarfjärden

Figure 3-41 shows the groundwater levels in monitoring wells located below and around Lake Bolundsfjärden (for the locations of the wells, see Figure 3-27), and the water level in the lake. During most of the time, the lake acts as a discharge area with the groundwater levels above the lake water level (SFM0040). However, in the dry summer of 2003 the groundwater levels measured below the lake (SFM0023) and in some of the nearby groundwater monitoring wells were below the lake water level, thereby indicating conditions where the lake acted as a source of groundwater recharge.

It can be seen in Figure 3-41 that the gradients between the lake and the monitoring wells around the lake change direction, but also that their magnitudes and the relations between the different wells are preserved; the well that normally shows the highest groundwater level (SFM0030 located just west of the lake) has the lowest level during the summer of 2003. Furthermore, some anthropogenic disturbances can be observed; these were caused by a pumping test and water sampling during May–July, 2004.

Figure 3-42 shows similar data for Lake Eckarfjärden and some monitoring wells below and around the lake. The situation with a lake water level above the groundwater levels during part of the summer 2003, providing conditions for the lake to act as a groundwater recharge source, is the same. In fact, the situation in which the groundwater level below the lake (SFM0015) is lower than the water level in the lake (SFM0041) is shown more clearly and appears to be at hand during more "events" for Lake Eckarfjärden than for Lake Bolundsfjärden.

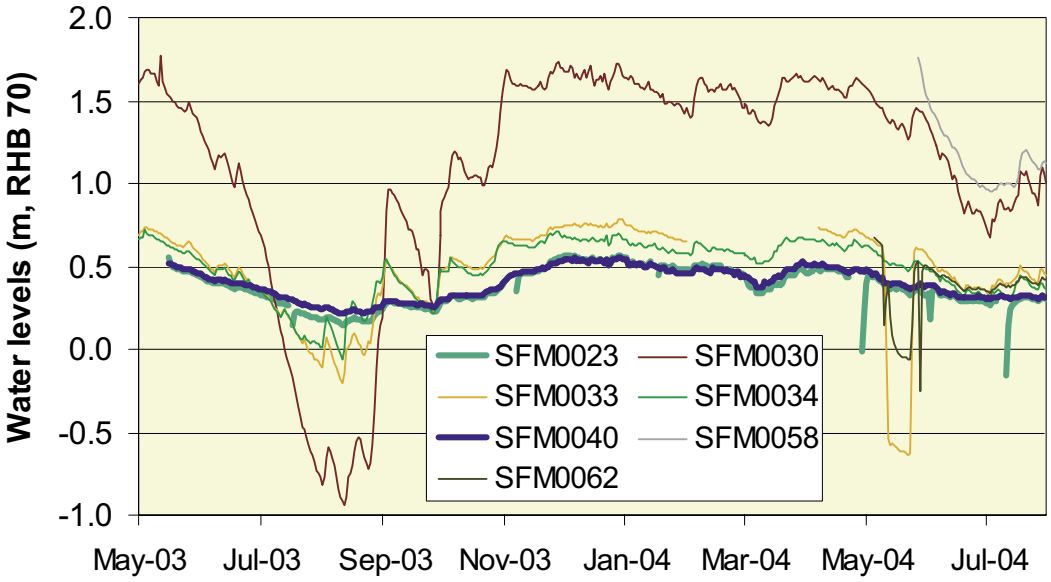

Figure 3-41. *Water level in Lake Bolundsfjärden (SFM0040) and groundwater levels below (SFM0023) and around the lake.*

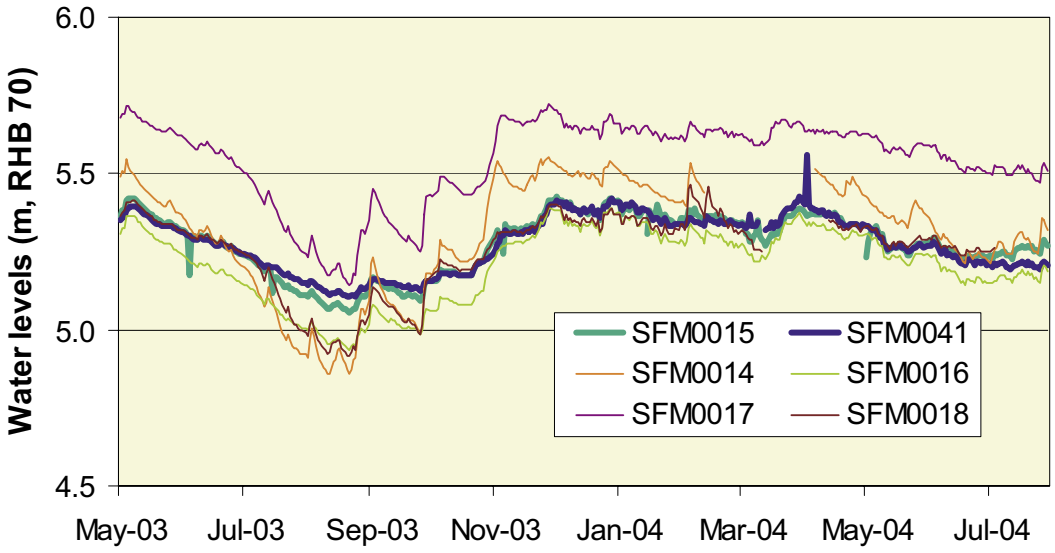

Figure 3-42. *Water level in Lake Eckarfjärden (SFM0041) and groundwater levels below (SFM0015) and around the lake.*

In general, the relations between the lake water level and the groundwater levels measured in the surrounding monitoring wells are also less consistent for Lake Eckarfjärden. Similar to Lake Bolundsfjärden, the main insight provided by the water level measurements is that the lake can be a source of groundwater recharge under certain "dry" conditions; how common these conditions are will be revealed when longer time series become available.

Diurnal groundwater level fluctuations

Diurnal fluctuations driven by evapotranspiration (ET) cycles were evident in groundwater monitoring well data obtained during warm dry periods. Figure 3-43 and Figure 3-44 show examples of diurnal ET-driven cycles in groundwater levels for a very shallow groundwater level (SFM0034) and a somewhat deeper groundwater level (SFM0030), respectively, measured with one-hour resolution during an eight-day period in August 2003. The figures also show the potential evapotranspiration (PET), which was calculated, as described above, based on measured meteorological data. In Figure 3-43, the PET and the groundwater level display similar diurnal cycles, where the increases in PET appear to be directly related to decreases in the groundwater level (and decreases in PET to increasing levels).

As would be expected, the location with a shallower groundwater table exhibited a stronger diurnal response (~6 cm) compared to the location with deeper a groundwater table (~0.5 cm). In addition, it was observed that the shallow system exhibited a sharper and higher amplitude response to the precipitation event beginning on August 12. However, the differences in the shape of the pulse following the precipitation event can be considered more pronounced than the differences in the total change in groundwater level.

Figure 3-43 also shows that the response of the shallow system was much stronger to this first event(s) than to the smaller August 14 event. The responses to the different precipitation events are much more difficult to distinguish in the data from the deeper groundwater level system in Figure 3-44.

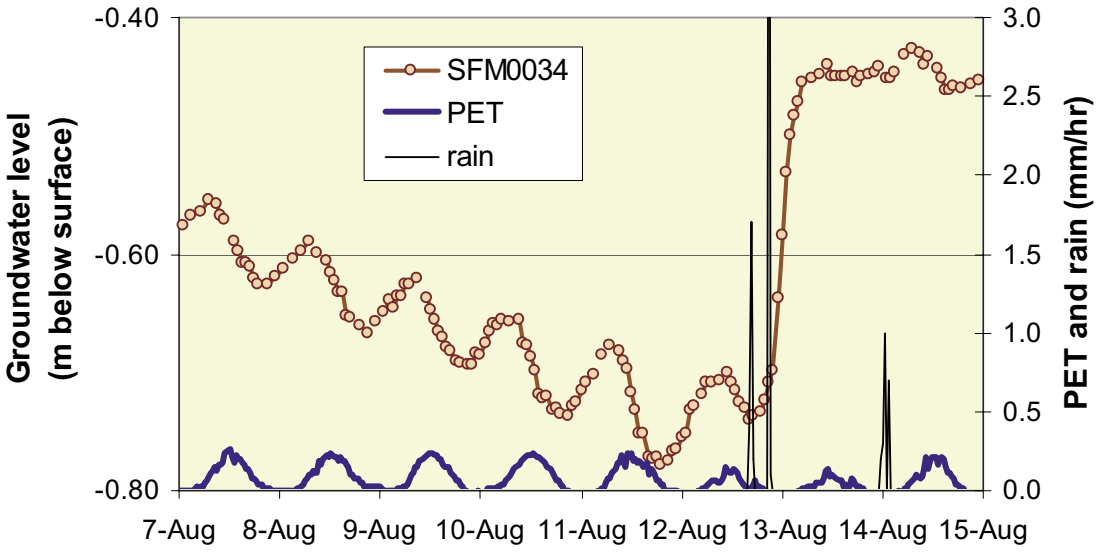

Figure 3-43. *Diurnal fluctuations in groundwater level in a typical location with shallow groundwater.*

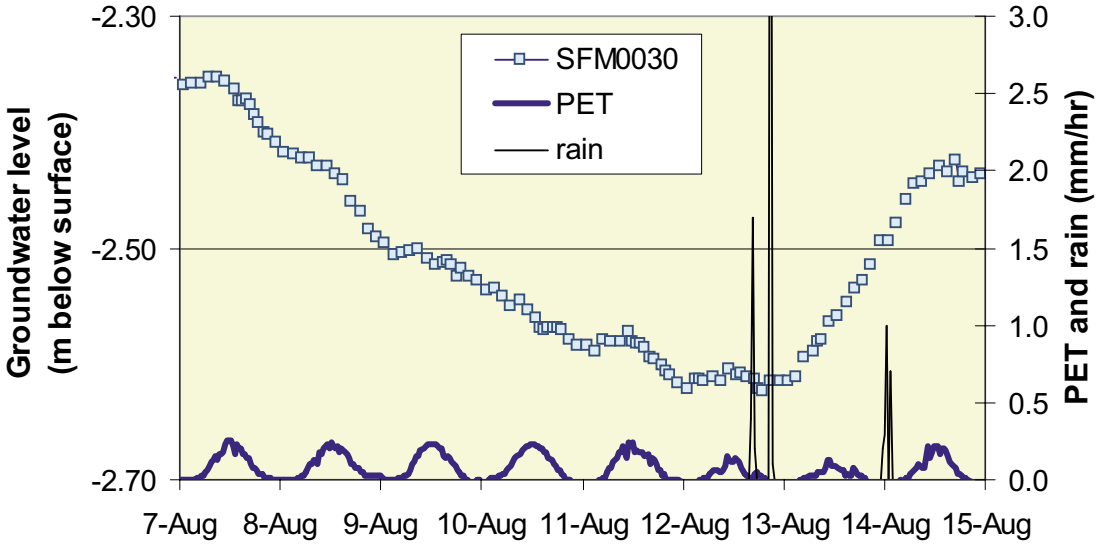

Figure 3-44. *Diurnal fluctuations in groundwater level in a typical location with deeper groundwater.*

Comparison of groundwater levels in the QD and in the shallow bedrock

Comparisons have been made between groundwater level time series from monitoring wells in the QD and in the percussion drilled boreholes in the bedrock. Results are presented from wells in the vicinity of the core-drill sites 1 and 2 (boreholes KFM01 and KFM02), referred to as Site 1 and Site 2, respectively, in the following. The locations of monitoring wells and percussion drilled boreholes near these sites are shown in Figure 3-45.

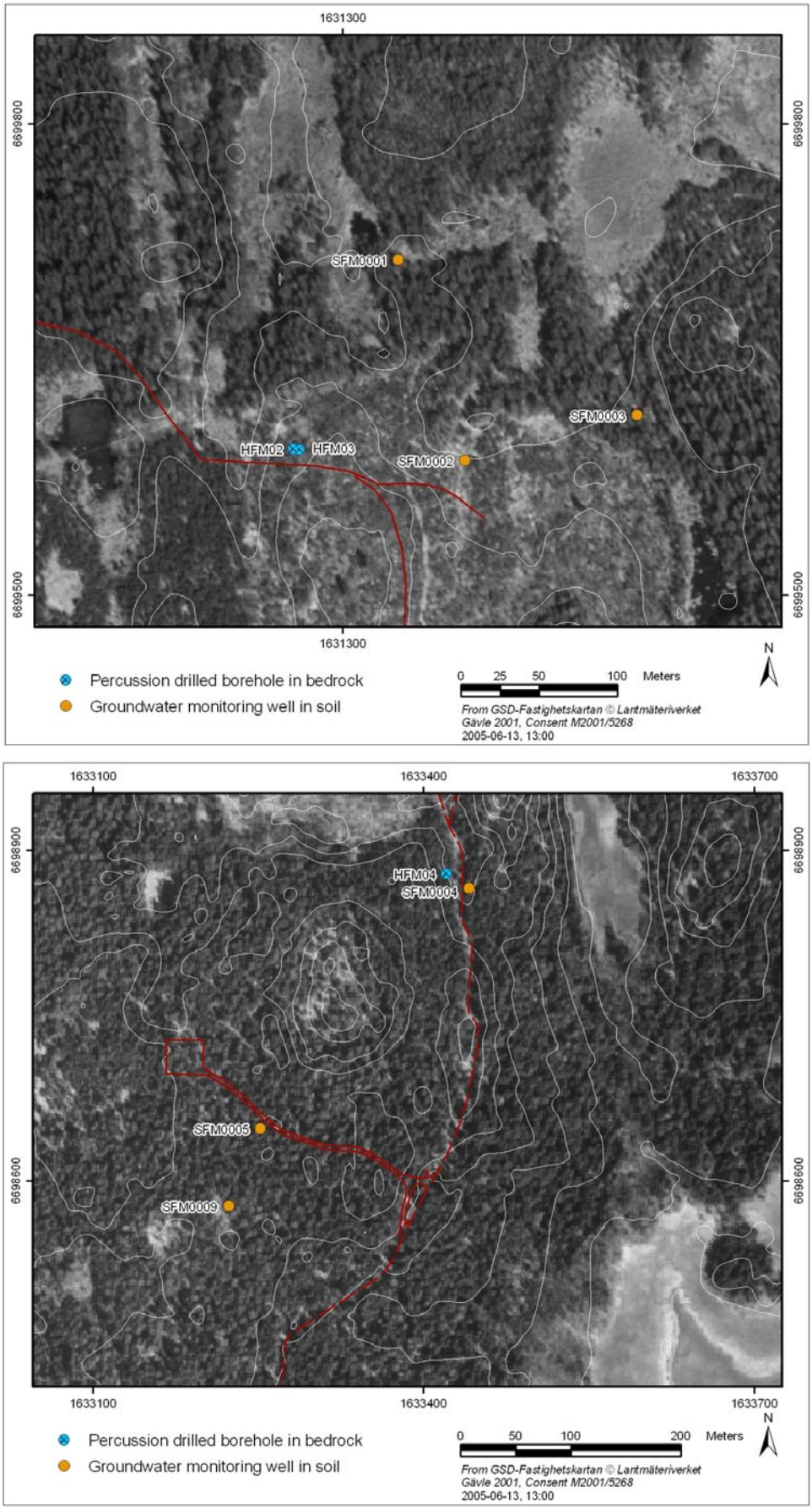

Figure 3-45. *Groundwater level measurement locations in the vicinity of Site 1(top) and Site 2 (bottom).*

Core-drill site 1

Figure 3-46 shows groundwater elevations and depths below ground surface for near-surface and percussion well locations in the vicinity of Site 1. Table 3-11 shows the distances between the well locations. Smaller distances between the wells, in the range of 20–30 m rather than 100–220 m, would have provided a stronger basis for drawing conclusions on the vertical direction of groundwater flow. Over larger distances, the effects of ground surface topography complicate the assessment. For instance, reported groundwater elevations at SFM0001 are indeed lower than at HFM02.1 and HFM03.1 for part of the time series. However, the ground elevation at SFM0001 is approximately 2 m lower than at either of the percussion well sites, and it is more than 100 m away.

When the data is presented in terms of water depth below surface, a consistent downward flow direction seems evident. In cases such as this, with greater than desirable distances between well locations, the groundwater elevations and depths below ground surface must be interpreted together to assess the vertical direction of groundwater flow. In general, it appears that the groundwater flow consistently had a downward direction at Site 1 during the studied period. The obvious disturbances observed in the percussion wells are connected to activities in the core-drill holes KFM01B and KFM05A and to pumping activities in HFM01 and HFM13.

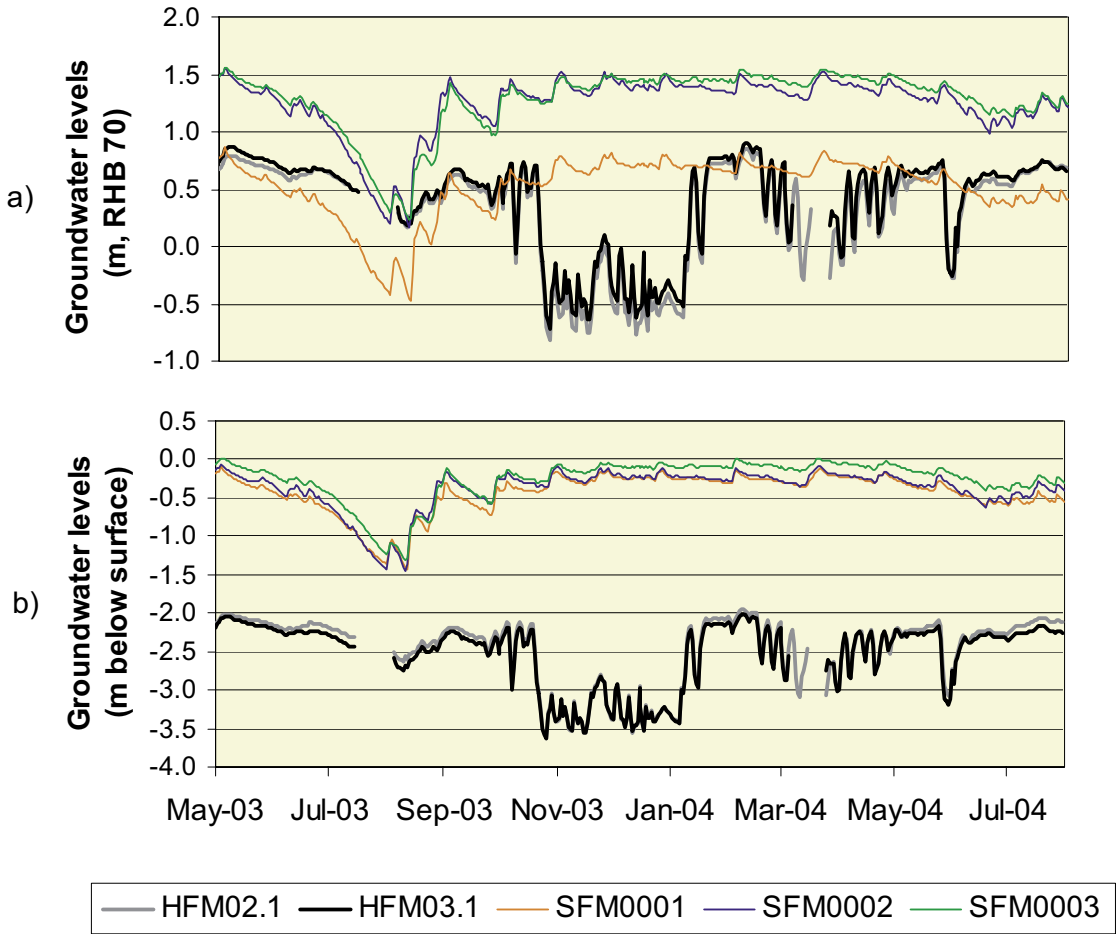

Figure 3-46. *Groundwater elevations and depths below ground surface for groundwater monitoring wells in QD (SFM) and percussion wells in bedrock (HFM) at Site 1.*

Table 3-11. Distances in meters between groundwater monitoring wells in QD and percussion-drilled wells in the vicinity of Site 1.

	SFM0001	SFM0002	SFM0003
HFM02	137	109	220
HFM03	136	105	216

Figure 3-47 shows a close-up of five-months of the groundwater data that was plotted in Figure 3-46. In this plot, percussion well data is plotted on an enlarged scale on the second (right) Y-axis. Clearly, there is a strong correlation between the near-surface (QD) and percussion well time series over this time interval, but the amplitude of the deeper groundwater level variations is diminished (less than half) in comparison to the variations in the near-surface system.

These data suggest that there is a coupling between groundwater in the QD and in the near-surface bedrock. It is also evident, however, that the variations in the bedrock are reduced, indicating that the connection takes place only through pathways of relatively low hydraulic conductivities.

Figures 3-48 and 3-49 show groundwater elevations in different sections of the percussion wells HFM02 and HFM03, respectively; these sections were separated by well packers. Generally, the differences in groundwater level between the sections are small. Some differences can be observed in HFM02, where it can be noted that the relation between the different sections changes with time. During the first part of the studied time period (in April and May), the highest levels are measured in the uppermost section (HFM02.3). Conversely, this section has the lowest groundwater levels in (most of) June and in July.

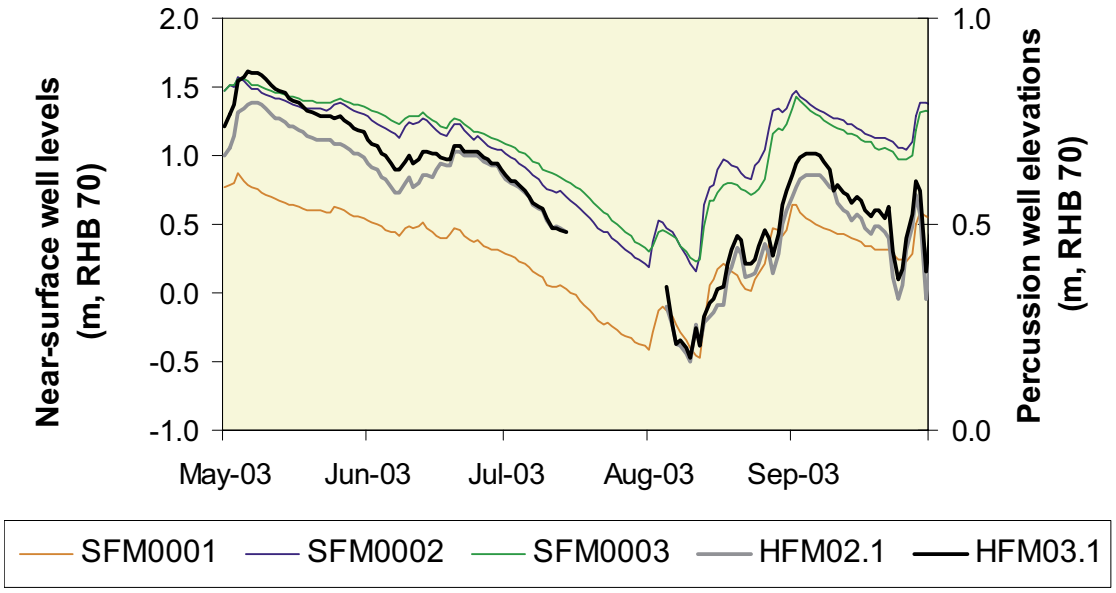

Figure 3-47. *Close-up view of groundwater elevations for a 5-month period at Site 1 with near-surface (QD) and percussion well data plotted on separate axes for improved resolution.*

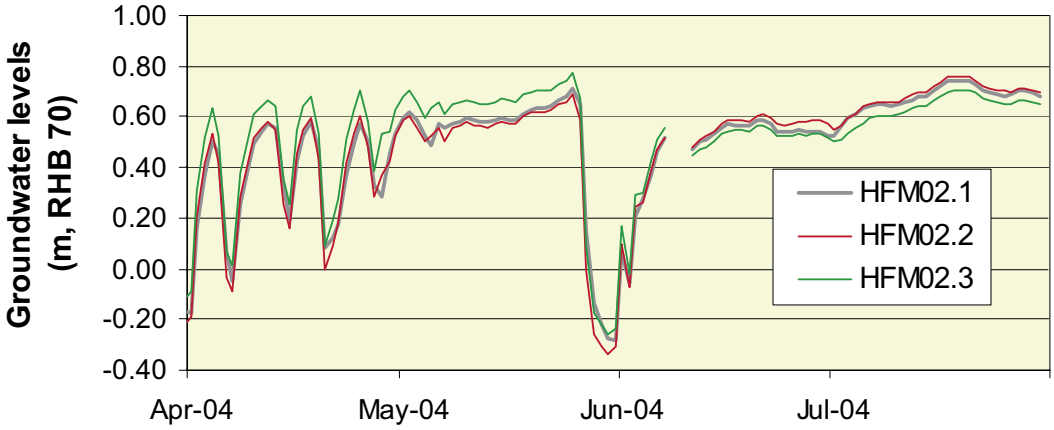

Figure 3-48. *Groundwater elevations in three sections in HFM02 (separated by packers). HFM02.1 measures groundwater elevation 49–100 m below ground, HFM02.2 38–48 m below ground, and HFM02.3 above 37 m below ground.*

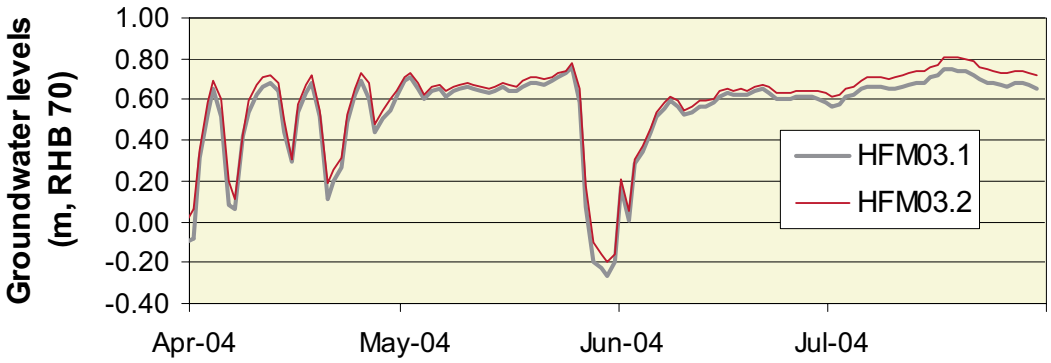

Figure 3-49. *Groundwater elevations in two sections in HFM03 (separated by packers). HFM03.1 measures groundwater elevation 19–26 m below ground, and HFM03.2 above 18 m below ground.*

The results from HFM03 are more consistent regarding the relation between the two sections where measurements were made; the highest groundwater level was recorded in the upper section (HFM03.2). However, the groundwater levels in the two sections follow each other closely during the whole period, except for the last month when a somewhat larger difference can be observed.

Core-drill site 2

Figure 3-50 shows groundwater elevations and depths below ground surface for percussion-drilled wells and near-surface wells in QD at and in the vicinity of Site 2 (cf Figures 3-27 and 3-45). The groundwater monitoring well SFM0004 is located close to HFM04, the distance between them is approximately 25 m, and at the same ground elevation, whereas SFM0009 is located approximately 360 m away where the ground elevation is about 1 m higher. There are several lengthy periods of missing data in the percussion well time series, but the data indicate that a consistent downward groundwater flow gradient existed in this region during the studied time period.

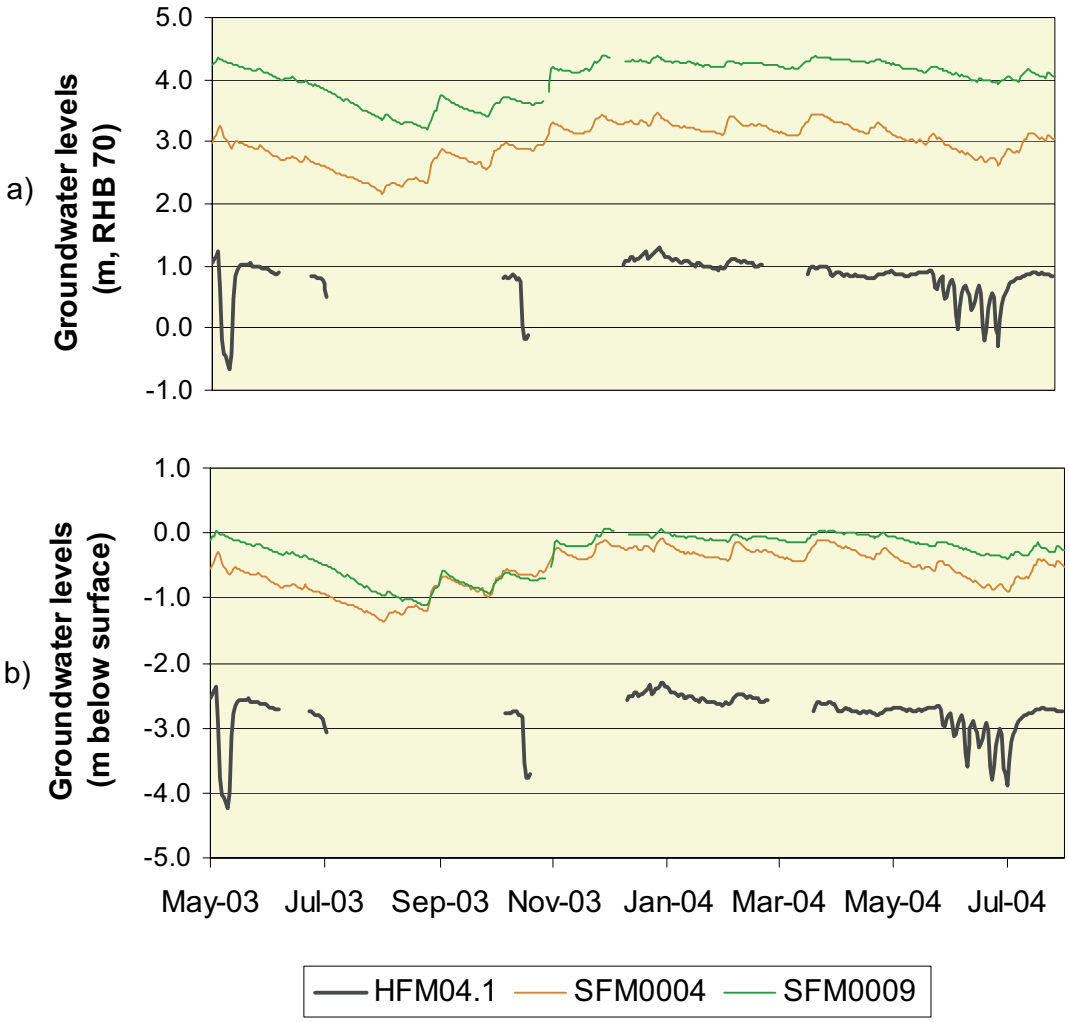

Figure 3-50. *Groundwater elevations and depths below ground surface for groundwater monitoring wells in QD (SFM) and percussion wells in bedrock (HFM) at Site 2.*

The close-up of data shown in Figure 3-51 suggests that some coupling exists between near-surface and deeper groundwater elevations; note the similarities in overall slope, as well as in the responses to some specific events. However, the coupling does not appear as strong as was observed for Site 1 (see Figure 3-47). Figure 3-52 shows a plot of groundwater elevations from three sections in HFM04 that were separated by packers. The shallowest section has an about 0.3 m higher groundwater level than the two lower sections. The disturbances that can be observed in the HFM04 data are caused by activities in core-drill borehole KFM02A and by pumping in HFM05.

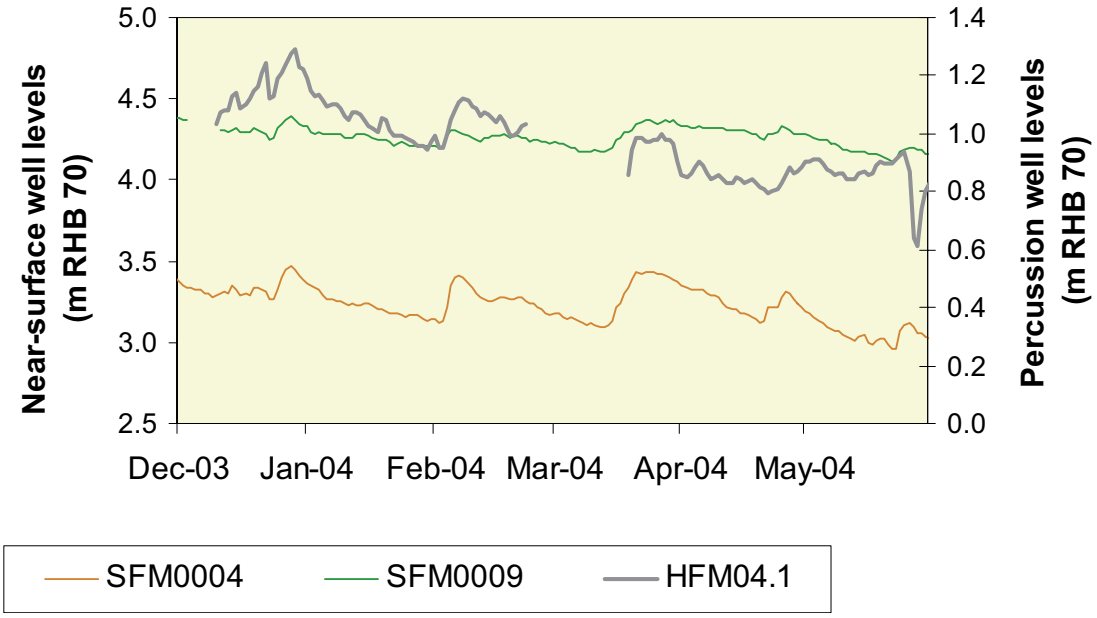

Figure 3-51. *Close-up view of groundwater elevations for a 6-month period at Site 2 with near-surface(QD) and percussion well data plotted on separate axes for improved resolution.*

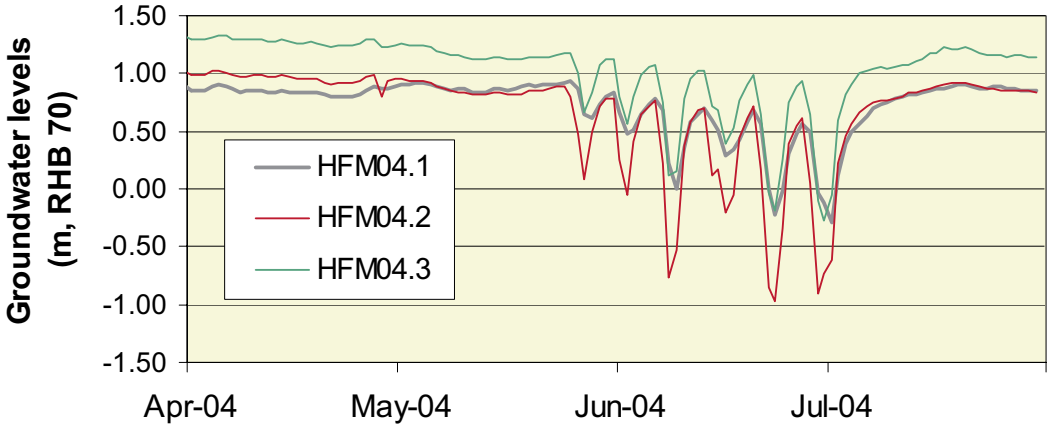

Figure 3-52. *Groundwater elevations in three sections in HFM04 (separated by packers). HFM04.1 measures groundwater elevation 66.9–221.7 m below ground, HFM04.2 57.9–65.9 m below ground, and HFM04.3 above 56.9 m below ground.*

3.3.4 Private wells and water prospecting wells

Private wells and water prospecting wells in the Forsmark area were investigated by /Ludvigson, 2002/. A total of 40 wells (27 private wells and 13 water prospecting wells) were identified. The locations of the identified wells are shown in Figure 3-53. The investigation included a gathering of basic well data, field checks, and water sampling in 25 of the private wells. Also included was a summary of geological and hydrogeological investigations, performed in Forsmark prior to the site investigations /Ludvigson, 2002/.

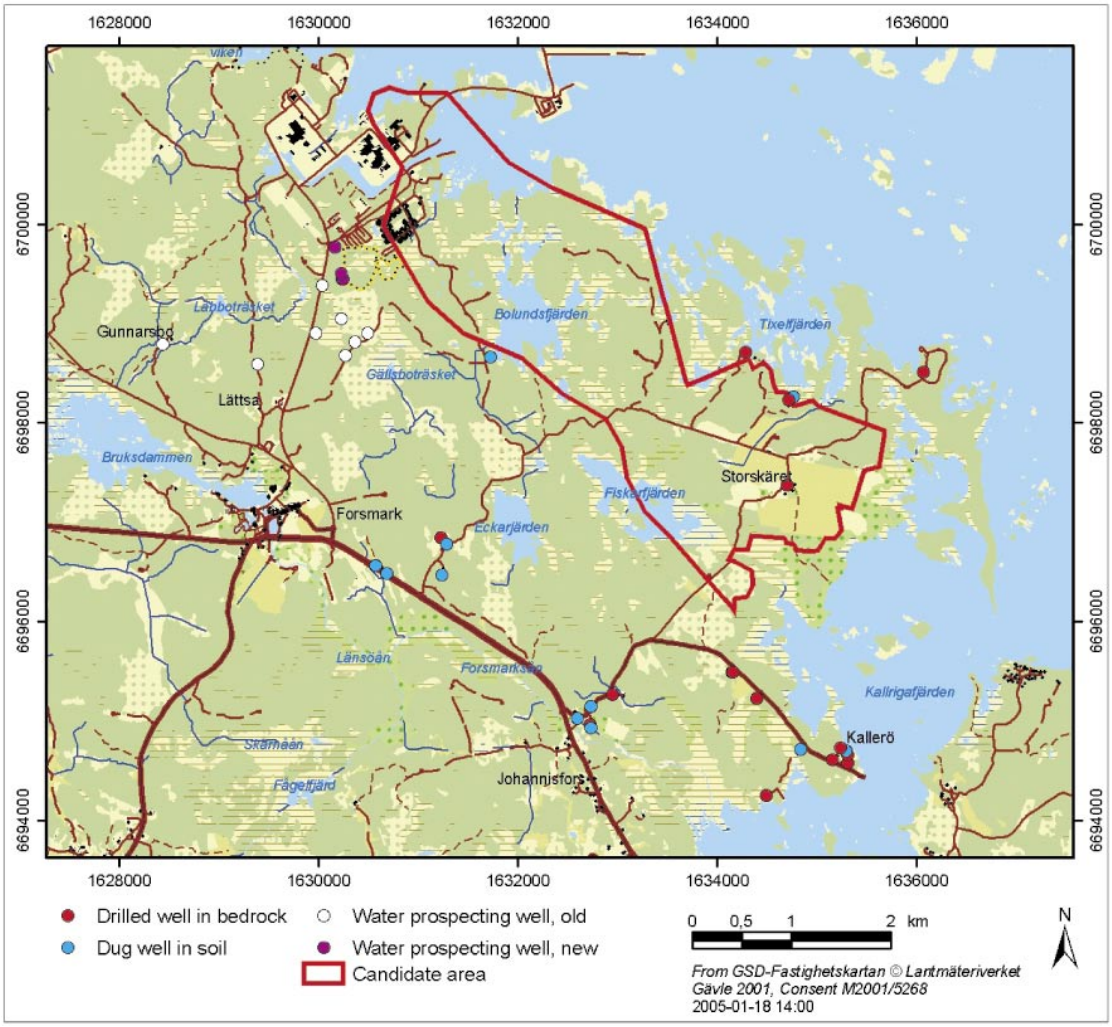

Figure 3-53. *Locations of identified private wells and water prospecting wells in the Forsmark area.*

The private wells include 15 wells drilled into the bedrock, and 12 dug wells in QD. As shown in Figure 3-53, most of these wells are located in, or immediately outside of, the western part of the candidate area, or south of this area. Only one well was found in the central part of area considered in the hydrological modelling (i.e. the area between the three main lakes, see Chapter 4). This well is situated just south of Lake Bolundsfjärden, but is reportedly not in use /Ludvigson, 2002/. Furthermore, some wells are located in the area west of Lake Eckarfjärden. It should also be noted that no private wells were found in the central and north-western parts of the candidate area.

The water prospecting wells were drilled by Vattenfall/Forsmarks Kraftgrupp in connection with investigations performed in order to find a new freshwater supply to the Forsmark nuclear power plant. These investigations are summarised by /Ludvigson, 2002/. (The present supply, of both drinking water and process water, is based on surface water from "Bruksdammen" at Forsmark.) The water prospecting for the power plant is an on-going process. It can be seen that the most of water prospecting wells are located in the area north-west of Lake Gällsboträsket.

The water sampled in 25 of the private wells was analysed for chemical and microbiological parameters. According to the results of the analyses, the water quality shows large variations between different wells. The water from some of the wells can be used as drinking water, whereas the water quality is poor in other wells.

4 Conceptual and descriptive modelling

4.1 Introduction

According to the definitions given by /Rhén et al. 2003/, the *conceptual model* should define the framework in which the problem is to be solved, the size of the modelled volume, the boundary conditions, and the equations describing the processes. The (hydrogeological) *descriptive model* defines, based on a specified conceptual model, geometries of domains and parameters assigned to these domains.

The aim of the present chapter is to provide a conceptual and descriptive model of the surface-hydrological and near-surface hydrogeological system of the Forsmark area. The model should, based on site-specific, regional and generic data, describe this system and provide the necessary input to the quantitative flow modelling (Chapter 5). The model of the system should include descriptions of

- boundaries,
- flow domains and their interfaces,
- infiltration and groundwater recharge,
- flow systems and discharge.

The database for the conceptual and descriptive model is mainly the data presented and referred to in Chapter 3. However, examples will also be given of supporting evidence from other disciplines of the site investigation. Furthermore, regional and generic data are used for the development of the model. The uncertainties related to the presented model are discussed in Chapter 6.

Figure 4-1 illustrates SKB's systems approach to hydrogeological modelling. The division into three types of hydraulic domains (overburden/QD, rock mass, and conductors in rock) constitutes the basis for the quantitative models. From a hydrogeological perspective, the geological data and related interpretations constitute the basis for the geometrical modelling of the different hydraulic domains. Thus, the investigations and documentation of the QD and the upper part of the bedrock, provide input to

- the distribution of QD (HSD), including genesis, composition, stratification, thickness and total depth,
- the geometry of deterministic fracture zones, or lineaments, if needed (HCD), and the bedrock in between (HRD).

In the present context, where the HSDs are investigated in detail, a further division is made of the near-surface hydrogeology (in terms of domains and interfaces) than shown in Figure 4-1.

A complete conceptual and descriptive model of the surface hydrology and the hydrogeology at a site involves a description of the integrated (continuous) hydrological-hydrogeological system, i.e. surface waters, groundwater in QD and groundwater in bedrock. The focus of the modelling presented here is on the surface and near-surface conditions. The hydrogeological properties of the bedrock and the lower boundary condition used in the quantitative modelling are therefore not described in the conceptual model. The description of the bedrock properties and the interaction between QD and bedrock in the quantitative flow modelling are presented in Chapter 5.

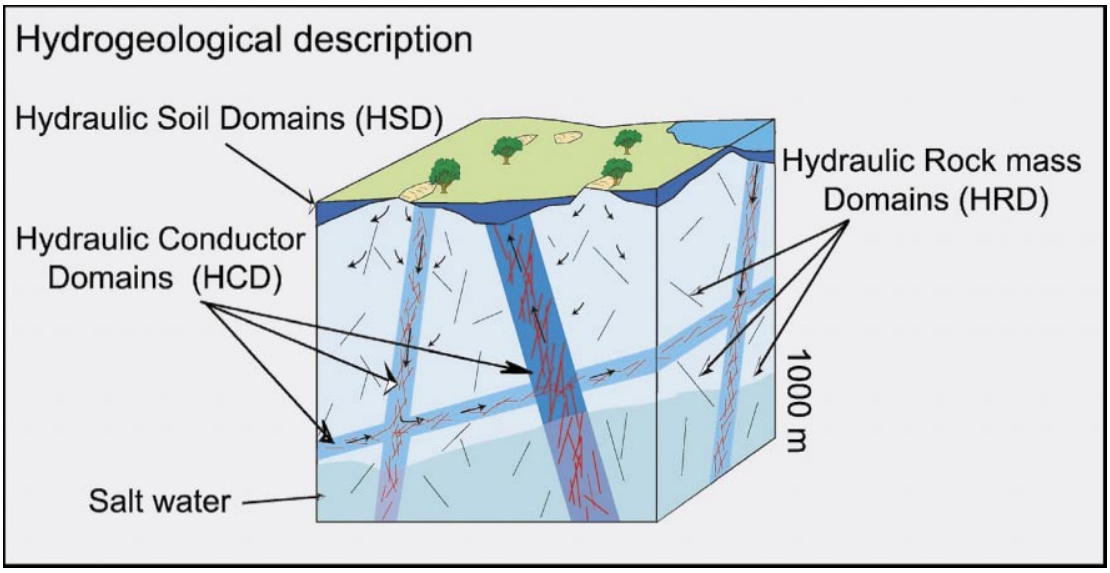

Figure 4-1. *Division of the overburden/QD and the bedrock into hydraulic domains representing the QD (HSD) and the rock domains (HRD) between fracture zones modelled as conductor domains (HCD). Within each domain the hydraulic properties are represented by mean values, or by statistical distributions /Rhén et al. 2003/.*

4.2 Boundaries

The conceptual and descriptive model covers the area northeast of the main water divide to the catchment area of Forsmarksån, between the nuclear power plant in the north and Kallrigafjärden in the south. Thus, the model area is the same as that covered by the detailed catchment area mapping, but includes also the areas draining directly to the Baltic Sea and the cooling water intake canal of the power plant, see Figure 4-2.

In the modelling, it is assumed that surface water and near-surface groundwater divides coincide. The boundary towards Forsmarksån is considered as a surface water and groundwater divide, i.e. as a no-flow boundary. Also the north-western boundary is considered as a surface water and groundwater divide. The boundary to the cooling water canal and the Baltic Sea is a flow boundary, normally an outflow boundary. However, as indicated by the measurement presented in Figures 3-16, 3-19 and 3-20, the flat topography allows sea water inflow to some of the lakes during periods of very high sea water levels.

As discussed above, the groundwater levels in the groundwater monitoring wells generally show very weak correlations with the sea water level (Figure 3-39). The only wells showing strong correlations with the sea water level are SFM0024 and SFM0025, located below open water directly influenced by the sea water level, and SFM0059 and SFM0061 at the Börstilåsen esker. From existing time series, it is evident that the sea water level is sometimes higher than the groundwater levels measured in these wells, which implies possibilities for sea water intrusion.

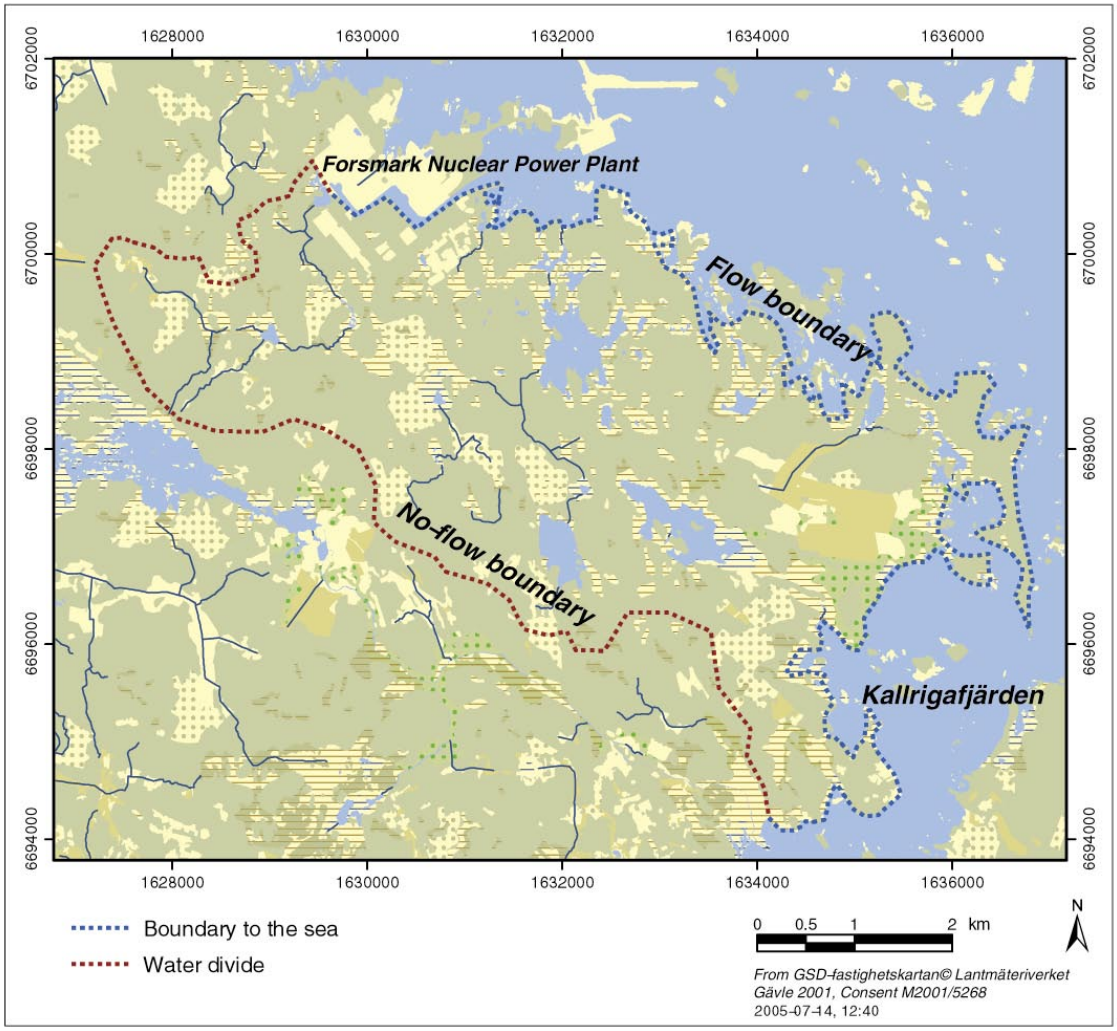

Figure 4-2. *Area considered in the conceptual and descriptive modelling.*

4.3 Flow domains and their interfaces

With reference to the three types of hydraulic domains in SKB's systems approach to hydrogeological modelling, see Figure 4-1, the focus of the description below will on surface water and near-surface groundwater in the QD (HSD) and their interfaces to the two bedrock domains (HCD and HRD).

4.3.1 Lakes

The area is characterized by a low relief with a small-scale topography. Almost the whole area considered in the conceptual and descriptive modelling is below 20 m a s l (metres above sea level), see Figure 3-27 and Figure 3-32. As described by /Brunberg et al. 2004/, 25 "lake-centered" catchments and sub-catchments have been delineated, ranging in size from 0.03 km^2 to 8.67 km^2 (cf Figure 3-13 and Table 3-4).

The 25 mapped lakes range in size from 0.006 km^2 (lake in sub-catchment 7:3) to 0.752 km^2 (Lake Fiskarfjärden). The main lakes besides Lake Fiskarfjärden are Lake Bolundsfjärden (0.609 km^2), Lake Eckarfjärden (0.282 km^2) and Lake Gällsboträsket (0.185 km^2). The lakes are shallow with mean depths and maximum depths ranging from approximately 0.1 to 1 m and 0.4 to 2 m, respectively, see Table 3-5 and /Brunberg et al. 2004/.

4.3.2 Water courses

No major water courses flow through the area covered by the conceptual model. The most important brooks are those dewatering catchments Forsmark 1 and 2, i.e. sub-catchments 1:1–1:4 and 2:1–2:11, respectively, in Figure 3-13. The brooks downstream Lake Gunnarsboträsket in catchment Forsmark 1 and downstream Lake Eckarfjärden and Lake Gällsboträsket in catchment Forsmark 2 carry water most of the year, but can still be dry for long time periods during dry years such as 2003 (see Figures 3-23 to 3-26).

Many brooks in the area have been deepened for considerable distances for draining purposes. However, still the riparian zone is wide at many locations and relatively large areas are inundated during periods of high water levels. A detailed surveying of slope and cross-sections of the major brooks has been initiated (see Section 3.2.4).

4.3.3 Wetlands

Wetlands are frequent and cover 10%, 12% and 17% of the major catchments Forsmark 1, 2 and 8, respectively. For some of the sub-catchments, wetlands cover between 25% and 35% (Table 3-4). The distribution of the wetlands according to the vegetation map was presented in Figure 3-14. From a hydrological point of view, it is useful to distinguish between bogs, fens and marshes /Kellner, 2004/. Bogs are peat covered areas where the precipitation falling within the area is the only source of water for the vegetation (ombrotrophic). Bogs are found in the most elevated parts of the area only. These bogs are small and the peat cover is not very thick (< 3 m) /Fredriksson, 2004/.

Fens are peat covered areas where the vegetation at least partly is supplied by inflowing surface water and/or groundwater. Marshes are wetlands with little or no peat. Fens and marshes are frequent in the more low-lying parts of the area. No comprehensive investigation of the stratigraphy or hydrology of the wetlands has been performed so far. The two fens studied in detail were both located in the western, most elevated part of the area. These fens were about one metre deep /Fredriksson, 2004/. From existing borings /Johansson, 2003; Werner and Lundholm, 2004a/, it is also known that the peat in the wetlands can rest directly on till, or be underlain by gyttja and/or clay above the till. This means that the hydraulic contact with the surrounding groundwater system varies among and within the wetlands in the area.

4.3.4 Quaternary deposits

A map of the Quaternary deposits (QD) is shown in Figure 4-3. This detailed map, compiled within the site investigation, is intended to be presented in the scale 1:10,000. It does not cover the whole area considered in the present modelling; the north-western part of the model area is not included. For the part where detailed mapping has not been performed, the existing map in 1:50,000 scale from SGU (Geological Survey of Sweden) /Persson, 1985, 1986/ must be used.

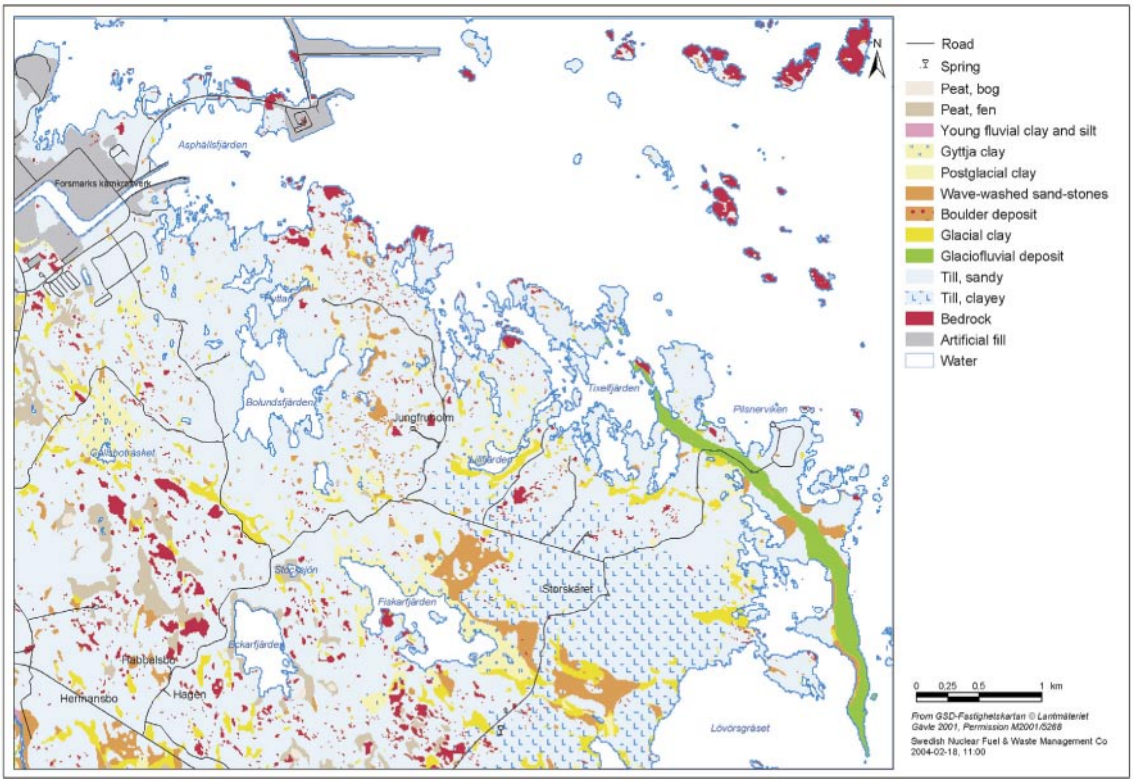

Figure 4-3. *Detailed map of QD /Sohlenius et al. 2004/.*

From the map in Figure 4-3 it is obvious that till is the dominating QD, covering approximately 75% of the mapped area. Bedrock outcrops are frequent, but constitute only approximately 5% of the area. Wave-washed sand and gravel, clay, gyttja clay and peat cover 3–4% each. The only glaciofluvial deposit, the Börstilåsen esker, runs in a north-south direction along the coast (cf the "green belt" on the map). The QD are shallow, usually less than 5 m deep /Sohlenius et al. 2004/. The greatest depth to bedrock, recorded in a drilling south-east of Lake Fiskarfjärden, is 16 m.

Three areas with different types of till have been distinguished /SKB, 2004a; Sohlenius et al. 2004/. In the western and northern parts of the mapped area, sandy till is dominating, whereas clayey till dominates at Storskäret and east of Lake Fiskarfjärden. In the easternmost part of the area, close to the Börstilåsen esker, the till has a high frequency of large boulders. Generally, the till deposits seem to be deeper in the south-east, in areas covered by clayey till. A preliminary model of the total depth and stratigraphy of the QD in the area has been developed, based on drillings and geophysical investigations /Vikström, 2005/, and included in the quantitative flow modelling (see Chapter 5). The median QD depth for all grid points within the modelled area, points with outcropping bedrock excluded, was calculated to 1.9 m.

The hydraulic properties of the till are mainly determined by the grain size distribution, the compactness, and structures such as lenses of sorted material. In the upper approximately one metre of the QD, the hydraulic conductivity (K) and effective porosity are much higher than further down the profile /Lundin, 1982; Johansson, 1986, 1987a,b; Espeby, 1989; Lind and Lundin, 1990/. This is mainly due to soil forming processes, probably with ground frost as the single most important process, resulting in higher porosity and formation of macro-pores. However, wave washing also implies that the till at exposed locations is coarser at the ground surface, and at some locations coarse out-washed material has been deposited.

Based on generic data, the saturated hydraulic conductivity in the upper one metre can be estimated to 10^{-5}–10^{-4} m·s^{-1} and the effective porosity to between 10% and 20%, with the higher values close to the surface (effective porosity is here used a common term for specific yield and kinematic porosity). The total porosity can typically be estimated to 30–40% mainly depending on depth. Only very few site-specific data exist for the hydraulic conductivity of the uppermost part of the profile (Figure 3-30). The quantitative modelling of unsaturated and saturated flow in the uppermost part of the profile in F1.2 has to mainly rely on generic data (see Chapter 5). Some additional site-specific data on hydraulic conductivity and water retention properties will be available for the next model version.

Below the depth interval strongly influenced by the soil forming processes, the hydraulic conductivity and the porosity of the till are considerably lower. The results from the slug tests indicate a higher hydraulic conductivity in the QD/rock contact zone than in the till itself, with geometric mean values of $1.3 \cdot 10^{-5}$ m·s^{-1} and $1.2 \cdot 10^{-6}$ m·s^{-1} (not including wells installed below open water), respectively (Figure 3-30). Comparing K-values from slug-tests with values calculated from grain-size distributions, the slug-test values are considerably higher in the QD/rock contact zone (differences from less than one order of magnitude for coarse till to 3 orders of magnitude for fine-grained till), whereas the results for the two methods are similar for tests in the till itself.

Also, if a division is made into coarse till (sandy and gravelly) and fine-grained till (clayey and silty) of the slug test results in the QD/rock contact zone, the geometric means of the K-values are almost the same. These results indicate that the relatively high K-values in the contact zone between QD and rock are mainly caused by the bedrock properties, i.e. by fractures in the upper part of the rock. However, in the zone between the upper one metre of the QD and the QD/rock contact, it is motivated to make a distinction between the coarse till and the fine-grained till.

The old, very compact till found at the bottom of the QD profile at some locations in the area most probably has a very low hydraulic conductivity and porosity. Since this material so far has been found only at a few locations, it is suggested not to include it as a separate unit in the quantitative modelling. According to generic data, the total and effective porosity of the till below the upper one metre typically can be estimated to 20–30% and 2–5%, respectively.

All site-specific hydraulic conductivity data are from test measuring the horizontal conductivity. The primary sedimentary structures of till have been shown to influence the hydraulic conductivity /Lind and Lundin, 1990; Lind et al. 1994/. The consistency of such structures depends on the genesis of the till; the consistency is higher in lodgement till than in meltout till and flow till. No systematic classification of the till genesis at the site has been conducted so far. For the present model version, it is recommended that sensitivity analysis is used to investigate the influence of anisotropy in the hydraulic conductivity. Generic data indicate that the hydraulic conductivity can vary with more than one order of magnitude in different directions /Lind et al. 1994/.

Based on the presented site-specific and generic data, the mean values of the saturated hydraulic conductivity, total porosity and effective porosity shown in Table 4-1 are proposed for a simplified three-layer model of the till profile in Forsmark (including the QD/rock contact zone), as a starting point for the quantitative modelling. The results of the hydraulic tests show a high variance (see Figure 3-29 and Figure 3-30), and the values should be considered as type values. A schematic profile illustrating the conceptual model is shown in Figure 4-4.

Table 4-1. Proposed mean values of horizontal saturated hydraulic conductivity, total porosity and effective porosity for a simplified three-layer till profile.

Layer/material	Horizontal saturated hydraulic conductivity ($m \cdot s^{-1}$)	Total porosity (%)	Effective porosity (%)
0 to 1 m below ground	$1.5 \cdot 10^{-5}$	35	15
Middle layer:			
Coarse till	$1.5 \cdot 10^{-6}$	25	5
Fine-grained till	$1.5 \cdot 10^{-7}$	25	3
0 to 1 m above the bedrock	$1.5 \cdot 10^{-5}$	25	5

For the only glaciofluvial deposit in the area, the Börstilåsen esker, the obtained K-value of $2 \cdot 10^{-4}$ $m \cdot s^{-1}$ is relatively low, and the storativity of $2 \cdot 10^{-3}$ indicates mainly confined conditions. In a simplified model, the small areas with shallow deposits of wave washed sand can be given the same hydraulic properties as the uppermost till layer.

No site-specific hydraulic data exist for clay, gyttja or peat. Therefore, the quantitative modelling must rely on generic data on these materials (see Chapter 5). The existence and hydraulic conductivity of clay and gyttja below wetlands and lakes are important factors for the surface water-groundwater interaction. As discussed above, no comprehensive investigation has been conducted of the stratigraphy of the wetlands.

The stratigraphy of bottom sediments in lakes has been investigated, and typical profiles have been identified for some of the lakes /Hedenström 2003, 2004; Vikström 2005/. Typically, the sediment stratigraphy from down and up is glacial and/or postglacial clay, sand and gravel, and nested layers of gyttja in different fractions. The clay layer is missing in major parts of the area below Lake Bolundsfjärden. However, still a pumping test in the vicinity of this lake indicated a very limited hydraulic contact between the lake and groundwater in till below the lake. The differences between the water level in the lake and the groundwater level below the lake under undisturbed conditions, as shown in Figure 3-41, give the same indication.

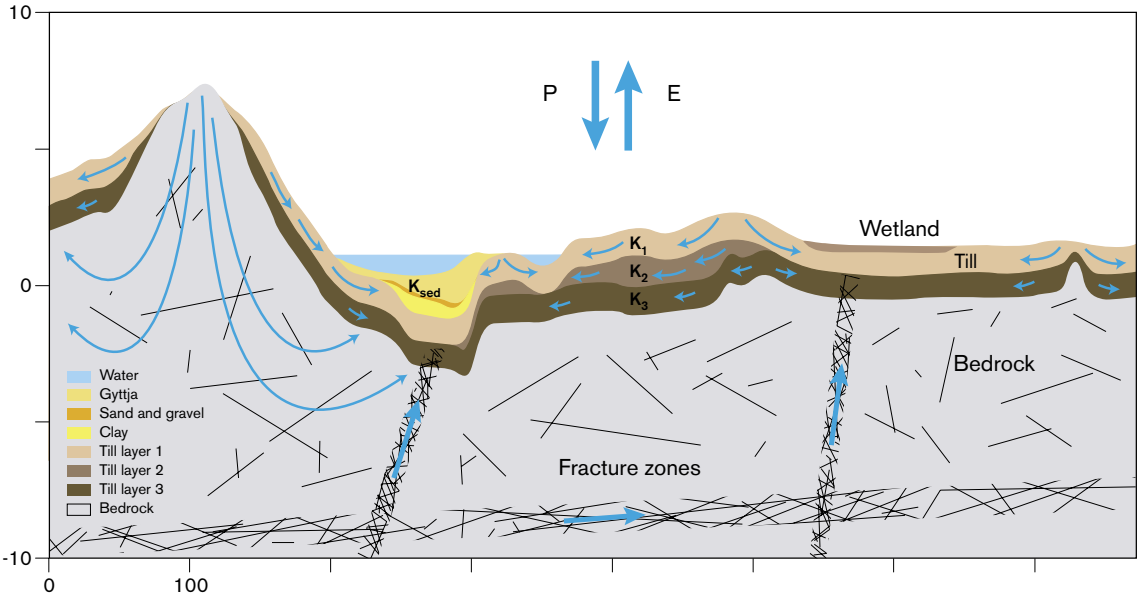

Figure 4-4. *Schematic profile illustrating the conceptual model.*

4.4 Infiltration and groundwater recharge

During the one-year period for which local measurements exist, August 1, 2003 – July 31, 2004, the corrected precipitation was 630 mm (Figure 3-6). The short period for which overlapping time series were available indicated that the precipitation in the study area is 5–10% larger than at the SMHI station at Örskär (Figure 3-7). The average annual (corrected) precipitation at Örskär is 588 mm, which indicates that the value for the one-year period of 630 mm in Forsmark should be close to the average annual precipitation there.

The total "potential evapotranspiration" for a short crop, calculated by the Penman equation based on the measurements in Forsmark, was 472 mm. According to simulations with the CoupModel, using the Penman-Monteith equations, the actual evapotranspirations for the same one-year period was slightly more than 400 mm for a mature coniferous forest in fresh to dry areas, and considerably lower, approximately 330 mm, in wet areas /Gustafsson et al. 2005/. The lower values in the wet areas are explained by the limited transpiration taking place when the groundwater level is very close to the ground surface.

In the calculations referred to above, root depth was not varied for dry, fresh and wet conditions. If an adaptation of the root depth in wet areas had been made, the difference in transpiration between dry and wet areas probably would have been smaller. The calculated evaporation directly from interception was approximately 130 mm. Typically, the total annual actual evapotranspiration does not differ very much for a forest and an agricultural crop, but the seasonal pattern is not the same /Gustafsson et al. 2004/. Due to higher interception evaporation, the evapotranspiration is higher in the forest during the cold part of the year.

In forested areas, constituting approximately 75% of the model area, the interception value presented above indicates that approximately 500 mm was available for infiltration. The infiltration capacity exceeds the rainfall and snowmelt intensity with few exceptions. Unsaturated (Hortonian) overland flow may appear over short distances, mainly on agricultural land covered with clayey till and on frozen ground where the soil water content was high during freezing. Also on outcropping bedrock unsaturated overland flow may appear, but just over very short distances before the water reaches open fractures or the contact zone between bedrock and QD. In a simplified quantitative model, unsaturated overland flow can be assumed to be negligible.

The flat terrain and the shallow groundwater levels mean that there will be a strong interaction between evapotranspiration, soil moisture and groundwater. The time series presented in Figure 3-34 and Figure 3-36 show that the groundwater level in most monitoring wells was within one metre below the ground all the year, and that the groundwater level on average was less than 0.5 m below ground during 50% of the time. A reservation should be made regarding the representativity of the monitoring well locations, with topographically low-lying areas over-represented. However, also in what can be considered as typical recharge areas the average groundwater level is not more than approximately one metre below ground. Only in locally elevated areas with relative steep slopes, considerably deeper groundwater levels can be assumed to exist, see, e.g. the results for SFM0008 in Figure 3-34. The annual variation in the groundwater level is often less than 0.5 m in low-lying areas, and approximately 1 m in typical recharge areas.

The prevailing conditions imply that a clear definition of groundwater recharge is required. The common definition is "the process by which water is added to the zone of saturation". In the present situation, however, with very shallow groundwater, there is a large difference between gross and net recharge. The diurnal groundwater level fluctuations shown in

Figure 3-43 and Figure 3-44 clearly illustrate the influence of evapotranspiration on the groundwater zone during dry periods. Of course, this influence is most accentuated in locations with very shallow groundwater, but it is also evident in areas where the groundwater table is at depths of more than two metres. The modelling results presented above for a forested dry area, typically a recharge area, of an annual evapotranspiration slightly larger than 400 mm, indicate that the net groundwater recharge is approximately 225 mm in such an area.

Direct recharge from precipitation is the dominant source of groundwater recharge. However, the groundwater level measurements in the vicinity of Lake Bolundsfjärden and Lake Eckarfjärden presented in Figure 3-41 and Figure 3-42 show that the lakes may act as recharge sources to the till aquifers in the immediate vicinity of the lakes during the summer. The gradients from the lake to the surrounding areas are created by direct and indirect groundwater abstraction by evapotranspiration. Due to the low permeability of the bottom sediments, the resulting water fluxes can be assumed to be small. Also the Baltic Sea can potentially act as a source of groundwater recharge, especially during periods of high sea water levels. However, as illustrated in Figure 3-39 there is no correlation between the sea water level and the groundwater levels on land for most monitoring wells. Therefore, the influence of this recharge can be assumed to be restricted to areas below the sea and areas in the immediate vicinity of the coast line.

4.5 Flow systems and discharge

Similar to the external boundaries of the model area, the internal surface water and near-surface groundwater divides are assumed to coincide. The small-scale topography implies that many small catchments will be formed with local, shallow groundwater flow systems in the QD. With reference to the hydraulic conductivity profile of the tills dominating in the area, it is evident that a dominating part of the groundwater will move along very shallow flow paths. These local, small-scale recharge and discharge areas will overlay the more large-scale flow systems associated with groundwater flow at greater depths.

Interesting observations can be made in groundwater level time series from nearby wells in till and bedrock, as illustrated in Figures 3-46 to 3-52. Specifically, the groundwater level in the till seems to be considerably higher than that in the rock, both relative to the ground surface and in terms of absolute levels. Relative to the ground surface, the difference is 1.5–2 m. This difference exists even though the screens of the wells in till are installed at the QD/rock interface. The differences between the levels in till and rock are much larger than between different sections in the bedrock boreholes sealed off by packers. However, the groundwater levels in the bedrock boreholes are still above the QD/rock interface, indicating that no unsaturated zone exists below the interface.

As shown in Figure 3-49, groundwater levels in the till and the bedrock are correlated. The natural groundwater level fluctuations are, however, much smaller in the bedrock. The prevailing conditions mean that the groundwater flow has a downward component at the sites studied, i.e. there is an inflow from the till into the bedrock, although probably small. The difference between the levels in till and bedrock does not agree with the concept of a good hydraulic contact between QD and rock in a zone of relatively high hydraulic conductivity. A possible explanation for the low levels measured in the bedrock boreholes is that these intersect one/some of the highly conductive horizontal to sub-horizontal zones shown to exist in the shallow bedrock in the Forsmark area /SKB, 2005a/.

The permeability and storage characteristics of the materials in the till profile mean that very little water needs to be added to raise the groundwater table below a depth of approximately one metre. A groundwater recharge of 10 mm will give a 20 to 50 cm increase in groundwater level. During periods of abundant groundwater recharge, the groundwater level, also in most recharge areas, reaches the shallow part of the QD profile where the hydraulic conductivity is much higher and a significant lateral groundwater flow will take place. However, the transmissivity of this upper layer is so high that the groundwater level does not reach much closer to the ground surface than 0.5–1 m in typical recharge areas.

In discharge areas, defined as areas where the groundwater flow has an upward component, by definition no groundwater recharge takes place. However, not all discharge areas are saturated up to the ground surface, but water flows in the uppermost most permeable part of the profile. In unsaturated discharge areas, the soil water deficit is usually very small and in these areas water levels respond quickly to rainfall and snowmelt and contribute to runoff generation. So called saturated overland flow appears in discharge areas where the groundwater level reaches the ground surface.

In the F1.1 model, the lakes were assumed to be important permanent discharge areas. The new data presented in this report indicate that the situation can be more complicated. The groundwater level time series from Lake Bolundsfjärden and Lake Eckarfjärden discussed above show flow gradients from the lakes to the riparian zones during parts of the summer. Results from continued level measurements will show if this is a common situation, or if the conditions prevailing during summer of 2003 were extreme in this sense.

The hydraulic contact between the lakes and the groundwater zone is highly dependent on the hydraulic conductivity of the bottom sediments. Borings in the lake sediments show relatively thick sediments consisting of gyttja and thin layers of clay at most locations. In Lake Bolundsfjärden, the clay layer appears to be missing under large parts of the lake. However, the groundwater level time series in the vicinity of both Lake Eckarfjärden and Lake Bolundsfjärden (Figure 3-41 and Figure 3-42) and the pumping test at Lake Bolundsfjärden (Section 3.3.2) indicate low-permeable bottom sediments.

The brooks are considered as permanent discharge areas, although dry during parts of the year. The wetlands can either be in direct contact with the groundwater zone and constitute typical discharge areas or be separate hydrological systems with low-permeable bottom materials that have little or no hydraulic contact with the underlying aquifer. Information should be gathered to clarify the hydraulic contact between the major wetlands and the adjacent aquifers. The flat terrain within the model area implies that the spatial extents of recharge and discharge areas may vary during the year. The time dependence of the recharge-discharge pattern is further discussed in Chapter 5.

4.6 Hydrochemical data for interpretation of flow systems

By use of oxygen-18 as a tracer, information can be obtained on the runoff generation process as well on groundwater reservoir volumes /Lindström and Rodhe, 1986; Johansson, 1987b; Rodhe, 1987/. In particular, /Rodhe, 1987/ studied the runoff generation process by oxygen-18 in several small Swedish catchment areas. The results showed that also in peak runoff events groundwater (pre-event water) often constitutes the dominating fraction of the discharge. The infiltrating water pushes the “old” water downstream to form the peak runoff.

Also in an area with shallow QD, like the Forsmark area, the total reservoir volume in the till is larger than the annual groundwater recharge. The water stored in a 3 meter thick saturated till profile corresponds to 3–4 years of groundwater recharge. In traditional hydrological linear reservoir modeling, the active storage used is usually much smaller than the total storage. However, in hydrochemical and contaminant transport modelling also the total storage is of major interest.

Several other hydrochemical parameters, e.g. parameters derived from hydrogen and chloride isotope concentrations, are often used to characterise hydrogeological conditions. Such parameters are also included in SKB's programme for sampling and analyses of surface water and near-surface groundwater, but the results available in the F1.2 data freeze were limited.

A first attempt on coupled hydrochemical and hydrogeological modelling of shallow groundwater has been performed as a part of the hydrogeochemical modelling /SKB, 2005b/. The data presented and discussed below are from this report. In Figure 4-5, Piper diagrams for water samples from groundwater monitoring wells in QD and from percussion drilled boreholes in the bedrock are shown. From Figure 4-5 it is evident that both Ca-HCO_3 and Na-HCO_3,Cl type waters are represented among the samples from the groundwater monitoring wells in QD, whereas all the bedrock samples are of the Na-HCO_3,Cl water type.

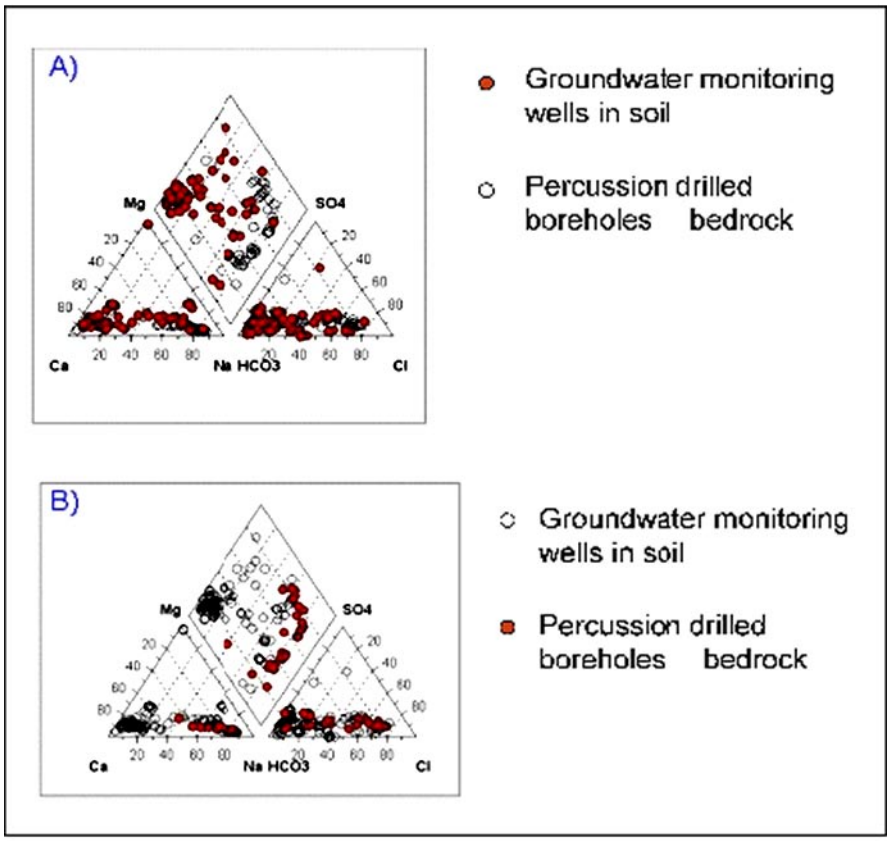

Figure 4-5. *Piper diagrams for groundwater samples from groundwater monitoring wells in QD and from percussion drilled boreholes in bedrock /SKB, 2005b/.*

The locations of the groundwater monitoring wells in QD that clearly belong to one of the two different water types are shown in Figure 4-6, together with the wells where the water can be characterised as "intermediate" in relation to these two types. It can be seen that the wells with the Na-HCO_3,Cl type water all are located at local topographic minima and that several of them are below lakes or the Baltic Sea.

In Figure 4-7 and Figure 4-8, chloride concentrations measured in precipitation samples and samples from groundwater monitoring wells in QD are plotted versus tritium and oxygen-18, respectively. The lowest tritium concentrations are found below Lake Bolundsfjärden, Lake Gällsboträsket and Lake Eckarfjärden. However, the chloride concentrations below the lakes are quite different. In Figure 4-8, it can be seen that the groundwater below the lakes plot along a hypothetical mixing line between the Littorina water and the wells on land.

In a recharge-discharge area perspective, it can be assumed that groundwater samples from both recharge and discharge areas in the local and very shallow systems in the QD belong to the Ca-HCO_3 type of water. Due to the high calcite content in the QD, the water will quickly be calcite saturated or oversaturated.

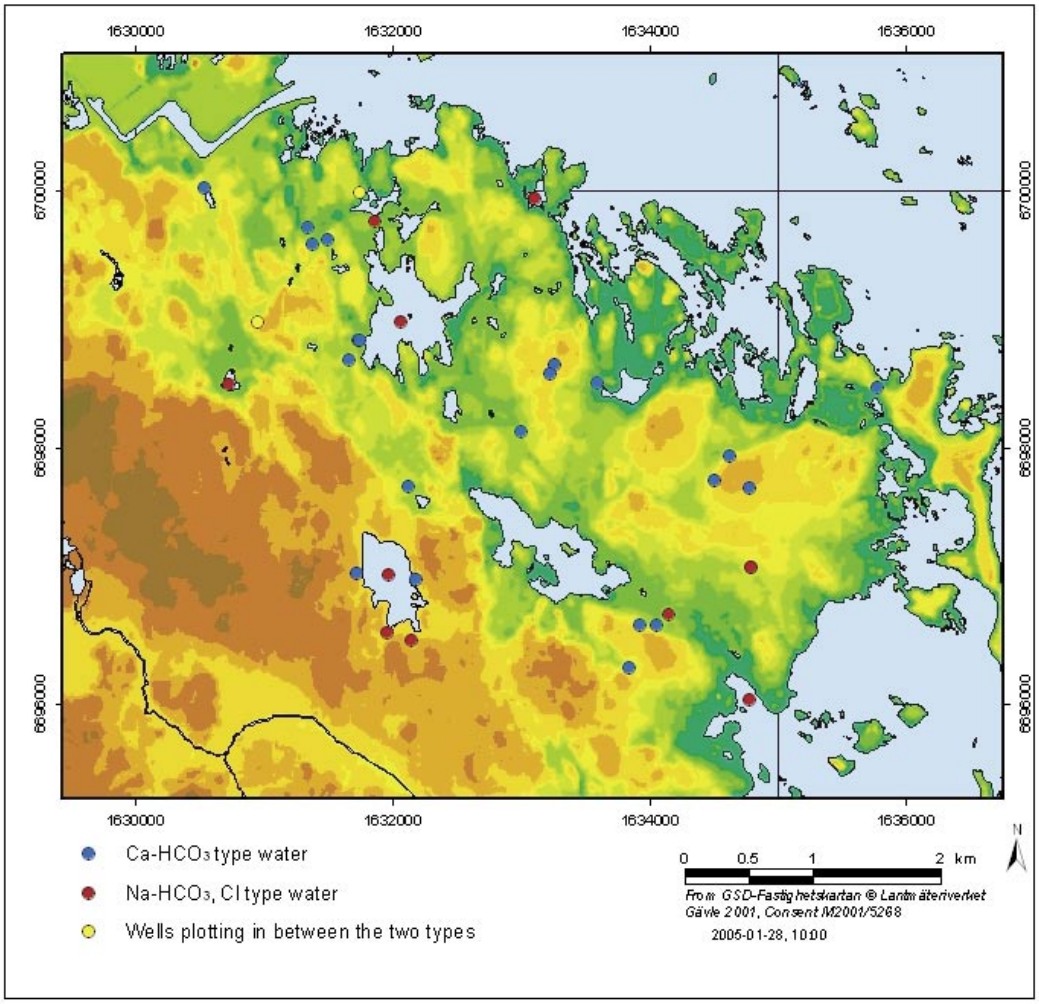

Figure 4-6. *Location of the groundwater monitoring wells in QD with Ca-HCO_3 (blue) and Na-HCO_3 ,Cl type water (red), and wells plotting in between the two types (yellow) /SKB, 2005b/.*

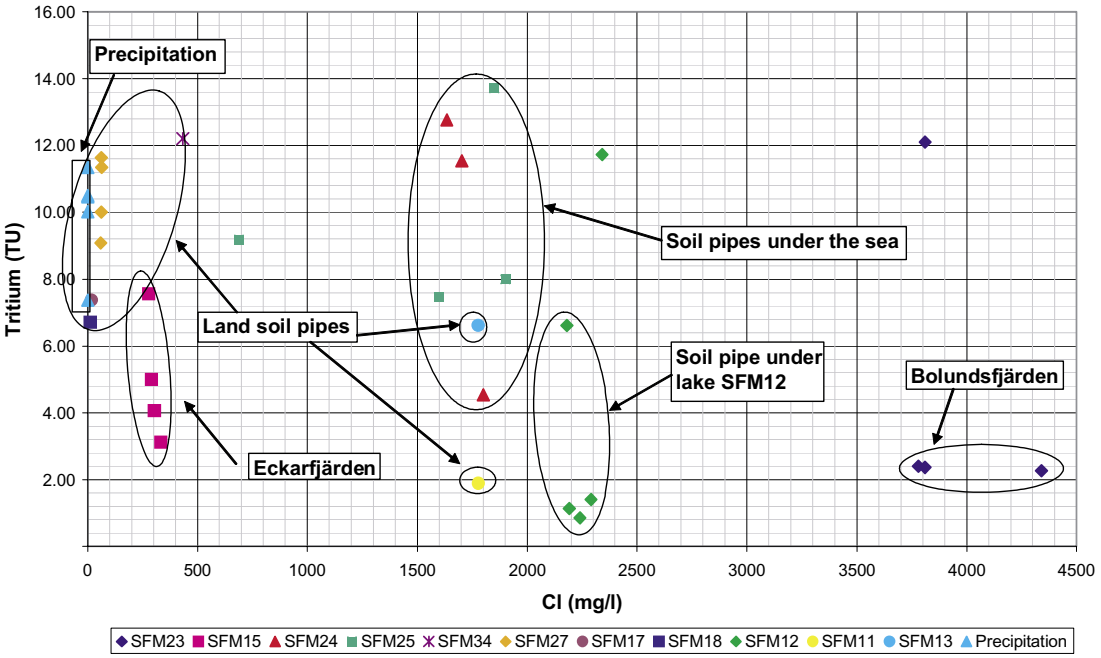

Figure 4-7. *Tritium versus chloride for some groundwater monitoring wells in QD /SKB, 2005b/.*

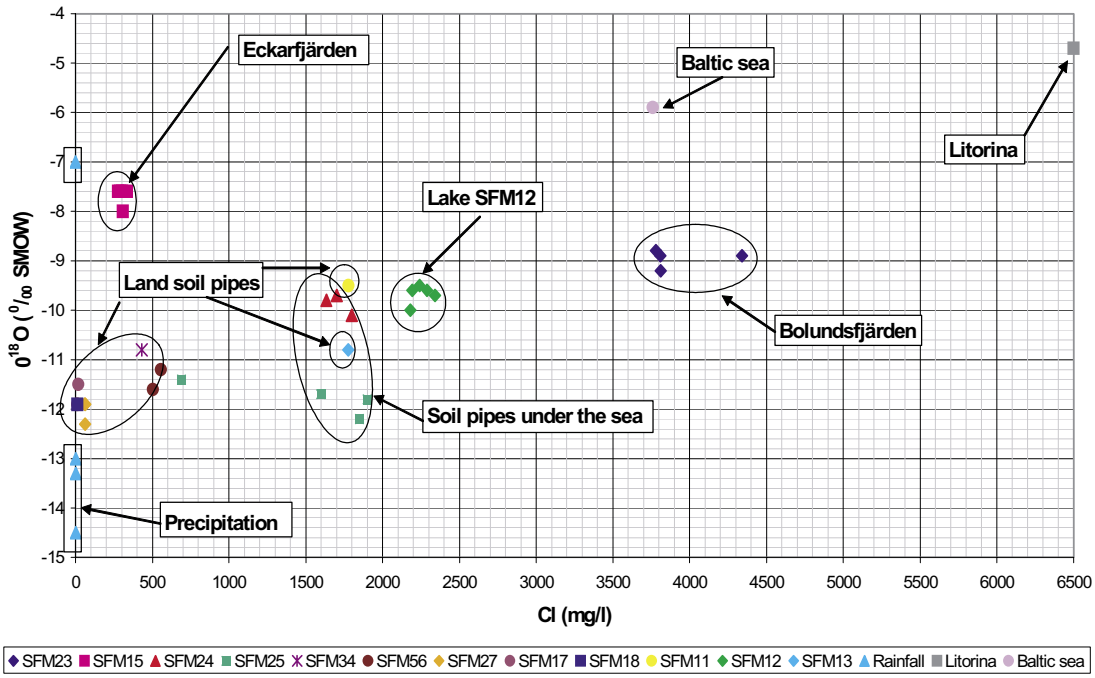

Figure 4-8. *Oxygen-18 versus chloride for some groundwater monitoring wells in QD /SKB, 2005b/.*

The “old” water with high chloride content that has been found below the lakes (and also in some wells in the immediate vicinity of the lakes) can be interpreted in two alternative ways. It can either be interpreted as typical discharge areas for deeper systems with a continuous flow of old, more saline water from below, or as areas with more or less stagnant water, perhaps even underlain by younger and less saline water in the highly conductive

horizontal to sub-horizontal zones of the shallow bedrock. For the overall understanding of the hydrogeology in the area, it is important to resolve which of these two interpretations that is correct.

4.7 Other supporting data and models

The descriptive model of surface hydrology and near-surface hydrogeology can be supported by a number of different types of data and models, both hydrological/ hydrogeological and from other modelling disciplines. Important aspects that can be evaluated using data and models from other disciplines include the overall flow pattern, especially the spatial distribution of recharge and discharge areas, and residence times of water in different parts of the system. The data and methods for support and evaluation of the descriptive model can be summarised as follows.

Hydrological and hydrogeological data: Mapping/comparison of "independent" data, i.e. data not used in the model development (e.g. measured groundwater levels or flow rates).

GIS-based hydrological modelling: Flow modelling based on topography and possibly also other meteorological, geological and/or land-use parameters (see Chapter 5).

Hydrological and hydrogeological process modelling: Flow modelling based on analytical or numerical solutions of flow equations, integrating various hydrological/ hydrogeological data with other inputs (see Chapter 5).

Mapping of QD, soil types and vegetation: Comparison of flow pattern with spatial distributions of QD, soil types and vegetation; the evaluation is based on assumed or observed correlations between geology/soil type/vegetation and hydrological/ hydrogeological characteristics.

Topographical data and tools and classification systems based on topographical data: Direct comparisons with the Digital Elevation Model (DEM) or classifications based on quantities derived from the DEM (slope or higher-order derivatives); the TOPMODEL system has been applied within the site investigations /Lundin et al. 2004/.

Hydrochemical data and coupled hydrogeological-hydrogeochemical modelling: Direct comparisons with spatial distributions of hydrochemical parameters (main elements and specific components such as isotopes can be used to distinguish "water types" and to infer information on the flow pattern), and use of coupled quantitative modelling of flow and hydrogeochemical processes for joint evaluation of hydrogeochemical and hydrological/ hydrogeological data (see Section 4.6).

Whereas most of the data and models listed above are or will be available within the site investigations, the supporting activities performed in connection with the present model version were limited. This is mainly due to time constraints. However, first attempts on GIS-based and process-based hydrological modelling are presented in Chapter 5 of this report. Furthermore, evaluations of the available hydrochemical data are presented in the main SurfaceNet report /Lindborg (ed), 2005/ and in the background report from the hydrogeochemical modelling /SKB, 2005b/, see also Section 4.6. The use of, primarily, topographical and hydrochemical data and models in connection with the hydrological/ hydrogeological modelling of the surface system will be explored in the next model version.

5 Quantitative flow modelling

5.1 Introduction and general objectives

As described by /Rhén et al. 2003/, quantitative flow modelling is performed as an integrated part of the site descriptive modelling. Specifically, the flow modelling serves the following three main purposes (see also /SKB, 2004a/):

Model testing: Simulations of different geometric interpretations or boundary conditions, carried out in order to try to disprove a given geometric interpretation or boundary condition, and thus reduce the number of alternative conceptual models of the system.

Calibration and sensitivity analyses: Flow modelling performed in order to explore the impact of different assumptions related to initial and boundary conditions and hydraulic properties.

Description of flow paths and flow conditions: Model calculations aimed to enhance the general understanding of the site-specific groundwater flow system.

In view of these main purposes and the present status of the surface hydrological and near-surface hydrogeological modelling, the overall objectives of the quantitative flow modelling in F1.2 were to

- start developing the site understanding by testing some selected aspects of the descriptive model,
- deliver specific output data to the ecological systems modelling,
- test selected modelling tools within the SKB environment.

Although the flow modelling is presented separately and without detailed references to the conceptual and descriptive modelling, the activities related to conceptual/descriptive and quantitative modelling have been integrated. However, the first-attempt character of the modelling work, in combination with the time constraints, enabled less interactions (and iterations) between the conceptual/descriptive and quantitative modelling than in a "complete modelling process". This has also been the case for the interactions with other modelling disciplines, such as the hydrogeological and hydrogeochemical modelling of the rock.

5.2 GIS-based modelling with ArcGIS

5.2.1 Model components

The extension "Hydrological modelling" in ArcGIS 8.3 is a modelling tool in which relatively simple, topography-driven hydrological models can be developed. The tool requires a Digital Elevation Model (DEM) as input. The DEM is the basis for the flow direction and flow accumulation calculations. In the model, the water is flowing down gradient towards areas of lower elevation. No other driving forces or processes than the differences in elevation are considered. There are three main functions in the ArcGIS Hydrological modelling extension, as follows:

Fill sinks: A correction of the DEM, in which local sinks are filled up to the level of the lowest neighbouring cell.

Flow direction: Calculation of the flow direction for each cell resulting in a grid referred to as the "direction grid".

Flow accumulation: Using the "direction grid" as input, the number of cells generating water to a specific cell is calculated; the resulting grid is referred to as the "accumulation grid".

Since a low value in the accumulation grid indicates that there are few upstream cells, the grid can be used to identify recharge areas. Consequently, a high value in the accumulation grid specifies a discharge area, e.g. a stream. By using the accumulation grid and a specified value of the specific discharge in the area as input (must be obtained from elsewhere), the discharge in each cell can be calculated. Thus, the results for a cell located at a stream outlet to the sea provide an estimate of the discharge from the catchment area associated with that outlet.

5.2.2 Objectives

The main objective of the F1.2 hydrological modelling with ArcGIS 8.3 was to calculate the spatial distribution of total runoff, which is used in the ecological systems modelling. These calculations have been performed and the results have been delivered to the users. Furthermore, the GIS-based modelling is used to illustrate the overall flow pattern within the Forsmark area, to estimate discharges in water courses, and to evaluate uncertainties related to the DEM.

5.2.3 Assumptions and input data

The only input data used in the ArcGIS-based hydrological model is the Digital Elevation Model (DEM) of the Forsmark area /Brydsten, 2004/ and an estimate of the specific discharge. The flow modelling with ArcGIS is performed assuming a spatially uniform specific discharge. Specifically, the estimate presented in the F1.1 model, i.e. a specific discharge of 6.5 $l \cdot s^{-1} \cdot km^{-2}$ /SKB, 2004a/ in the Forsmark area, is used in present work.

As described above, the model is driven by topographical gradients only. It is a steady-state model and the input value on the specific discharge is an annual mean value derived from discharge measurements further inland and an estimated difference between these inland locations and the coast. The model considers the total runoff only, which means that no distinction is made between surface water and groundwater flows. Thus, the calculated discharges can be assumed to represent surface water flows in the downstream part of a catchment, and the sum of surface water and groundwater flows in the upstream part. This also implies that surface water divides are assumed to coincide with groundwater divides.

In addition, it should be noted that the modelling is subject to uncertainties related to the DEM. Specifically, ditches and other "constructions" resulting from water-related activities that alter the "natural" flow field (e.g. deepening of existing brooks, cf Section 4.3.2) may be lost in the interpolations underlying the DEM. This may result in differences between actual flow directions and those indicated by the overall topography.

5.2.4 Results

The GIS model has been applied to the whole regional model area of Forsmark. The results shown in the following are a few examples from the GIS modelling work.

Runoff and water courses

A high value in the "accumulation grid" can be taken as an indication of a water course. Figure 5-1 shows a comparison of the modelled water courses and the water courses obtained from the Fastighetskartan map (the Real Estate map). Specifically, the modelled water courses (the red lines) are the grid cells that have a mean annual discharge above 0.5 $l \cdot s^{-1}$, which means that even very small streams are included in the figure. The majority of these small streams are dry during most of the year.

Since the model is driven by topography only, as given by the DEM, there are some areas where the modelled water courses do not match the actual ones on the Fastighetskartan map. This can be seen in the water system in the area between Lake Bolundsfjärden, Lake Gällsboträsket and Lake Eckarfjärden (Figure 5-1). In this area, the model results indicate that the surface water system may have been altered by human impact, which, as described in Section 4.3.2, also is the case.

For example, the figure shows a modelled water course between Lake Labboträsket and Lake Gällsboträsket. This water course does not exist in reality. There is a field controlled water divide between these two lakes. The calculated flow direction in this area is indicated by a red arrow in Figure 5-1, whereas the mapped flow direction is indicated by a blue arrow. Other reasons for deviations from the mapped water courses can be associated with the resolution of the DEM. Since the DEM grid cells are 10 m by 10 m, small ditches or sinks are not included in the modelling. The terrain in Forsmark is very flat and there are no large water courses within the model area. Water courses that are dry during long periods are not marked on the Fastighetskartan map. However, the model result can also be viewed as an illustration of where the water is accumulating when heavy rains occur (rather than as a map of permanent water courses).

The calculated discharges at the points marked in Figure 5-1, which in most cases correspond to outlets from the model area to the sea, are listed in Table 5-1. The discharges in the water courses no 3–5 (Q_3, Q_4 and Q_5) are negligible compared to the flow in the other water courses. These water courses can be expected to be dry during most of the year, such that flow occurs only after rainstorms and during wet periods. The dominating discharge occurs in Q_2, which is the outlet of the water course dewatering the catchment of Lake Norra basängen, Forsmark 2 /Brunberg et al. 2004/. In this outlet, the mean annual discharge is 88 $l \cdot s^{-1}$. However, it should be noted that the calculated discharges in Q_2, Q_3 and Q_6 are affected by the difference between the modelled and real flow directions in the Labboträsket-Gällsboträsket area (cf the red and blue arrows in Figure 5-1).

Table 5-1. Calculated discharges in the Forsmark area (cf Figure 5-1).

	Discharge ($l \cdot s^{-1}$)
Q_1	23
Q_2	88
Q_3	1
Q_4	11
Q_5	4
Q_6	46
Q_7	18

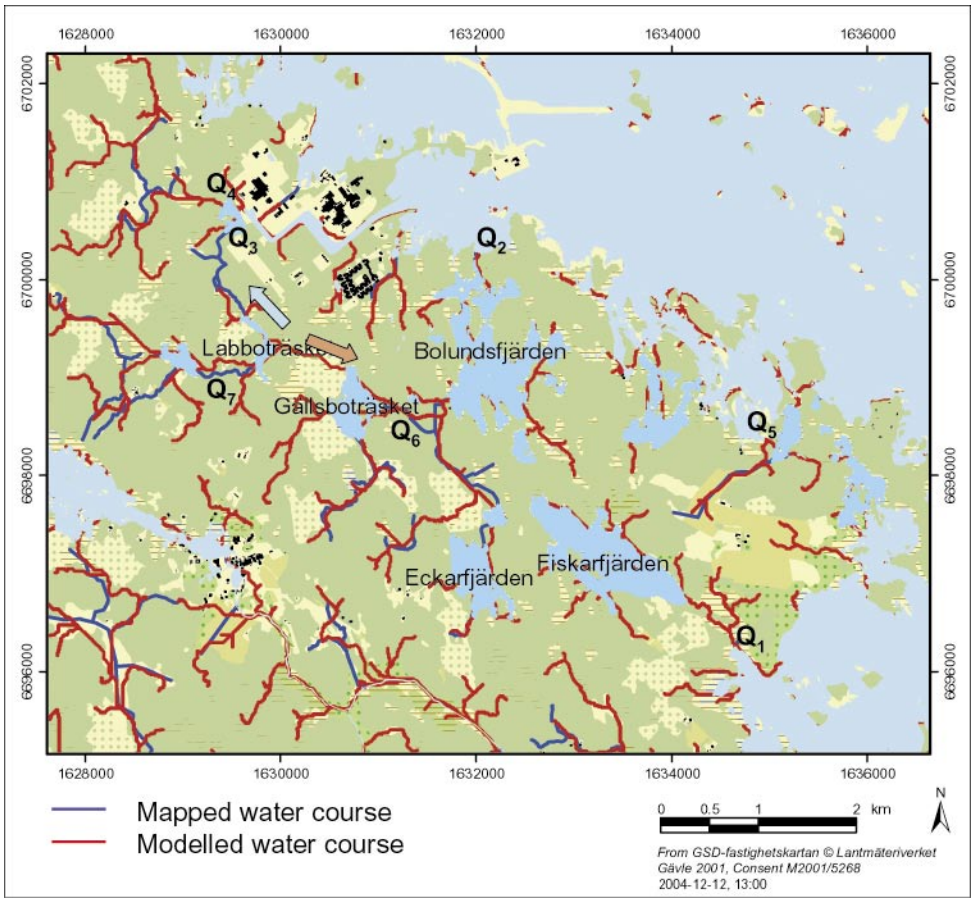

Figure 5-1. *Modelled water courses and water courses from the Fastighetskartan map. The red arrow indicates the calculated flow direction and the blue arrow the mapped ("true") direction (see text).*

Recharge and discharge areas

Recharge and discharge areas have been identified with the ArcGIS model. In this modelling, areas consisting of cells with zero values in the "accumulation grid", i.e. cells without upstream cells providing inflow, were defined as recharge areas. These areas are marked with red colour in Figure 5-2. In this figure, areas consisting of cells with accumulation grid values above 500 are marked with blue colour. Since each grid cell is 10 m by 10 m, this implies that cells receiving water from areas larger than 0.05 km^2 are defined as discharge areas.

Figure 5-2 clearly illustrates the local, small-scale character of the flow system described in the preceding chapters. Thus, the modelling results support the observations in Chapter 3 and the description in Chapter 4. The locations of recharge and discharge areas are strongly influenced by the local topography. In the present steady-state modelling context, the lakes in the area are most probably discharge areas. However, the GIS model does not take the lakes into consideration; they are represented as flat water surfaces in the DEM. In the descriptive model, the "river valleys" and water courses are assumed to be discharge areas throughout the year. This assumption is in agreement with the modelling results.

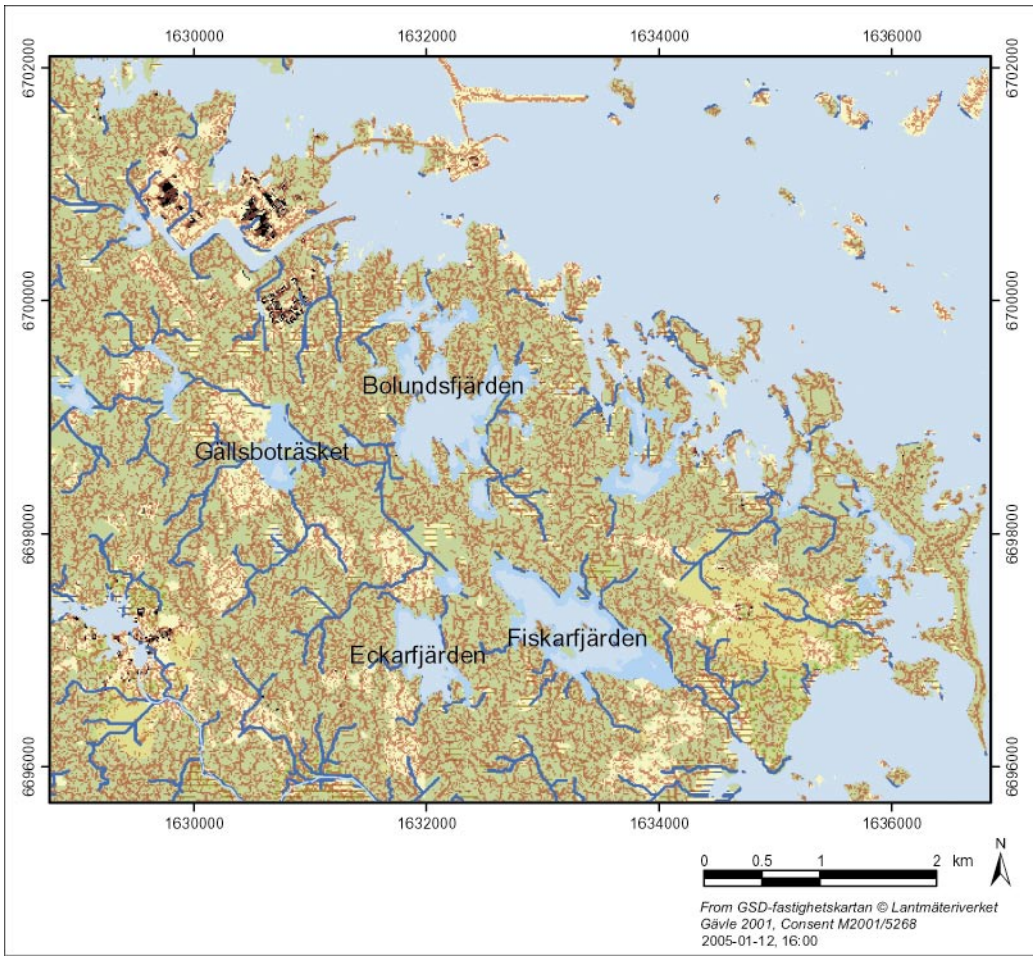

Figure 5-2. *Recharge (red) and discharge (blue) areas identified with the GIS model. Areas of colours other than red or blue are "intermediate areas", i.e. neither recharge nor discharge areas according to the definitions employed in this modelling (see text).*

Flow pattern

The GIS-modelled flow pattern provides a visualisation of the surface water flow system in the model area. The flow pattern in the catchment of Lake Eckarfjärden is shown in Figure 5-3. The arrows are flow weighted, which means that a long arrow corresponds to a high value in the "accumulation grid". By following the field controlled water divide (red line) one can investigate the accuracy of the model. It can be seen that water flows from the catchment boundaries towards the lake in most of the catchment area.

As shown in the more detailed representation of the southern part of the catchment area in Figure 5-4, there also exist places where water flows towards the field controlled water divide. This type of errors can be related to errors in the DEM. Thus, the model can be used to identify errors in the DEM, and to quantify uncertainties related to these errors. Such analyses are of interest to all users of the DEM, especially those using it as input to flow modelling (e.g. in groundwater flow modelling of the deep rock when the topography is used as upper (pressure) boundary condition). It should be noted, however, that the GIS modelling itself is sensitive to parameters associated with the "Fill sinks" function. Therefore, a complete analysis of the implications of uncertainties related to the DEM should involve also this sensitivity.

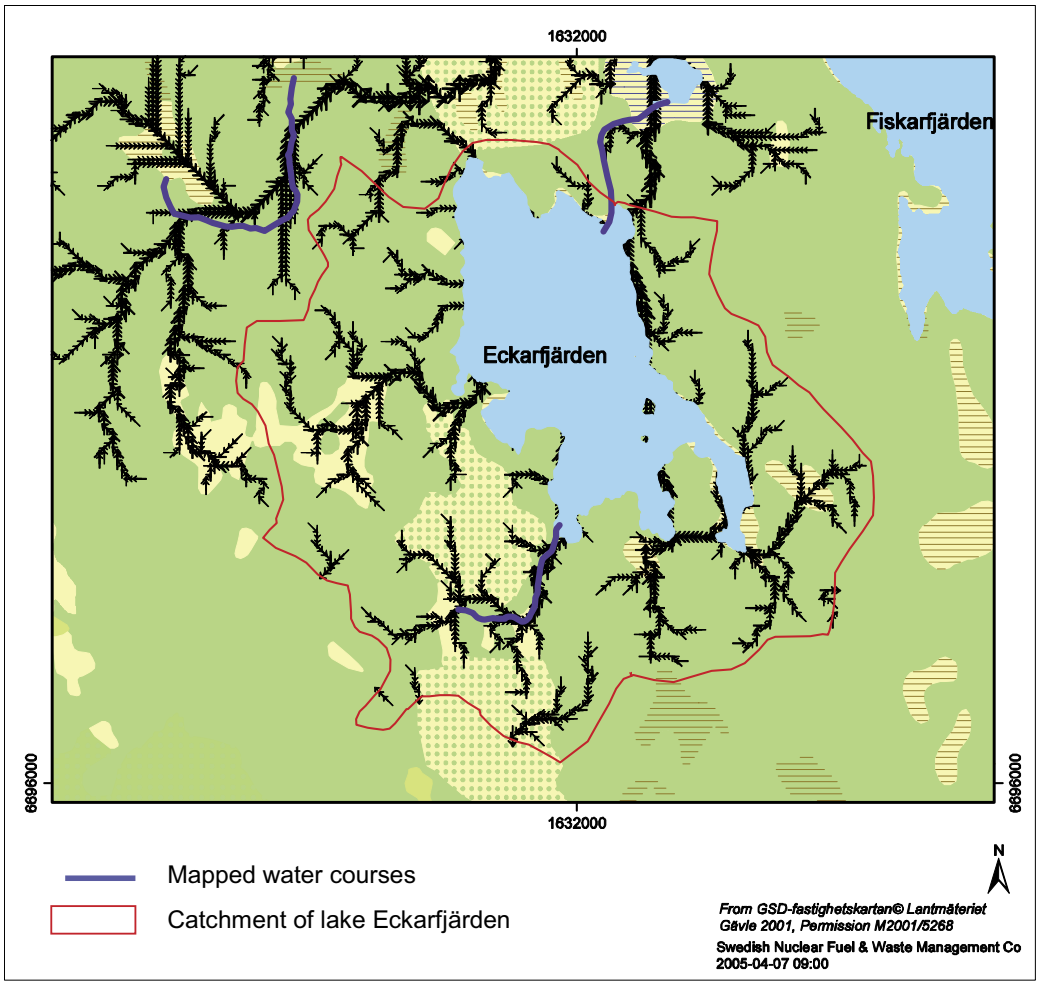

Figure 5-3. *Flow pattern in the catchment of Lake Eckarfjärden.*

Identification of catchment areas

In the Forsmark area, 25 catchment areas have been identified and described, see Section 3.2.1 and /Brunberg et al. 2004/. All catchment area boundaries in the area are controlled in the field. However, the GIS-based model can be used to identify sub-catchments, e.g. the drainage area to a specific wetland area, which is particularly useful when extracting hydrological information for use in the ecosystems modelling. In the following, a comparison is made between the field-controlled catchments and those obtained from the ArcGIS model (i.e. more or less directly based on the DEM). Although dealing with catchment areas only, this comparison also gives an indication of the uncertainties associated with the use of GIS-modelled hydrological data for other spatial objects.

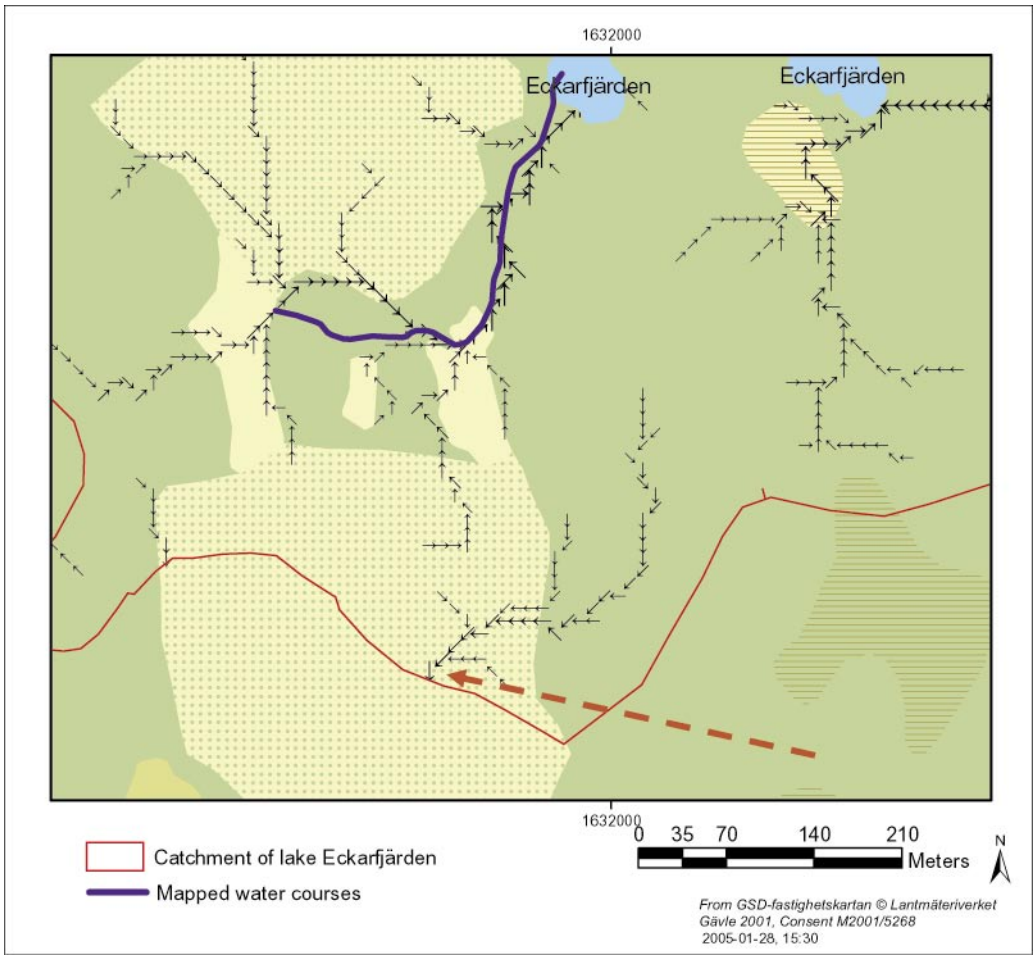

Figure 5-4. *Detail of flow pattern in the southern part of the catchment of Lake Eckarfjärden. The red arrow indicates one of the places where the modelled flow direction contradicts with the field-controlled water divide.*

As shown in Figure 5-5, the modelled catchments coincide with the field controlled catchment area boundaries in most of the model area. The field controlled boundaries are marked with dashed lines and the number of each catchment is marked in the figure. The modelled catchments are marked with different colours. All the 25 catchment areas can be located with the GIS model. Catchment areas no 2:4 and 3:1 consist in the GIS model of two sub-catchments each. However, in both cases the total areas of the two sub-catchments are almost the same as the areas of the field-controlled catchment areas.

There is an obvious divergence between the field-controlled catchment boundary and the model result for the boundary between catchments 1:3 and 2:8. In the model, water flows across the field controlled boundary from area 1:3 to area 2:8. According to /Brunberg et al. 2004/ this is a no-flow boundary and the outlet from catchment no 1 (including 1:3) is just south of the nuclear power plant. In the GIS model, the water from most of catchment no 1 discharges through catchment no 2. This explains the small calculated discharge in point Q_3 in Table 5-1. Figure 5-5 illustrates this difference in flow patterns; the black arrows are the flow pattern according to the GIS model, and the red arrows show how the water flows in reality.

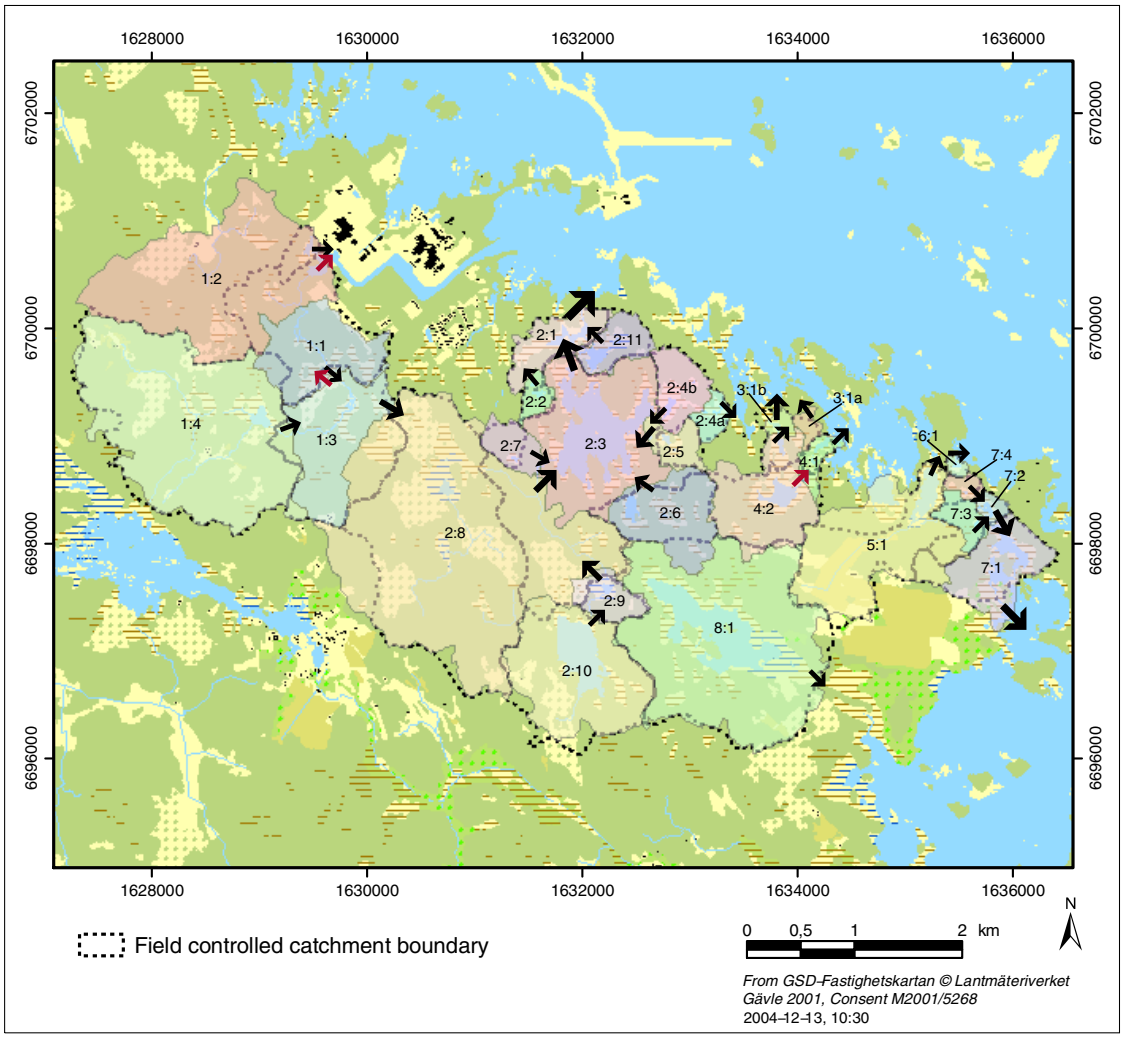

Figure 5-5. *Comparison of modelled and field controlled catchment area boundaries.*

The comparison illustrated in Figure 5-5 and quantified in terms of absolute and relative differences in Table 5-2 (a negative difference means that the area estimated by the GIS model is smaller than the field-controlled area) shows that the differences between modelled and field-controlled areas range from zero to be on the order of the size of the catchment area (with catchment no 1:2 as the only exception). However, the difference between the total area of the field-controlled catchments and that of the modelled catchments is relatively small, 1.5 km^2 (7.4%).

Concerning the catchment areas of the main lakes in the area, it can be noted that the catchment areas of Lake Eckarfjärden (2:10) and Lake Fiskarfjärden (8:1) are well predicted by the GIS model, whereas the deviations between modelled and field-controlled areas are large for Lake Bolundfjärden (2:3) and Lake Gällsboträsket (2:8). It can be noted that deviations for the two latter lakes concern approximately the same area, appearing as a negative difference for Lake Bolundsfjärden and a positive one for Lake Gällsboträsket.

Table 5-2. Comparison between field-controlled and GIS-modelled catchment areas. The largest absolute and relative differences are marked with green and yellow, respectively.

Catchment area no	Field-controlled area (km²)	Modelled area (km²)	Difference (km²)	Relative difference (%)
1:1	1.09	0.71	–0.38	–34.9
1:2	0.10	2.16	+2.06	+2,060.0
1:3	1.19	0.81	–0.38	–31.9
1:4	2.74	2.78	+0.04	+1.5
2:1	0.35	0.35	0.00	0.0
2:2	0.07	0.10	+0.03	+42.9
2:3	2.50	1.39	–1.11	–44.4
2:4*	0.40	0.41	+0.01	+2.5
2:5	0.14	0.18	+0.04	+28.6
2:6	0.48	0.64	+0.16	+33.3
2:7	0.13	0.20	+0.07	+53.8
2:8	2.89	4.30	+1.41	+48.8
2:9	0.18	0.23	+0.05	+27.8
2:10	1.30	1.24	–0.06	–4.6
2:11	0.24	0.25	+0.01	+4.2
3:1*	0.22	0.11	–0.11	–50.0
4:1	0.07	0.11	+0.04	+57.1
4:2	0.62	0.75	+0.13	+21.0
5:1	0.94	1.32	+0.38	+40.4
6:1	0.04	0.03	–0.01	–25.0
7:1	0.56	0.56	0.00	0.0
7:2	0.70	0.07	–0.63	–90.0
7:3	0.20	0.15	–0.05	–25.0
7:4	0.08	0.06	–0.02	–25.0
8:1	2.93	2.74	–0.19	–6.5

* Modelled catchments no 2:4 and 3:1 consist of two sub-catchments.

5.2.5 Evaluation of uncertainties

Five main groups of uncertainties associated with the GIS-based flow modelling have been identified. These are the uncertainties related to

- the Digital Elevation Model (DEM),
- the GIS modelling functions,
- the basic assumptions and restrictions of the GIS model,
- the conceptual model of the site,
- the other input data used in the modelling.

The main uncertainties in the present GIS-based model are associated with the DEM and the fact that the model is driven by the modelled topography only. Since the horizontal resolution of the DEM is 10 metres, all details in the topography are not included in the modelling. Due to the interpolations made in the model development, large divergences from the real topography occur in some parts of the DEM, not only in areas with small ditches or local sinks and heights.

The calculated catchments do not always coincide with the field controlled water divides. In areas with a flat terrain, small errors in the DEM may cause large differences in flow patterns. The fact that the DEM does not take the details of human impacts, such as ditching, into account is an important source to uncertainty in the runoff estimates for the individual catchments. This uncertainty will to large extent be resolved when more field data on the water courses become available.

For areas where information about ditching is already available, the model can be used to investigate the effects of human impact on the flow pattern. Evaluations of the effects of errors in the DEM are valuable because the DEM is used as input data in other hydrological and hydrogeological modelling, including the modelling of surface hydrology and near-surface hydrogeology and the hydrogeological modelling of the deep rock.

The uncertainty related to the "fill sink function" is judged to be the most important one associated with the GIS modelling functions. As described above, this function fills up a local sink to the lowest level of the adjacent cells. This means that no surrounding cell has a lower elevation than the actual cell. This may cause "artificial" flow patterns. The sensitivity to the parameters governing the "fill sink function" has not been evaluated in this work.

In the conceptual model presented in Chapter 4, it is assumed that the groundwater divides coincide with the surface water divides. If the actual water divides for surface water and groundwater differ significantly, the GIS model would strictly be valid for the surface water system only. It should be noted that the ArcGIS model discussed here provides quantitative information on the total runoff only; the division of the total runoff into groundwater and surface water flows is not quantified. Furthermore, the GIS model is restricted to steady-state conditions, which implies that the significance of transients for the discharge estimates cannot be tested.

The specific discharge is the only additional input parameter that could cause uncertainty in the flow model. In the present model, the value for the specific discharge is based on measurements outside the Forsmark area and an estimated gradient from the inland area where the measurements were made to the coastal model area. The value can be considered a rough estimate of the average discharge in the area. Thus, no spatial variations in the specific discharge within the model area are considered.

5.3 GIS-based modelling with PCRaster-POLFLOW

Other GIS-based hydrological modelling tools provide extended capabilities compared to the model based on the ArcGIS "Hydrological modelling" extension discussed above; the modelling in Section 5.2 was based on a direct application of the DEM and a constant specific discharge. Such extended capabilities could concern transient flow conditions, the processing of the topographical data, the quantification of the specific discharge, or the interactions between surface water and groundwater.

The PCRaster-POLFLOW approach uses a single language for performing both GIS and process modelling operations, and allows for analyses of temporally and spatially varying flow and transport processes within catchments on various spatial-temporal scales /Darracq and Destouni, 2005; Darracq et al. 2005; Prieto, 2005; Destouni et al. 2005/. PCRaster-POLFLOW has been applied to pre site-investigation data from the Forsmark area /Jarsjö et al. 2004/. For the present report, the model presented by /Jarsjö et al. 2004/ has been updated with Forsmark 1.2 site investigation data. The results from this updated model are described below (a complete presentation of the updated model will be provided in a forthcoming report by J Jarsjö and co-workers). For a more detailed description of the modelling approach and the original Forsmark model, the reader is referred to /Jarsjö et al. 2004/.

Previously, PCRaster-POLFLOW was primarily applied at relatively large river basins and catchments, such as Rhine, Elbe and Norrström, see, e.g. /Greffe, 2003/. A main goal with the Forsmark site application was to investigate whether the model at this much smaller scale can provide results that are consistent with independently measured stream flow data or area averaged runoff. For this purpose, a relatively simple steady-state version of the model could be and was used. In the Forsmark application, the PCRaster-POLFLOW modelling approach used empirical equations and data for quantification of the specific discharge and its distribution on surface and subsurface flows. Specifically, the input data included spatially variable meteorological, geological and land use parameters, which are used either in empirical equations or as a basis for a classification of different subareas within the model area.

5.3.1 Model components

In the PCRaster-POLFLOW approach, a GIS-based processing similar to that described in Section 5.2.1 is performed to obtain flow directions and flow accumulation in the model grid. However, additional calculations are made to quantify the spatially variable input to the system and the distribution of this input on different sub-systems.

The calculation scheme is summarised in Figures 5-6 and 5-7. First, a precipitation surplus, PS, is calculated for each grid-cell (in $mm \cdot year^{-1}$) as the difference between the precipitation, P, and actual evapotranspiration, E, i.e. PS = P – E (see “Step 1” of Figure 5-6). Two different and independent methods are used to estimate the actual evapotranspiration, namely

- **Method 1** – using empirical equations expressing the actual evapotranspiration as a function of precipitation and potential evapotranspiration (which, in turn, depends on the temperature).
- **Method 2** – based on a classification of texture and land cover, where different classes are assigned different actual evapotranspiration values using calibrated data from catchments in Germany.

It should be noted that PCRaster is flexible and allows the empirical relations to be modified or changed if needed.

Following the quantification of PS, it is assumed that a certain fraction of PS is available for groundwater recharge, according to a groundwater recharge index f_{gw}, which takes on values between 0 and 1 (“Step 2” of Figure 5-6). The groundwater recharge index is determined as a function of ground surface slope and land cover. The remaining fraction ($1-f_{gw}$) is then available for surface water runoff from the grid cell directly from the precipitation surplus in the cell. The resulting total runoff of water precipitated within the cell, R, must be equal

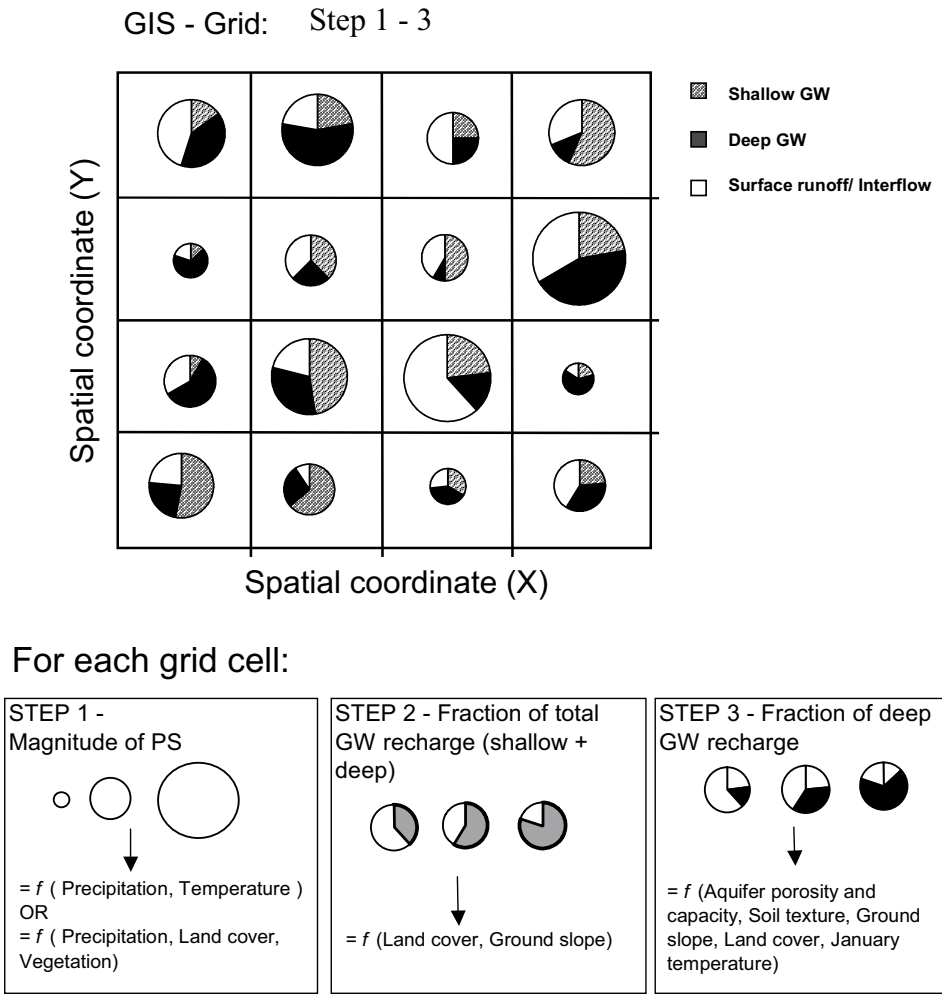

Figure 5-6. *Estimating the distribution of available precipitation surplus, PS, on recharge (in mm·year^{-1}) of deep groundwater and shallow groundwater, and surface water discharge in each grid cell /Jarsjö et al. 2004/.*

to PS at steady-state and is expressed as the sum of the surface runoff and soil interflow contribution, R_S, and the groundwater discharge contribution R_{gw}, i.e. $R = R_S + R_{gw} = PS$, where $R_{gw} = GW = f_{gw} \times PS$ and $R_S = (1\text{-}f_{gw}) \times PS$.

/Jarsjö et al. 2004/ also describe a further sub-division of the groundwater recharge into near-surface and deep recharge components ("Step 3" of Figure 5-6). However, no such sub-division is made in the Forsmark calculations. For estimation of the total water discharge through each grid cell, local flow directions of surface water and possibly also groundwater (arrows in Figure 5-7) are estimated on the basis of the digital elevation model. Each cell is then associated with a unique flow direction, into the neighbour with the lowest elevation. For each cell i, an associated sub-catchment area Ω_i is defined according to Figure 5-7, including all cells upstream of cell i that contribute to the flow through the cell, on the basis of all upstream defined flow directions. Thus, the total flow through cell i is the sum of the PS generated locally within the cell, and the inflow from the sub-catchment area Ω_i.

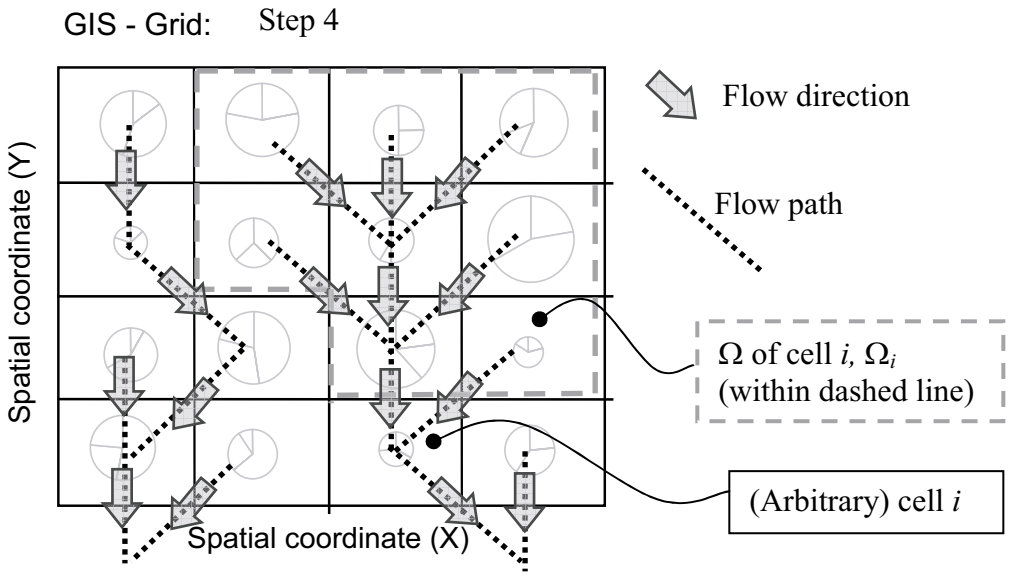

Figure 5-7. *Estimating the total water discharge through each grid cell i within upstream sub-catchment area* Ω_i */Jarsjö et al. 2004/.*

This flow represents the sum of surface water and groundwater discharge from each cell to downstream areas, with a main underlying assumption being that the sub-catchments and the mean flow directions for both the surface water and the groundwater discharge out from each sub-catchment are at least approximately the same; this assumption will generally be more valid for greater sub-catchments, i.e. the further downstream one goes within the main catchment. The calculations illustrated in Figure 5-7 are similar to those performed in the GIS-based modelling described in Section 5.2. However, some additional modifications of the DEM were made in the PCRaster-POLFLOW modelling. In particular, the ground surface level was lowered along the mapped water courses, in order to account for the local depressions determining the surface runoff.

In cells where the headwater reaches of main streams first appear, such that these cells but not their upstream sub-catchments Ω_i include a main stream reach, the upstream groundwater flow contribution may be assumed to discharge into, and directly add to, the total stream water flow of the stream reach in cell i. The groundwater discharge is then added either totally where the headwater reaches first appear (for simplicity), or, for instance, distributed along the stream according to some distribution function.

If a main stream is present in the considered cell, its stream water flow will generally be much greater than the groundwater flow not discharging into the stream, and hence the total flow can then on sound physical grounds be assumed to provide a good estimate of the stream water flow. In addition, the Forsmark application is primarily focused on water discharges in relatively large sub-catchments and coastal outlets of the Forsmark catchment, for which the flow can be assumed to consist almost only of stream water.

On the other hand, if a main stream and thereby a clear groundwater discharge area is not present in the considered cell and its sub-catchment area Ω_i, then the groundwater flow can be at least approximately quantified by substituting PS for $GW = f_{gw} \times PS$ in the flow calculation. The corresponding surface water flow occurring in minor streams or as overland flow within the cell and its sub-catchment is then obtained by substituting PS for $R_S = (1\text{-}f_{gw}) \times PS$ in the summation of the flow through cell i.

5.3.2 Objectives

The objective of the original study reported by /Jarsjö et al. 2004/ was to develop a GIS-based surface water model of the Forsmark area on the basis of the then available (pre site-investigation) dataset, using the PCRaster toolkit. The specific objective of the model update presented herein (also performed by J Jarsjö and co-workers) is to include the presently available site investigation data in the model, and thereby provide a common basis for comparisons with other model results obtained within the site descriptive modelling.

In particular, the update facilitates a comparison between the PCRaster-POLFLOW model and the GIS model developed using the ArcGIS "Hydrological modelling" extension only, which can be used to assess the effects of the additional features considered in the former modelling approach. However, it should be noted that the update of the PCRaster-POLFLOW model does not involve calibration against, for instance, discharge measurements. This implies that the same, generic equations and data are used in the calculations of PS and f_{gw} as in /Jarsjö et al. 2004/.

5.3.3 Assumptions and input data

The assumptions and input data in the first PCRaster-POLFLOW model of the Forsmark area are described by /Jarsjö et al. 2004/. The model area considered in the update of the model is shown in Figure 5-8, where also the coastal outlets in which the discharge is calculated are indicated. As compared to the original model, the area has been extended to include also the large number of small areas of direct runoff to the sea that are found along the coastline; this is the reason for the large number of coastal outlets (1532).

The following input data are affected by the update:

- The digital elevation model (DEM).
- The map of Quaternary deposits (QD).
- The land use (vegetation) map.

The methods and procedures that were used for obtaining the updated results are, with a few exceptions, identical to those described by /Jarsjö et al. 2004/; the exceptions are:

- Peat is introduced as a separate QD class in the processing of hydrological data.
- New QD and land-use categories are accounted for in the processing (a need that emerged due to new classes in the updated QD and land use maps).
- The model area is extended all the way to the coastline, enabling consideration of interactions with seawater in future studies.

The main assumptions associated with the flow direction and flow accumulation calculations are the same as for the GIS-based modelling described in Section 5.2. However, in the calculation of discharges, spatially uniform regional estimates of the specific runoff are replaced by generic constitutive equations with regional meteorological input data (method 1) or a classification based on site-specific data with evapotranspiration data from elsewhere (method 2). Hence, it is assumed that these generic equations and data are relevant for describing the site conditions.

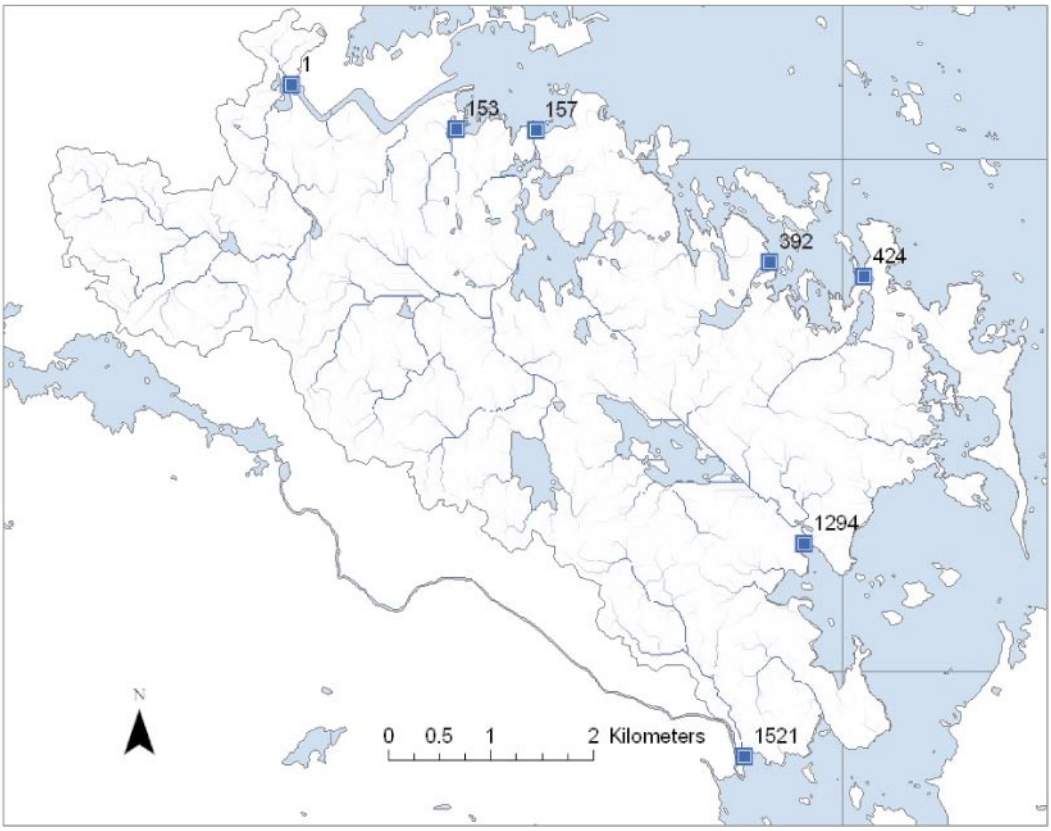

Figure 5-8. *Location of catchment boundary (black line) and streams (blue lines), as well as location and ID of the top seven coastal outlets with regard to high discharge values, out of the 1532 outlets.*

5.3.4 Results

Below, a brief summary of the updated modelling results is given. A detailed description of the results of the modelling based on pre site-investigation data was given by /Jarsjö et al. 2004/.

Precipitation surplus and groundwater recharge

In method 1 for calculation of the actual evapotranspiration, spatially variable meteorological data for the model area are obtained by interpolation between SMHI stations in surrounding areas. The resulting distributions of meteorological parameters (precipitation, temperature and potential evapotranspiration), actual evapotranspiration (E) and precipitation surplus (PS) show relatively small variations within the model area. Therefore, the presentation of spatially distributed parameters is focused on results obtained with method 2.

Method 2 uses geological (texture) and land use/vegetation data to develop a classification of different subareas within the model area. Each class is then assigned a value of the actual evapotranspiration. Since these values in the present modelling are obtained from elsewhere (calibrated data from catchments in Germany), this means that the classification and thereby the overall pattern of variability are determined from site-specific data, whereas the actual values and differences between subareas are not. In principle, the generic evapotranspiration data for the different classes could be replaced by site-specific data, based on modelling and/or measurements, when such data become available.

Figure 5-9 shows the actual evapotranspiration calculated using method 2. It can be seen that the calculated evapotranspiration is 460–600 mm·year^{-1} in most of the model area. These large values reflect the fact that the calculation is based on non site-specific input data; the data used for parametrisation of the individual classes are imported from an area with warmer climate than that in Forsmark. However, it can also be seen that there are subareas where the evapotranspiration is much smaller, 300–400 mm·year^{-1}, indicating a relatively high degree of spatial variability.

The corresponding local values of the precipitation surplus (PS = P – E), i.e. the local contributions to the total runoff, are presented in Figure 5-10. The figure shows that most of the model area has PS values less than 200 mm·year^{-1}, i.e. relative low values consistent with the large evapotranspiration in the model. Considerable spatial variability can be observed also for this parameter. PS is generally in the interval 200–300 mm·year^{-1} in the western part of the model area, whereas low values, 60–80 mm·year^{-1}, are obtained in some areas. Many low-PS areas coincide with lakes.

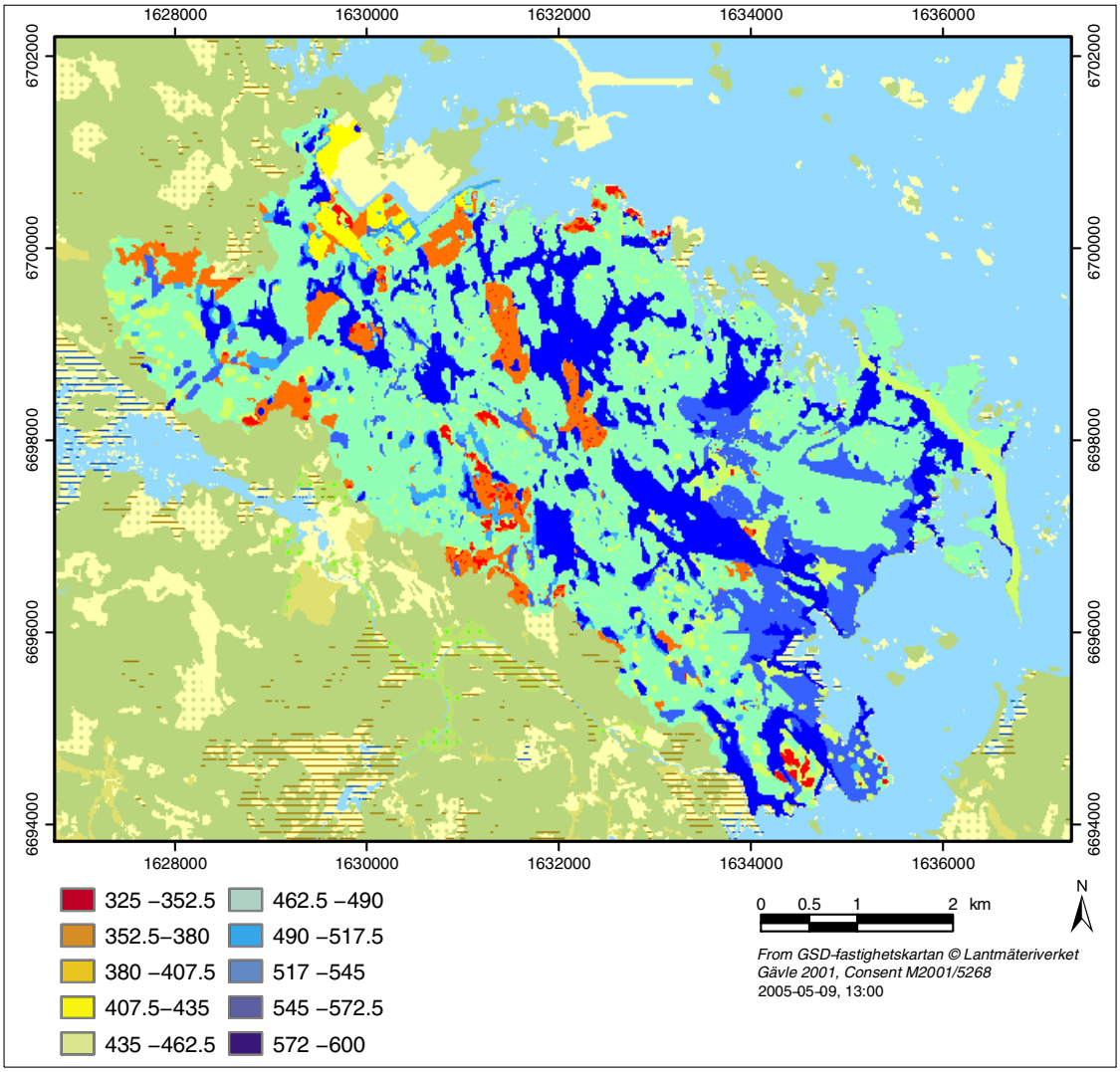

Figure 5-9. *Actual evapotranspiration (in mm·year^{-1}) calculated using method 2.*

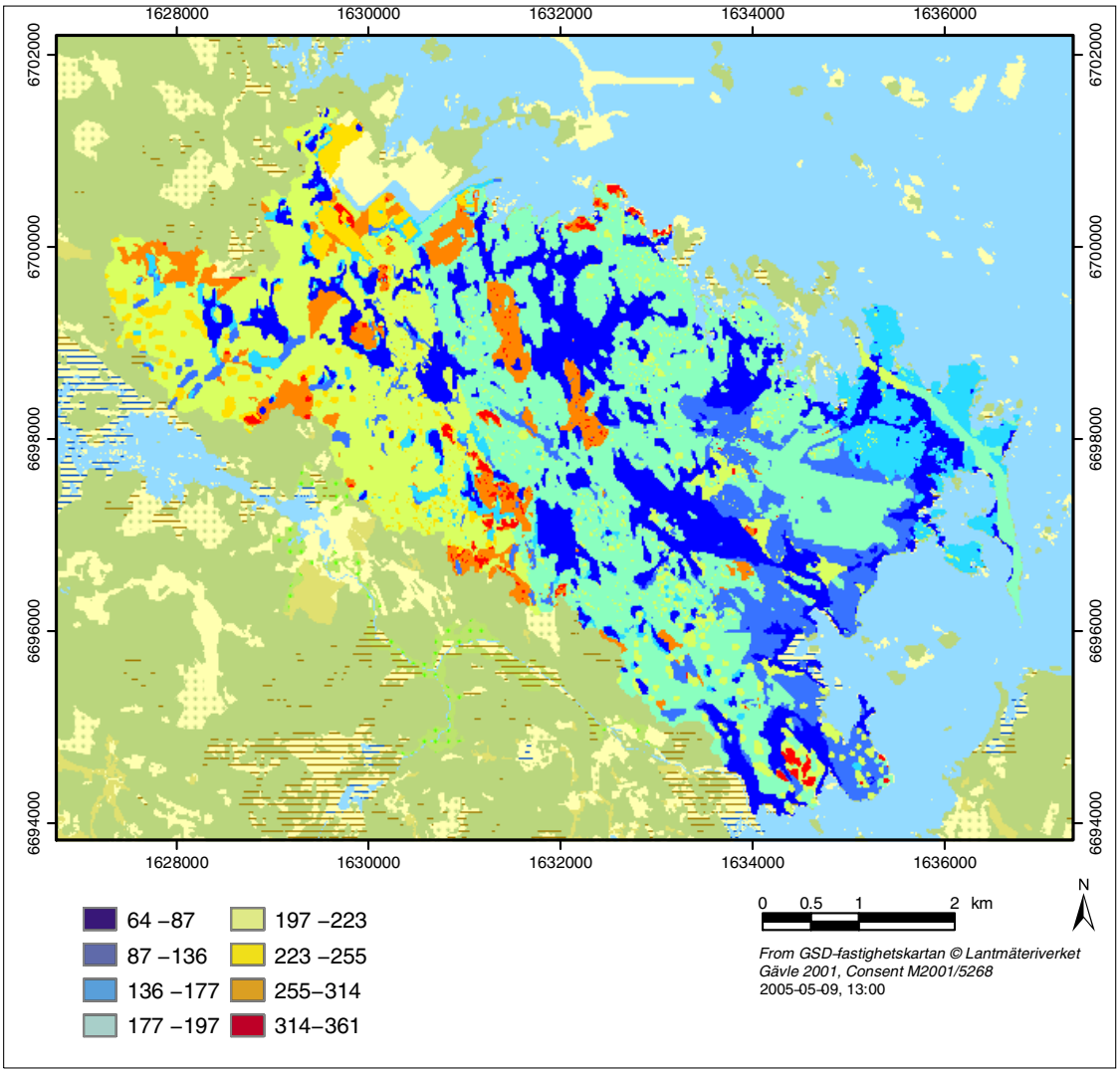

Figure 5-10. *Local precipitation surplus (in mm·year^{-1}), PS, which also equals total locally created runoff calculated using method 2.*

Figure 5-11 and 5-12 show the groundwater recharge index, f_{gw}, i.e. the local fraction of PS that discharges as groundwater from each grid cell, and the corresponding calculated local groundwater recharge, GW = $f_{gw} \times$ PS, which equals the locally generated groundwater discharge, R_{gw}, respectively. Also these parameters display spatial variability as a result of the differences in parameters assigned to the different subareas (classes). In most of the model area, f_{gw} varies between 0.5 and 0.8 (Figure 5-11), but also areas of much lower (mainly associated with lakes) and higher values can be found. The recharge index depends on the topographic gradient and the land cover. It is seen that the small-scale topographic variations in the Forsmark area are reflected as similar variations in f_{gw}.

The groundwater recharge (Figure 5-12), which combines the results in Figure 5-10 (PS) with those in Figure 5-11 (f_{gw}), varies between 0 and 300 mm·year^{-1}, with some (barely visible) exceptions. The calculated groundwater recharge is small in and around lakes and along the coastline. The largest recharge takes place in the western part of the model area, mainly in higher-altitude areas and along the intake canal to the nuclear power plant in the north (possibly a boundary effect).

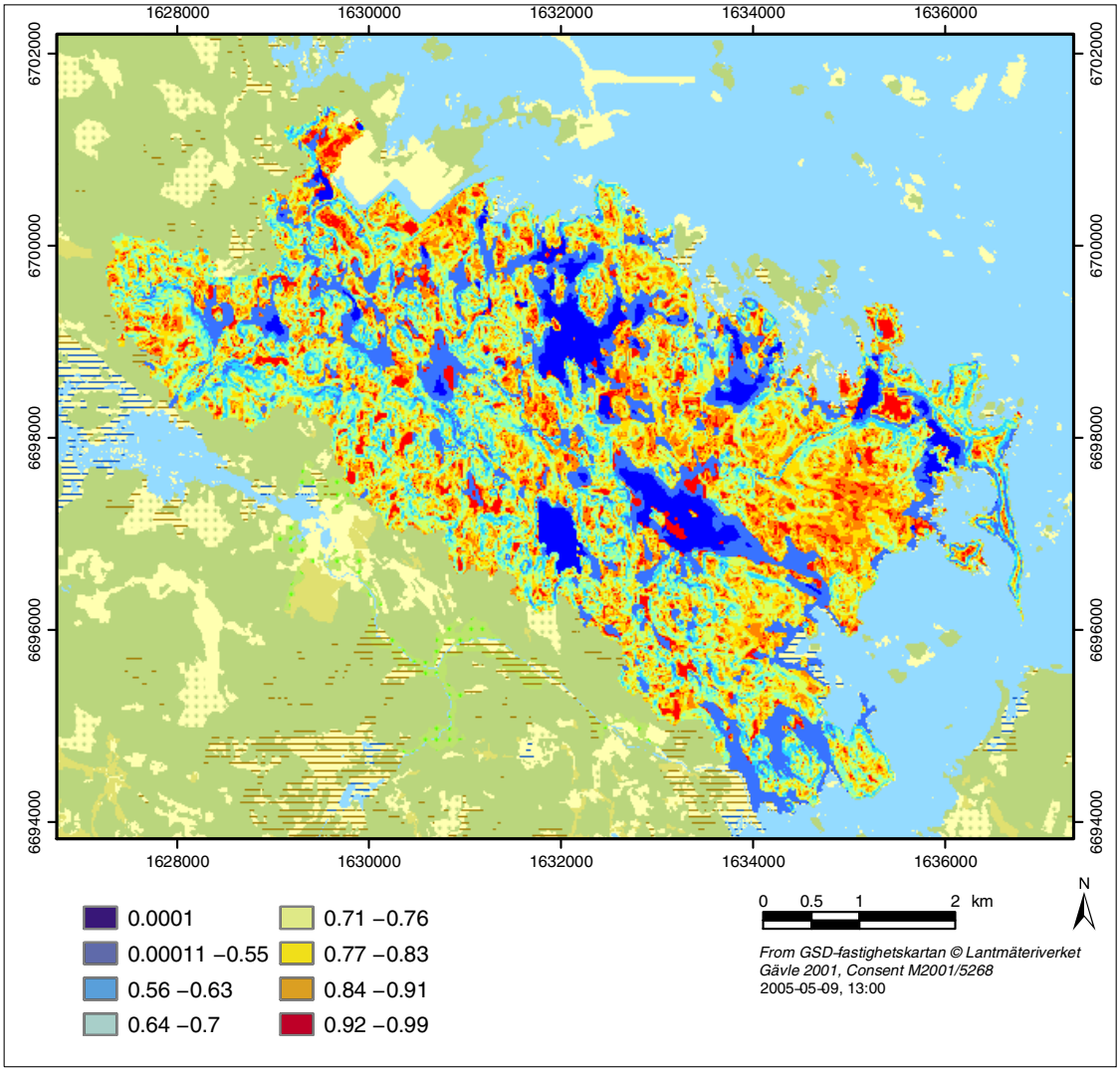

Figure 5-11. *The calculated groundwater recharge index, f_{gw} (dimensionless fraction of precipitation surplus, PS).*

Area-averaged runoff and discharge in coastal outlets

The specific runoff in Forsmark regional model area has been estimated to 6.5 $l \cdot s^{-1} \cdot km^{-2}$ (205 $mm \cdot year^{-1}$) based on regional meteorological and hydrological data /SKB, 2004a/. The calculation performed with evapotranspiration method 1 gives an area-averaged specific discharge of 8.8 $l \cdot s^{-1} \cdot km^{-2}$ (277 $mm \cdot year^{-1}$), which is 35% larger than the estimate. Thus, the generic constitutive equation employed in method 1 results in a smaller actual evapotranspiration and a larger runoff than the estimate obtained from regional data.

Evapotranspiration method 2 results in an area-averaged specific discharge of 4.6 $l \cdot s^{-1} \cdot km^{-2}$ (145 $mm \cdot year^{-1}$), 29% smaller than the estimate based on regional data. This indicates that the data used to parametrise the different classes in the GIS model overestimate the evapotranspiration and hence underestimate the runoff. The estimate in the descriptive model (6.5 $l \cdot s^{-1} \cdot km^{-2}$) is obviously associated with uncertainty, and should not be taken as an exact site-specific value to be used in model evaluation. However, it seems clear that a calibration or "site adaption" of the constitutive equations (method 1) and/or the evapotranspiration values assigned to the land cover/land use classes (method 2) is needed to obtain site-specific estimates of absolute discharge values for the Forsmark area from the PCRaster-POLFLOW model.

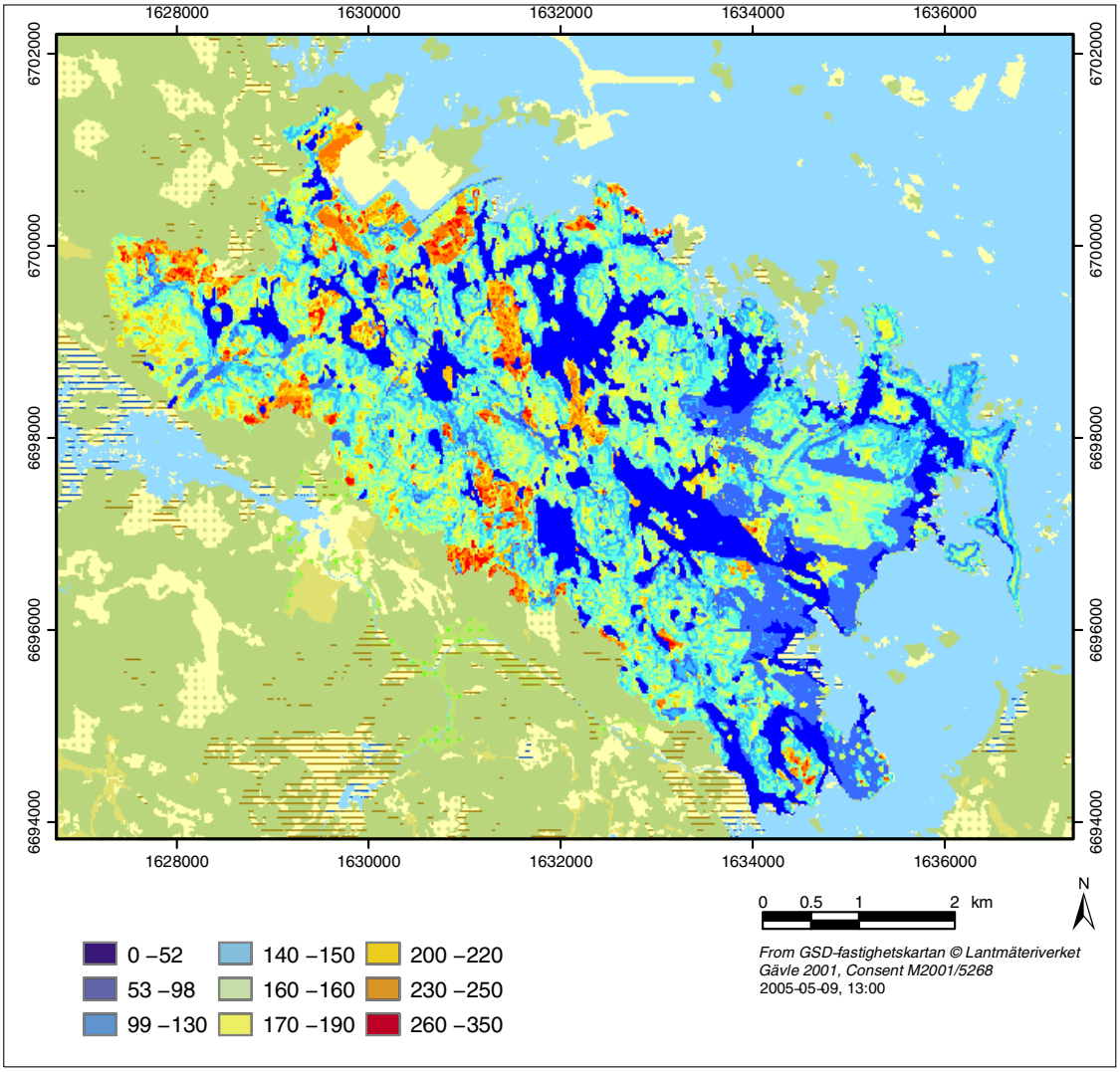

Figure 5-12. *Calculated local groundwater recharge, GW (in mm·year^{-1}), and corresponding locally created groundwater discharge R_{GW} = GW (Equation (3)), adding to local stream runoff, or flowing as groundwater and adding to stream runoff further downstream using method 2.*

The results from the PCRaster modelling also include discharges in the coastal outlets shown in Figure 5-8, for average seasonal and annual conditions, and at discharge measurement locations in the water courses. One conclusion from the calculated distributions among the coastal outlets is that one single calibration factor appears to be sufficient for correcting the results for the bias indicated by the overall area-averaged discharges. The results for the coastal outlets are further discussed below.

Comparison with ArcGIS results

Since the ArcGIS modelling described in Section 5.2 uses a spatially uniform specific runoff estimated on the basis on the regional meteorological and hydrological data (i.e. 6.5 l·s^{-1}·km^{-2}, as discussed above), both the overall, area-averaged discharge and the spatial distribution of the local discharge differs between ArcGIS and PCRaster models. Specifically, the ArcGIS "PS map" corresponding to Figure 5-10 would have a constant value of 205 mm·year^{-1} over the whole model area.

The differences in the overall magnitude and spatial distribution of the specific discharge lead to differences in the runoff pattern ("flow accumulation") and the discharges in the coastal outlets. Furthermore, the PCRaster modelling included modifications of the DEM, which also affected the modelling results. These modifications consisted of a lowering of the ground surface level along the mapped water courses, thereby emphasising their importance for the runoff pattern relative to the gradients obtained by interpolation of ground surface levels only.

The differences in calculated discharges in coastal outlets are illustrated in Figure 5-13 (absolute values) and Figure 5-14 (relative values normalised with the total discharge in each model); the locations and ID numbers of the outlets are shown in Figure 5-8. The most notable difference between the ArcGIS and PCRaster results, except for the differences in total discharges discussed above, is that the outlet with ID 1 located in the northern part of the model area has no discharge in the ArcGIS model, but non-zero discharges in the PCRaster results. This is also the case for outlet ID 1521.

The observed differences between the PCRaster and ArcGIS results in the northern part of the area are consistent with the differences between field-controlled and ArcGIS-modelled catchment areas described in Section 5.2.4 (see Figure 5-5). In particular, the GIS model predicted that part of the discharge from the "Forsmark 1" catchment area discharged through "Forsmark 2", which corresponds to the redistribution of discharge between outlets 1 and 157 indicated by the relative discharges in Figure 5-14.

The comparison between ArcGIS and PCRaster indicates that the modifications of the DEM performed in the latter model lead to a better agreement between modelled and observed surface water runoff. Similar to the analyses in Section 5.2, the results also show that errors associated with the DEM (i.e. both actual errors in the interpolation and objects not represented due to the limited resolution) may have relatively large effects

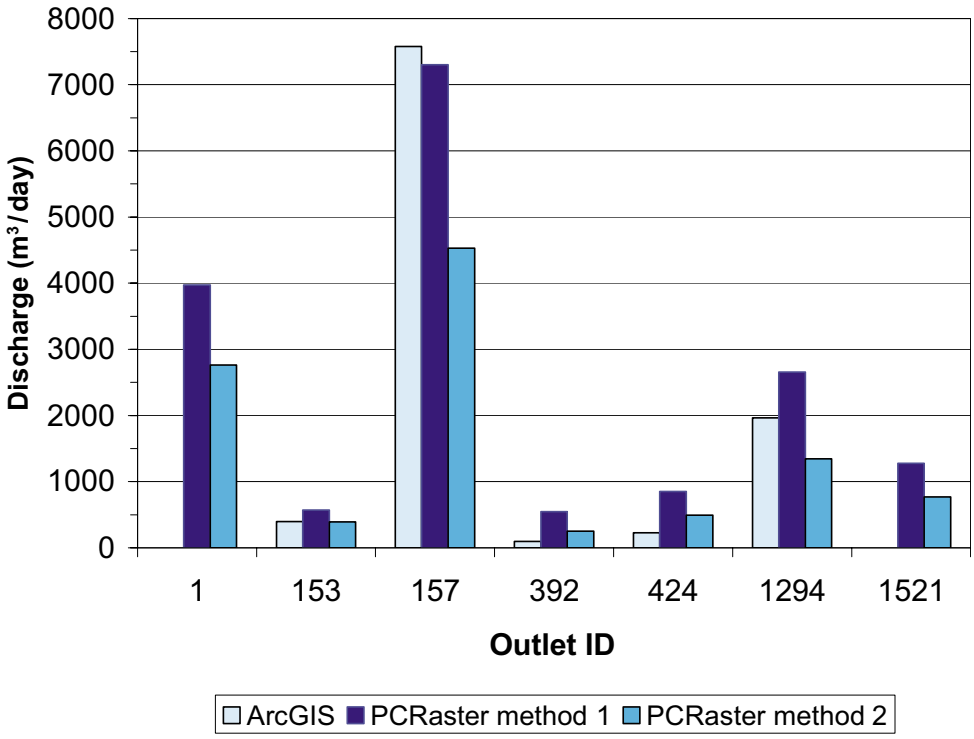

Figure 5-13. *Discharges in coastal outlets calculated with different GIS-based models.*

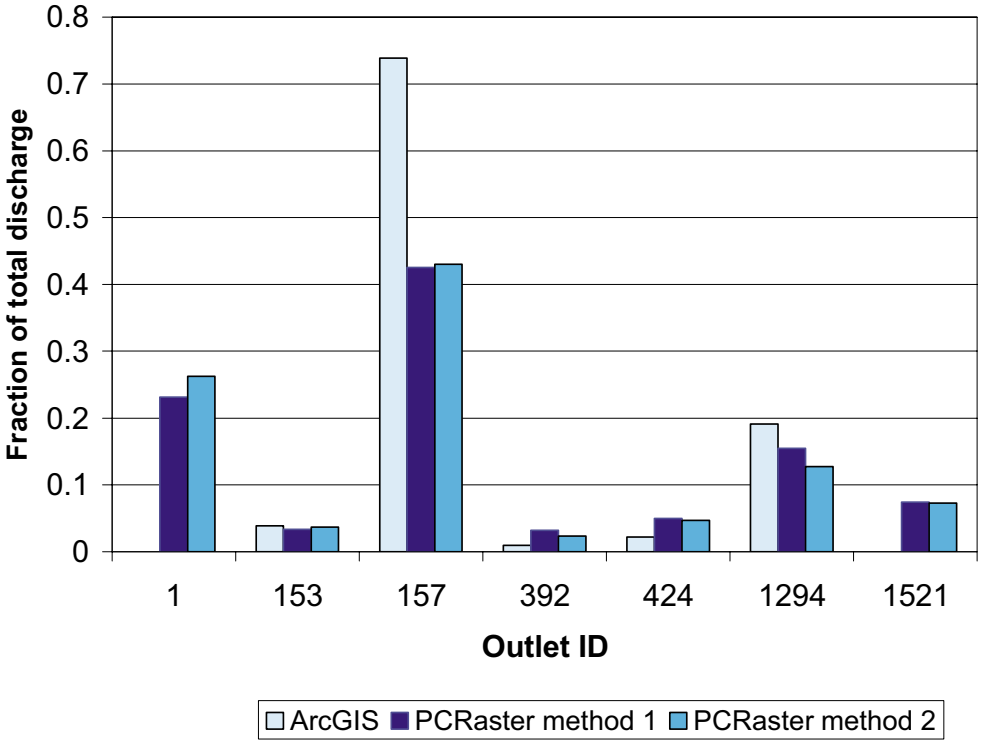

Figure 5-14. *Relative discharges in coastal outlets in different GIS-based models (discharges in individual outlets normalised with the total discharge in each model).*

on discharge predictions. Furthermore, the PCRaster results, at least those obtained using evapotranspiration model 2, indicate that spatial variability in the locally generated discharge is an important factor, also in predictions of the discharges from relatively large areas and in the main coastal outlets.

5.3.5 Evaluation of uncertainties

The main uncertainties related to the PCRaster-POLFLOW modelling of the Forsmark site are the same as for the ArcGIS modelling; see the discussion in Section 5.2.5. Additional, PCRaster-specific uncertainties are those introduced by the generic data and equations employed in the modelling of the evapotranspiration and the groundwater recharge index. A quantification of these uncertainties is given by the comparison of area-averaged runoff values above; the deviations relative to the previously estimate of the specific runoff in the area is ±35% for the two evapotranspiration methods considered.

Obviously, this uncertainty range would decrease if the generic input could be replaced by site-specific information. It may be argued that a development of site-specific correlations for use in the PCRaster-POLFLOW model is not needed, given that detailed process-based modelling is performed with other tools (see next section). However, the PCRaster-POLFLOW approach provides a suitable framework for analysing the effects of hydrological spatial variability with limited computational effort. This implies that it probably is most useful as a basis for investigating the uncertainties in flow and transport models of the surface system.

5.4 Hydrological process modelling with MIKE SHE

5.4.1 Overview of tools and capabilities

MIKE SHE (SHE = Système Hydrologique Europeen) is a physically based, distributed model that simulates water flows from rainfall to river flow. It is a commercial code, developed by the Danish Hydraulic Institute (DHI). This sub-section summarises the basic processes and the governing equations in MIKE SHE. For a more detailed description, see the user's guide and technical reference /DHI Software, 2003/.

MIKE SHE describes the main processes in the land phase of the hydrological cycle. The precipitation can either be intercepted by the vegetation or fall to the ground. The water on the ground surface can infiltrate, evaporate or form overland flow. Once the water has infiltrated the soil, it enters the unsaturated zone. In the unsaturated zone, it can either be extracted by roots and leave the system as transpiration, or it can percolate down to the saturated zone, see Figure 5-15. MIKE SHE is fully integrated with a channel-flow code, MIKE 11. The exchange of water between the two modelling tools takes place during the whole simulation, i.e. the two programs run simultaneously.

MIKE SHE is developed primarily for modelling of groundwater flow in porous media. However, in the present modelling the bedrock is also included. The bedrock is parameterised by use of data from the Forsmark 1.1 groundwater flow model developed using the DarcyTools code /SKB, 2004a/. In DarcyTools, a discrete fracture network (DFN) is used as a basis for generating hydrogeological properties for a continuum model /Svensson et al. 2004/. Thus, hydrogeological parameters can be imported directly to the corresponding elements in the MIKE SHE model, provided the spatial resolution is the same.

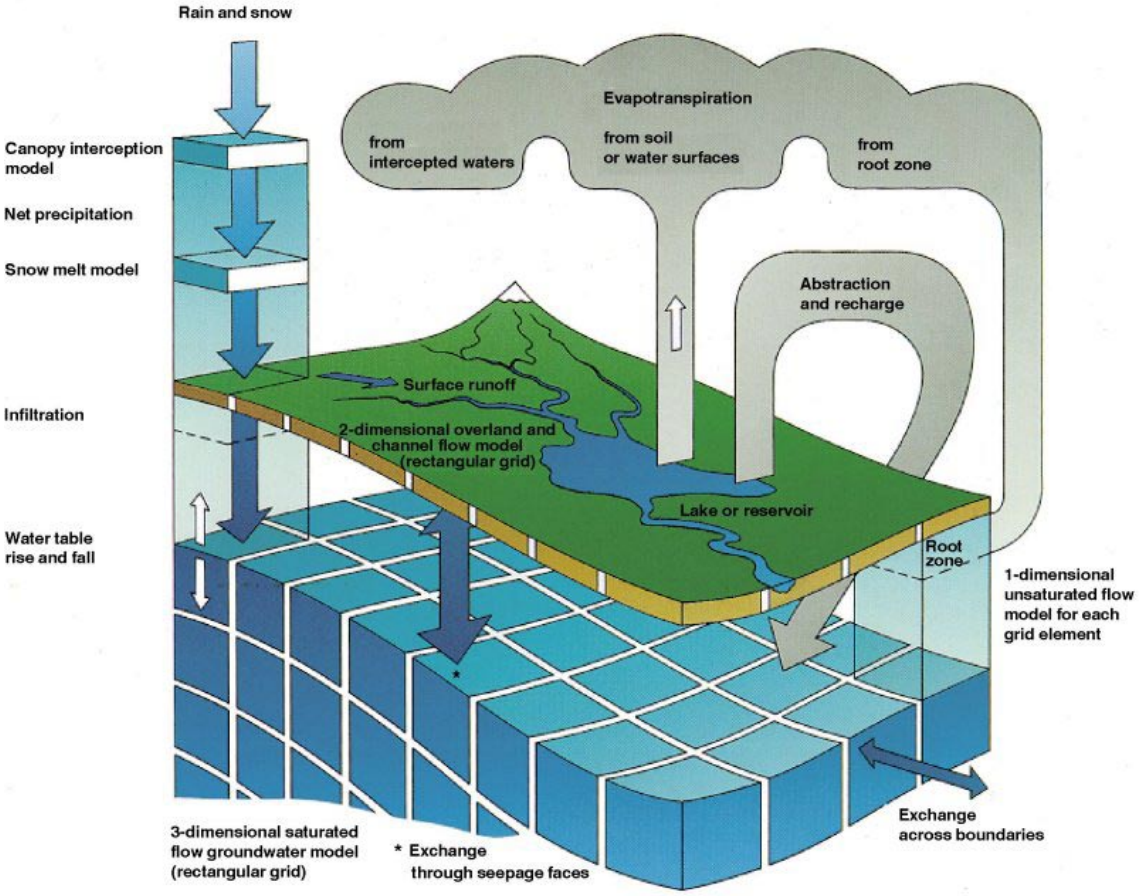

Figure 5-15. *Overview of the MIKE SHE model /DHI Sverige, 1998/.*

The MIKE SHE model consists of the following five compartments:

- Overland flow (OL).
- Evapotranspiration.
- Unsaturated zone (UZ).
- Saturated zone (SZ).
- Channel flow.

The water flow is calculated in different ways in each compartment. In addition to the different compartments, there is a frame component that runs simultaneously with the other components of the model. For a detailed description of each compartment, see /Werner et al. 2005/ and the user's guide and technical reference /DHI Software, 2003/.

Input data

The input data to the MIKE SHE model include data on topography, land use, geology, hydrogeology and meteorology. In addition, MIKE 11 requires information on the river network within the model area. Table 5-3 lists the different input data needed for each compartment of the model. There is a direct coupling between the GIS program ArcMap and MIKE SHE. This is an advantage for the present modelling, since most of the input data can be obtained in GIS format. It is possible to use both shape files and ESRI grid files as input.

Table 5-3. Input data required for the MIKE SHE modelling.

Compartment	Input data
Frame	Topography
	Model boundary (e.g. water divide)
Evapotranspiration/snow routine	Potential evapotranspiration
	Precipitation
	Snow melt constants
	Temperature
	Vegetation
	Leaf Area Index (LAI)
	Root depth
	Root distribution
	K_c-value
Overland flow/channel flow	River network
	Cross-sections
	Permeability of the river bed
	Manning's number
Unsaturated flow	Map of QD
	Hydraulic parameters for unsaturated flow
Saturated flow	Geological model
	Horizontal saturated hydraulic conductivity
	Vertical saturated hydraulic conductivity
	Storage coefficient
	Specific yield
Particle tracking	Kinematic (effective) porosity

The geological layers and the computational layers are separated in MIKE SHE. The user starts by defining the geological model and the different geological layers. The thickness of a geological layer can be zero, which implies that it is possible to describe a geological layer that exists in parts of the model area only. The next step is to define the computational layers and the boundary conditions for each layer. The thickness of both the computational layers and the geological layers can vary within the model area.

Summary of model simplifications

The main simplifications in the MIKE SHE model are made in the modelling of unsaturated flow and the processes associated with freezing/thawing of the soil materials. Specifically, unsaturated flow is calculated in one dimension only, i.e. in the vertical direction. Freeze/thaw processes are not included in MIKE SHE. The snow routine takes snow accumulation and snow melt into consideration (based on air temperature), but the detailed processes within the porous medium, and the associated effects on the hydrogeological properties and processes, are not modelled explicitly.

5.4.2 Objectives

The general objectives of the quantitative modelling in F1.2 are described in Section 5.1. The specific objectives of the MIKE SHE modelling are to

- test the MIKE SHE tool, including its coupling to GeoEditor and MIKE 11, within the SKB environment,
- perform initial modelling studies of site-specific conditions with regard to (1) the hydraulic contact between groundwater in QD and in fractured rock, (2) the water exchange between groundwater and surface waters, (3) the spatial distribution of recharge and discharge areas, and (4) the temporal variations in the various components of the water balance,
- deliver output data on the components of the water balance (evapotranspiration, surface water and groundwater flows) to the ecological systems modelling.

The assumptions and conclusions made in the conceptual and descriptive modelling, presented in Chapter 4, are demonstrated and tested in the numerical modelling. The overall conceptual model and the parameters in the descriptive model provide the basis for the quantitative numerical modelling. However, it is recognised that in the present model version the interactions between descriptive modelling and flow modelling have not been developed to the extent proposed in the modelling strategy. This is mainly due to time constraints.

The aim is to simulate the groundwater flow in the Quaternary deposits (QD) and the interaction between surface water and groundwater. Furthermore, the purpose is to model the coupling of surface waters and the deep groundwater. Normally, it is assumed that the bottom boundary condition in a near-surface groundwater flow model is a no-flow boundary. In this application, the boundary at the bottom of the model is a “head-controlled flux boundary” which provides an opportunity to simulate the flow of water between “deep” and “near-surface” groundwater.

Since the flows of matter in different ecosystems are strongly dependent on the hydrology, the model results are important for the ecosystems modelling. Information on the water balance, especially the evapotranspiration from different parts of the model area, are results that have been used in the ecosystems modelling. As compared to the GIS-based

hydrological modelling, transient process-based modelling provides opportunities to explore a multitude of additional aspects and properties of the system, such as time-dependent processes and interactions between different sub-systems.

5.4.3 Model area

The central part of the land area within the regional model area is included in the MIKE SHE modelling of Forsmark, cf Figure 5-16. The model area is 21.5 km^2 and consists of 19 sub-catchments. The properties of the sub-catchments are described in detail in /Brunberg et al. 2004/, see also Section 3.2.1. The model area includes a river network and several lakes, which implies that all five compartments in MIKE SHE are activated during the simulation.

The horizontal resolution of the calculation grid is 40 m by 40 m. The vertical resolution varies with depth. The upper calculation layers, containing the QD, follow the geological layers. The deeper calculation layers have an average depth of 20 meters. In total, the model contains 12 calculation layers and it has a total vertical extent of approximately 170 meters.

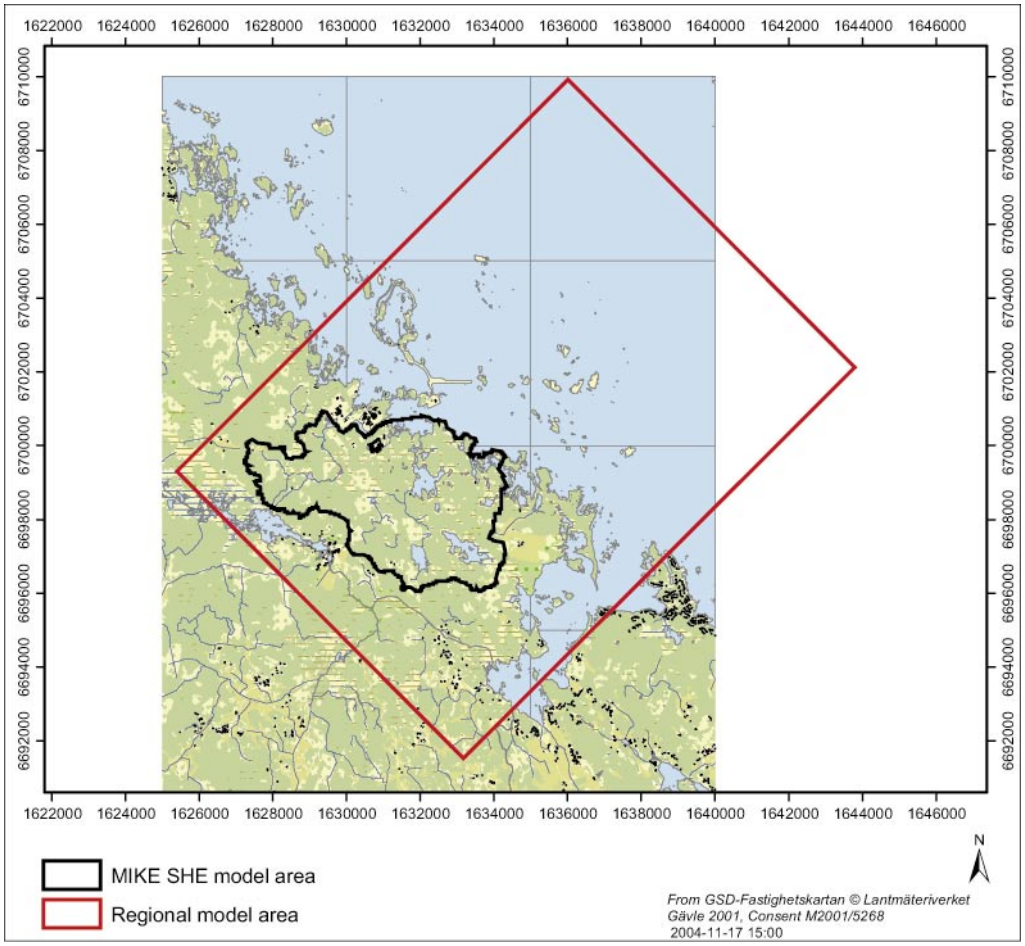

Figure 5-16. *The model area in the MIKE SHE modelling of the Forsmark site.*

5.4.4 Input data

As shown in Table 5-3, many different types of input data are required to develop a MIKE SHE model. At present, site-specific data are not available on all the input parameters in the model. However, the site investigations are not completed, and the input data will be updated in future versions of the flow models of the Forsmark area. Table 5-4 gives information on whether the various types of data used in the F1.2 model application are site-specific, and provides references to the relevant data reports. In addition, some references to generic (literature) data are given in the text.

Table 5-4. Input data used in the MIKE SHE model of the Forsmark area.

Compartment	Input data	Site specific	Data report
Frame	Topography	X	P-04-03
	Model boundary (e.g. water divide)	X	P-04-25
Evapotranspiration/ snow routine	Potential evapotranspiration	X[1]	TR-02-02
	Precipitation	X[1]	TR-02-02
	Snow melt constants		
	Temperature	X[1]	TR-02-02
	Vegetation	X	P-03-83
	Leaf area index (LAI)		
	Root depth		
	Root distribution		
	K_c-value		
Overland flow/ channel flow	River network	X	SKB-GIS[2]
	Cross-sections	X	SKB-GIS[2]
	Permeability of the river bed		
	Manning's number		
Unsaturated flow	Map of QD	X	P-04-39
	Hydraulic parameters for unsaturated flow		
Saturated flow	Geological model	X	R-04-15
	Horizontal hydraulic conductivity	X	P-03-65
	Vertical hydraulic conductivity	X	P-03-65
	Storage coefficient		
	Specific yield		
Particle tracking	Kinematic (effective) porosity of the bedrock[3]	X	R-04-15

[1] Version 0 data, judged representative for the model area (i.e. not site investigation data).

[2] P-reports not available at the time of writing.

[3] Effective porosity of QD assumed equal to specific yield (which is based on generic data).

Meteorological input data

The meteorological input data are taken from the SMHI (Swedish Meteorological and Hydrological Institute) station no 10832 at Örskär. As shown in Figure 5-17, this station is located approximately ten kilometres north of the north-eastern boundary of the Forsmark regional model area. Data from 1988 are used in the modelling; this year has been identified as a statistically representative year during the period 1961–2000 /Larsson-McCann et al. 2002/. The dataset contains precipitation data measured every twelfth hour and temperature data for every third hour, whereas monthly mean values are used for the potential evaporation. The annual precipitation and potential evapotranspiration at Örskär during 1988 was 551 mm and 538 mm, respectively

Since there are losses due to wind, evaporation and adhesion, the measured precipitation is always less than the real. Therefore, the precipitation time series has been corrected. The corrections factors for annual and monthly mean values given in /Larsson-McCann et al. 2002/ were used to correct the precipitation data from 1988. The total corrected precipitation for the year was calculated to 674 mm. For a more detailed description of the meteorological conditions and the available data, see Chapter 3.

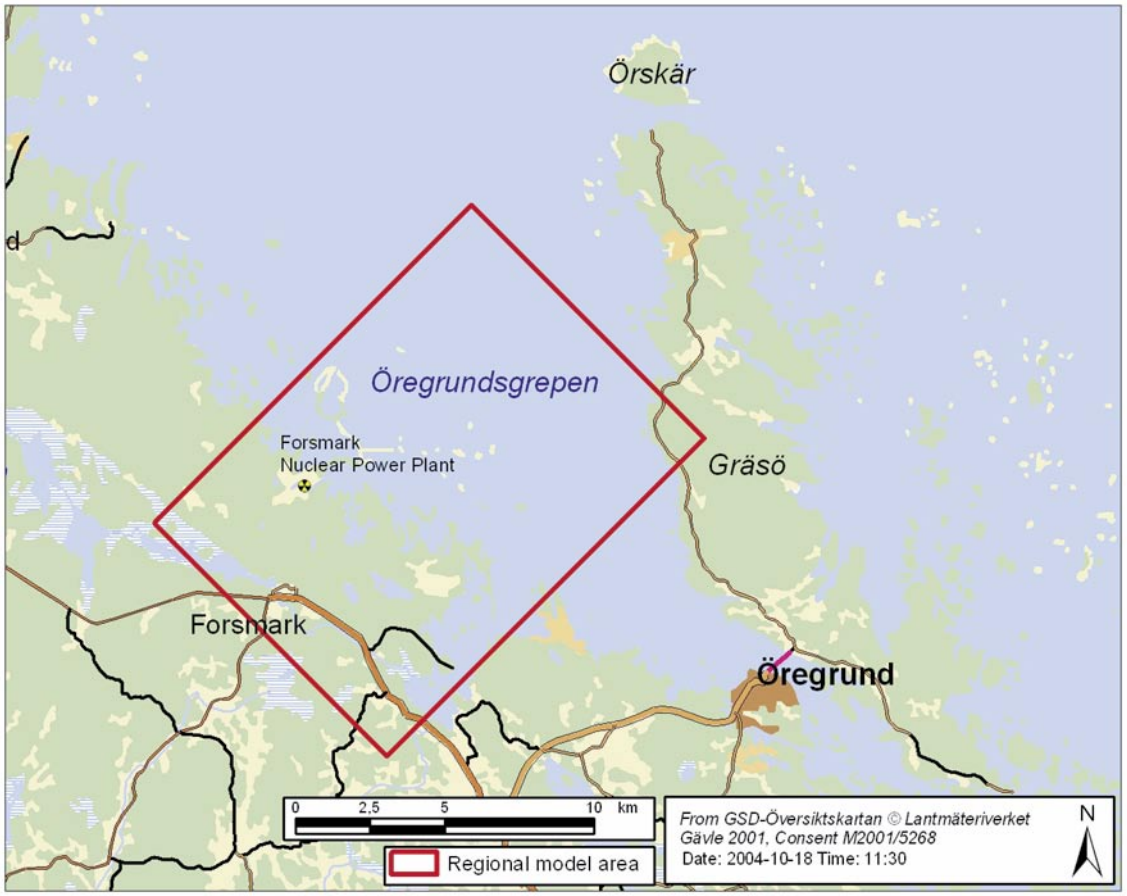

Figure 5-17. *The meteorological station no 10832 at Örskär and the regional model area in Forsmark.*

Geological model and hydraulic properties

Bedrock

The part of the geological model that consists of rock is described by data taken from the F1.1 hydrogeological modelling performed with the DarcyTools code /SKB, 2004a/. The reason for using the F1.1 hydrogeological model of the rock is that the F1.2 model was not available when the MIKE SHE modelling started. Thus, it should be noted that the results presented herein reflect the deformation zones (geometry and properties) presented in the F1.1 hydrogeological model, and that these have changed considerably in the F1.2 model.

Data on hydrogeological properties were taken from three different levels in the DarcyTools model, at 20, 60 and 150 metres below sea level (m b s l). Specifically, the bedrock is described in terms of its vertical and horizontal hydraulic conductivities. The horizontal hydraulic conductivity at 150 m b s l is shown in Figure 5-18. The areas with colours deviating from the background correspond to intersections between the visualised plane and the deformation zones represented in the F1.1 hydrogeological model of the rock. Generic data are used for the specific yield and the storage coefficient. The values are based on data from previous MIKE SHE applications /DHI Sverige, 1998/. The specific yield for the bedrock is set to 0.01 (–) and the storage coefficient for the bedrock is set to $1 \cdot 10^{-5}$ m^{-1}.

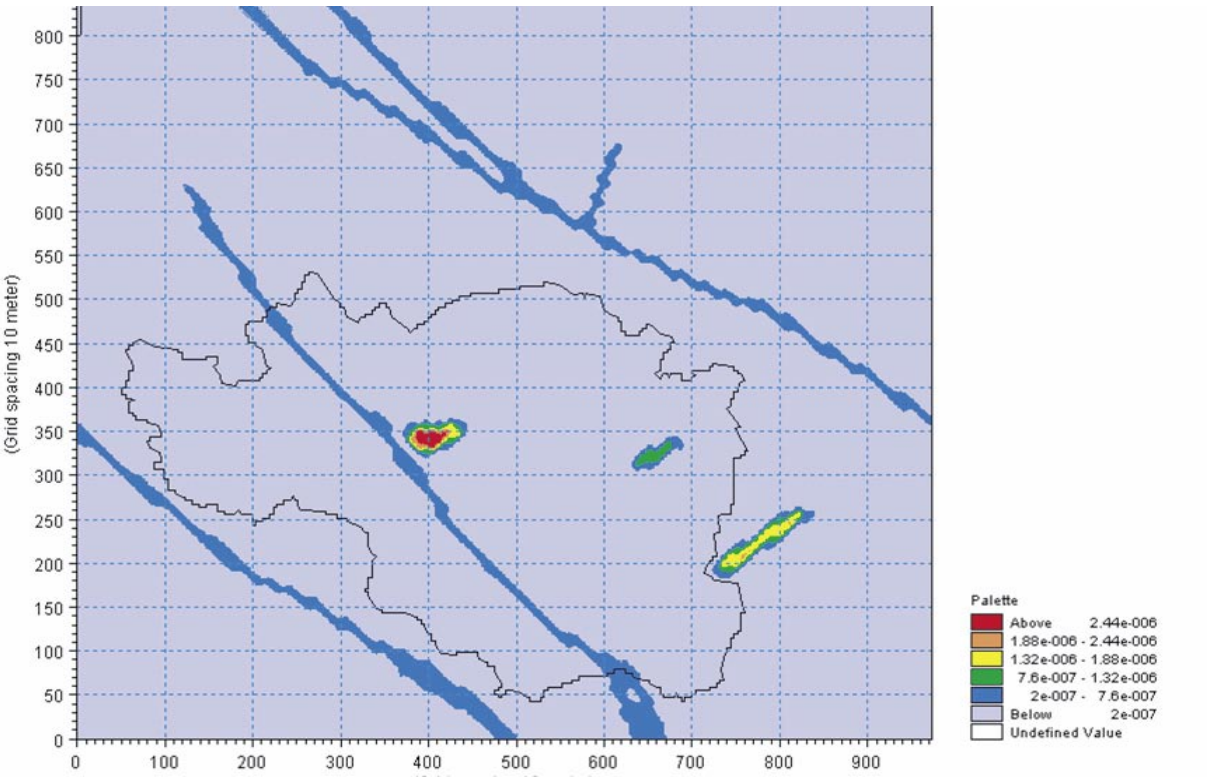

Figure 5-18. *Horizontal hydraulic conductivity (ms^{-1}) at 150 m b s l (metres below sea level).*

Quaternary deposits

The geological modelling of the Quaternary deposits (QD) is performed using the GIS extension GeoEditor, see /Vikström, 2005/ for a detailed description of the tool and the modelling procedure. Since the hydraulic properties are changing within the stratigraphical profile, the till is divided into three layers, which are denoted Z1, Z2 and Z3 (see Figure 5-19). In the geological model, these layers are described geometrically, i.e. in terms of their respective thicknesses at each location within the model area, based on the DEM, an interpolated rock surface level, and a set of "rules".

The hydraulic properties of the top layer, Z1, are affected by plant roots and other soil-forming processes. In general, the hydraulic conductivity is higher in this zone than in the underlying parts of the QD, see Section 3.3.2. This relatively high-conductive layer is followed by a more compact, less conductive layer, Z2. The third and deepest layer, Z3, represents the more high-conductive (as compared to Z2) QD/rock contact zone indicated by the hydraulic tests (Section 3.3.2). Below wetlands and lakes this three-layer principle is complemented by geological lenses. These lenses have hydraulic properties that differ from those of the surrounding till materials.

The thickness of each layer in the model illustrated in Figure 5-19 depends on the total thickness of the QD, i.e. the difference between the ground surface level (GSL) and the rock surface level (RSL). In the present model, it is assumed that layers Z1 and Z3 each has a thickness of 1 m if the total thickness of the QD exceeds 2 m. With this basic assumption, there are three possible cases to be considered when determining the levels of the internal interfaces (the top surface levels of Z2 and Z3 are referred to as TSL_{Z2} and TSL_{Z3}, respectively) and the thickness of each layer (denoted D_{Z1}, D_{Z2} and D_{Z3}):

1. The total thickness of the QD is larger than 2 m ($GSL - RSL > 2$ m)
   $\Rightarrow$ three till layers (Z1, Z2 and Z3):

   $TSL_{Z2} = GSL - 1$ m
   $TSL_{Z3} = RSL + 1$ m
   $D_{Z1} = 1$ m
   $D_{Z2} = TSL_{Z2} - TSL_{Z3}$
   $D_{Z3} = 1$ m

2. The total thickness of the QD is between 1 m and 2 m ($1 \text{ m} \leq GSL - RSL < 2$ m)
   $\Rightarrow$ two till layers (Z1 and Z3):

   $TSL_{Z3} = GSL - 1$ m
   $D_{Z1} = 1$ m
   $D_{Z2} = 0$
   $D_{Z3} = TSL_{Z3} - RSL$

3. The total thickness of the QD is less than 1 m ($GSL - RSL \leq 1$ m)
   $\Rightarrow$ one till layer (Z1):

   $D_{Z1} = GSL - RSL$
   $D_{Z2} = 0$
   $D_{Z3} = 0$

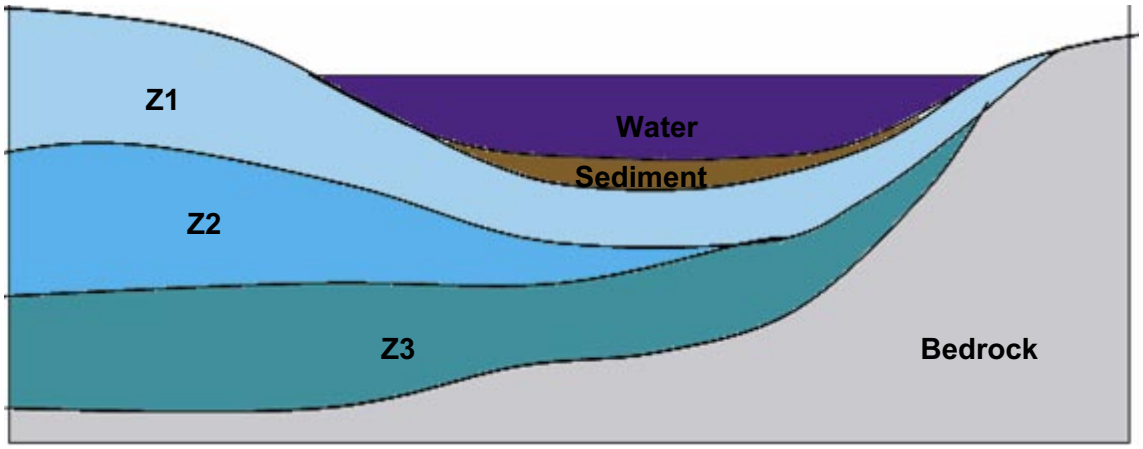

Figure 5-19. *Geological section illustrating the three-layer principle adopted for the till deposits and a sediment lens under a lake.*

As described in Chapters 3 and 4, the QD in most of the model area are dominated by sandy till. Stratigraphical investigations (drillings and excavations) have been performed within the site investigations. The available data consist of field classifications of the till stratigraphy and analyses of grain size distributions. The information gained from these point observations was used to estimate the hydraulic conductivity of the till in the MIKE SHE model. After assigning a grain size curve to each site-specific till type, these curves were compared to grain size curves in generic data stored in a database connected to the CoupModel program /Jansson and Karlberg, 2004/.

The grain size curves obtained from samples classified as sandy till were found to correspond to those of samples no 204:3 and 203:2 in the CoupModel database. Sample no 204:3 was taken from the upper part of the profile; therefore, it was used to represent the uppermost till layer, Z1. Sample no 203:2 was taken at some depth in the profile, and was taken to represent the till in the second layer, Z2.

The hydraulic conductivities of the till materials in layers Z1 and Z2 were taken from the CoupModel database, whereas the hydraulic conductivity assigned to layer Z3 was based on slug tests performed during the site investigation (see Chapters 3 and 4). Specifically, the hydraulic conductivity of layer Z3 is $6.9 \cdot 10^{-5}$ m·s^{-1}, which is the arithmetic mean conductivity obtained from the F1.1 slug tests /Werner and Johansson, 2003/. This K-value is larger than the corresponding value in the descriptive model (Table 4-1). The reason for the discrepancy is that the numerical model, due to the limited time available for the modelling, must be parameterised using the first set of field test results. Thus, the numerical model is not based on the complete F1.2 dataset presented in Chapter 3 and the final interpretations presented in the descriptive model. All QD types in Z1 and the sandy till in Z2 are listed in Table 5-5, together with the saturated hydraulic conductivities assigned to these materials.

Table 5-5. QD types from the CoupModel database; K_s is saturated hydraulic conductivity.

Material	Database ID	Profile depth (m)	K_s ($m \cdot s^{-1}$)
Till, sandy	204:3	0.22–0.32	$4.20 \cdot 10^{-5}$
Till,sandy	203:2	1.2–4.0	$9.60 \cdot 10^{-6}$
Till, clayey-sandy-silty	212:3	0.2–0.4	$3.25 \cdot 10^{-6}$
Peat*	503:1		$2.80 \cdot 10^{-9}$
Clay	58:1	0.5–0.6	$2.80 \cdot 10^{-9}$
Sand/gravel	205:2	0.1–0.25	$1.88 \cdot 10^{-4}$

* arbitrary organic soil from the database.

The spatial distribution of the QD in layer Z1 is based on the detailed map presented in /Sohlenius et al. 2004/. The uppermost layer has been has been divided into seven classes, including bedrock outcrops (cf Figure 5-20). Layers Z2 and Z3 are assumed to consist of sandy till only. The hydraulic properties in the Z1 layer vary within the model area. Each class has been assigned a material-specific set of parameters, see Table 5-5 and Table 5-6.

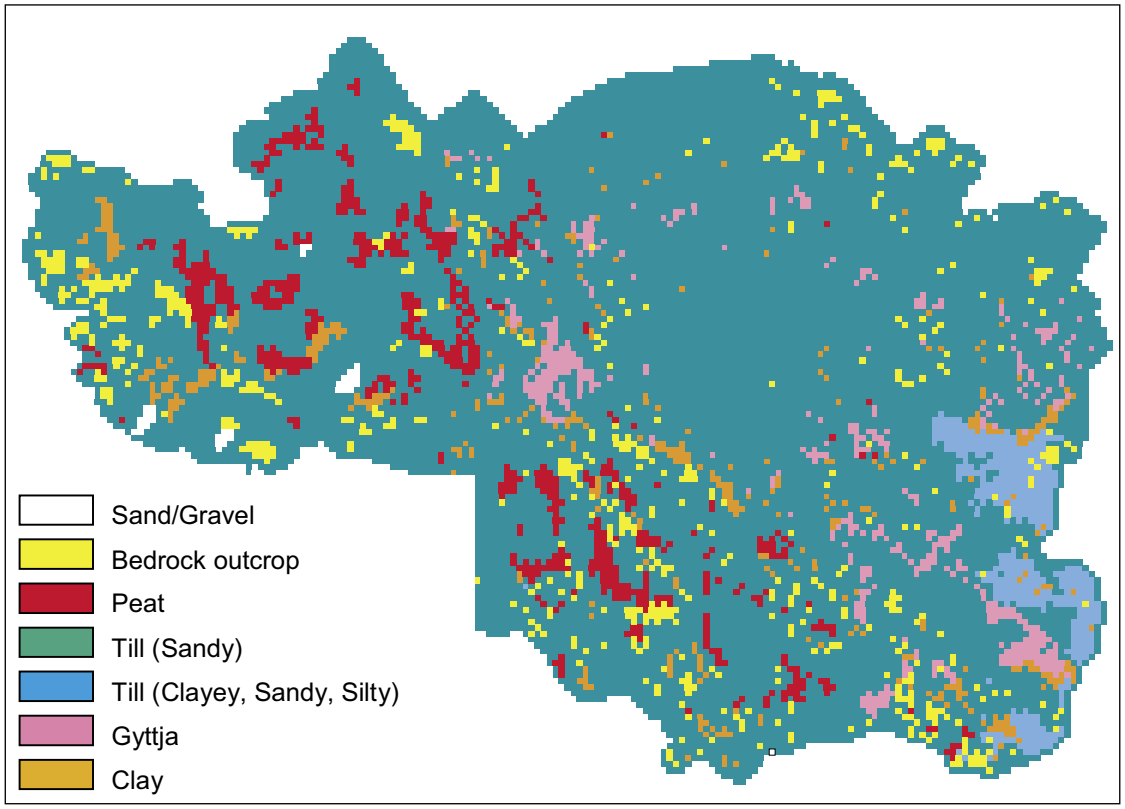

Figure 5-20. *Spatial distribution of QD in the uppermost layer (Z1).*

The parameters for unsaturated flow are taken from the database in the MIKE SHE program. Generic data from /Domenico and Schwartz, 1998/ are used for the specific yield (Table 5-6). The values for "Till, sand", "Till, silt", "Sand, coarse", "Clay" and "Peat" are used in the model. There is no variation of these properties of the till with depth since unsaturated flow is calculated with the full Richard's equation in the uppermost calculation layer only. The storage coefficient of the QD is set to 0.001 m^{-1} in the whole model area; this value is taken from /DHI Sverige, 1998/.

Table 5-6. Specific yield for different types of QD /Domenico and Schwartz, 1998/.

Material	Specific yield (%)
Gravel, coarse	23
Gravel, medium	24
Gravel, fine	25
Sand, coarse	27
Sand, medium	28
Sand, fine	23
Silt	8
Clay	3
Peat	44
Till, silt	6
Till, sand	16
Till, gravel	16

The lake sediments are divided into three layers. The uppermost layer consists of gyttja, which is underlain by sand. The deepest layer is a clay layer. The parameters assigned to the lake sediments are listed in Table 5-7. The specific yield is used under open aquifer conditions and the storage coefficient under confined conditions. The values of the specific yield are taken from Table 5-6. In the model, the lenses under wetland areas are not divided into layers. They are all assumed to consist of peat.

Table 5-7. Properties for lake sediments and peat lenses.

	K_s ($m \cdot s^{-1}$)	Specific yield (–)	Storage coefficient (m^{-1})
Gyttja	$1 \cdot 10^{-7}$	0.03	0.001
Sand	$5 \cdot 10^{-4}$	0.23	0.001
Clay	$1 \cdot 10^{-8}$	0.03	0.001
Peat	$2 \cdot 10^{-5}$	0.44	0.001

Vegetation-related parameters

A classification of the vegetation was made based on the tree layer from the inventory of the vegetation in the model area /Boresjö Bronge and Wester, 2003/. In this classification, the vegetation was divided into four vegetation groups: coniferous forest, deciduous forest, shrubs and water, cf Figure 5-21. The areas where no tree layer had been identified were classified as shrubs.

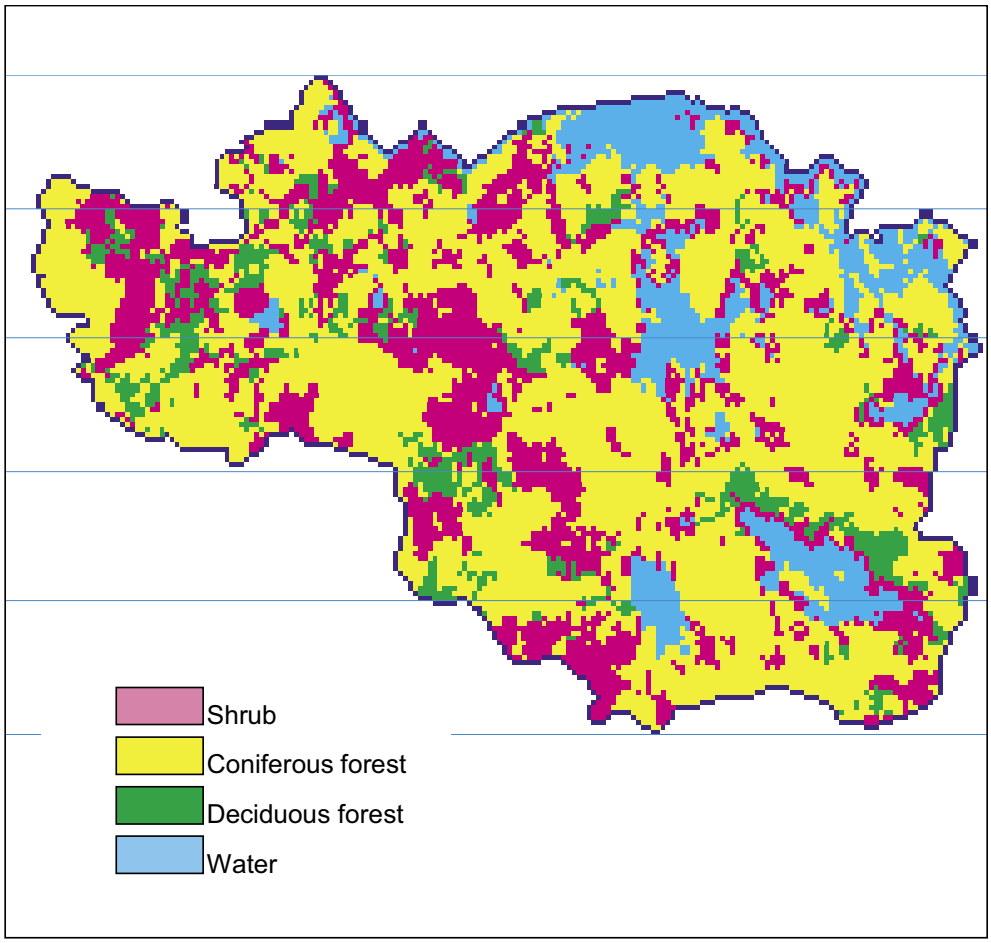

Figure 5-21. *Classification of the vegetation in the model area.*

The properties of each vegetation group are expressed in terms of the parameters Leaf Area Index (LAI), root depth, K_c-value, and the empirical parameters used in the Kristensen and Jensen model /Kristensen and Jensen, 1975/. The values for the different properties are taken from the vegetation database associated with the MIKE SHE program. Root depth and LAI for water are zero, which implies that the transpiration component of the total actual transpiration is zero in these areas.

5.4.5 Initial and boundary conditions

A so-called "hot start" is used to generate the initial conditions of the model. The model is run until semi steady-state conditions are reached. This means that the model is run, with the time-dependent boundary conditions given by the meteorological data for the reference year, until the variations during the year have stabilised (e.g. the pressure at a certain point shows more or less the same variation from one year to the next). The results from this simulation are used as initial conditions for a more detailed one-year simulation. The model has been run for three years, based on data from 1988, to get proper initial conditions.

The surface water divides are assumed to coincide with the groundwater divides. Thus, a no-flow boundary condition is used for vertical boundaries, except for the boundary along the coastline (see Figure 4-2). The coastline boundary is modelled as a head boundary condition with the head set to zero in the uppermost calculation layer. The head increases

towards the bottom calculation layer. Data from the F1.1 DarcyTools simulations have been used to set the boundary condition at the coast line. Specifically, hydraulic head data were received from three levels, 20, 60 and 150 m b s l. The head at the coastline has been linearly interpolated between each level for which data are available. There is an almost linear head increase between the sea level and 150 m b s l. The hydraulic head at 150 m is 1.4 m along the line corresponding to the coast line in calculation layer no 1 (the uppermost layer).

The top boundary condition is expressed in terms of precipitation and potential evapo-transpiration. The precipitation is assumed to be uniformly distributed over the model area, and is given as a time series. The boundary condition for the saturated zone is described by the processes in the unsaturated zone. Water is taken out from the model by the MIKE 11 "river network". Some of the water courses in the model cross the model boundary; at these places, surface water is transported out from the model area. The amount of water flowing to the channel flow compartment (MIKE 11) is dependent on the conditions in the other compartments of the model. Water is transported to the water courses via overland flow, and from the saturated zone.

The bottom boundary condition is a fixed head boundary condition. Model results from the F1.1 DarcyTools groundwater flow modelling /SKB, 2004a/ are used as input data when setting the bottom boundary condition; the calculated hydraulic head from 150 m b s l is imported to the MIKE SHE model (Figure 5-22). The time step used in the DarcyTools simulations (one year) is much longer than that in the MIKE SHE modelling, which implies that short-term temporal variations cannot be captured. Thus, the bottom boundary condition in the MIKE SHE model is constant with time.

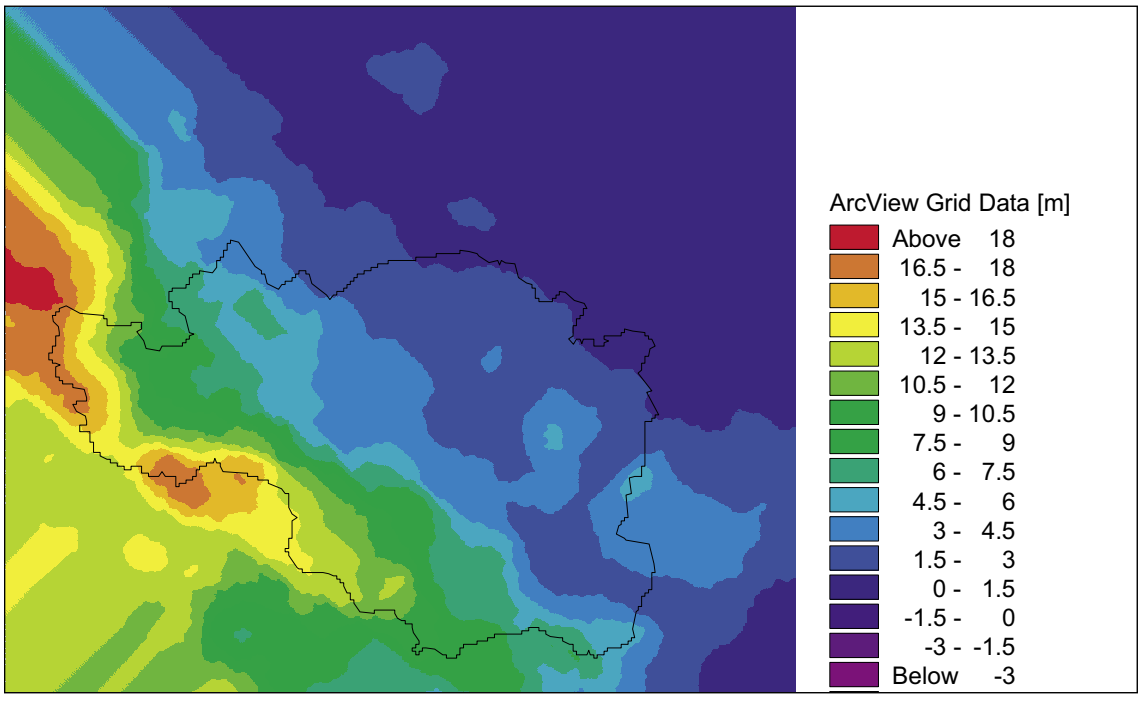

Figure 5-22. *Calculated hydraulic head at 150 m b s l.*

5.4.6 Flow modelling results

As described above, the MIKE SHE modelling was based on meteorological data from the SMHI station Örskär. High-resolution data from 1988 were used in the simulations. The annual corrected precipitation for the modelled year was 674 mm and the potential evapotranspiration was calculated to 538 mm. Thus, it should be noted that all results presented below are based on these input data, and not on the site data from 2003–2004 described in Chapter 3. Furthermore, all references to "dry" and "wet" periods concern different periods of the modelled year, not long-term extreme values.

The model was run until semi steady-state conditions were reached, in order to get proper initial conditions for the detailed simulations. A time period of one year was considered in the detailed simulations. Below, only a small subset of the available results is presented, focusing on the water balance and the groundwater flow in the model area. No calibration against measured site data was performed (because site-specific groundwater level data and meteorological input data were from different time periods, and no discharge data from the site were available). However, differences between modelled and observed water-saturated areas are discussed.

Water balance and surface water discharge

In the F1.1 site description, the total runoff in the model area was estimated to 6.5 $l \cdot s^{-1} \cdot km^{-2}$ /SKB, 2004a/, which corresponds to 205 $mm \cdot year^{-1}$. The modelled specific runoff in the present MIKE SHE model is 7.1 $l \cdot s^{-1} \cdot km^{-2}$, which corresponds to 226 $mm \cdot year^{-1}$. The total actual evapotranspiration (averaged over the model area) was calculated to 441 $mm \cdot year^{-1}$. Thus, the calculated water balance agrees relatively well with the previous estimate, and with other modelling results discussed in Chapter 4.

Figure 5-23 illustrates the calculated water balance and the exchange of water between the different compartments of the model. The error in the water balance is small (1 mm). The water balance was calculated for all compartments of the model. Thus, there are arrows labelled "evaporation" both in the overland compartment and the unsaturated zone compartment. The total actual evapotranspiration is a sum of evaporation from snow, interception, soil surface, ponded water and transpiration.

The calculated evaporation directly from interception was 163 $mm \cdot year^{-1}$, which was larger than the interception calculated with the CoupModel, 130 $mm \cdot year^{-1}$ (see Section 4.4). The total transpiration for the whole area was calculated to 70 $mm \cdot year^{-1}$. If the water balance is calculated only for areas covered with vegetation, the corresponding value is 102 $mm \cdot year^{-1}$. Lakes and areas with ponded water do not generate transpiration. The calculated transpiration in MIKE SHE is low compared to the transpiration calculated with the CoupModel, where the corresponding value for a fresh forest is 196 $mm \cdot year^{-1}$. The calculated transpiration for a wet forest in the CoupModel is 100 $mm \cdot year^{-1}$, which is in the same range as the MIKE SHE results.

As indicated by the various arrows in Figure 5-23, more detailed water balance data than the total evaporation and runoff quantifications presented in the figure can be obtained from the modelling results. The calculated evapotranspiration and runoff components are shown in Table 5-8, where also the flows across the model boundaries are given; boundary inflow/outflow consists of water entering or leaving the model volume as groundwater, whereas the runoff components are surface water flows (overland flow and flow in water courses). The results in Table 5-8 are expressed in terms of averages over the model area (in $mm \cdot year^{-1}$), which implies that, for instance, the evaporation from open water areas depends on both the specific evaporation from these areas and their areal extent within the model area.

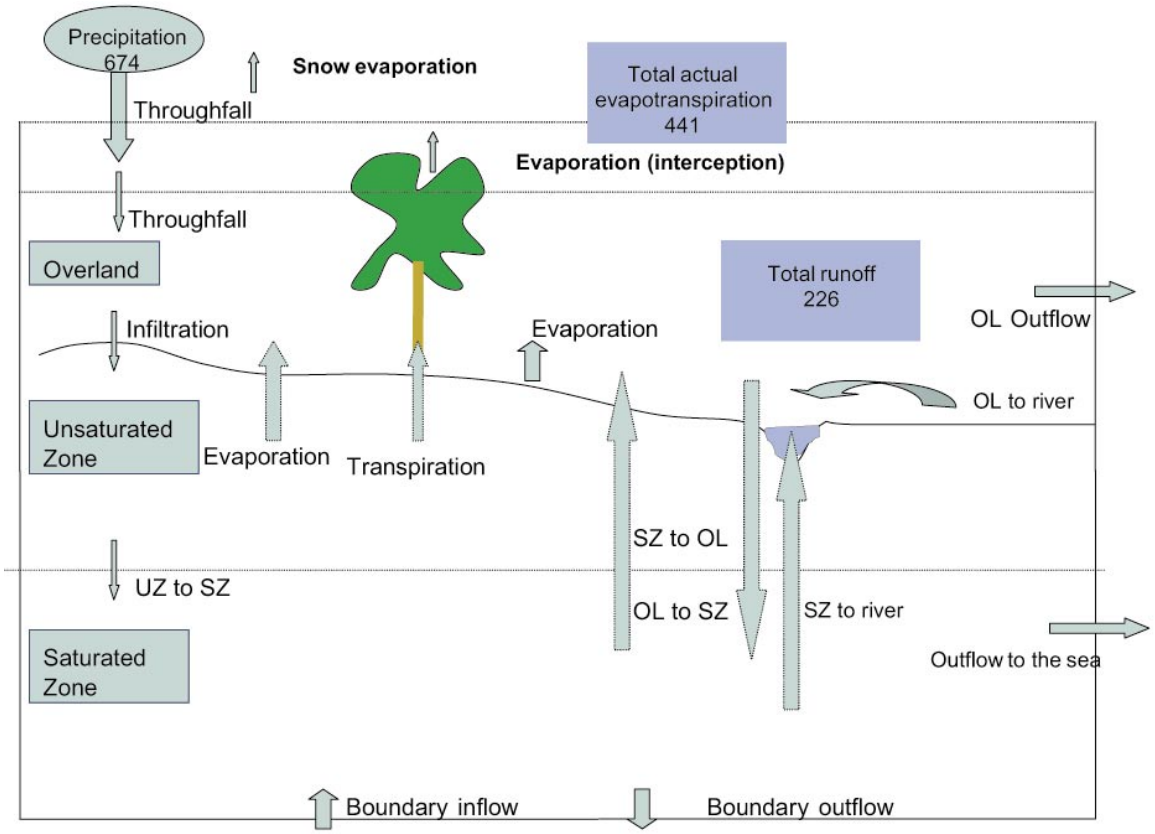

Figure 5-23. *Water balance for the model area and water exchanges between the different compartments of the model.*

Table 5-8 shows that the evaporation components related to intercepted water (on vegetation) and open water (lakes) give similar contributions to the total evapotranspiration from the model area. The contribution from transpiration (water uptake in plants) is about half as large as each of these components. The runoff is dominated by water entering the water courses from overland flow, whereas the groundwater flow across the sea and bottom boundaries is very small compared to most of the other water balance components.

According to the water balance calculation, approximately 480 mm·year^{-1} of the annual precipitation of 674 mm·year^{-1} reach the overland flow compartment in the model; the difference is due to interception and evaporation from snow. The annual flow from the overland flow compartment to the unsaturated zone is c. 170 mm, whereas the annual flow from the unsaturated zone to the saturated zone is nearly 80 mm. In addition, there is an exchange of water directly between the overland and saturated zone compartments. The net flow in this exchange is 55 mm·year^{-1}, mainly consisting of groundwater discharge in the vicinity of water courses and lakes.

As shown above, the runoff is calculated as the net flow of water to the MIKE 11 model plus the water that leaves the model area as overland flow. MIKE 11 calculates the actual discharges and water levels in the water courses. Figure 5-24 shows the hydrograph in three different water courses within the model area, i.e. the outlets of the “Forsmark 1” catchment, Lake Bolundsfjärden in “Forsmark 2”, and the “Forsmark 8” catchment. The hydrograph calculated for Forsmark 1 has many peaks and is highly transient during the year. This indicates that the flow is highly dependent on the weather conditions.

Table 5-8. Results of water balance calculations with MIKE SHE (meteorological data from Örskär for the reference year 1988).

	Water flow (mm·year^{-1})
Total evapotranspiration	**441**
Evaporation from interception	163
Evaporation from soil	24
Evaporation from the saturated zone	5
Evaporation from open/ponded water	144
Evaporation from snow	35
Transpiration	70
Total surface water runoff	**226**
Direct runoff from model area as overland flow	47
Overland flow to water courses	113
Groundwater flow to water courses	66
Net groundwater outflow across boundaries	**5**
Inflow across bottom boundary	–2.0
Outflow across bottom boundary	0.5
Outflow across sea boundary	6.5

The results for the discharge from Lake Bolundsfjärden (Forsmark 2) indicate that the lake reduces the temporal discharge variations in the water course. The discharge in the water course at the outlet of Forsmark 8 (downstream Lake Fiskarfjärden) is smaller than the discharge from Lake Bolundsfjärden, due to the smaller catchment area, but shows a similar pattern of temporal variability. The maximum calculated discharge in the three water courses during the simulation period, approximately 80 l·s^{-1}, occurs in the water course from the Forsmark 1 catchment. However, Figure 5-24 shows that the total annual discharge from Lake Bolundfjärden in Forsmark 2 is much larger than that from Forsmark 1.

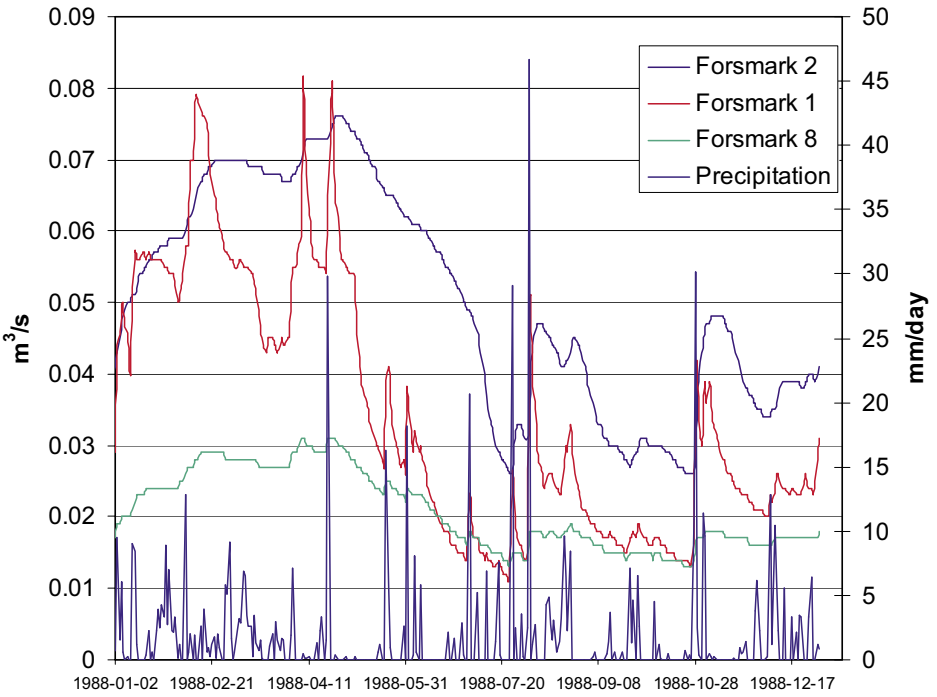

Figure 5-24. *Modelled discharges from three catchments within the model area.*

Groundwater levels

Generally, the calculated groundwater level within the model area was close to the ground surface. For example, the mean groundwater level (i.e. spatially averaged over the model area) in the end of June was 0.2 m below the ground surface, cf Figure 5-25. However, there was a certain temporal variation during the year. As shown in the figure, the calculated depth to the groundwater table in the end of June varied within the model area. The maximum depth was approximately 7 metres below the ground surface, and was found at the topographic heights south of Lake Gällsboträsket.

The mapped water courses and the contours of mapped lakes and wetlands within the model area are marked in Figure 5-25. Yellow, orange or red colours indicate ponded water on the ground surface. It was found that the simulated water depths in the lakes were in accordance with measured depths. The water depths in some wetlands were 0.5–1 m, implying that shallow lakes, rather than wetlands, were obtained in the model.

As described in Chapter 4, the Forsmark model area consists of many small catchment areas, and the groundwater table is generally very shallow. Thus, the model results support these aspects of the descriptive model. As described above, the modelling resulted in too much water ponding on the ground surface in some wetland areas. This result can to some extent be related to errors in the DEM and to man-made structures not included in the

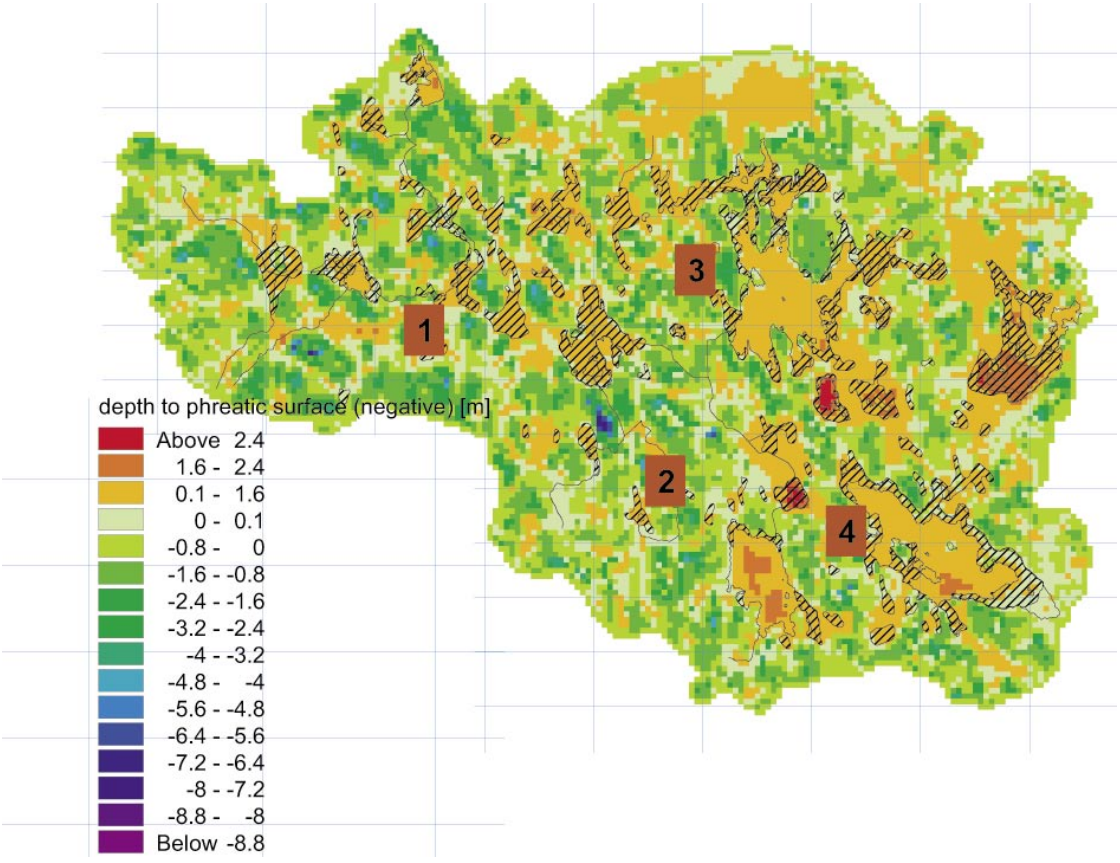

Figure 5-25. *Simulated depth to groundwater table (depth relative to the ground surface) in the end of June during the modelled one-year period. The mapped water courses and lake shorelines are marked by black contour lines, whereas wetlands are indicated by a pattern of diagonal lines. Yellow, orange or red colours indicate ponded water on the ground surface*

present model. For example, there may be ditches or man-made redirections of the surface waters that cause a more effective runoff than that simulated by the river network in the present MIKE 11 model. Another factor that may have contributed to the ponding of water is the hydraulic conductivity values used in the model, i.e. that the values assigned to the QD were incorrect (too low).

Time series showing the fluctuations in the groundwater levels, expressed relative to the ground level, at the points numbered 1 through 4 in Figure 5-25 are shown in Figures 5-26 and 5-27. Points no 3 and no 4 are at locations characterised by a shallow groundwater table, whereas points no 1 and no 2 are located at topographic heights where the depth to the groundwater table is larger. Note that the figures display two different depth intervals, but that the vertical resolution is the same.

Comparing the results in Figures 5-26 and 5-27, it is seen that the two groups of observation points show differences in the temporal variations of the groundwater table. In the points with shallow groundwater, the calculated groundwater levels show short-term variations and a seasonal pattern indicating a strong influence of the variations in the meteorological conditions. Figure 5-26 shows a seasonal variation with groundwater levels above or very close to the ground surface during spring, and decreasing levels during the summer. The groundwater levels are relatively stable during late summer and autumn, and then increase slightly in October–November.

As shown in Figure 5-27, the curves for the points with deeper groundwater tables are smoother, showing less evidence of being affected by short-term meteorological variations. However, the two points also display some differences, with point no 1 showing a larger seasonal variation that resembles the one described above for the shallow groundwater. The seasonal variation at point no 2 is smaller and somewhat delayed compared to the other observation points, even though the groundwater depth is larger at point no 1.

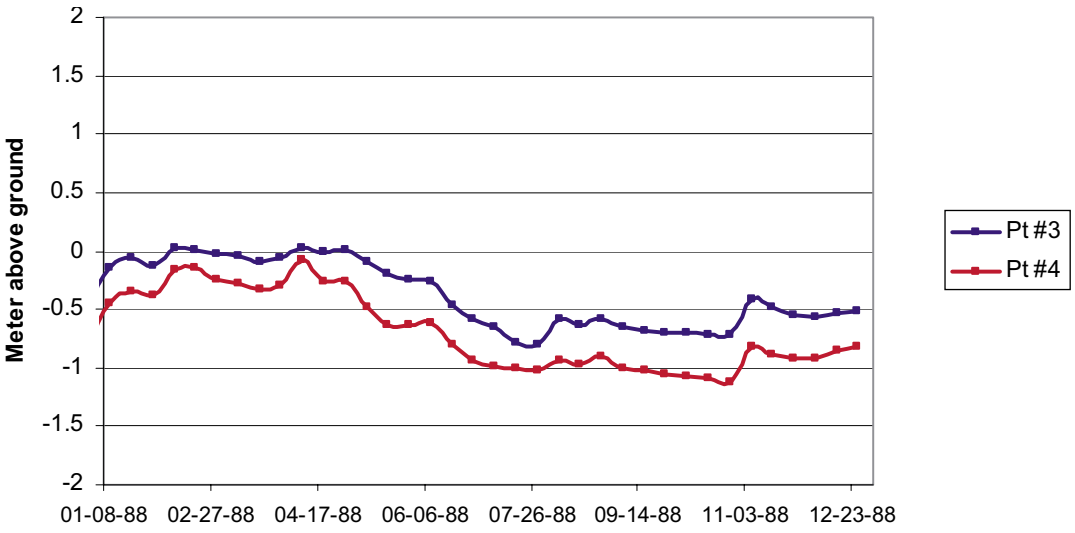

Figure 5-26. *Time series of calculated groundwater levels (relative to the ground surface) at points of shallow groundwater tables (locations shown in Figure 5-25).*

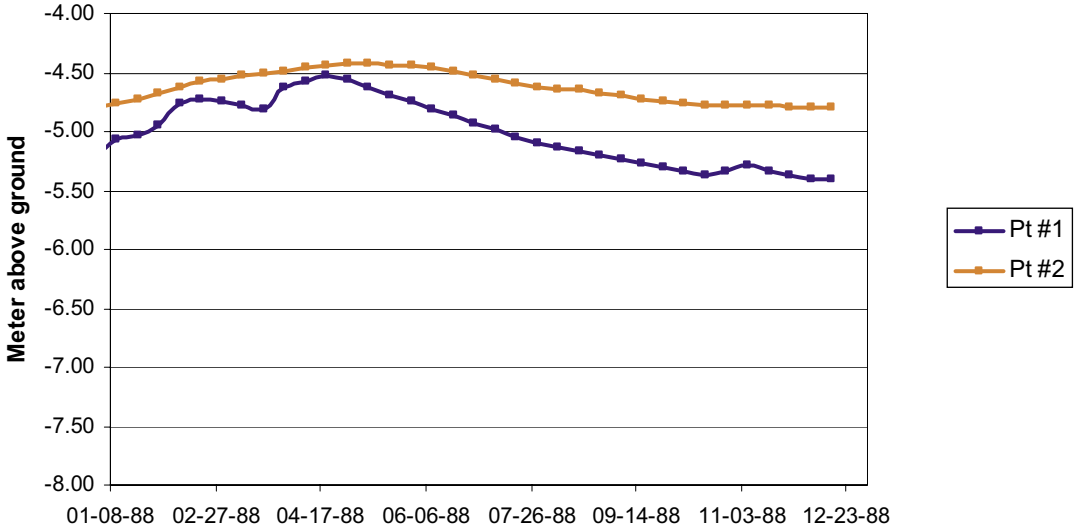

Figure 5-27. *Time series of calculated groundwater levels (relative to the ground surface) at points of deep groundwater tables (locations shown in Figure 5-25).*

The calculated hydraulic head in January in the uppermost layer of the saturated zone (calculation layer 1) is illustrated in Figure 5-28. The red and yellow areas are typical recharge areas. The dark blue areas are discharge areas during most of the year. The contours of the lakes and water courses are marked in the figure. The figure shows that all lakes are discharge areas at the time for which results are presented. The locations of recharge and discharge areas are affected by the meteorological conditions. The simulations show that the red and yellow areas in Figure 5-28 are typical recharge areas during the whole year, whereas the lakes and the water courses are discharge areas throughout the year. The head is decreasing towards the sea, such that the overall flow direction in the area is from the south-western model boundary towards the sea.

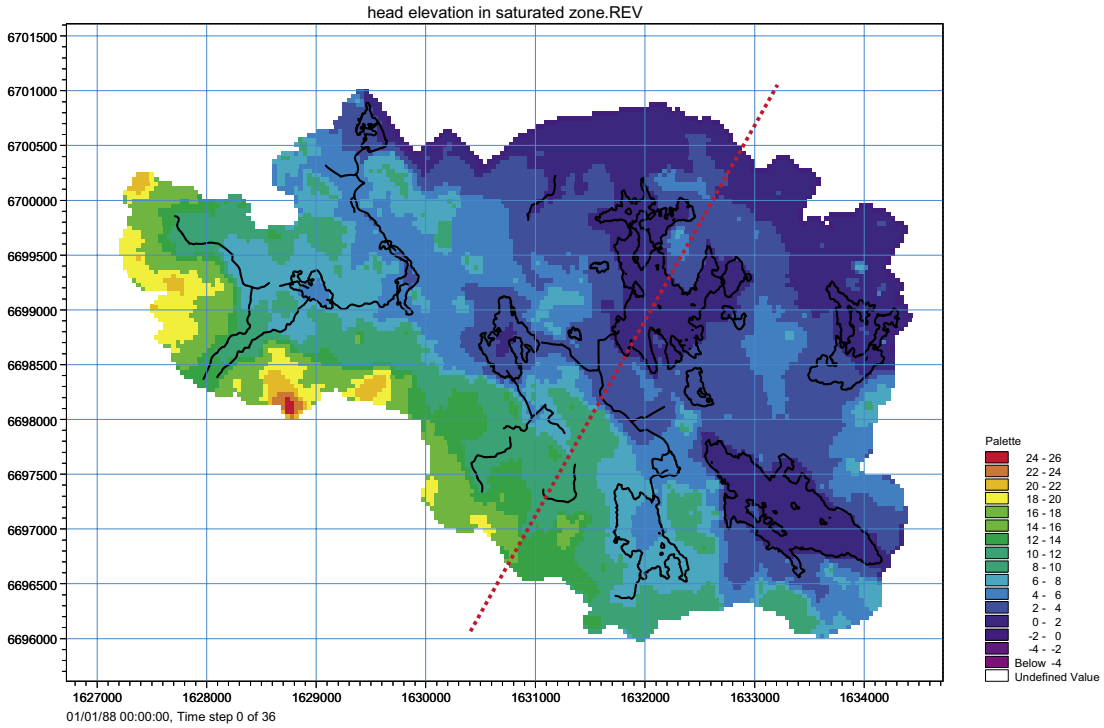

Figure 5-28. *Head elevation in the uppermost calculation layer in the saturated zone (January 1988).*

Figure 5-29 shows a cross-section with the calculated hydraulic heads in each of the twelve calculation layers; the red dotted line in Figure 5-28 shows where the cross section is taken. The positions of the calculation layers in the vertical profile are indicated by the colours of the lines; the lighter green the head elevation curve, the more shallow the calculation layer. The location of Lake Bolundsfjärden is marked in the figure.

It can be seen in Figure 5-29 that the hydraulic head generally is higher at the topographic heights. The topographic heights are typical recharge areas and the lowest points, around the lake and the water course, are discharge areas. This is shown by the order in which the curves for the different layers appear in the figure. In the higher-altitude areas, the more shallow (lighter green) layers show the highest hydraulic heads, indicating a downward flow through the QD profile (recharge). Conversely, the shallow layers display the lowest hydraulic heads in the lower-altitude areas, which indicates upward flow (discharge).

Thus, the shift in the relative positions of the different calculation layers along the cross-section illustrates the large-scale shift from recharge to discharge conditions within the model area. However, it can be seen that also more local changes between recharge and discharge conditions take place in the studied cross-section, in connection with local depressions in the topography.

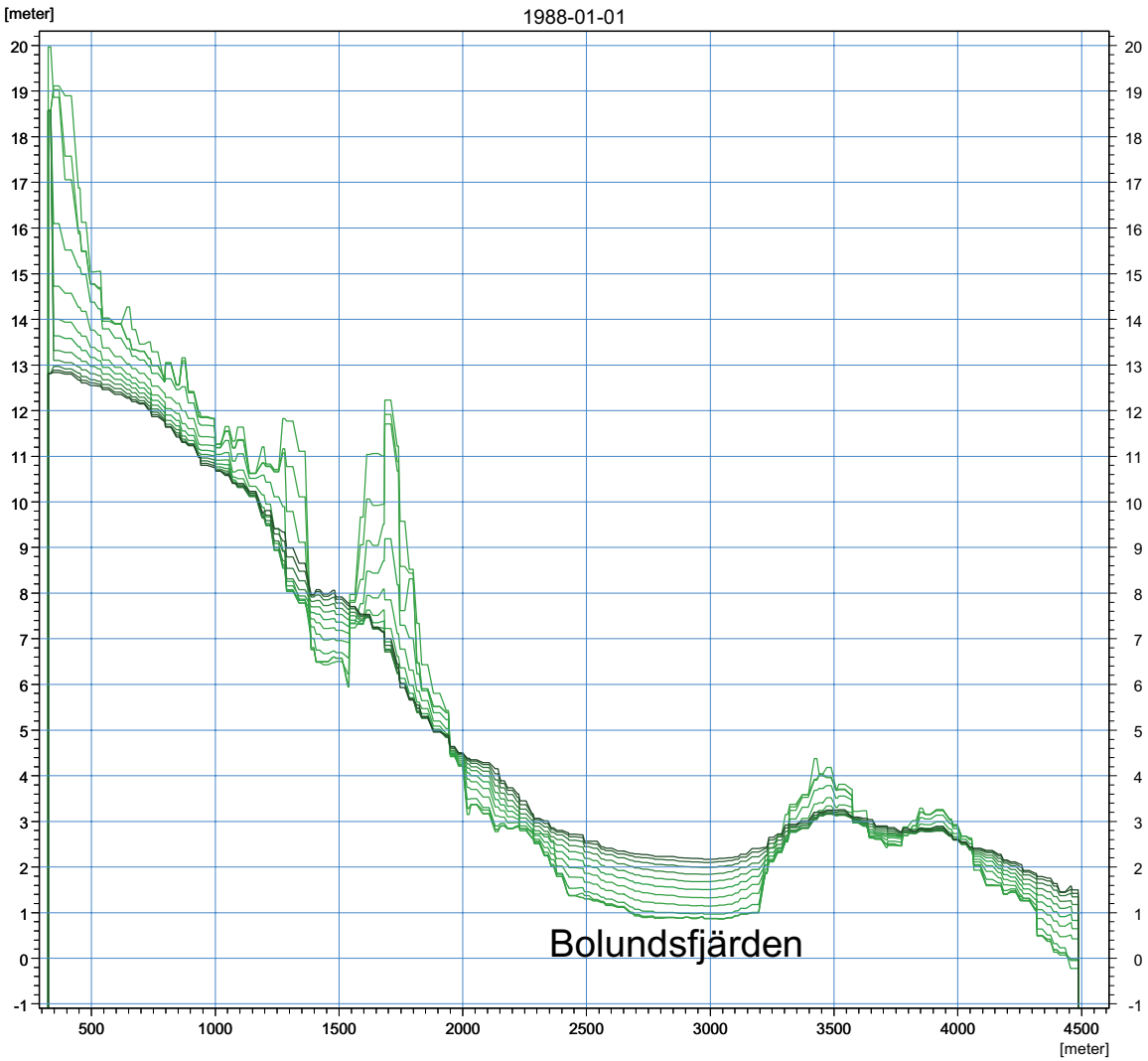

Figure 5-29. *Calculated head elevations (January 1988) in the calculation layers in the saturated zone along the section indicated in Figure 5-28; the lighter green the head elevation curve, the more shallow the calculation layer.*

Spatial distribution of recharge and discharge areas

In accordance with the conceptual model presented in Chapter 4, the QD consisted of three till layers in the MIKE SHE model, except for in areas below lakes and where the total depth of the QD was small, as given by the difference between the ground surface and the bedrock surface in the geological model. As described in Section 5.4.4 (Figure 5-19), the till layers are referred to as layer Z1, Z2 and Z3, respectively, with Z1 being the uppermost layer. Simulation results for saturated groundwater flow in Z1, Z2 and Z3 are presented in Figures 5-30 to 5-33. This means that only the saturated part of the flow system is considered in grid cells that are not fully saturated.

The figures illustrate the angle between the groundwater velocity (Darcy velocity) in the xy-plane and in the z-direction, thereby showing if the flow in each grid cell is horizontal or vertical. In particular, the water flow is vertical and directed upwards if the calculated angle is +90 degrees. If the angle is between –45 and +45 degrees, the groundwater flow is dominated by the horizontal component. Yellow and turquoise areas are areas where the groundwater flow is mainly in the horizontal direction, whereas blue and red areas have vertical upward and downward flow, respectively.

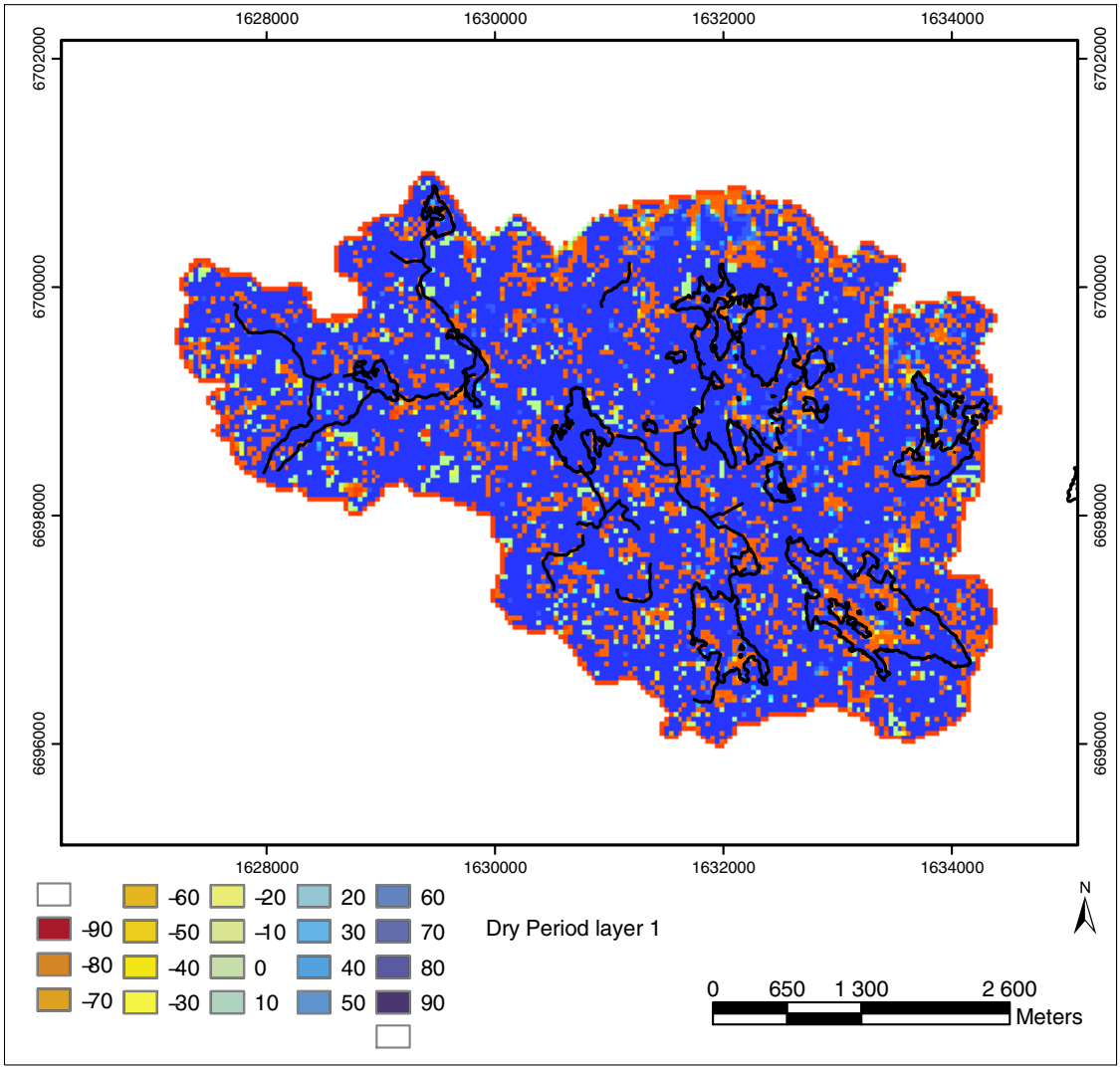

Figure 5-30. *Flow direction relative to the horizontal plane in layer Z1 during a dry period. The legend refers to the angle (in degrees) of the flow vector relative to the horizontal plane; +90 (blue) is up and –90 (red) is down.*

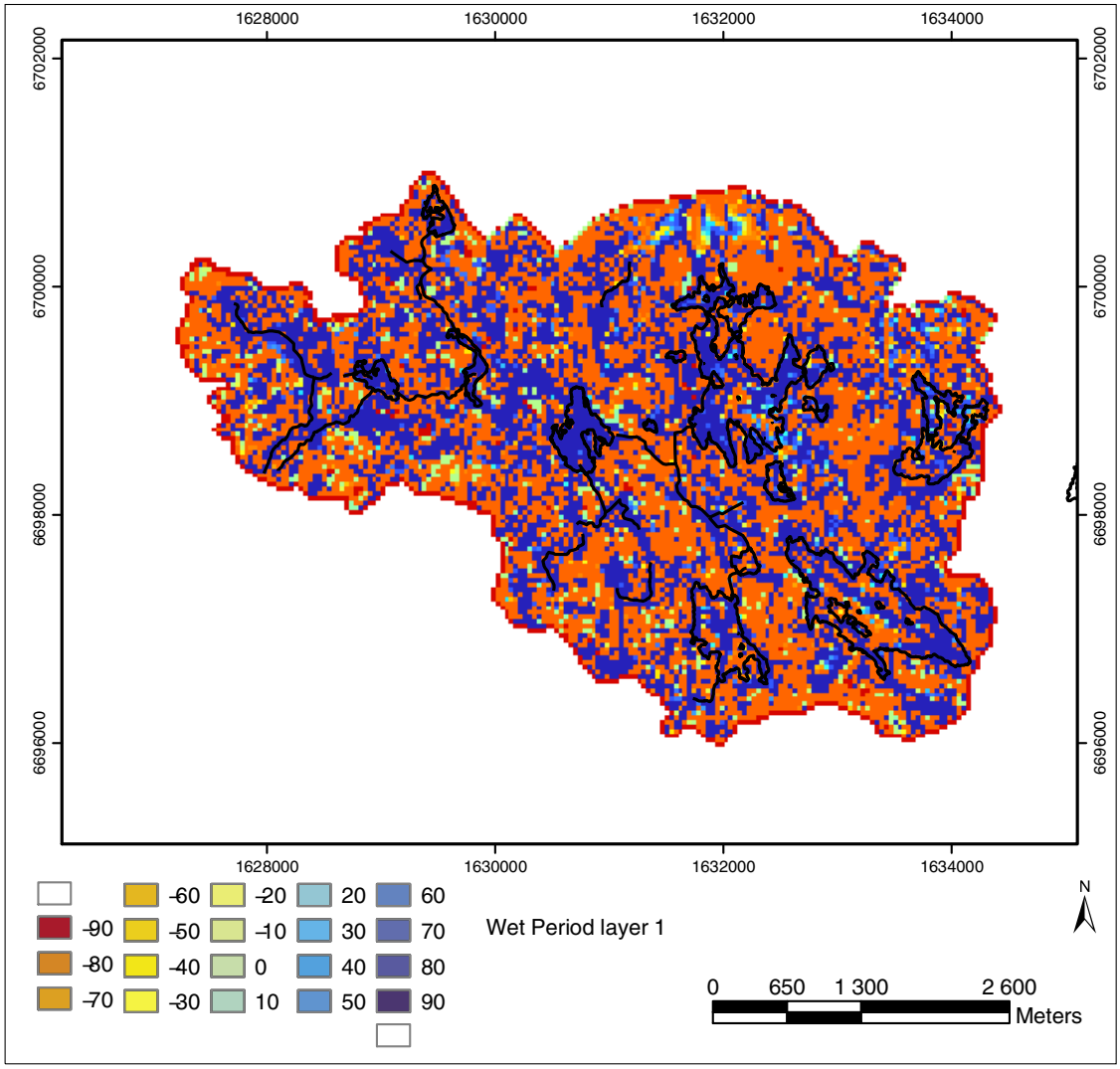

Figure 5-31. *Flow direction relative to the horizontal plane in layer Z1 during a wet period. The legend refers to the angle (in degrees) of the flow vector relative to the horizontal plane; +90 (blue) is up and –90 (red) is down.*

The results in Figures 5-30 and 5-31 show that the calculated groundwater flow in layer Z1 was dominated by its vertical component. During a dry period (in the summer), the evapotranspiration had a strong influence on the water movement in the uppermost layer, see Figure 5-30, such that the uptake of water by the roots in the unsaturated zone caused an upward groundwater flow. The results for Z1 during a wet period, Figure 5-31, showed that the groundwater flow was dominated by vertical flow directed downwards. Areas with upward flow, i.e. blue areas, coincide with lakes and areas in the vicinity of water courses.

The two figures above illustrate how the local topography and the meteorological conditions influence the locations of recharge and discharge areas. The topographic heights were recharge areas in both cases and the areas around the water courses and the lakes were discharge areas during both the dry and the wet periods. The flat areas between the local heights and the topographic minima were recharge or discharge areas depending on the meteorological conditions.

The calculated groundwater flow directions in layer Z2, see Figure 5-32, were also dominated by the vertical component, but also some areas dominated by horizontal flow could be observed. In layer Z2, the spatial distribution of vertical and horizontal flow areas was almost the same during dry and wet periods; Figure 5-32 illustrates the groundwater flow conditions during a dry period. Figures 5-30 to 5-32 illustrate the local character of the near-surface hydrogeology in the Forsmark area, thereby supporting the description in the preceding chapter. The groundwater flow in the upper part of the QD was found to be highly dependent on the meteorological conditions and dominated by the vertical component (either upward or downward flow, depending on the meteorological conditions).

As shown in Figure 5-33, the groundwater flow is dominated by the vertical component also in layer Z3. Also in this layer, the pattern of vertical flow was similar under dry and wet conditions. However, it can be observed that the pattern of upward and downward flow was less "patchy" in layer Z3 than in the layers above it. One reason for this is that calculation layer Z3 only partly consists of QD, i.e. the calculation layers are not identical with the

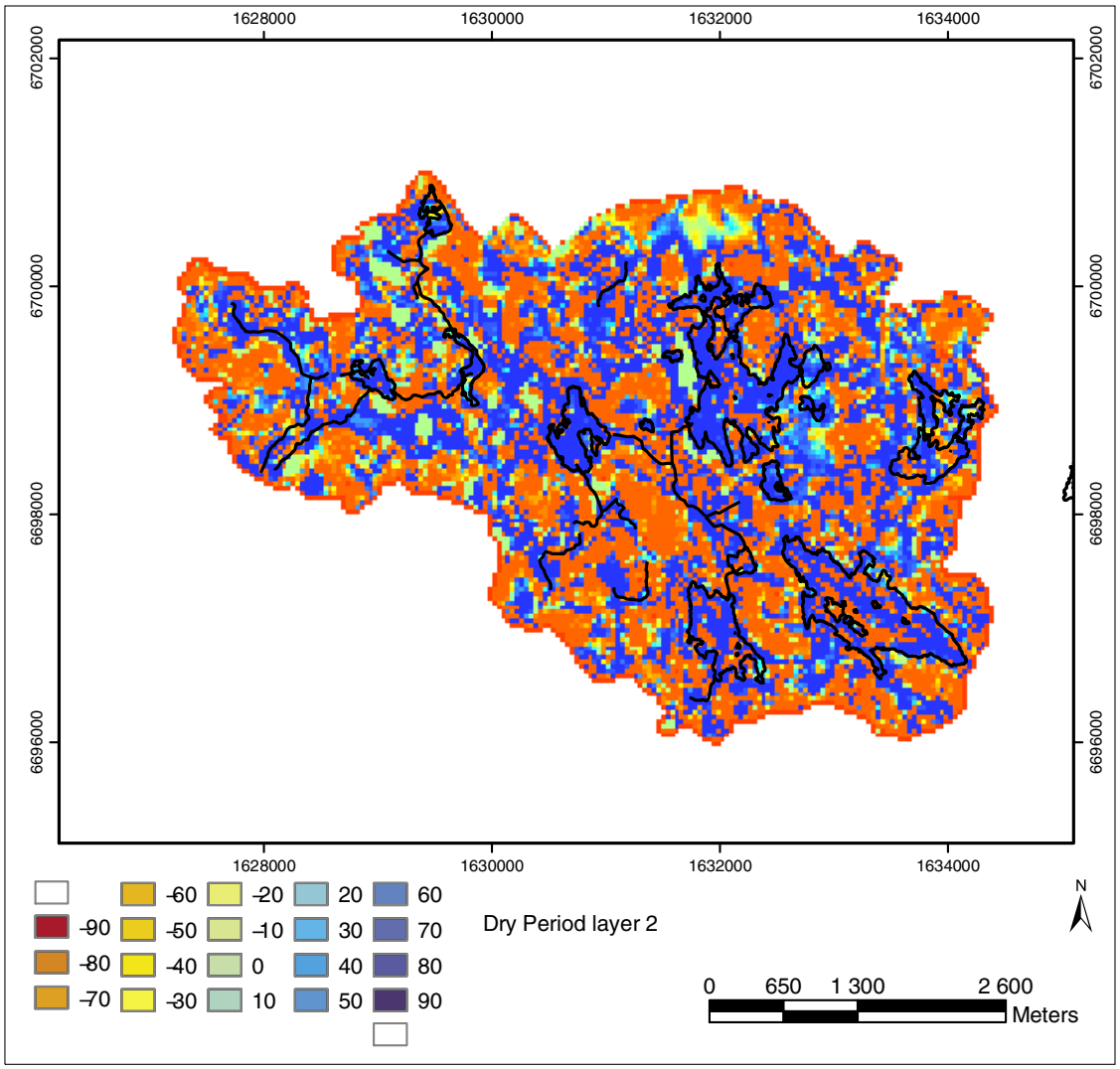

Figure 5-32. *Flow direction relative to the horizontal plane in layer Z2 during a dry period. The legend refers to the angle (in degrees) of the flow vector relative to the horizontal plane; +90 (blue) is up and –90 (red) is down.*

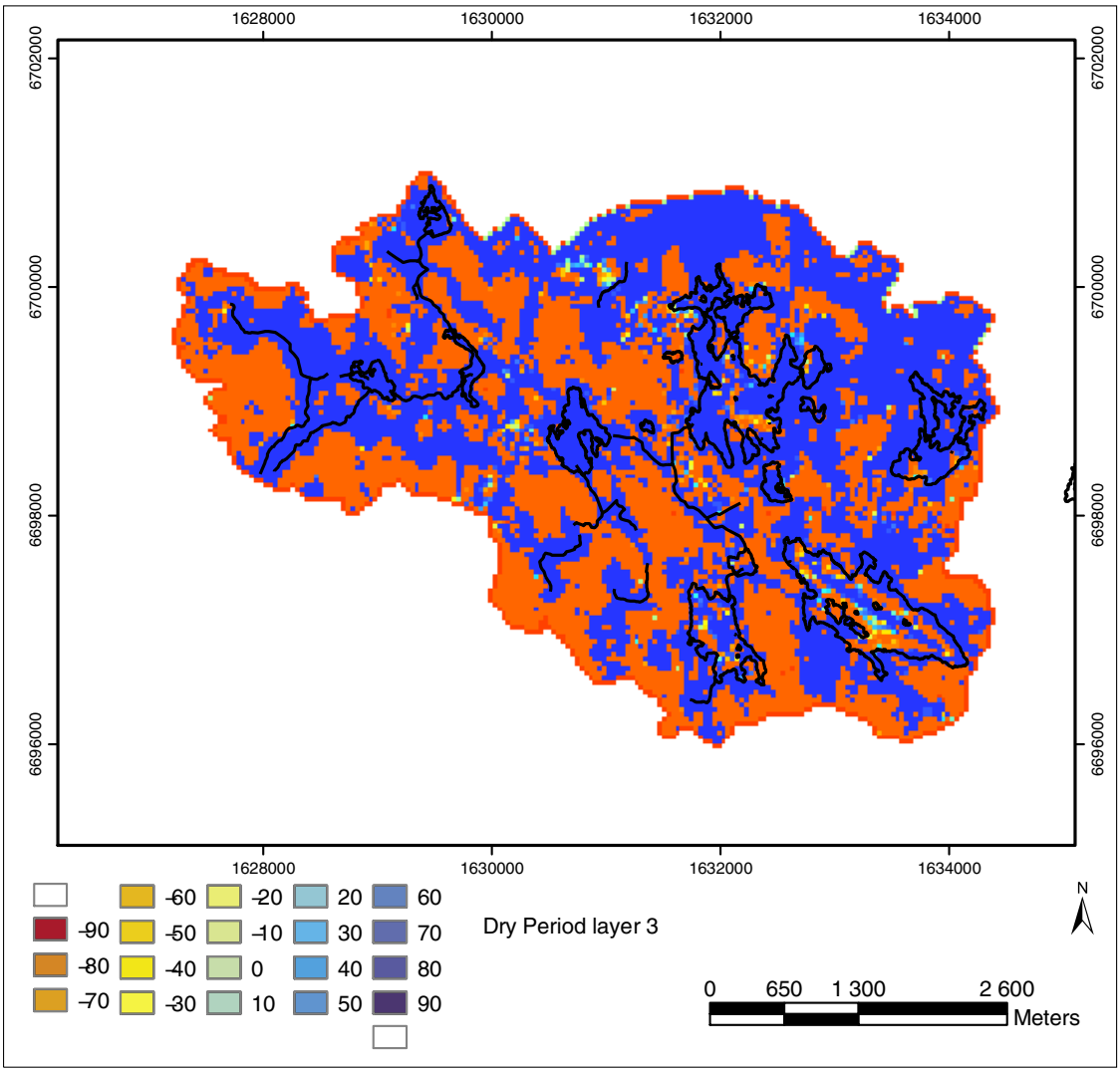

Figure 5-33. *Flow direction relative to the horizontal plane in layer Z3 during a dry period. The legend refers to the angle (in degrees) of the flow vector relative to the horizontal plane; +90 (blue) is up and –90 (red) is down.*

geological layers. Specifically, the calculation layers follow the geological layers with the condition that the minimum thickness of a calculation layer is one meter, which implies that layer Z3 consists of both bedrock and QD. The areas where layer Z3 is dominated by QD are concentrated to the "valleys" and the lakes. In general, the flow in layer Z3 is directed upwards in areas where the layer consists of QD and directed downwards in areas where it mainly consists of bedrock.

The main horizontal flow appeared to occur in layer Z2. In the conceptual modelling, it was assumed that most of the flow takes place in the uppermost, more permeable till layer. If this apparent difference is due to, for instance, insufficient vertical resolution or too small hydraulic conductivity contrasts between the layers, will be investigated in future model versions.

Water exchange with deep groundwater

The bottom boundary condition in the MIKE SHE model is a so-called head-controlled flux boundary condition. The prescribed head at the boundary (represented by the head at 150 m b s l), taken from the F1.1 DarcyTools model /SKB, 2004a/, generates a flux over the bottom boundary. Thus, results from the modelling of groundwater flow in the fractured rock are used as input to the MIKE SHE modelling, which provides a coupling between the deep rock and near-surface groundwater flow systems.

Figure 5-34 shows the vertical groundwater (Darcy) velocity across the bottom boundary in the MIKE SHE model. Green and blue colours indicate inflow to and yellow and red colours outflow from the model volume. The figure illustrates that the main groundwater flow at the bottom boundary took place in the fracture zones. The groundwater flow pattern reflected the extent of the large fracture zone crossing the model area in the F1.1 geological and hydrogeological models of the rock.

There was a net inflow of water to the MIKE SHE model volume during the simulation period. The accumulated net flow over the bottom boundary during one year was 1.3 mm. The corresponding annual flow rate at this depth in the DarcyTools model was calculated to 2.3 mm (also net upward flow). The vertical discretisation in the two models differs, which implies that it is difficult to make an exact comparison of the two model results. However, it can be concluded that the calculated vertical net groundwater flow rates at the level of the bottom boundary in the MIKE SHE model had the same direction and were of the same order of magnitude.

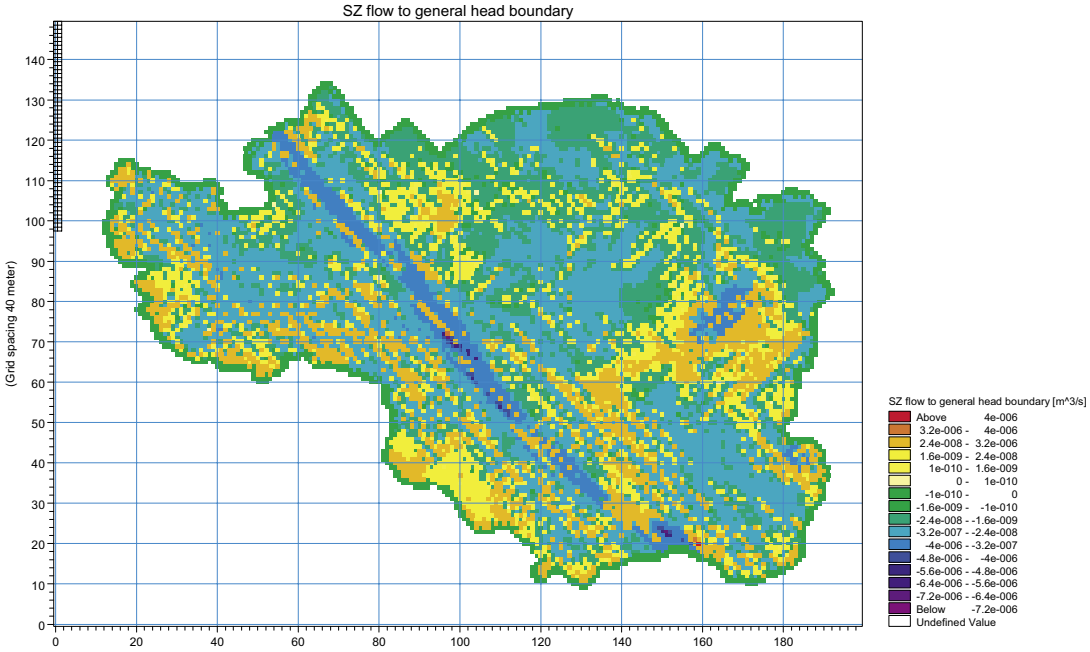

Figure 5-34. *Calculated water exchange with deep groundwater (m^3s^{-1}) in each grid cell (40 m × 40 m) at the end of the calculation year (December 1988).*

Figure 5-35 shows the calculated vertical groundwater flow in all calculation layers along the cross-section indicated in the smaller figure inserted in the lower right corner. The figure shows a snapshot of the groundwater flow taken from the end of December 1988 (i.e. at the end of the calculation year). The pattern of the groundwater flow in the bedrock is similar throughout the calculation year, whereas the flow direction in the uppermost calculation layers changes with the meteorological conditions (cf above). The inserted figure also shows the horizontal hydraulic conductivity in the bedrock (cf Figure 5-18), thereby indicating where the section goes through fracture zones. The arrows show the vertical groundwater flow in all the calculation layers (directions and relative magnitudes). The thickness of the uppermost calculation layers in the QD is much smaller than the thickness of the calculation layers in the bedrock. Therefore, there is just one arrow representing all the three QD layers, whereas the small arrows in the fracture zone represent the flow in each specific calculation layer.

It is clearly seen in Figure 5-35 that the flow rates generally are much higher in the uppermost layers in the QD than in the bedrock, and that the fracture zone dominates the flow in the rock (no flow vectors are visible in the rock outside the zone). The water movement below Lake Eckarfjärden has an upward direction. The groundwater flow in QD in other parts of the cross-section is influenced by the local topography, and can be directed both upwards and downwards. It should be noted that in some locations the direction of the flow vector changes during the year, in connection with, e.g. heavy rains and dry periods.

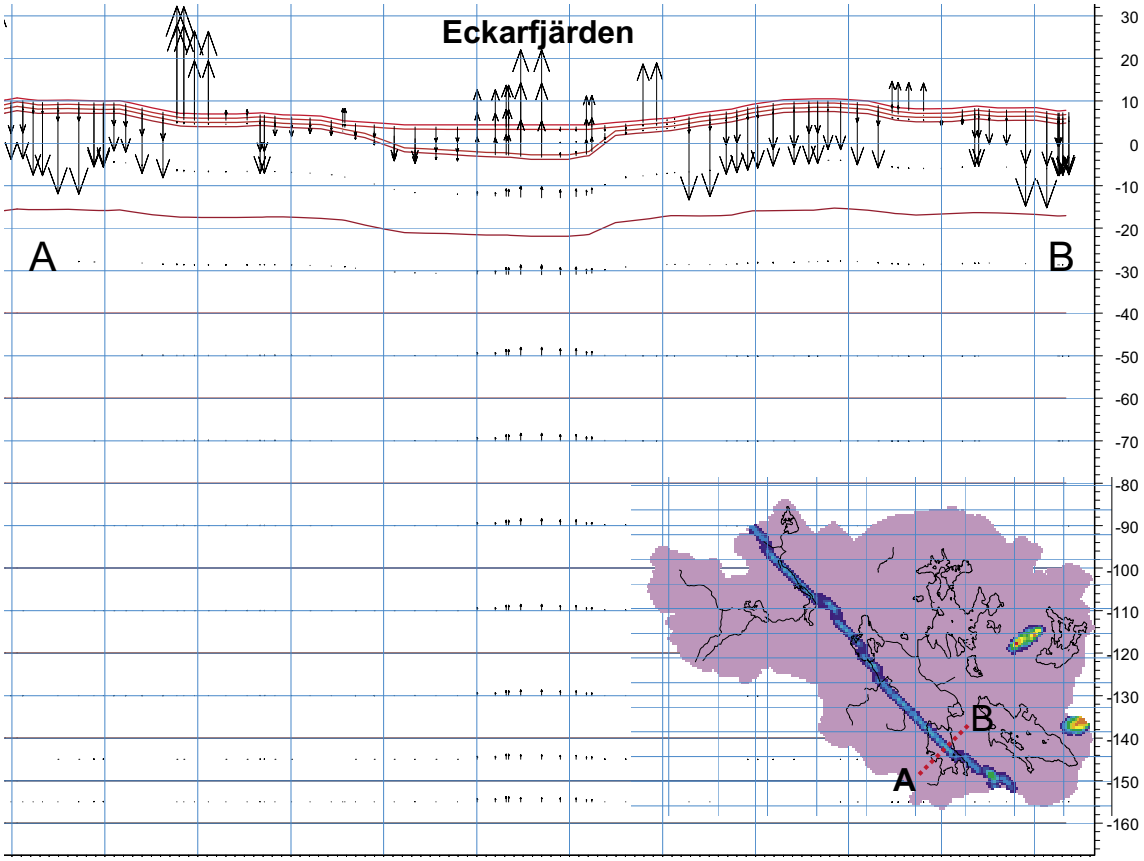

Figure 5-35. *Vertical flow in the calculation layers along cross-section indicated by the red dotted line in the inserted figure. The red lines correspond to the lower levels of each calculation layer. The insert shows the hydraulic conductivity of the bedrock, i.e. the contrast corresponding to the fracture zone.*

5.4.7 Particle tracking results

Particle tracking makes it possible to calculate the flow paths of hypothetical particles as they are transported by water flow within the model volume. The calculated three dimensional flow field is the basis for the movement of the particles. The particles are transported according to the local groundwater velocity calculated in the MIKE SHE water movement module. Additional input data required for the particle tracking simulations are the effective porosity, the number of particles introduced and the starting point for each particle. The effective porosity of the bedrock is imported from the DarcyTools model (Table 5-4), whereas the effective porosity of each QD material is assumed to be equivalent to the specific yield of that material (Table 5-6). The particle tracking simulation is made in the saturated groundwater zone only; particles that leave the saturated zone are not traced further. However, it is possible to identify what kind of sinks the particles have moved to, i.e. water courses, "overland water", the unsaturated zone, model boundaries, or wells (no wells are included in the present MIKE SHE modelling of the Forsmark area).

Two cases were studied in the particle tracking simulations. In both cases, the particles were introduced in the layer above the bottom lower boundary layer (the second lowest layer in the model; it is not possible to introduce particles in boundary cells). The first case ("Case 1" below) considered a uniform injection, in which eight particles were introduced in each grid cell. In the second case ("Case 2"), the introduction of particles was flow-weighted, which means that the number of particles introduced in a given cell was proportional to the vertical groundwater velocity in that cell. All cells in the injection layer that had an upward flow were assigned at least one particle.

The simulation time was 150 years in both release cases, using the calculated transient flow results during the modelled single "representative year". Thus, the model results from the MIKE SHE water movement calculation for this single year were cycled 150 times. A number of "registration zones" in the uppermost calculation layer was defined. These zones make it possible for the user to study where in the model volume a specific particle emerges, i.e. the arrival of the particle in each pre-defined zone can be monitored. It is also possible to calculate the travel times for a particle to each specific registration zone. In the present modelling of the Forsmark area, each sub-catchment and each lake was defined as a separate registration zone.

In Case 1, 45% of the particles left the model volume through the bottom boundary (34%) or through the boundary towards the sea (11%). The Case 2 results showed that only 13% of the particles were crossing the model boundary; the smaller fraction of "escaping" particles is due to the fact that particles were introduced in cells with upward flow only.

Case 1 results

Figure 5-36 shows model results from Case 1. The figure illustrates to which catchment registration zone the particles injected at each release location moved. Specifically, the colour of a cell indicates to which catchment the particles injected at that x,y-position travelled. For example, a cell marked with pink colour indicates that the particles released at that position within the injection layer were traced to the Forsmark 2 catchment (referred to as "Norra bassängen"). It follows that all the particles that emerged in Forsmark 2 were released within the pink area in the figure. In this case, the registration zone reported for each particle was the one where the particle left the saturated zone, which means that the results show the last registration zone along the path.

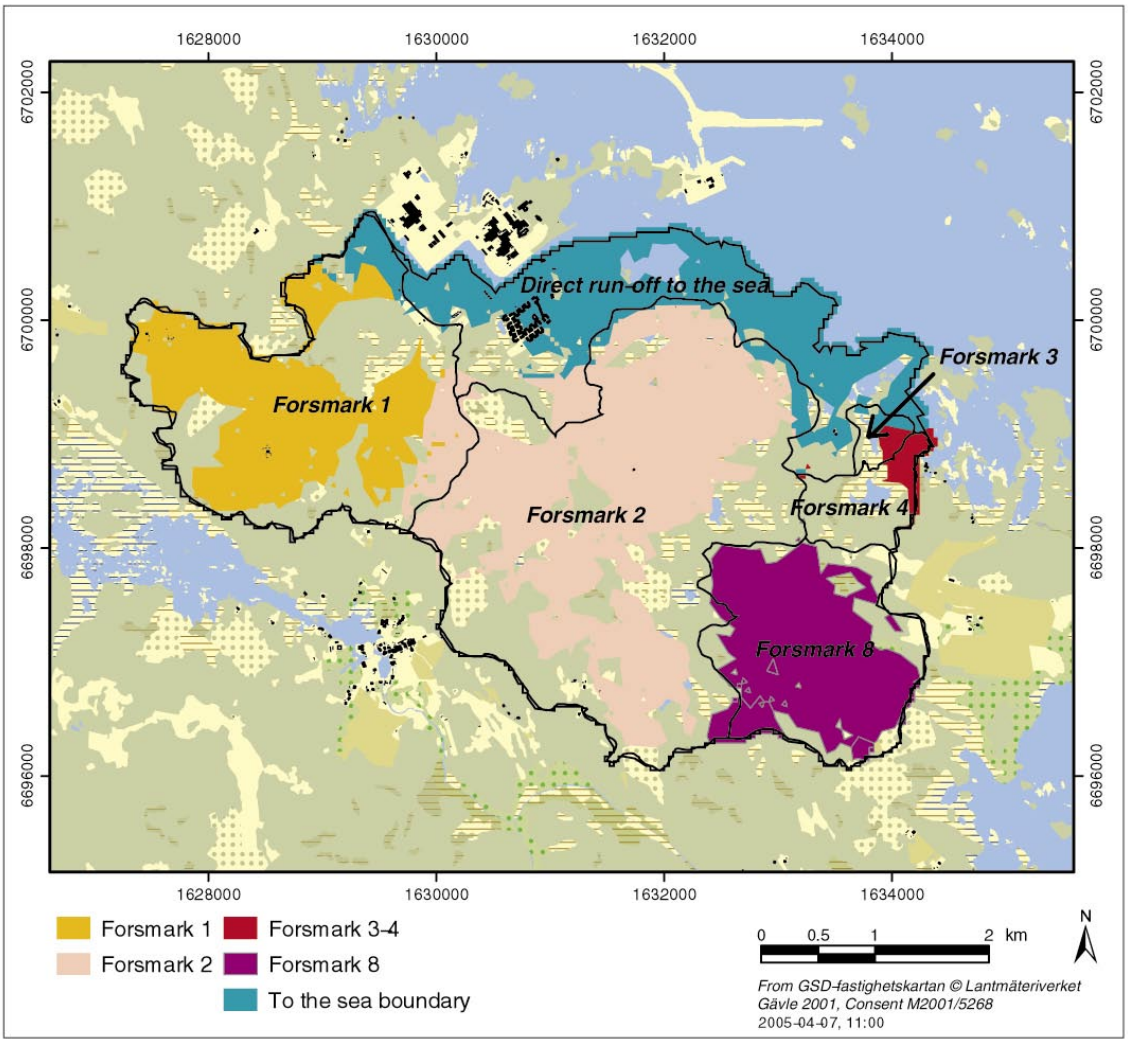

Figure 5-36. *Results of particle tracking simulations, Case 1 (uniform injection). The colour of a cell indicates in which catchment a particle injected at that x,y-position was registered (particles injected in empty cells left the model through the bottom boundary).*

Each colour in the figure is associated with a catchment area, i.e. a registration zone. Empty (non-coloured) areas in the figure indicate that the particles released there left the model through the bottom boundary. The catchment boundaries (the boundaries of the different registration zones) are marked with black lines in the figure. The results in Figure 5-36 show that the particle transport is mainly vertical, such that, e.g. no particles released in the southern part of the model area emerge in the northern part.

In both Case 1 and Case 2, the largest amount of particles was registered in the Forsmark 2 catchment. Thus, the particle tracking simulations indicate that Forsmark 2 is the main discharge area for particles injected at depth in the rock within the whole model area. Table 5-9 summarises the Case 1 particle tracking results, showing the amount of particles registered in each catchment and in the lakes within the catchments. Specifically, 36% of the particles that did not cross the model boundaries at depth were registered in the Forsmark 2 catchment. Almost 50% of these particles were traced to Lake Bolundsfjärden, which was the lake receiving the largest amount of particles. Forsmark 1 received the second largest amount of particles, 17%, followed by Forsmark 8 with 15%.

Table 5-9. Registered particles in different catchments and lakes, Case 1, expressed in terms of absolute numbers and fractions of the total number of particles that did not leave the model volume through the bottom or sea boundaries ("Fraction of all particles") and fractions of the total number of particles registered in each catchment ("Fraction registered in lakes").

	Number of particles registered	Fraction of all particles (%)	Fraction registered in lakes (%)
Forsmark 1	11,498	17	34
Particles registered in L Labboträsket	2,000		
Particles registered in L Gunnarsboträsket	1,882		
Forsmark 2 (Norra bassängen)	24,022	36	79
Particles registered in L Bolundsfjärden	11,294		
Particles registered in L Eckarfjärden	2,890		
Particles registered in L Gällsboträsket	4,902		
Forsmark 8 (Fiskarfjärden)	10,450	15	90
Particles registered in L Fiskarfjärden	9,413		
Forsmark 3 and Forsmark 4	1,104	2	17
Particles registered in L Tallsundet and L Lillfjärden	183		
Total number of particles registered in areas with direct surface runoff to the sea	14,743	22	
Total number of particles registered in water courses	5,650	8	
Total number of particles reaching the surface system	67,467	100	

As explained above, the particle tracking results show where the particles left the saturated zone. Particles registered in the catchment areas could either discharge into the lakes, or travel to the unsaturated zone or the overland water within the catchment. Since the water courses are defined as a separate registration zone, particles travelling directly to them from the saturated zone are reported separately. Table 5-9 shows that 8% of the particles took this path, whereas 22% emerged in areas with direct surface runoff to the sea.

Also listed in Table 5-9 are the fractions of particles registered in lakes, i.e. the number of particles registered in lakes within a catchment divided by the total number of particles registered in that catchment. It is seen that these fractions vary among the catchments; in Forsmark 2 and Forsmark 8, most of the particles (79% and 90%, respectively) discharge into lakes, whereas the corresponding fractions are much smaller for the other catchments.

Table 5-10 lists the results for each lake, expressed as fractions of the total number of particles that were registered in the lakes. Of the total amount of particles left in the model area, almost 50% were traced to a lake. This result supports the assumption that the lakes are important discharge areas. Most of the particles registered in the lakes were traced to Lake Bolundsfjärden (35%) and Lake Fiskarfjärden (29%).

The calculated advective travel time in Case 1 from each cell to the last registration zone, i.e. catchment or lake (the average travel time for all particles injected in the cell), is shown in Figure 5-37. The figure illustrates that the main fracture zone within the area has a strong influence on the travel times; particles released in the fracture zone have very short travel times to the near-surface system. The red areas in Figure 5-37 are areas where the travel time to the uppermost calculation layer (layer Z1) was less than 10 years.

Table 5-10. Particles registered in the lakes in Case 1 (fractions of all particles registered in the lakes).

Lake	Fraction (%)
Bolundsfjärden	35
Eckarfjärden	9
Fiskarfjärden	29
Gällsboträsket	15
Labboträsket	6
Gunnarsboträsket	6
Total	100

Also the areas very close to the sea boundary had short travel times. However, this does not necessarily mean that these particles left the model volume in the uppermost calculation layer. The particles that crossed the model boundary towards the sea were registered in all calculation layers. Therefore, the short travel times near the sea boundary may be related to shorter flow paths, indicating a boundary effect caused by the limited horizontal extent of the model (only land areas were included). Conversely, the particles registered in catchments and lakes had travelled through all layers in the model, i.e. approximately 170 m in the vertical direction.

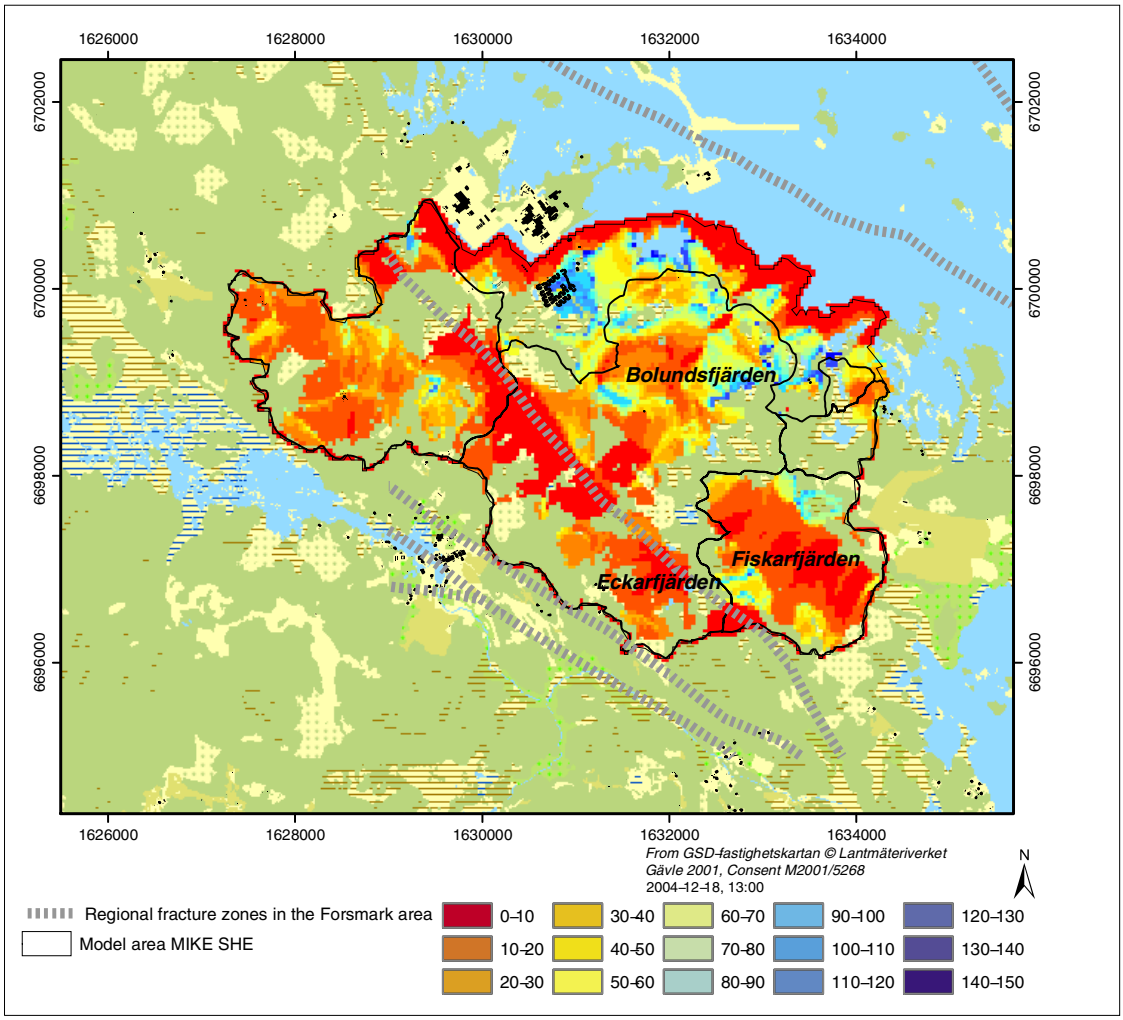

Figure 5-37. *Advective travel times (years) for particles released uniformly near the bottom boundary of the MIKE SHE model (Case 1).*

Case 2 results

In Case 2, the number of particles injected in each cell varied within the model area. Particles were only introduced in areas where the vertical component of the groundwater flow was directed upwards. The injection was flow-weighted, i.e. the higher the flow velocity in an injection cell, the larger the amount of particles introduced into that cell. A total number of 72,099 particles were introduced in the second lowest calculation layer. In this case, only 13% of the particles left the model volume through the boundaries, 10% via the bottom boundary and 3% via the sea boundary.

Figure 5-38 shows the number of particles introduced into each cell. It can be seen that the spatial distribution reflects that of the hydraulic conductivity (cf Figure 5-18). The number of particles injected into a single cell varies from 1 particle per cell to more than 250 particles per cell.

Figure 5-39 shows to which catchments the particles moved in the Case 2 particle tracking simulation. The presentation is similar to that of the Case 1 results discussed above (Figure 5-36), which means that the colour of a cell shows which catchment the particle injected at that x,y-position travelled to and that the results show the last registration zone along each path (i.e. where the particle left saturated zone).

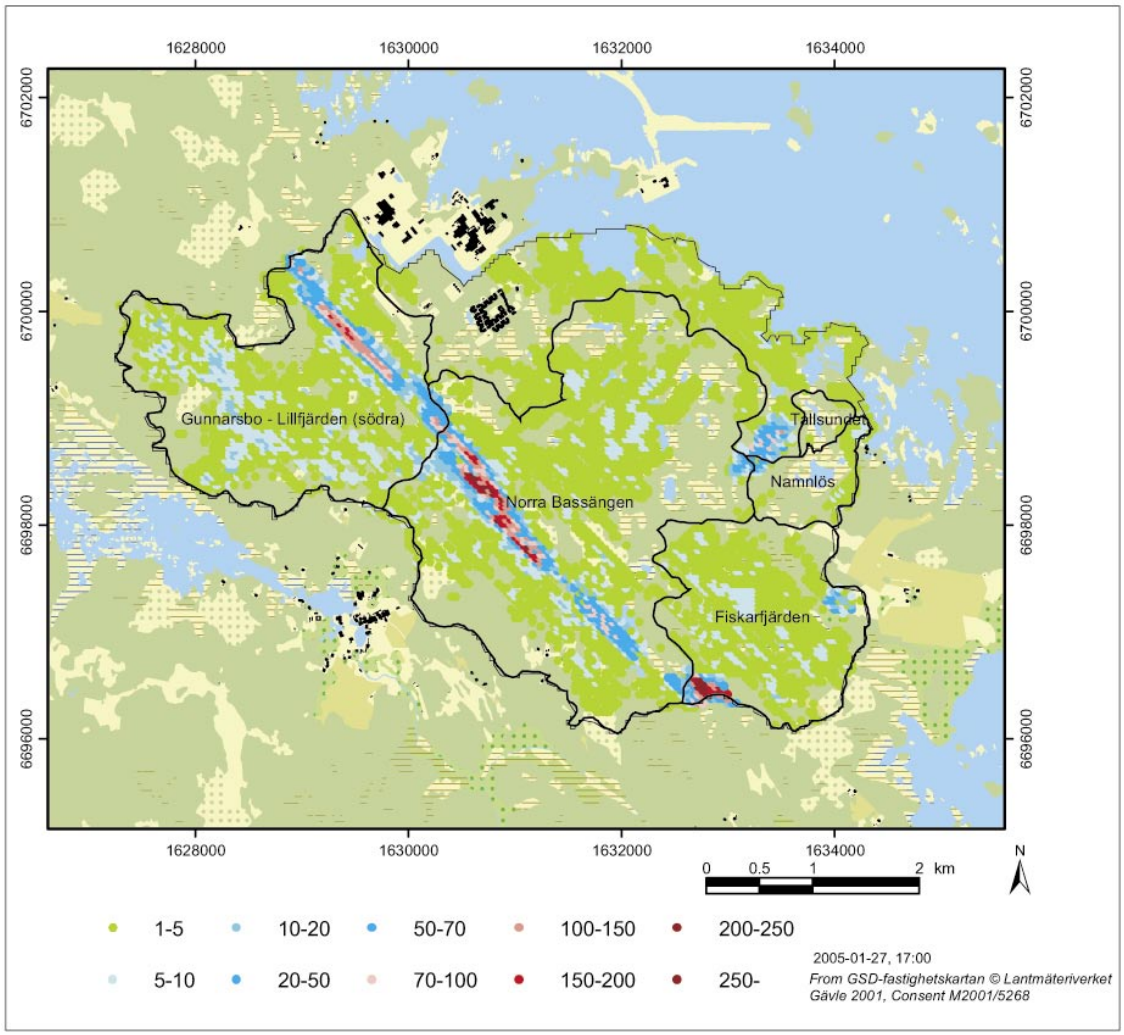

Figure 5-38. *Number of particles introduced into each cell in Case 2 (flow-weighted injection).*

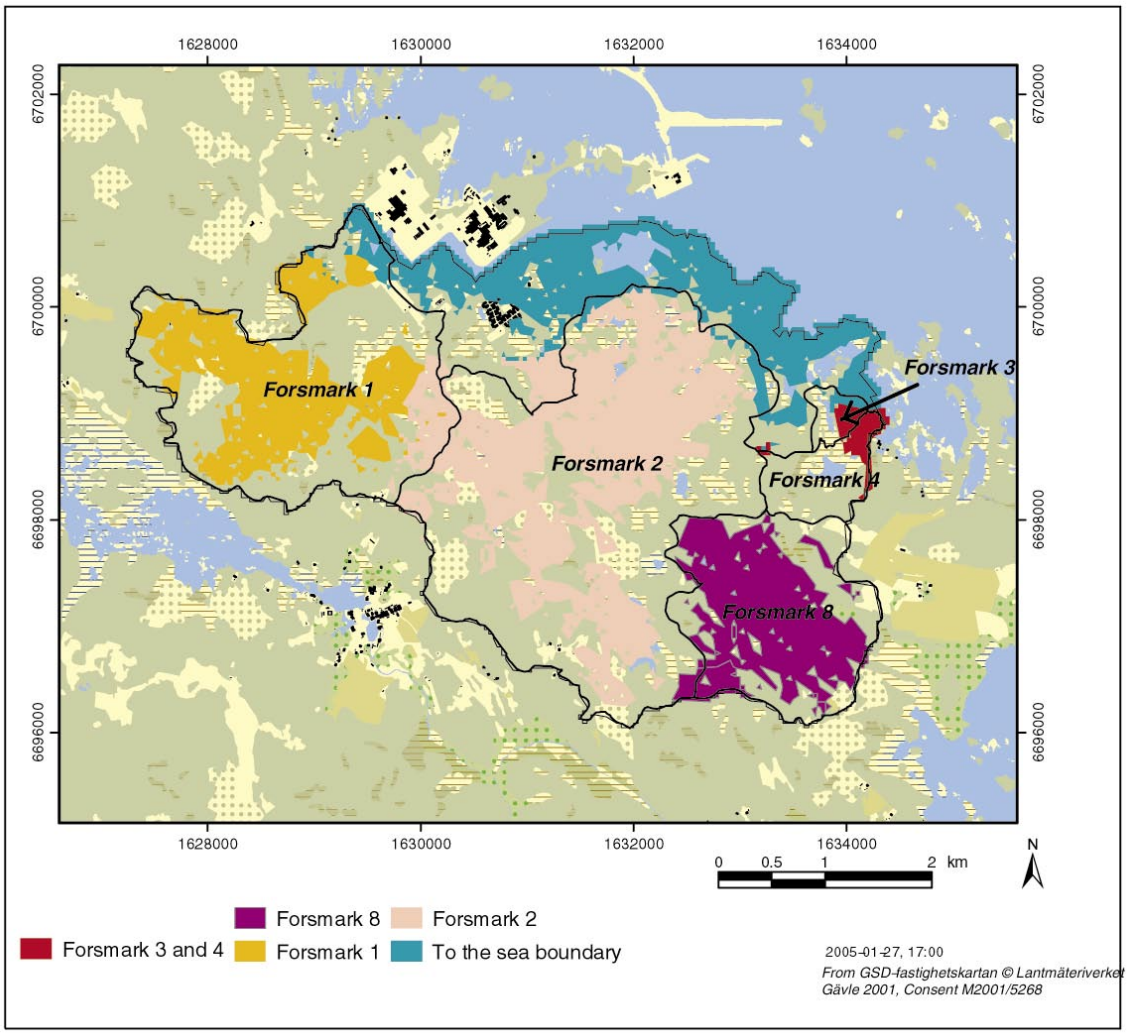

Figure 5-39. *Results of particle tracking simulations, Case 2 (flow-weighted injection). The colour of a cell indicates in which catchment a particle injected at that x,y-position was registered (empty cells indicate that no particles were injected or that the particles left the model through the bottom boundary).*

The results appear to be quite similar to those in Figure 5-36 (Case 1), with some minor differences that probably can be related to the injection procedure. These differences are indicated by a slight reduction of the coloured areas. It can be seen that an overall result characterised by particles emerging within the catchment areas where they were released is obtained also in Case 2.

Table 5-11 lists the amounts of particles registered in each catchment, and the particles emerging in the lakes within the catchments. Also in Case 2, the largest amount of particles was registered in the catchment of Norra Bassängen (Forsmark 2); in this case, 50% of the particles that did not leave the model volume through the boundaries went to Forsmark 2. Forsmark 8 received 16% of the particles and Forsmark 1 12%, whereas 16% went from the saturated zone directly to the water courses.

Table 5-11. Registered particles in different catchments and lakes, Case 2, expressed in terms of absolute numbers and fractions of the total number of particles that did not leave the model volume through the bottom or sea boundaries ("Fraction of all particles") and fractions of the total number of particles registered in each catchment ("Fraction registered in lakes").

	Number of particles registered	Fraction of all particles (%)	Fraction registered in lakes (%)
Forsmark 1	7,415	12	40
Particles registered in L Labboträsket	2,516		
Particles registered in L Gunnarsboträsket	442		
Forsmark 2 (Norra bassängen)	31,130	50	74
Particles registered in L Bolundsfjärden	2,559		
Particles registered in L Eckarfjärden	4,118		
Particles registered in L Gällsboträsket	16,442		
Forsmark 8 (Fiskarfjärden)	10,256	16	28
Particles registered in L Fiskarfjärden	2,831		
Forsmark 3 and Forsmark 4	227	1	28
Particles registered in L Tallsundet and L Lillfjärden	63		
Total number of particles registered in areas with direct surface runoff to the sea	3,061	5	
Total number of particles registered in water courses	10,234	16	
Total number of particles reaching the surface system	62,323	100	

Of the particles registered in Forsmark 2, 53% were traced to Lake Gällsboträsket. This lake is situated above the main fracture zone crossing the model area. Since most of the flow in the rock occurs in the fracture zones, the largest amounts of particles were introduced into the fracture zone cells. Most of these particles have nearly vertical flow paths, and are thus registered in the lakes underlain by the fracture zone. Table 5-11 also shows that most of the particles registered in Forsmark 2, 74%, went to the lakes within the catchment; the corresponding fractions were much smaller for the other catchments, 40% or less.

Comparing the Case 2 results in Table 5-11 with the Case 1 results in Table 5-9, it can be seen that there are some differences in the relative order and particle fractions of the various registration zones, even though the overall pictures are more or less the same. In particular, Case 2 shows a stronger emphasis on Forsmark 2 and the water courses than Case 1. Furthermore, the distribution of the particles on the different lakes within Forsmark 2 changes considerably; Lake Bolundsfjärden dominates in Case 1, whereas Lake Gällsboträsket by far is the most important lake in Case 2. It can also be noted that Lake Fiskarfjärden is a much more important discharge area for particles within Forsmark 8 in Case 1 than in Case 2.

Table 5-12 lists the fractions of all particles reaching the lakes that were registered in each specific lake. In this case, 46% of the total amount of particles not leaving the model through the boundaries was traced to a lake. Also this result supports the assumption that the lakes are distinct discharge areas. As discussed above, the main part of the particles registered in the lakes emerged in Lake Gällsboträsket (57%). Most of these particles are introduced in the fracture zone below the lake, which indicates that the fracture zone in the bedrock and the QD below the lake have a strong hydraulic contact. However, it should be noted that the parametrisation of both the QD and the fracture zone is associated with large uncertainties, implying that also the degree of hydraulic contact is uncertain.

Table 5-12. Particles registered in the lakes in Case 2 (fractions of all particles registered in the lakes).

Lake	Fraction (%)
Bolundsfjärden	9
Eckarfjärden	14
Fiskarfjärden	10
Gällsboträsket	57
Labboträsket	9
Gunnarsboträsket	1
Total	100

The calculated advective travel times in Case 2, reported as average travel times from an injection cell to the last registration zone (catchment or lake) for all particles injected within that cell, are shown in Figure 5-40. The figure shows that the Case 2 travel times follow the same pattern as the travel times in Case 1 (Figure 5-37). The shortest travel times are found in areas close to the fracture zones. Similar to the comparison of registration zones (Figure 5-36 and 5-39), only relatively small differences, mainly in the internal distributions within the individual catchment areas, are identified when comparing the travel time results.

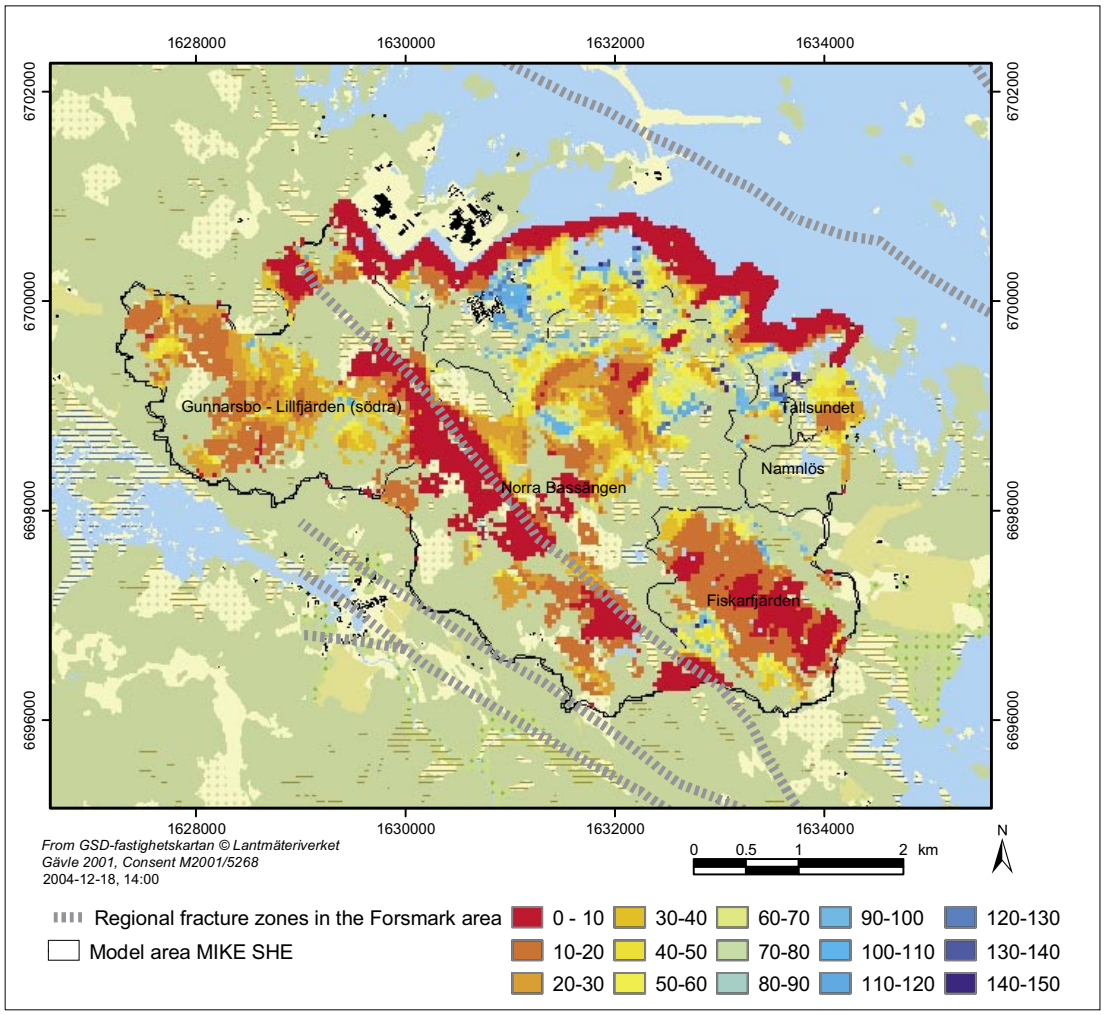

Figure 5-40. *Advective travel times (years) for a flow weighted release of particles near the bottom boundary of the MIKE SHE model (Case 2).*

In summary, the two particle tracking cases showed similar spatial distributions of the particle registration zones. Most of the particles emerged in the lakes. The "Norra bassängen" catchment (Forsmark 2) received most of the particles in both release cases. The largest difference between Case 1 and Case 2 was that most of the particles in Case 1 were traced to Lake Bolundsfjärden, whereas in Case 2 Lake Gällsboträsket was the lake where most of the particles were registered. This result is related to the number of particles introduced in the fracture zone below Lake Gällboträsket; more particles were released in the fracture zone in Case 2. The particle tracking results agree with the results shown in Figure 5-30 to 5-33, emphasising the vertical component of the groundwater flow in the near-surface system.

5.4.8 Evaluation of uncertainties

The present MIKE SHE simulations of the Forsmark area are based on regional (i.e. non site-specific, considered "representative") and spatially uniform meteorological data, and on limited site data on the geological and hydrogeological properties of the modelled system. Specifically, a simplified stratigraphic model of the QD is used, and the available hydraulic dataset does not include site-specific parameters for all materials represented in the flow model.

It follows that there are a number of uncertainties associated with the application of the simulation results for describing the present surface hydrological and near-surface hydrogeological conditions within the Forsmark area. The main uncertainties can be summarised as follows:

- Uncertainties in input data and models from other disciplines:
  - The topographical description (the DEM).
  - The geological descriptions of bedrock and QD (spatial distribution and stratigraphy).
  - The vegetation map.
- Uncertainties in the classification and parametrisation of different types of vegetation for use in the modelling of evapotranspiration and unsaturated flow.
- Uncertainties in the hydraulic parameters for saturated flow in QD and fractured rock, and in the parameters for unsaturated flow.
- Uncertainties in the delineation of catchment boundaries (the boundaries of the model) and in the description of the water courses (positions and cross-sections).
- Uncertainties related to simplifications in process models in MIKE SHE, primarily in the modelling of unsaturated flow and soil freezing/thawing.
- Uncertainties in other input data, primarily the meteorological parameters and their spatial and temporal variability within the model area.

Generally, the uncertainties associated with the limited application of site data in the flow modelling are judged most important at the present stage of model development. The reasons for these uncertainties are related both to the limited availability of site data and to limitations in the analyses performed. The present data gaps concern both basic properties of the system (e.g. hydrogeological parameters for some QD) and data needed to evaluate the model (e.g. measured flow rates).

Perhaps more important for the overall uncertainty is that the analyses performed so far are quite limited when it comes to calibration and sensitivity exercises. It may be noted that the full potential of the dataset presented in this report has not been used in the flow modelling; this is primarily due to time constraints. Since no systematic sensitivity and input data uncertainty analyses were performed in the present model version, there exists only very

limited quantitative input to an uncertainty evaluation. Thus, the uncertainty evaluation provided here is primarily of qualitative character, focusing on identification and qualitative description rather than quantification.

A more detailed evaluation of site data on the variations in hydraulic properties within the model area could improve the model. Some preliminary sensitivity studies have been undertaken in order to investigate the effects of anisotropy in the hydraulic properties of the QD. Although these studies have indicated only small effects on the overall flow pattern and flow rates, extended sensitivity studies will be valuable for assessing geological and hydrogeological uncertainties. However, site data are needed to constrain these sensitivity studies.

In the present descriptive and mathematical models, it is assumed that the hydraulic conductivities of QD are isotropic. One simulation with anisotropic conditions has been performed. In this simulation, the vertical hydraulic conductivity was reduced by a factor of ten. No significant differences in the groundwater levels in the area were observed. In particular, the change in the vertical hydraulic conductivity did not significantly affect the groundwater levels in the observation points in Figure 5-26 and 5-27. However, more extensive analyses are required to investigate the sensitivity to the hydraulic properties of the QD.

The geological/hydrogeological model of the bedrock is taken from the F1.1 modelling /SKB, 2004a/. Since there is a large contrast in hydraulic conductivity between fracture zones and rock mass, with most of the hydrogeological interactions between rock and QD taking place in connection with the fracture zones, uncertainties in the hydrogeological model for the rock and the associated hydrogeological parameters could be important for the surface system model. Therefore, it should be noted that the present model of the surface/near-surface system is based on the F1.1 model of the rock, and that relatively large changes have been made in the F1.2 hydrogeological model of the bedrock.

As indicated by the water balance calculations, it can be expected that the surface hydrology/near-surface hydrogeology is more important for the deep rock hydrogeology than vice versa. However, it should be noted that the details of these interactions are crucial for the modelling of radionuclide transport to and within the surface system. In the present model, the hydraulic properties assigned to QD other than till are based on literature data. This implies relatively large uncertainties in the present description of some materials that may be important for the interactions between rock and overburden, such as lake sediments and fine-grained materials found below lakes and wetlands.

The vegetation classification is based on field inventory of the tree layer. The classification and the parameters describing the properties of each vegetation class are associated with uncertainties; these parameters affect the water balance through the modelling of the evapotranspiration. The potential evapotranspiration is calculated for a grass field. The K_c-value (defined as actual transpiration/potential evapotranspiration) is used to quantify the transpiration capacities of different plants; in some cases, the K_c-value can make the actual transpiration larger than the potential evapotranspiration. Different K_c-values have been investigated in the CoupModel simulations reported by /Gustafsson et al. 2005/. The intention is to use the results of their study as input in future MIKE SHE simulations of the Forsmark area.

The description of the surface water system is important for the modelling of surface hydrology and near-surface hydrogeology. In particular, the various threshold levels and flow resistances in the water courses determine, together with the hydrogeological properties, the distribution of the total runoff on the surface and subsurface systems.

There has been a field inventory of the cross sections and the slope of the river bed in some of the water courses in Forsmark, see Section 3.2.4. For water courses that have not been investigated in the field, the cross sections in the MIKE 11 river network are assumed to have a triangular shapes and the depth from the bank level to the bottom is set to one metre. The field inventory of water courses has been complemented after the F1.2 data freeze, and more data will be available for the forthcoming model versions.

In the MIKE SHE code, the snow cover is simulated with the degree-day-method. The degree-day factor is the amount of snow that melts each day when the temperature is above the threshold temperature (the temperature at which the snow starts to melt). Furthermore, the soil freezing processes are not included in MIKE SHE. These processes are modelled in the one-dimensional "CoupModel", which is used within the SurfaceNet modelling /Lindborg (ed), 2005/. Thus, comparisons between MIKE SHE and "CoupModel" can be made in order to address the process model simplifications in the former model.

5.5 Concluding remarks

The F1.2 quantitative flow modelling includes GIS-based modelling of steady-state flow (total runoff), using the DEM and either a spatially uniform specific discharge estimated from regional meteorological data or spatially variable local discharges obtained from generic data as inputs, and process-based hydrological and hydrogeological modelling with MIKE SHE, using temporally variable meteorological data for a "representative" regional site during a "representative" year. In addition, the MIKE SHE model is based on geological, hydrogeological and vegetation data from the Forsmark area, as well as generic data.

It should be emphasised that the quantitative flow modelling of the Forsmark area has only just started. So far, the modelling has to large extent been focused on the production of outputs required for the ecosystems modelling, and on model testing. Sensitivity analysis is an obvious "missing component" in the work performed to date, which will be an important part of the continued modelling. In particular, such analysis is important for identifying the key processes and parameters, and those that may be handled in a simplified manner.

The modelling presented in this report does not include calibration exercises or detailed comparisons between modelled and measured data. This is mainly due to the fact that the considered meteorological input is non site-specific and that it covers a different time period than the available measurements at the site; therefore, detailed comparisons between measurements and modelling results were not considered meaningful. In future models, the understanding of the hydrological and hydrogeological conditions at the site will be improved by integration of simulations and site data, primarily in the form of site-specific time series of groundwater levels, discharges in water courses and meteorological parameters.

Most of the aspects of the descriptive model that were tested were also confirmed by the modelling results, at least to the degree of detail considered in the present evaluation. The local topography has a strong influence on the surface and near-surface flow pattern in the area. Due to the flat topography, the modelling results are sensitive to errors in the DEM. Within the Forsmark area, the lakes are obvious potential discharge areas, and the topographic heights are recharge areas. However, the measurements at the site show that the lakes may act as recharge areas during dry summer periods. This behaviour has not been observed in the modelling results, which may be a result of the considered meteorological input for the representative year not including "sufficiently extreme" periods or that

the hydraulic properties need to be modified. No site-specific hydraulic parameters are available on materials other than till, such as clay and other materials of importance for the hydraulic contact between groundwater and surface water.

The implications of the simplifications in the modelling of unsaturated flow and freezing should be further analysed. In particular, processes in connection with soil freezing could be important for the retention of water and components transported by water. As discussed above, comparisons between MIKE SHE-results and results from CoupModel simulations could be useful for this purpose. Concerning the unsaturated zone, it is also noted that no site-specific water retention parameters were available for the present modelling. Such data will be available in the future.

Most of the water turnover in the integrated hydrological-hydrogeological system at the site takes place in the QD. According to the presently available information, the groundwater exchange between QD and rock is very small, only a few millimeters per year on average. This was also the conclusion of the coupled hydrogeological and hydrogeochemical evaluations reported by the Hydrogeochemical Analysis Group, HAG /SKB, 2005b/. Therefore, it is important to develop a proper stratigraphical model of the QD, and to obtain adequate hydraulic parameters for the various geological materials.

The fracture zones in the rock dominate the hydrogeological interactions between the rock and QD. This implies that the details of the hydraulic properties of deposits overlying fracture zones must be adequately described. The properties of these materials are of particular importance for radionuclide transport simulations, and for assessing the effects of groundwater level drawdown during the construction and operation phases of the nuclear waste deposit.

6 Resulting description of the Forsmark site

6.1 Development since previous model version

Site-specific data on climate, surface hydrology and near-surface hydrogeology were very limited in Forsmark 1.1 (F1.1). For the present model version, the following additional site-specific data have been available:

- Local meteorological data from two stations (time series of approximately one year).
- Measurements of lake thresholds, and hydraulic gradients and cross-sections in some of the water courses in the area.
- Manual discharge measurements in water courses (time series for an additional 15 months).
- Stratigraphy of Quaternary deposits (QD) from additional drillings performed in connection with installations of groundwater monitoring wells (16 new drillings).
- Hydraulic parameter data from additional slug tests (12) and pumping tests (2).
- Time series of sea, lake and groundwater levels (up to 15 months long).
- Chemical data from surface water and near-surface groundwater.

Based on these additional site-specific data, the conceptual and descriptive models have been improved and given more details. The three-layer model of the till dominating the QD that was proposed in F1.1 still appears to be a reasonable simplification and has got some additional support from the new drillings and hydraulic tests. The available time series of surface and groundwater levels illustrate the close interactions between evapo-transpiration, surface water and near-surface groundwater. The water level time series and the hydrochemistry of the near-surface groundwater indicate complex flow patterns in some important discharge areas.

Preliminary quantitative flow modelling has been performed as a part of Forsmark 1.2 (F1.2) modelling work. The modelling activities included GIS-based hydrological modelling, using the hydrological modelling extension in ArcGIS 8.3 and PCRaster-POLFLOW, as well as more detailed process modelling using the MIKE SHE code. Modelling results have been delivered to the ecological systems modelling, and the modelling has also contributed to and confirmed the site understanding expressed in the descriptive model.

6.2 Summary of present knowledge

6.2.1 Conceptual and descriptive model

The present knowledge, as inferred from data evaluations and expressed in the conceptual and descriptive modelling, can be summarised as follows:

- Data from the local meteorological stations and nearby SMHI regional stations indicate an average corrected annual precipitation of 600–650 mm in the Forsmark area.

- The mean annual evapotranspiration in the dominating forested areas can be estimated to a little more than 400 mm, leaving approximately 200 mm·year^{-1} for runoff.

- The area covered in the conceptual and descriptive modelling is characterised by a low relief and a small-scale topography. Almost the whole area is located below 20 m a s l.

- In total, 25 "lake-centered" catchments, ranging in size from 0.03 km^2 to 8.67 km^2 have been delineated and described within the model area.

- The 25 mapped lakes range in size from 0.006 km^2 to 0.752 km^2. The lakes are very shallow with maximum depths ranging from 0.4 m to 2 m. The major lakes are Lake Fiskarfjärden, Lake Eckarfjärden, and Lake Bolundsfjärden. The bottom sediments mostly consist of a relatively thick gyttja layer underlain by thin layers of sand and clay. However, in Lake Bolundsfjärden the clay layer is missing under a large part of the lake.

- No major water courses flow through the model area. The brooks downstream Lake Gunnarsboträsket, Lake Gällsboträsket, Lake Eckarfjärden and Lake Fiskarfjärden carry water most of the year, whereas the remaining brooks are dry for long periods. No automatic continuous discharge measurements were available for F1.2, but four stations have now been established.

- Wetlands are frequent and cover 10–20% of the areas of the three major catchments, and up to 25–35% of some sub-catchments. The stratigraphy of the wetlands has not been investigated in detail. Peat has developed in the more elevated areas; the thickness of the peat is mostly less than one meter. In more low-lying areas, the peat layer is very thin or missing. The peat is underlain by gyttja and sometimes also by sand and clay layers. The hydraulic contact between the wetlands and the surrounding shallow groundwater largely depends on the stratigraphy. It can be assumed that both wetlands more or less isolated from the nearby shallow groundwater and wetlands with a continuous inflow of groundwater from upgradient areas exist within the model area.

- Till is the dominating Quaternary deposit covering approximately 75% of the area. In most of the area, the till is sandy. However, at Storskäret in the southeast, clayey till dominates. Bedrock outcrops are frequent but cover only approximately 5% of the area. Wave washed sand and gravel, clay, gyttja clay and peat cover about 3–4% each. The till is relatively shallow, usually less than 5 m. The greatest depth of Quaternary deposits (QD) recorded is 16 m. A median depth of 1.9 m, excluding areas with outcropping bedrock, was calculated based on data from drillings, pits and geophysical investigations.

- Based on site-specific and generic data, a three-layer model is proposed for the hydraulic properties of the dominating till, see Table 6-1. The uppermost layer is assigned relatively high hydraulic conductivity and porosity values due to the impact of soil forming processes. The middle layer is given lower values of both conductivity and porosity, in agreement with both site-specific and generic data. A differentiation is proposed between areas with coarse and fine-grained till. The bottom layer, resting on the bedrock, is in accordance with site-specific data assigned a higher conductivity value than the middle layer. However, it is still an open question if the relatively high values obtained in the slug tests are caused by a higher conductivity in the till at the QD/rock interface or if they mainly depend on the properties of a fractured uppermost part of the bedrock.

Table 6-1. Proposed mean values of horizontal saturated hydraulic conductivity, total porosity and effective porosity for a simplified three-layer till profile.

Layer	Horizontal saturated hydraulic conductivity ($m \cdot s^{-1}$)	Total porosity (%)	Effective porosity (%)
0 to 1 m below ground	$1.5 \cdot 10^{-5}$	35	15
Middle layer:			
Coarse till	$1.5 \cdot 10^{-6}$	25	5
Fine-grained till	$1.5 \cdot 10^{-7}$	25	3
0 to 1 m above the bedrock	$1.5 \cdot 10^{-5}$	25	5

- The infiltration capacity exceeds the rainfall and snowmelt intensities with few exceptions. Unsaturated (Hortonian) overland flow only appears over short distances on agricultural land covered by clayey till, on frozen ground where the soil water content is high during freezing, and on outcropping bedrock.

- Direct groundwater recharge from precipitation is the dominant source of groundwater recharge. However, groundwater level measurements in the vicinity of the two lakes Bolundsfjärden and Eckarfjärden show that gradients are from the lakes to the riparian zones during periods of dry summer conditions. Due to the low hydraulic conductivities of the QD materials involved, the flow rates during these periods can be assumed to be small.

- The groundwater is very shallow; groundwater levels are within one meter below ground as an annual mean for almost all groundwater monitoring wells. Also, the annual groundwater level amplitude is less than 1.5 m for most wells. The shallow groundwater levels mean that there is a strong interaction between evapotranspiration, soil moisture and groundwater. This is clearly illustrated by the measured fast groundwater level decline and diurnal groundwater level fluctuations during dry, warm periods. The present situation implies that it is important to make a difference between gross and net groundwater recharge, i.e. transients are important.

- Strong correlations are obtained between groundwater level variations in different groundwater monitoring wells, and between groundwater levels and the cumulative P-ET difference (precipitation minus evapotranspiration). Very strong correlations were also observed between measured groundwater levels and levels simulated based on a simple conceptual hydrological model.

- The correlations between the sea water level and the measured groundwater levels were weak, except for two wells located below open water directly influenced by the sea water and for the two wells at the Börstilåsen esker. The relations between the sea water level and the water levels in Lake Norra Bassängen, Lake Bolundsfjärden and Lake Lillfjärden show that inflow of sea water can occur during periods of high sea water levels.

- Surface water and near-surface groundwater divides are assumed to coincide. The small-scale topography implies that many local, shallow groundwater flow systems are formed in the QD. The hydraulic conductivity profile of the dominating till implies that a dominating part of the groundwater flow will take place along very shallow flow paths. These local and small-scale recharge and discharge areas will overlay more large-scale flow systems associated groundwater flows at greater depths.

- Groundwater level time series from wells in till and bedrock within the same areas show a considerably higher groundwater level in the till than in the bedrock. The observed differences in levels are not fully consistent with the good hydraulic contact between QD and bedrock indicated by the hydraulic tests in the QD. However, the relatively lower groundwater levels in the bedrock may be caused by the horizontal to sub-horizontal highly conductive zones shown to exist in the upper bedrock.

- Not all discharge areas are saturated up to the ground surface, but water flows in the uppermost highly permeable part of the QD profile. "Saturated overland flow" occurs in discharge areas where the groundwater level reaches the ground level. The flat terrain, in combination with the shallow groundwater levels, results in temporal variations in the extents of recharge and discharge areas during the year.

- The sediment stratigraphies of lakes and wetlands are crucial for their function as discharge areas. Low-permeable sediments will restrict the discharge and result in a relocation of the discharge to areas where such sediments are missing.

- "Old" water with high chloride content has been found below Lake Bolundsfjärden, Lake Eckarfjärden and Lake Gällsboträsket. These observations can either be interpreted as the result of a continuous discharge of deep water, or as evidence of more or less stagnant water below the lakes. The two alternative interpretations lead to different conceptual models regarding the role of the lakes as discharge areas for groundwater from greater depths.

6.2.2 Quantitative flow modelling

The observations and conclusions from the quantitative flow modelling with the GIS and MIKE SHE modelling tools can be summarised as follows:

- The results from the hydrological GIS modelling support the assumptions and conclusions in the descriptive model. The flow model is highly sensitive to the topography, as this is the only parameter determining the flow pattern. Consequently, the simulated locations of recharge and discharge areas are strongly influenced by the local topography. In addition, the flat topography implies that small errors in the topographical model (the DEM) may have large effects on the modelled flow pattern. The present analysis shows that there are errors in the DEM, especially along the boundary between the "Forsmark 1" and "Forsmark 2" catchments. If the DEM is used in combination with the field controlled catchment boundaries, boundary effects (flow anomalies) may occur in such areas.

- The GIS-based modelling performed using the PCRaster-POLFLOW tool demonstrated that relatively small modifications of the DEM (i.e. a lowering of the ground surface along the mapped water courses) lead to a much better correspondence between modelled and observed surface water flow patterns than in the analysis based on a direct application of the DEM. A conclusion from the PCRaster calculations of discharges in the coastal outlets is that one single calibration factor appears to be sufficient for correcting the results for the bias indicated by the overall area-averaged discharges. Furthermore, the PCRaster results indicate that spatial variability in the locally generated discharge is an important factor, also in predictions of the discharges from relatively large areas and in the main coastal outlets.

- Ditches, diverted water courses and other human impacts on the system are important in some parts of the model area. These and other types of "man-made structures" are not fully considered in the DEM, and therefore need to be investigated further in order to get a proper description of the surface water and near-surface groundwater systems.

- The water balance for the Forsmark area, as calculated with the MIKE SHE modelling tool, agrees with the presented conceptual and descriptive models of the flow system. The transient model simulations for the selected reference year (1988) result in an annual total runoff of 226 mm and a total actual evapotranspiration of 441 mm. These values are considered to be reasonable for the Forsmark area, but cannot at present be tested against site-specific measurements. The MIKE SHE model produces a shallow groundwater table, which is in accordance with groundwater level measurements within the area, and with the overall conceptualisation of the system.

- The modelling results show that most of the groundwater flow occurs in the QD. During dry summer periods, the evapotranspiration has a strong influence on the groundwater flow. Except from within typical recharge areas, the dominant water flow direction during dry summer periods is upwards. The groundwater flow is dominated by its vertical component. The horizontal groundwater flow paths are short, indicating small-scale local flow systems.

- The results also illustrate the importance of the fracture zones for the groundwater recharge to, or discharge from, the bedrock (the model includes the bedrock to a depth of 150 m, based on the Forsmark 1.1 description of rock hydraulic properties). There is a hydraulic contact between the QD and the fracture zones, where the calculated flow is upwards, although the flow rates are small relative to other components of the water balance. The groundwater flow in the bedrock between the fracture zones is very small. There is a small exchange of groundwater across the bottom boundary of the model (at 150 m depth); the flow direction and magnitude is consistent with the results obtained with the corresponding F1.1 DarcyTools groundwater flow model /SKB, 2004a/.

- Similar to the GIS modelling, the process-based modelling with the MIKE SHE model shows that the locations of recharge and discharge areas are strongly influenced by the local topography. Meteorological parameters (precipitation, snow melt and temperature) also affect the locations of recharge and discharge areas. Within the studied area, the model simulates topographic heights as recharge areas and water courses and lakes as discharge areas throughout the year. However, the locations of local recharge and discharge areas in between these two "extremes" are influenced by the meteorological conditions, and may thus vary during the year.

- The results from the particle tracking simulations show that the groundwater flow is dominated by its vertical component. The catchment "Norra bassängen" (Forsmark 2) receives the main portion of the introduced particles in both of the particle release cases studied (uniform release and flow-weighted release). The dominant transport of particles occurs in the fracture zones, which makes the results of the two cases similar. The travel time of a particle is highly dependent on its release position. The shortest travel times are observed for the registration/observation areas underlain by large fracture zones. However, it should be noted that these results are based on the F1.1 hydrogeological model of the rock, and that large modifications have been made in the F1.2 model. Thus, large changes in the spatial patterns of particle release areas can be expected when the present model is updated in accordance with the F1.2 hydrogeological model of the rock.

6.3 Evaluation of uncertainties

As described in Chapter 2, a relatively large amount of new data has been available for the F1.2 modelling. Specifically, the evaluation of time series of local meteorological data and surface water and groundwater levels, enabling comparisons between different processes and hydrological sub-systems, has lead to an improved understanding of the site that supports some of the fundamental aspects of the descriptive model. However, significant uncertainties still exist regarding the interactions between different sub-systems and the spatial and temporal variability of model parameters. In particular, the site-specific basis for setting boundary conditions in hydrological models (i.e. meteorological data) and for evaluating calculated water balances and surface water discharges (i.e. discharge measurements) is still weak.

The main uncertainties in the present descriptive model can be summarised as follows:

- The available local meteorological time series are very short and longer time series are needed to get reliable correlations to nearby regional SMHI-stations that will allow long-term hydrological and near-surface hydrogeological modelling.

- Local continuous discharge measurements were not available for version F1.2. Time series from such measurements will be most valuable for the derivation of a more accurate total water balance, and can be used for calibration and validation of the quantitative models. Four discharge stations are now running, producing data that will be used in forthcoming model versions.

- The groundwater levels in the area are very shallow. However, there is a bias towards local topographical minima in the location of the monitoring wells. Some additional wells should be installed at typical local topographical maxima (i.e. in recharge areas).

- The evident difference in groundwater levels between the QD and the upper bedrock observed at some of the core-drill sites should be further investigated for a better understanding of the hydraulic contact between the QD and the rock. The sites studied are considered to be recharge areas. A similar study in a local discharge area is recommended.

- More information on the hydraulic conditions around and below lakes and wetlands is essential, since they have been identified as important discharge areas. Further field investigations, including drillings and hydraulic tests, are recommended to reduce this uncertainty.

- The locations of recharge and discharge areas at different scales are crucial for the understanding of the groundwater flow system. A combination of complementary field investigations, including hydrogeological and hydrogeochemical methods, and modelling exercises using models based on morphological parameters as well as hydrogeological modelling is recommended. The model results should be compared with, e.g. the vegetation map, the soil type map and the map of QD.

The present descriptive model of the surface-hydrological and near-surface hydrogeological system is considered to be acceptable in a qualitative sense, which means that the general description of the hydrological and hydrogeological driving forces and the overall flow pattern will not change much in future models. Furthermore, there exists a relatively large amount of quantitative information on, primarily, the hydraulic properties of the QD.

As described above, significant uncertainties remain regarding certain aspects of the model. However, no systematic or complete quantification of uncertainties has been performed in the present model version. Some sensitivity studies have been reported, for instance, the comparison of field controlled and DEM-based catchment areas and the flow modelling with different degrees of anisotropy in the hydraulic conductivity. In addition, the statistics of measured hydraulic conductivities are presented, which gives an indication of the uncertainty associated with spatial variability. It is expected that sensitivity studies with flow models will be an important part of future modelling efforts.

6.4 Implications for future investigations

Presentation and evaluation of the existing database has been an important component of the F1.2 modelling of surface hydrology and near-surface hydrogeology. Based on this work, complemented by a first set of flow simulations, the main uncertainties and the investigations required to reduce these uncertainties have been identified (cf above). Thus, the present modelling results will serve as a basis for the continued site investigations. It can be noted that the investigations identified as important for reducing the uncertainties in the descriptive model include both extensions of presently on-going measurements (e.g. continued meteorological, water level and discharge measurements) and new investigations of, for instance, wetlands.

References

Andersson A-C, Andersson O, Gustafson G, 1984. Brunnar. Undersökning – Dimensionering – Drift. BFR Report R42:1984. Byggforskningsrådet (BFR). (In Swedish.)

Boresjö Bronge L, Wester K, 2003. Vegetation mapping with satellite data of the Forsmark, Tierp and Oskarshamn regions. SKB P-03-83. Svensk Kärnbränslehantering AB.

Brunberg A-K, Blomqvist P, 1998. Vatten i Uppsala län. 1997. Beskrivning, utvärdering, åtgärdsförslag. Rapport nr 8/1998. Upplandsstiftelsen. (In Swedish.)

Brunberg A-K, Carlsson T, Blomqvist P, Brydsten L, Strömgren M, 2004. Identification of catchments, lake-related drainage parameters and lake habitats. SKB P-04-25. Svensk Kärnbränslehantering AB.

Brydsten L, 2004. A method for construction of digital elevation models for site investigation program in Forsmark and Simpevarp. SKB P-04-03. Svensk Kärnbränslehantering AB.

Butler J J Jr, 1998. The design, performance and analysis of slug tests. Lewis Publisher, Boca Raton, Florida, U.S.A.

Carlsson B, Bergström S, Brandt M, Lindström G, 1987. PULS-modellen: Struktur och tillämpningar. SMHI Rapporter Hydrologi Nr. 8. Sveriges Meteorologiska och Hydrologiska Institut (SMHI). (In Swedish.)

Cooper H H Jr, Bredehoeft J D, Papadopoulos I S, 1967. Response of a finite-diameter well to an instantaneous charge of water. Water Resour. Res. 3(1), 263–269.

Darracq A, Destouni G, 2005. In-stream nitrogen attenuation: model-aggregation effects and implications for coastal nitrogen impacts. Environmental Science and Technology, 39(10), 3716–3722, DOI: 10.1021/es049740o.

Darracq A, Greffe F, Hannerz F, Destouni G, Cvetkovic V, 2005. Nutrient transport scenarios in a changing Stockholm and Mälaren valley region. Water Science and Technology, 51(3–4), 31–38.

Destouni G, Hannerz F, Jarsjö J, Prieto C, Shibuo Y, 2005. Distribution and observation gaps of hydrological water-solute pathways from land to coast (submitted to an international journal with peer-review).

DHI Software, 2003. MIKE SHE User's Guide.

DHI Sverige, 1998. VBB VIAK, Kristianstads kommun, 1998. Dokumentation av MIKE SHE-modellen för Kristianstadsslätten. (In Swedish.)

Domenico P-A, Schwartz F W, 1998. Physical and chemical hydrogeology (2nd ed.). John Wiley & Sons Inc, New York, U.S.A.

Eriksson B, 1981. Den "potentiella" evapotranspirationen i Sverige. SMHI RMK Nr 28. Sveriges Meteorologiska och Hydrologiska Institut (SMHI). (In Swedish.)

Espeby B, 1989. Water flow in a forested till slope – field studies and physically based modeling. Report Trita-Kut No 1052. Dept. of Land and Water Resources, Royal Institute of Technology (KTH), Stockholm.

Fredriksson D, 2004. Peatland investigation Forsmark. SKB P-04-127. Svensk Kärnbränslehantering AB.

Freeze R A, Cherry J A, 1979. Groundwater. Prentice-Hall Inc, Englewood Cliffs, New Jersey, U.S.A.

Greffe F, 2003. Material transport in the Norrström drainage basin: Integrating GIS and hydrological process modelling. MSc thesis, Dept. of Land and Water Resources, Royal Institute of Technology (KTH), Stockholm.

Gustafsson D, Lewan L, Jansson P-E, 2004. Modeling water and heat balance of the Boreal Landscape – Comparison of forest and arable land in Scandinavia. J. Applied Meteorology, 43(11), 1750–1767.

Gustafsson D, Gärdenäs A, Jansson P-E, Eckersten H, 2005. Simulated carbon and water processes of forest ecosystems in Forsmark and Simpevarp during a 100 year-period. SKB report in progress. Svensk Kärnbränslehantering AB.

Hedenström A, 2003. Investigation of marine and lacustrine sediments in lakes. SKB P-03-24. Svensk Kärnbränslehantering AB.

Hedenström A, 2004. Investigation of marine and lacustrine sediments in lakes. Stratigraphical and analytical data. SKB P-04-86. Svensk Kärnbränslehantering AB.

Jansson P-E, Karlberg L, 2004. Coupled heat and mass transfer model for soil-plant-atmosphere systems. Dept. of Civil and Environmental Engineering, Royal Institute of Technology (KTH), Stockholm, 435 pp.
(available at ftp://www.lwr.kth.se/CoupModel/CoupModel.pdf)

Jarsjö J, Shibuo Y, Destouni G, 2004. Using the PCRaster-POLFLOW approach to GIS-based modelling of coupled groundwater-surface water hydrology in the Forsmark area. SKB R-04-54. Svensk Kärnbränslehantering AB.

Johansson P-O, 1986. Diurnal groundwater level fluctuations in sandy till – a model analysis. J. of Hydrology, 87, 125–134.

Johansson P-O, 1987a. Estimation of groundwater recharge in till with two different methods using groundwater level fluctuations. J. of Hydrology, 90, 183–198.

Johansson P-O, 1987b. Spring discharge and aquifer characteristics in a sandy till area in southeastern Sweden. Nordic Hydrology, 18, 203–218.

Johansson P-O, 2003. Drilling and sampling in soil. Installation of groundwater monitoring wells and surface water gauges. SKB P-03-64. Svensk Kärnbränslehantering AB.

Johansson P-O, 2004. Undisturbed pore water sampling and permeability measurements with BAT filter tips. Soil sampling for pore water analyses. SKB P-04-136. Svensk Kärnbränslehantering AB.

Kellner E, 2004. Wetlands – different types, their properties and functions. SKB TR-04-08. Svensk Kärnbränslehantering AB.

Kristensen K-J, Jensen S-E, 1975. A model for estimating actual evapotranspiration from potential evaporation. Nordic Hydrology, 6, 170–188.

Larsson-McCann S, Karlsson A, Nord M, Sjögren J, Johansson L, Ivarsson M, Kindell S, 2002. Meteorological, hydrological and oceanographical information and data for the site investigation program in the communities of Östhammar and Tierp in the northern part of Uppland. SKB TR-02-02. Svensk Kärnbränslehantering AB.

Lind B, Lundin L, 1990. Saturated hydraulic conductivity of Scandinavian tills. Nordic Hydrology, 21, 107–118.

Lind B, Ronnert L, Nyborg M, 1994. The hydraulic conductivity of different genetic till types – A geological approach. Trends in Hydrology, 1, 169–178.

Lindborg T (ed), 2005. Description of surface systems. Preliminary site description Forsmark area – version 1.2. SKB R-05-03. Svensk Kärnbränslehantering AB.

Lindell S, Ambjörn C, Juhlin B, Larsson-McCann S, Lindqvist K, 2000. Available climatological and oceanographical data for site investigation program. SKB R-99-70. Svensk Kärnbränslehantering AB.

Lindström G, Rodhe A, 1986. Modelling water exchange and transit times in till basins using oxygen-18. Nordic Hydrology, 17, 325–334.

Lindström G, Gardelin M, Johansson B, Persson, M, Bergström S, 1996. HBV-96: En areellt fördelad modell för vattenkrafthydrologin. SMHI Rapporter Hydrologi Nr 12. Sveriges Meteorologiska och Hydrologiska Institut (SMHI). (In Swedish.)

Ludvigson J-E, 2002. Brunnsinventering i Forsmark. SKB R-02-17. Svensk Kärnbränslehantering AB. (In Swedish.)

Lundin L, 1982. Soil and groundwater in moraine and the influence of the soil type on the runoff. Dept. of Phys. Geogr, Report No 56, University of Uppsala.

Lundin L, Lode E, Stendahl J, Melkerud P-A, Björkvald L, Thorstensson A, 2004. Soils and site types in the Forsmark area. SKB R-04-08. Svensk Kärnbränslehantering AB.

Nilsson A-C, Karlsson S, Borgiel M, 2003. Sampling and analyses of surface waters. Results from sampling in the Forsmark area, March 2002 to March 2003. SKB P-03-27. Svensk Kärnbränslehantering.

Nilsson A-C, Borgiel M, 2004. Sampling and analyses of surface waters. Results from sampling in the Forsmark area, March 2003 to March 2004. SKB P-04-146. Svensk Kärnbränslehantering AB.

Persson C, 1985. Jordartskarta 12I Östhammar NO med beskrivning. SGU Ae 73. Sverigens Geologiska Undersökning (SGU). (In Swedish with English summary.)

Persson C, 1986. Jordartskarta 13I Österlövsta/13J Grundkallen SV med beskrivning. SGU Ae 76. Sverigens Geologiska Undersökning (SGU). (In Swedish with English summary.)

Prieto C, 2005. Groundwater-seawater interactions: seawater intrusion, submarine groundwater discharge and temporal variability and randomness effects, Doctoral thesis in Water Resources Engineering, Royal Institute of Technology (KTH), Stockholm.

Rhén I, Follin S, Hermanson J, 2003. Hydrogeological site descriptive model. A strategy for model development during site investigations. SKB R-03-08. Svensk Kärnbränslehantering AB.

Rodhe A, 1987. The origin of streamwater traced by oxygen-18. Dept. of Phys. Geogr, Report Ser. A, No 41, University of Uppsala.

SGU, 1983. Description and appendices to the hydrogeological map of Uppsala County. Sveriges Geologiska Undersökning (SGU).

SKB, 2000. Förstudie Östhammar. Slutrapport. ISBN-91-972810-4-2. Svensk Kärnbränslehantering AB. (In Swedish.)

SKB, 2001. Site investigations. Investigation methods and general execution programme. SKB TR-01-29. Svensk Kärnbränslehantering AB.

SKB, 2002. Forsmark – site descriptive model version 0. SKB R-02-32. Svensk Kärnbränslehantering AB.

SKB, 2004a. Preliminary site description. Forsmark area – version 1.1. SKB R-04-15. Svensk Kärnbränslehantering AB.

SKB, 2004b. Preliminary site description. Simpevarp area – version 1.1. SKB R-04-25. Svensk Kärnbränslehantering AB.

SKB, 2004c. Interim main report of the safety assessment SR-Can. SKB TR-04-11. Svensk Kärnbränslehantering AB.

SKB, 2005a. Preliminary site description. Forsmark area – version 1.2. SKB R-05-18. Svensk Kärnbränslehantering AB.

SKB, 2005b. Hydrogeochemical evaluation of the Forsmark area, model version 1.2. SKB R-05-17. Svensk Kärnbränslehantering AB.

SMHI, 1985. Svenskt vattenarkiv. Vattendragsregistret. Sveriges Meteorologiska och Hydrologiska Institut (SMHI). (In Swedish.)

Sohlenius G, Rudmark L, Hedenström A, 2004. Mapping of unconsolidated Quaternary deposits 2002-2003. Map description. SKB R-04-39. Svensk Kärnbränslehantering AB.

Svensson U, Kuylenstierna H-O, Ferry M, 2004. Darcy Tools, Version 2.1. Concepts, methods, equations and demo simulations. SKB R-04-19. Svensk Kärnbränslehantering AB.

Vikström M, 2005. Modelling of soil depth and lake sediments. An example from the Forsmark site. SKB R-05-07. Svensk Kärnbränslehantering AB.

Werner K, Johansson P-O, 2003. Slug tests in groundwater monitoring wells in soil. SKB P-03-65. Svensk Kärnbränslehantering AB.

Werner K, 2004. Supplementary slug tests in groundwater monitoring wells in soil. SKB P-04-140. Svensk Kärnbränslehantering AB.

Werner K, Lundholm L, 2004a. Supplementary drilling and soil sampling, installation of groundwater level monitoring wells, a pumping well and surface water level gauges. SKB P-04-139. Svensk Kärnbränslehantering AB.

Werner K, Lundholm L, 2004b. Pumping test in well SFM0074. SKB P-04-142. Svensk Kärnbränslehantering AB.

Werner K, Lundholm L, Johansson P-O, 2004. Drilling and pumping test of wells at Börstilåsen. SKB P-04-138. Svensk Kärnbränslehantering AB.

Werner K, Bosson E, Berglund S, 2005. Description of climate, surface hydrology, and near-surface hydrogeology. Simpevarp 1.2. SKB R-05-04. Svensk Kärnbränslehantering AB.

Appendix 1

Description of measurement points

Surface water level gauges, groundwater monitoring wells, abstraction wells, and BAT-type filter tips

Coordinates, type, and length of time series at data freeze F1.2 (July 31, 2004).

Coordinate system: RT 90 2.5 gon W 0:–15, RHB 70.

Borehole	X	Y	Z	Z ground	Type of measurement point	Start date for data	No of data days
SFM0001	6699713.31	1631335.44	1.10	0.95	Groundwater monitoring well at core-drill site	1-May-03	457
SFM0002	6699585.84	1631377.69	2.02	1.62	Groundwater monitoring well at core-drill site	1-May-03	457
SFM0003	6699614.59	1631487.30	1.94	1.54	Groundwater monitoring well at core-drill site	1-May-03	457
SFM0004	6698865.76	1633441.21	4.14	3.54	Groundwater monitoring well at core-drill site	1-May-03	457
SFM0005	6698647.55	1633252.18	6.80	6.00	Groundwater monitoring well at core-drill site	10-Dec-03	364
SFM0006	6697747.16	1634501.93	6.29	5.89	Groundwater monitoring well at core-drill site	1-May-03	154
SFM0007	6697688.66	1634780.08	7.00	6.60	Groundwater monitoring well at core-drill site	–	0
SFM0008	6697930.56	1634622.99	3.77	3.37	Groundwater monitoring well at core-drill site	22-Aug-03	345
SFM0009	6698577.50	1633223.50	4.64	4.33	Groundwater monitoring well at core-drill site	1-May-03	448
SFM0010	6697313.87	1630734.94	13.54	12.90	Groundwater monitoring well, not at core-drill site	14-May-03	412
SFM0011	6699117.11	1630711.39	6.44	5.79	Groundwater monitoring well, not at core-drill site	1-May-03	457
SFM0012	6698492.25	1630719.10	2.85		Groundwater monitoring well below open water	9-May-03	449
SFM0013	6698698.54	1631122.63	4.40	3.68	Groundwater monitoring well, not at core-drill site	1-May-03	457
SFM0014	6697027.00	1631715.50	6.61	5.59	Groundwater monitoring well, not at core-drill site	1-May-03	404
SFM0015	6697009.79	1631964.04	5.77		Groundwater monitoring well below open water	1-May-03	453
SFM0016	6696976.14	1632173.94	6.19	5.22	Groundwater monitoring well, not at core-drill site	1-May-03	457
SFM0017	6696504.81	1632138.16	6.69	5.65	Groundwater monitoring well, not at core-drill site	1-May-03	457
SFM0018	6696557.50	1631950.00	6.67	5.77	Groundwater monitoring well, not at core-drill site	1-May-03	398
SFM0019	6697700.72	1632118.35	4.77	3.67	Groundwater monitoring well, not at core-drill site	1-May-03	457
SFM0020	6698126.80	1632993.65	2.25	1.67	Groundwater monitoring well, not at core-drill site	1-May-03	457
SFM0021	6699706.35	1632492.99	1.97	1.43	Groundwater monitoring well, not at core-drill site	1-May-03	423

Borehole	X	Y	Z	Z ground	Type of measurement point	Start date for data	No of data days
SFM0022	6697597.55	1632697.18	1.49		Groundwater monitoring well below open water	–	0
SFM0023	6698982.51	1632064.42	1.06		Groundwater monitoring well below open water	16-May-03	426
SFM0024	6699944.40	1633108.79	0.47		Groundwater monitoring well below open water	1-May-04	235
SFM0025	6696039.39	1634774.05	0.86		Groundwater monitoring well below open water	1-May-04	457
SFM0026	6696702.65	1634151.84	1.59	0.70	Groundwater monitoring well, not at core-drill site	18-Aug-03	348
SFM0027	6696685.21	1634146.66	1.75		Groundwater monitoring well, not at core-drill site	–	0
SFM0028	6698507.93	1633588.91	1.07	0.22	Groundwater monitoring well, not at core-drill site	1-May-03	450
SFM0029	6698510.19	1633588.89	1.08		Groundwater monitoring well, not at core-drill site	–	0
SFM0030	6698678.20	1631662.72	2.79	1.67	Groundwater monitoring well, not at core-drill site	1-May-03	457
SFM0031	6698681.55	1631661.09	2.63		Groundwater monitoring well, not at core-drill site	–	0
SFM0032	6698838.26	1631725.79	1.63	0.53	Groundwater monitoring well, not at core-drill site	–	0
SFM0033	6698839.01	1631728.18	1.69	0.67	Groundwater monitoring well, not at core-drill site	1-May-03	391
SFM0034	6699757.49	1631858.50	1.58	0.61	Groundwater monitoring well, not at core-drill site	1-May-03	457
SFM0035	6699756.25	16318592.16	1.49	0.66	Groundwater monitoring well, not at core-drill site	–	0
SFM0036	6699991.99	1631746.07	1.51	0.61	Groundwater monitoring well, not at core-drill site	1-May-03	457
SFM0037	6699991.93	1631744.41	1.50	0.60	Groundwater monitoring well, not at core-drill site	–	0
SFM0038*	6701375.07	1632560.63	2.55		Surface water level gauge	22-May-03	349
SFM0039	6699867.01	1631751.42	1.40		Surface water level gauge	1-May-03	451
SFM0040	6698983.16	1632063.77	1.57		Surface water level gauge	16-May-03	442
SFM0041	6697010.49	1631963.34	5.93		Surface water level gauge	1-May-03	454
SFM0042	6697598.02	1632696.42	1.53		Surface water level gauge	5-Feb-04	177
SFM0043	6696040.29	1634774.45	0.40		Surface water level gauge	1-May-03	267
SFM0049	6700027.55	1630533.057	4.03	2.93	Groundwater monitoring well, not at core-drill site	13-May-03	421
SFM0050	6699601.50	1631487.50	3.01	1.73	BAT filter tip for determination of K-value	–	0
SFM0051	6699600.00	1631488.00	2.18	1.48	BAT filter tip for water sampling	–	0
SFM0052	6698517.90	1633589.70	1.03	–0.27	BAT filter tip for determination of K-value	–	0
SFM0053	6698515.97	1633589.70	0.958	–0.33	BAT filter tip for water sampling	–	0
SFM0054	6697068.43	1634793.37	4.408	3.13	BAT filter tip for determination of K-value	–	0
SFM0055	6697068.55	1634792.70	6.611	3.13	Borehole for soil sampling	–	0

Borehole	X	Y	Z	Z ground	Type of measurement point	Start date for data	No of data days
SFM0056	6697068.43	1634791.67	3.897	2.89	BAT filter tip for water sampling	–	0
SFM0057	6698979.93	1630949.38	4.82	4.27	Groundwater monitoring well, at core-drill site	3-Dec-03	232
SFM0058	6699349.27	1631739.76	3.55	3.20	Groundwater monitoring well, at core-drill site	27-May-04	65
SFM0059	6698464.48	1635777.32	4..53	4.03	Groundwater monitoring well, not at core-drill site	16-Feb-04	166
SFM0060	6698379.81	1635923.87	4.91	4.26	Groundwater monitoring well, not at core-drill site	–	0
SFM0061	6698376.67	1635923.81	5.40	4.33	Abstraction well	16-Feb-04	166
SFM0062	6698838.72	1631807.99	1.18		Groundwater monitoring well below open water	5-May-04	87
SFM0063	6698839.05	1631851.41	1.28		Groundwater monitoring well below open water	–	0
SFM0064	6698491.57	1630718.38	2.80		Surface water level gauge	21-Apr-04	101
SFM0065	6698380.94	1633841.58	0.97		Groundwater monitoring well below open water	28-Apr-04	94
SFM0066	6698380.47	1633842.38	0.89		Surface water level gauge	6-May-04	86
SFM0067	6699120.60	1630713.36	6.37	2.11	Groundwater monitoring well, not at core-drill site	–	0
SFM0068	6699706.12	1632489.56	2.07	1.61	Groundwater monitoring well, not at core-drill site	–	0
SFM0069	6698680.22	1631662.25	2.50	1.87	Groundwater monitoring well, not at core-drill site	–	0
SFM0070	6697069.55	1634783.49	3.72	3.26	Groundwater monitoring well, not at core-drill site	–	0
SFM0071	6697069.45	1634785.08	3.60	3.29	Groundwater monitoring well, not at core-drill site	–	0
SFM0072	6697069.33	1634789.30	3.69	3.27	Groundwater monitoring well, not at core-drill site	–	0
SFM0073	6698513.24	1633585.10	0.63	0.23	Groundwater monitoring well, not at core-drill site	–	0
SFM0074	6698839.08	1631738.02	0.82	0.52	Abstraction well	–	0
SFM0075	6697069.45	1634786.84	3.78	3.27	Groundwater monitoring well, not at core-drill site	–	0
SFM0076	Not surveyed				Groundwater monitoring well at core-drill site	–	0

* Renamed PFM010038.

Correlations between groundwater level time series

Notation: In the table, 01 denotes SFM0001, 02 SFM0002, etc.

	01	02	03	04	05	06	08	09	10	11	12	13	14	15	16	17	18	19	20	21	23	24	25	26	28	30	33	34	36	49	57
01	**1,00**	0,98	0,98	0,91	0,92	0,92	0,82	0,81	0,89	0,84	0,80	0,89	0,90	0,78	0,80	0,84	0,82	0,94	0,92	0,95	0,76	-0,07	0,53	0,84	0,95	0,95	0,70	0,96	0,97	0,73	0,95
02		1,00	0,97	0,86	0,91	0,90	0,71	0,73	0,79	0,77	0,71	0,82	0,82	0,69	0,71	0,76	0,74	0,90	0,86	0,92	0,69	0,01	0,52	0,70	0,91	0,90	0,67	0,92	0,93	0,64	0,93
03			1,00	0,90	0,89	0,94	0,80	0,84	0,89	0,87	0,79	0,87	0,90	0,79	0,81	0,87	0,85	0,95	0,92	0,97	0,75	-0,06	0,55	0,87	0,94	0,96	0,68	0,94	0,96	0,78	0,91
04				1,00	0,92	0,92	0,90	0,87	0,84	0,83	0,84	0,93	0,93	0,84	0,87	0,84	0,83	0,94	0,95	0,92	0,81	-0,25	0,50	0,93	0,95	0,91	0,68	0,92	0,93	0,77	0,92
05					1,00	0,86	0,81	0,77	0,74	0,65	0,80	0,90	0,88	0,75	0,81	0,73	0,66	0,93	0,96	0,94	0,69	-0,47	0,16	0,77	0,94	0,83	0,54	0,89	0,89	0,56	0,87
06						1,00	0,79	0,92	0,93	0,81	0,74	0,84	0,90	0,77	0,84	0,90	0,73	0,93	0,86	0,91	0,66	0,41	0,04	0,88	0,89	0,96	0,29	0,92	0,95	0,78	0,83
08							1,00	0,83	0,79	0,86	0,90	0,91	0,86	0,87	0,90	0,81	0,85	0,79	0,86	0,77	0,80	-0,39	0,42	0,93	0,88	0,79	0,52	0,84	0,84	0,81	0,92
09								1,00	0,82	0,94	0,90	0,90	0,95	0,95	0,97	0,96	0,95	0,89	0,92	0,88	0,82	-0,29	0,58	0,95	0,89	0,91	0,60	0,85	0,88	0,98	0,93
10									1,00	0,85	0,87	0,91	0,92	0,81	0,87	0,89	0,88	0,91	0,89	0,89	0,81	-0,38	0,24	0,85	0,88	0,95	0,54	0,94	0,95	0,77	0,87
11										1,00	0,91	0,91	0,92	0,90	0,93	0,93	0,94	0,88	0,89	0,87	0,81	-0,22	0,55	0,92	0,88	0,91	0,61	0,87	0,89	0,94	0,82
12											1,00	0,96	0,94	0,92	0,96	0,91	0,91	0,85	0,89	0,84	0,89	-0,37	0,43	0,89	0,87	0,87	0,65	0,89	0,88	0,88	0,83
13												1,00	0,96	0,91	0,94	0,91	0,89	0,92	0,95	0,90	0,88	-0,32	0,46	0,90	0,94	0,92	0,70	0,95	0,94	0,85	0,91
14													1,00	0,95	0,96	0,97	0,96	0,95	0,98	0,94	0,88	-0,28	0,57	0,94	0,95	0,96	0,70	0,94	0,94	0,90	0,96
15														1,00	0,98	0,94	0,95	0,85	0,90	0,84	0,92	-0,37	0,58	0,94	0,88	0,87	0,68	0,85	0,85	0,93	0,84
16															1,00	0,96	0,95	0,88	0,92	0,86	0,89	-0,38	0,55	0,96	0,90	0,89	0,66	0,88	0,88	0,95	0,92
17																1,00	0,98	0,91	0,93	0,91	0,85	-0,27	0,57	0,92	0,90	0,94	0,66	0,89	0,89	0,94	0,94
18																	1,00	0,89	0,91	0,90	0,88	-0,25	0,67	0,94	0,88	0,92	0,66	0,87	0,86	0,94	0,84
19																		1,00	0,97	0,98	0,81	-0,23	0,53	0,85	0,96	0,98	0,71	0,94	0,94	0,80	0,94
20																			1,00	0,95	0,84	-0,25	0,56	0,90	0,97	0,95	0,71	0,94	0,94	0,85	0,95
21																				1,00	0,79	-0,17	0,58	0,85	0,95	0,98	0,71	0,93	0,94	0,81	0,92
23																					1,00	-0,35	0,49	0,82	0,85	0,82	0,65	0,86	0,83	0,79	0,74
24																						1,00	0,34	-0,49	-0,16	-0,22	-0,20	-0,19	-0,21	-0,32	0,18
25																							1,00	0,39	0,58	0,53	0,46	0,48	0,48	0,55	0,18
26																								1,00	0,90	0,89	0,50	0,84	0,89	0,91	0,95
28																									1,00	0,95	0,73	0,97	0,96	0,80	0,90
30																										1,00	0,69	0,94	0,96	0,85	0,91
33																											1,00	0,72	0,67	0,51	0,48
34																												1,00	0,98	0,78	0,93
36																													1,00	0,82	0,90
49																														1,00	0,87
57																															1,00

Shaded blue = wells below surface waters

Shaded red = correlation R^2>0.95

Excludes:

- water surface elevations
- data sets with < 200 days

Appendix 3

Modelling of near-surface groundwater monitoring well time series using a simple conceptual hydrological model

Background

A detailed analysis of data collected from 52 groundwater monitoring wells in Quaternary deposits within the Forsmark site investigation had suggested that correlations existed between most of these well time series with regional precipitation (P) events and potential evapotranspiration (PET) cycles. The modelling effort reported herein was proposed as an investigation to deepen our understanding of these relationships. In this effort, a simple conceptual hydrological model was calibrated on a well-by-well basis to best simulate well time series as a hydrologic response to P events and PET cycles.

Model selection

The intent was to apply a simple, well-established model structure, tested and validated for typically Swedish conditions. The model structure that was selected for this study was virtually identical to the PULS model /Carlsson et al. 1987/. The PULS model was developed from the HBV-model that is SMHI's standard model for hydrological forecasting /Lindström et al. 1996/. The HBV-model was used already in the early 80s to simulate groundwater levels /Sandberg, 1982/. The Swedish Geological Survey (SGU) also used a version of the HBV model to develop a method of simulation and forecasting of groundwater levels /Johnson, 1993/. In this study typical ranges for its calibration parameters were described.

Model structure

Figure A3-1 shows a schematic diagram of the PULS-like conceptual model that was calibrated to the well data time series. The key features of the model are briefly described here, but the reader is referred to /Carlsson el al. 1987/ for a more thorough presentation of the model and its equations.

The model utilized three input time series: daily P, PET, and mean air temperate. The snow routine "corrected" the precipitation time series when mean daily air temperatures were less than 0°C by storing precipitation that occurred below this temperature. The routine released the stored precipitation ("snow melt") as input to the unsaturated zone when air temperature once again exceeded 0°C at a daily rate proportional to the temperature difference above 0°C.

Water adds to the unsaturated storage via "adjusted" precipitation (after the snow routine) and capillary rise from the saturated zone. Water departs the unsaturated zone as evapotranspiration (ET) and vertical seepage to the saturated zone. The maximum soil moisture (SM) storage capacity of the unsaturated zone conceptually corresponded to "field capacity" (FC). Fluxes in and out of the unsaturated storage were each mathematically expressed as separate functions of SM (Figure A3-2). The simulated ET rate was determined with a piece-wise linear relationship to SM. When soil moisture was less than a specified fraction (LP) of FC, ET was equal to a corresponding fraction of PET. Above that threshold,

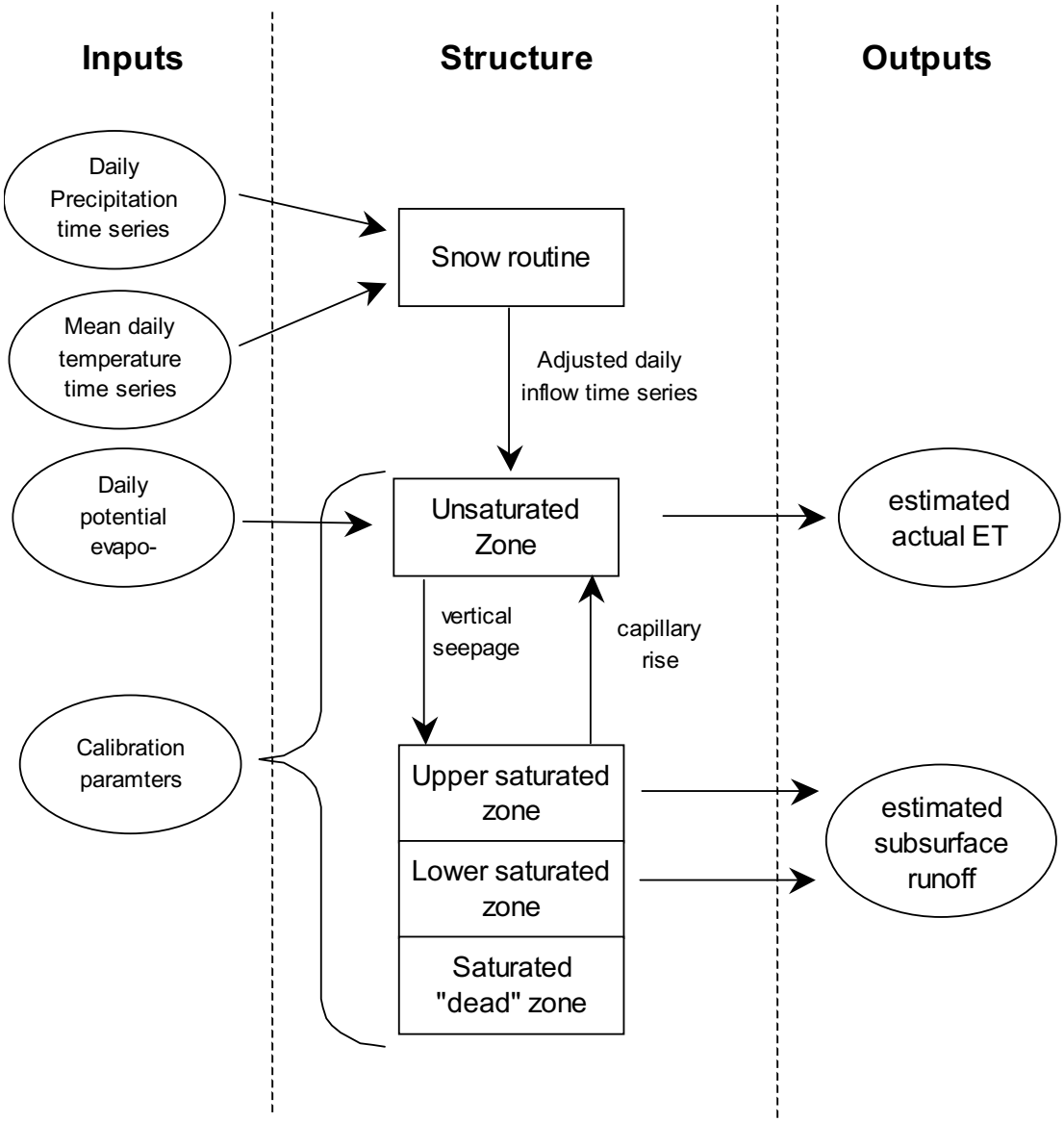

Figure A3-1. *Schematic diagram of the conceptual model calibrated to near-surface well data.*

ET equaled PET. Vertical seepage to the saturated zone was defined as a variable fraction of the adjusted precipitation dependent upon an exponential relationship with SM relative to FC. The residual precipitation that did not vertically seep through to the saturated storage on any given day accumulated in the unsaturated storage. The capillary rise was defined as a simple linear function of SM-FC.

Water adds to the saturated zone via vertical seepage and exits via capillary rise and subsurface outflows. The saturated storage is divided into three sub-compartments: upper, lower and dead storages. The upper and lower saturated zones each have separately specified linear outflow coefficients and porosity values for estimating groundwater levels from simulated storage volumes. The dead zone storage is the most significant deviation in the present model structure from the original PULS structure (PULS did not have a saturated dead zone). The dead zone represents a capacity to draw upon deeper inactive (in terms of outflow) waters if necessary to fulfill capillary rise during dry periods.

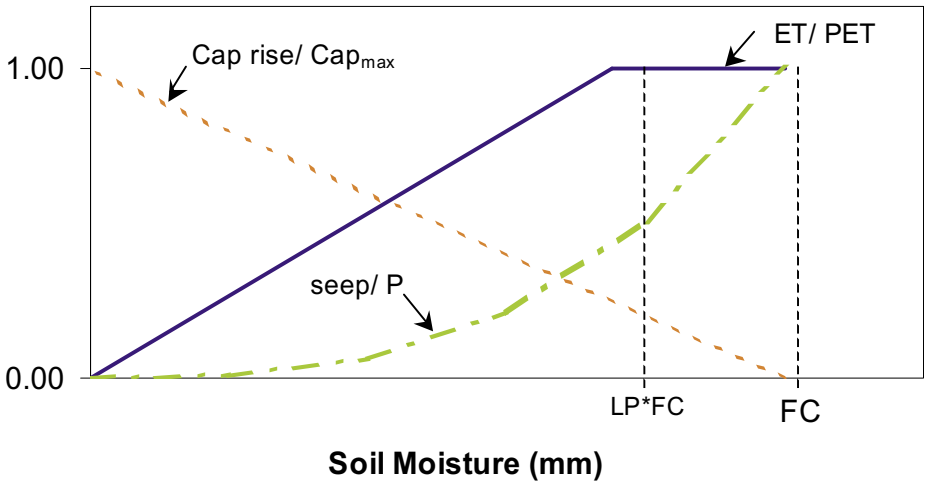

Figure A3-2. *Soil moisture relationships for inflows and outflows to and from the unsaturated storage in the conceptual model.*

In all, the model had 10 calibration parameters, which are listed and described in Table A3-1. The table also shows typical ranges for these parameters that were identified by /Johnson, 1993/. The last column indicates the range of parameters that were identified during the calibration effort for the near-surface wells in the Forsmark study area. These values will be discussed further in the next section.

Table A3-1. Summary of calibration parameters for the conceptual model.

Parameter	Description	Typical range *	Range in this study
K_{melt}	Melt coefficient for accumulated snow based on degrees above 0°C	N/A	1.16
FC	Storage capacity of the unsaturated zone (units = mm)	100–300	10–160
LP	Fraction of FC above which ET = PET	0.5–1.0	0.5 (fixed)
β	Exponent in power relationship that determined curvature in seepage relationship to the saturated zone from the unsaturated zone	1.5–4.0	0.6–4.0
C_{flux}	Maximum daily capillary rise from the saturated zone (units = mm/d)	N/A	0.0–1.6
ρ_{upper}	Porosity of the upper saturated zone	N/A	0.15 (fixed)
K_{upper}	First order outflow coefficient from the upper saturated zone	0.05–0.7	0.0–0.2
LZ_{max}	Storage capacity of the lower saturated zone (units = mm)	8–70	0–50
ρ_{lower}	Porosity of the lower saturated zone	N/A	0.03 (fixed)
K_{lower}	First order outflow coefficient from the lower saturated zone	0.002–0.05	0.0–0.06

* From Johnson, 1993.

Calibration and simulation technique

Snow routine

The snow routine was calibrated to snow depth and water content data collected in the Forsmark study area during winter 2003/04 and reported in /Heneryd, 2004/. Data from the three reported stations (AFM000071, AFM000072, and AFM001172) were averaged for each sampling date (typically, a biweekly interval). The melt coefficient, K_{melt}, was calibrated to minimize the sum of squared errors between the model and available data.

Groundwater routine

Coefficients for the near-surface groundwater model were determined using a stepping routine with a criterion to maximize the Nash-Sutcliffe coefficient /Lindström et al. 1996/. Each well data set was calibrated individually. Only the subset of 22 well data sets were considered that had at least 350 days of available data (max possible = 457 days).

The stepping routine sequentially compared model solutions for all combinations of parameters within user-specified ranges and stepping intervals. For example, solutions could be compared with field capacity (FC) varied between 30 and 130 mm with a 10 mm stepping interval in combination with similarly specified ranges for all other parameters. In this fashion, between 50,000 and 100,000 solutions were typically compared to any given well data time series to determine a "best-fit" parameter set. "Best-fit" was determined by maximizing the Nash-Sutcliffe (NS) coefficient:

$$NS = 1 - \frac{\sum_{i=1}^{n} \left(X_{sim}(i) - X_{obs}(i)\right)^2}{\sum_{i=1}^{n} \left(X_{sim}(i) - \overline{X}_{obs}\right)^2}$$

where

$X_{sim}(i)$ = simulated groundwater level time series,

$X_{obs}(i)$ = observed groundwater level time series,

$\overline{X}_{obs}$ = mean value of observed time series,

n = number of observed days in each time series.

The maximum possible value of the Nash-Sutcliffe coefficient is 1.0, which indicates a perfect fit to data. In addition to the Nash-Sutcliffe coefficient, the correlation coefficient (r^2) and standard error (SE) were also calculated for each best-fit simulation with the following equations:

$$r^2 = \frac{\sum_{i=1}^{n} \left(X_{obs}(i) - \overline{X}_{obs}\right)^2 \cdot \left(X_{sim}(i) - \overline{X}_{sim}\right)^2}{\sum_{i=1}^{n} \left(X_{obs}(i) - \overline{X}_{obs}\right)^2 \cdot \sum_{i=1}^{n} \left(X_{sim}(i) - \overline{X}_{sim}\right)^2}$$

$$SE = \left(\frac{\sum_{i=1}^{n} \left(X_{obs}(i) - X_{sim}(i) \right)^2}{n} \right)^{0.5}$$

where

$\overline{X}_{sim}$ = mean value of the simulated time series.

The calibration period was from May 1, 2003 thru July 31, 2004 (457 days). In order to automatically set initial conditions for each parameter set, the simulation was started 485 days prior to the calibration period (on January 1, 2002, based on average precipitation from Lövsta and Örskär and potential evapotranspiration calculated from Örskär data). At the start of the simulation, initial conditions were set equal to 0.5*FC for the unsaturated storage and equal to LZ_{max} for the saturated storage. This method provided robust and self-determined initial conditions for the groundwater storages that were independent of the start values that were assigned to each.

Model output for each solution (one for each well time series) included the following:

- Simulated “best-fit” time series.
- Values of the parameter set that provided “best-fit”.
- Nash-Sutcliffe coefficient from “best-fit”.
- Corresponding regression coefficient, R^2.
- Corresponding standard error, SE (average predictive error).
- Total annual simulated fluxes (for the period August 1, 2003 thru July 31, 2004) in, out and between unsaturated and saturated storages including predictions of total actual ET and subsurface outflow.
- A list of all model solutions (with output on the five previously listed items) that had Nash-Sutcliffe coefficients that were at least 90% of the “best-fit” value. This dataset provided insight into the robustness of solution parameter values and model predictions.

Initial investigations with the model suggested that it was over-specified in terms of calibration parameters. In other words, many different parameter sets with widely variant parameter values provided similar (indistinguishable) fit to the data. Therefore, three of the nine parameters in the groundwater model were given fixed values as follows:

- LP = 0.6
- $\rho_{upper} = 0.15$
- $\rho_{lower} = 0.03$

These three parameters were fixed at these values for all solutions while the other six parameters were varied. Unfortunately and as will be discussed in the Results section, this still did not lead to unique and robust solutions for the remaining six parameters, but excellent fits to the data were still achieved.

Limitations

There are several constraints and limitations to the simplified approach adopted in this investigation that could limit the strength of the results:

- The structure of the conceptual model, although proven to be well suited for a wide variety of applications /Johnson, 1993/, may have limitations when applied to shallow groundwater regions such as the Forsmark study area. In a shallow groundwater region, field capacity would actually vary as groundwater levels varied and would not remain independent as assumed in the conceptual model.
- At this point in time, the only available calibration data are the well time series data. A complimentary data set, such as measured discharge from gauge stations within the study area, would significantly contribute to the robustness of the calibration results.
- Furthermore, the calibration time series were relatively short for the complexity of the conceptual model, as indicated by the inability to identify unique optimal parameter sets (discussed below). The calibration effort will benefit when these time series are extended at least one additional year (after next year's data freeze), which could be used for validation and/or additional calibration data.

Variations on model structure

Two minor variations of the model structure were briefly investigated to identify if these or other variations warranted future investigation.

Interception storage

In this variation, an interception storage was added before the snow routine. This storage had a 2 mm capacity. Precipitation accumulated in this storage before passing thru to the snow routine. Evaporation was modeled as occurring preferentially from the interception storage (before taking from the unsaturated zone) at the daily PET rate (if the storage had adequately fill). The unfulfilled PET was then "passed on" to the unsaturated storage where ET was calculated with the piece-wise linear relationship discussed above (see Figure A3-2).

Non-linear capillary rise

In this variation, the linear relationship for capillary rise as a function of moisture storage in the unsaturated zone (see Figure A3-2) was changed to a non-linear (square-root) relationship such that capillary rise was increased at low soil moisture compared to the linear relationship.

Results

Snow routine

Calibration results from the snow routine are shown in Figure A3-3. The model was calibrated to water content data in order to minimize the sum of squared errors. However, water content data was only available from mid-January 2004. Therefore, snow depth data, which was available for the entire winter season, was used as a visual check for simulated accumulations in November and December 2003. The calibrated snowmelt coefficient was 1.16 mm/C and was applied when air temperatures exceeded 0°C.

Calibrated parameters and flows for best-fit time series

Figure A3-4 shows three examples of comparisons between simulated and observed groundwater level time series. The three examples represent the "worst", "median", and "best" calibrations to data of the 22 wells that were evaluated. Even the "worst" fit calibration (SFM0002) was impressive with an r^2 value equal to 0.87 (see Figure A3-4a). On the other hand, the "best" fit (SFM0019) was virtually indistinguishable from the observed data set (see Figure A3-4c).

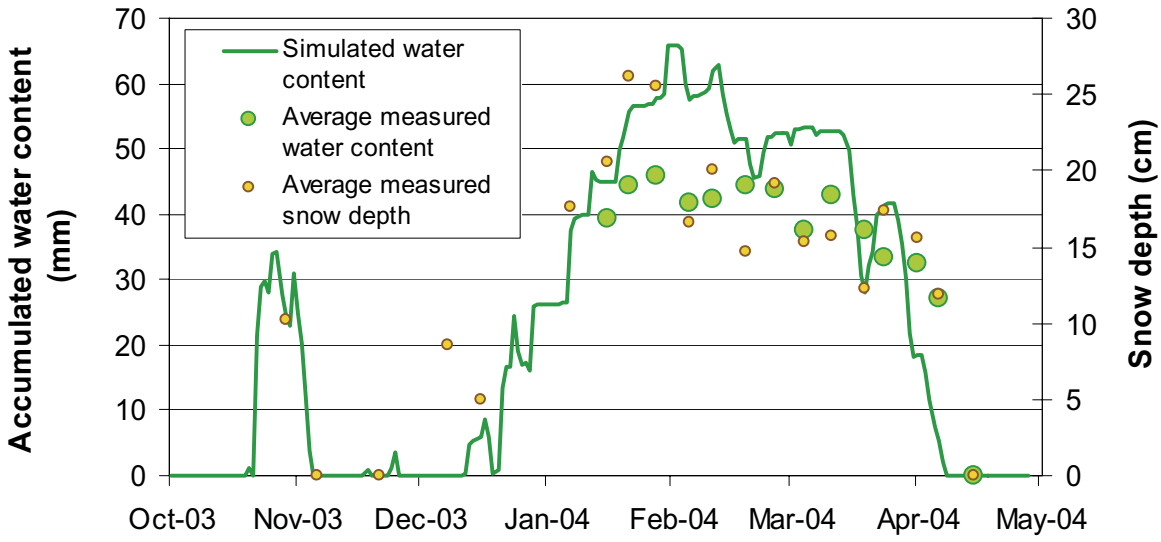

Figure A3-3. *Comparison of simulated water content in snow accumulation to measured data from the study area (average of AFM000071, AFM000072, and AFM001172).*

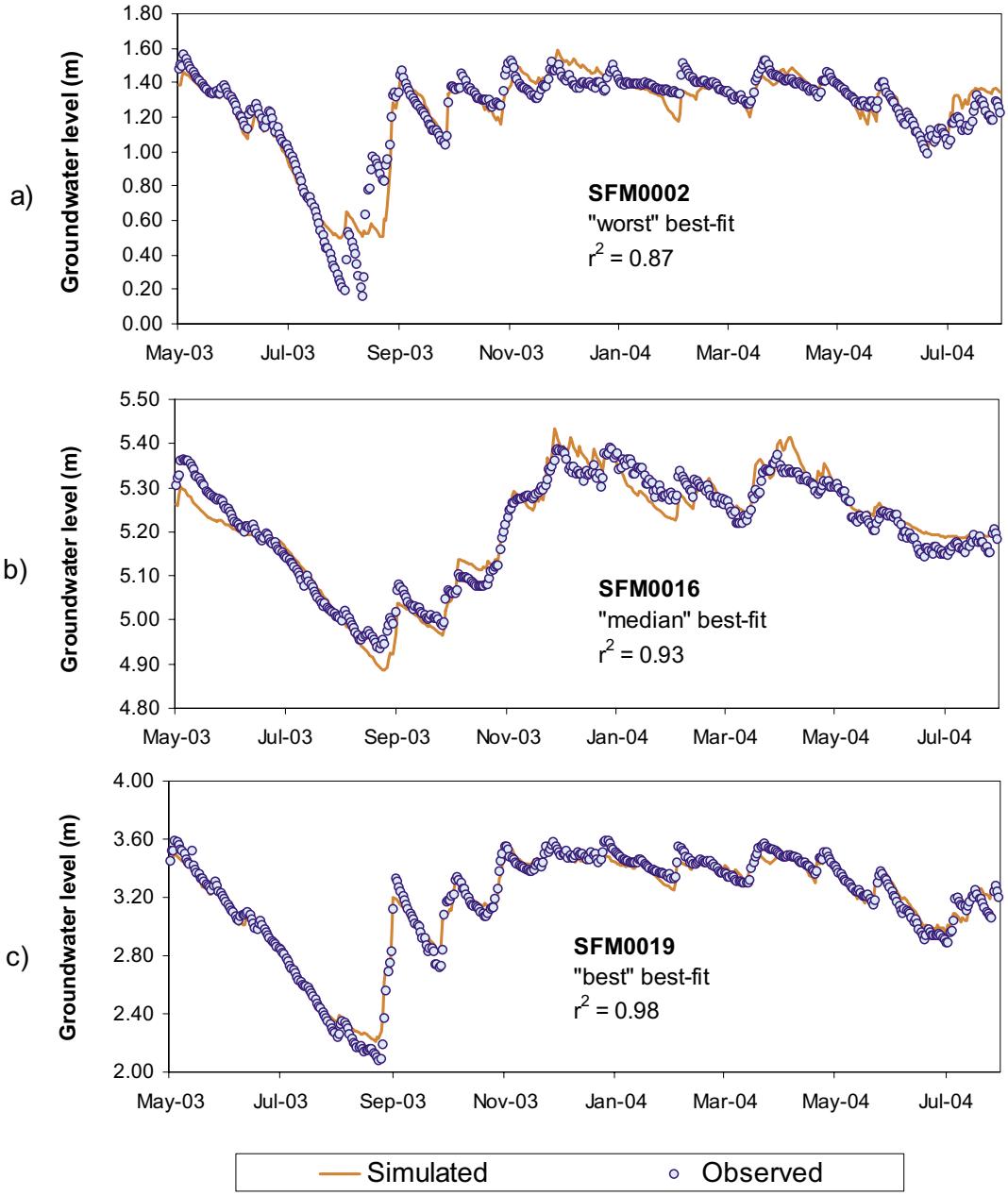

Figure A3-4. *Simulated time series compared to measured data for a) the "worst" data fit, b) the "median" data fit, and c) the "best" data fit. All groundwater levels represent meters above sea level (RHB 70).*

Figure A3-5 shows a graphical representation of total annual simulated fluxes in the conceptual model for the same three wells that were shown in Figure A3-4. The simulated fluxes varied considerably between wells. For these three cases, the model suggested that SFM0016 had the highest ET and lowest runoff rates compared to the other two locations. This well also had the lowest response amplitude of the three (0.45 m compared to 1.41 and 1.51 m, as seen in Figure A3-4).

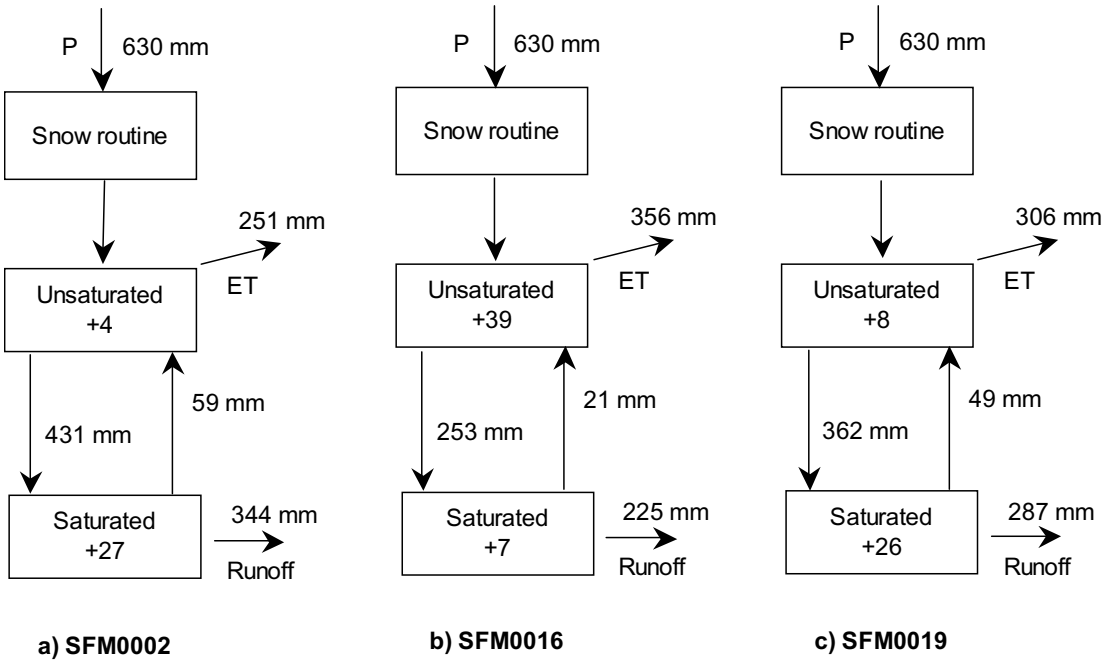

Figure A3-5. *Simulated total annual fluxes (August 1, 2003 to July 31, 2004) to, from, and between storage compartments for the same three wells shown in Figure A3-4.*

Table A3-2 shows a summary of Nash-Sutcliffe and correlation coefficients and standard errors that resulted from model calibrations to the 22 well time series. As suggested by the three time series graphs shown above in Figure A3-4, the calibration results demonstrated excellent fits to the observed data in all cases. The average r^2 value from all simulations was 0.93, the average Nash-Sutcliffe coefficient was 0.73, and the average standard error was 0.07 m. The table also shows estimates of total annual ET and runoff flows from each simulation. ET estimates ranged between 251–359 mm/yr, while runoff estimates ranged (in opposite balance) between 344–216 mm/yr.

For the 22 wells considered, we observed a very weak correlation ($r^2 = 0.15$) between the predicted ET rates and response amplitudes for groundwater level in the wells, but no correlation ($r^2 = 0.04$) was observed between ET rates and the average groundwater depths below surface. Perhaps these weak or non-existent correlations could be partially explained by the wide range of output that was observed for other calibration solutions that also provided similar "close" fits to the data, where in this case we define "close" as those solutions that had Nash-Sutcliffe coefficients within 10% of the "best-fit" value. The ranges of predicted ET and runoff for "close" fit solutions are shown for each well in the last two columns of Table A3-2 and typically varied around "best-fit" values by approximately ± 30%. The indefinite ranges of these solution sets will be discussed further in the next section.

Table A3-2. Summary of model calibration results for 22 near-surface wells.

	NS	r^2	SE (m)	ET (mm)	Outflow (mm)	Output range for solutions with NS > 0.9*NS_{max}	
						ET	Outflow
SFM0001	0.66	0.89	0.09	294	301	210–340	390–260
SFM0002	0.64	0.87	0.10	257	344	160–310	420–160
SFM0003	0.68	0.91	0.09	285	297	210–340	380–250
SFM0004	0.71	0.92	0.09	302	293	260–350	340–240
SFM0005	0.70	0.91	0.07	284	307	250–330	350–270
SFM0009	0.82	0.97	0.06	354	232	310–370	270–200
SFM0010	0.78	0.95	0.10	367	233	340–370	260–230
SFM0011	0.64	0.88	0.06	341	233	320–360	250–220
SFM0013	0.73	0.95	0.05	334	263	310–350	280–230
SFM0014	0.78	0.94	0.04	327	266	320–360	240–270
SFM0016	0.72	0.93	0.03	356	225	340–370	260–210
SFM0017	0.75	0.94	0.03	355	238	340–360	250–220
SFM0018	0.72	0.93	0.04	354	229	340–360	250–210
SFM0019	0.84	0.98	0.06	306	287	280–350	310–250
SFM0020	0.75	0.94	0.06	312	284	300–350	300–240
SFM0021	0.81	0.96	0.08	307	277	250–350	330–240
SFM0028	0.70	0.91	0.08	295	302	260–340	320–250
SFM0030	0.82	0.97	0.12	324	257	280–370	290–220
SFM0033	0.75	0.94	0.06	310	290	270–350	320–250
SFM0034	0.65	0.89	0.06	329	272	280–350	320–250
SFM0038	0.72	0.91	0.11	305	291	250–340	350–250
SFM0049	0.79	0.95	0.05	359	216	330–380	250–180
AVERAGE	0.73	0.93	0.07	321	270	–	–

Robustness and sensitivity

Calibration results for all wells exhibited relatively wide ranges of both parameter estimates and predicted ET and runoff rates for solutions that provided "close" fits (within 10% of best-fit solutions) to the groundwater level time series. In other words, the uniqueness of the calibration results were not robust, suggesting that amongst other factors the model was over-specified for the limited calibration data available. Figure A3-6 and Figure A3-7 show three time series simulations for SFM0002 and SFM0019, respectively, each providing an excellent fit to the time series data and also predicting widely different ET rates. In fact, of over 50,000 different combinations of model parameters that were evaluated for solutions to each of these calibrations, approximately 2,000 different solutions were available for each that provided "close" fits (within 10% of "best") to the observed data.

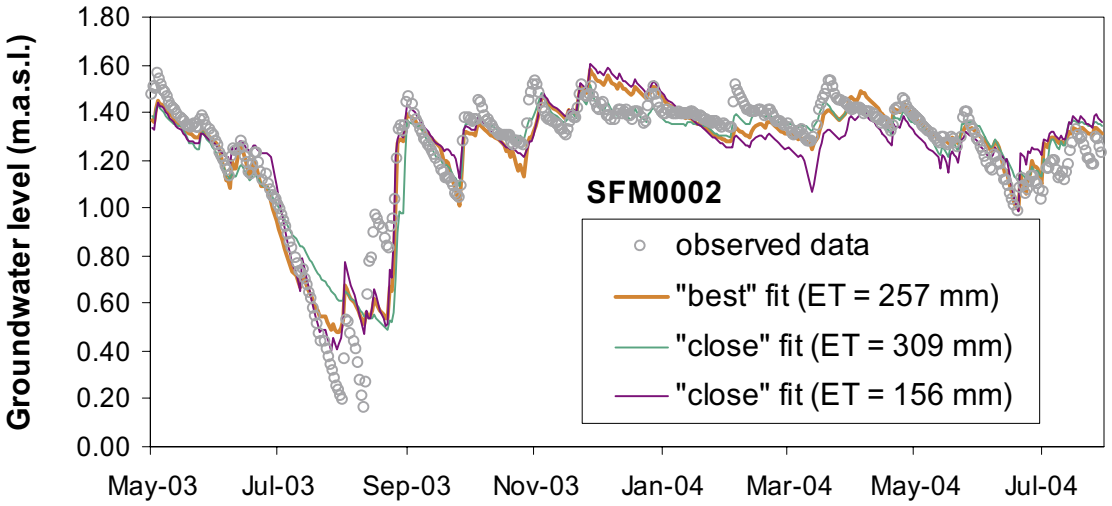

Figure A3-6. *Three solutions for SFM0002 that provide "close" fits to the time series (all have $r^2 > 0.83$) but that also predict widely different annual ET rates.*

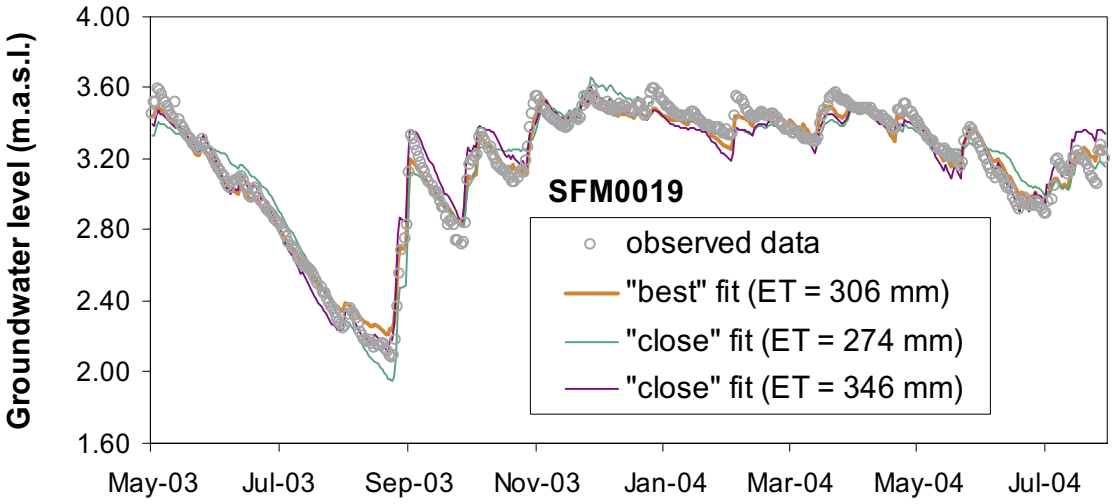

Figure A3-7. *Three solutions for SFM0019 that provide "close" fits to the time series (all have $r^2 > 0.95$) but that also predict widely different annual ET rates.*

Figure A3-8 shows frequency distributions of predicted ET rates from these solutions for SFM0002 and SFM0019. Parameter values for these solutions demonstrated similar variance. For instance, Figure A3-9 shows the frequency distribution of values for field capacity (FC) from the 2,000 or so solutions that provided "close" data fits. For SFM0002, "close" solutions were found with field capacity values ranging from 10 to 100 mm, while that range was between 30 to 100 mm for SFM0019. While clearly there is a difference in the central tendencies of these two distributions, it is also clear that unique parameter values cannot be stated with confidence at this point.

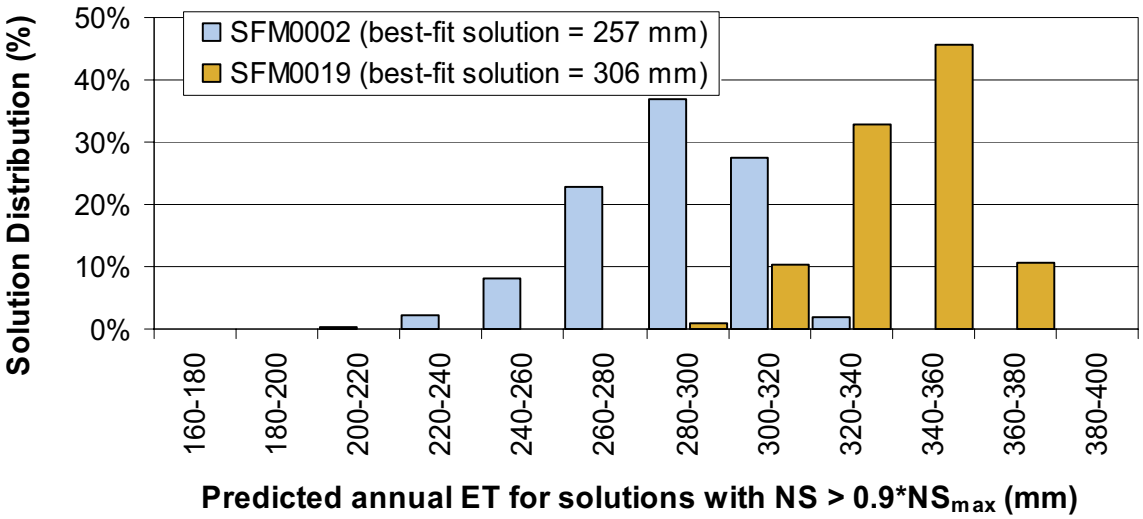

Figure A3-8. *Model solutions demonstrating the wide ranges of possible ET values that provided "close" fits to the data (within 10% of Nash-Sutcliffe "best-fit").*

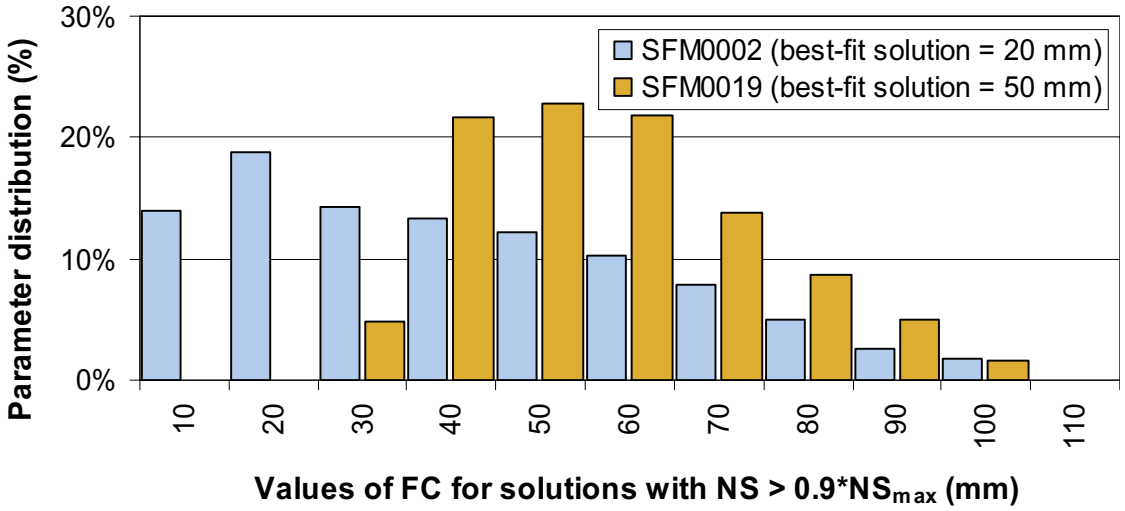

Figure A3-9. *Model solutions demonstrating the wide ranges of FC values that provided "close" fits to the data (within 10% of Nash-Sutcliffe "best-fit").*

Comparison to water balance results obtained from the CoupModel

According to simulations with the CoupModel using the Penman-Monteith equations the actual evapotranspirations for the same one-year period was slightly more than 400 mm for a mature coniferous forest in fresh to dry areas but considerably lower, approximately 330 mm in wet areas /Gustafsson et al. 2005/. The lower values in the wet areas are explained by restricted transpiration when the groundwater level is very close to the ground surface. However, root depth was not varied for dry, fresh and wet conditions. If an adaptation of the root depth in wet areas had been made, the difference in transpiration between dry and wet areas had been less accentuated. The evaporation directly from interception was approximately 130 mm.

The evapotranspiration values simulated by the CoupModel were generally higher than the results predicted by the conceptual model reported herein, for which predicted ET values were generally less than about 360 mm at even the maximum span for "close" fit simulations.

Investigation of variations in model structure

Table A3-3 summarizes simulation results from two variations on model structure that were investigated. The purpose of these simulations was to investigate if minor changes to the model structure could alter the predicted water balance and increase simulated annual ET rates to values similar to those reported from CoupModel simulations.

In general, the modifications had only a minor impact on ET rates, typically increasing values by 0–10%. The addition of the interception storage had a slightly greater impact than changing the slope of the capillary rise function. The interception storage provided for 109 mm of direct evaporation of precipitation before infiltration to the unsaturated storage. Subsequent fluxes between storage compartments in the conceptual model adjusted to accommodate the decreased infiltration volume (compared to the model structure with no interception storage). However, the net result was a combined ET rate just barely greater than what was predicted without the interception storage. The maximum predicted ET rates, even at the maximum span of "close" solutions, remained less than 380 mm/yr and therefore less than upper range of ET values that were predicted by CoupModel simulations.

Table A3-3. Summary of simulated annual ET for select wells using modified model structure. Values in parentheses indicate the range of predicted ET with "close" solutions.

	Baseline ET (mm/yr)	With non-linear capillary rise function (mm/yr)	With interception storage (mm/yr)
SFM0002	260	280	280
	(160–310)	(160–320)	(200–320)
SFM0005	280	300	310
	(250–330)	(250–330)	(180–320)
SFM0016	360	360	360
	(340–370)	(280–360)	(340–380)
SFM0019	310	320	330
	(280–350)	(280–360)	(280–350)
SFM0028	300	320	320
	(260–340)	(280–350)	(240–350)
SFM0030	320	320	340
	(280–370)	(310–370)	(310–370)

Discussion and recommendations

Overall, the calibration of a simple conceptual model based on a PULS-like structure provided consistently excellent simulation of time series of groundwater levels from 22 wells that were considered here and are within the study area. Correlation coefficients ranged from a minimum of $r^2 = 0.87$ to a maximum of $r^2 = 0.98$. These strong correlations suggest that the near-surface hydrology of the study area can be well explained as a hydrological response to precipitation events and ET cycles.

However, the results also indicated that there was a wide range of model parameters that provided accurate fits to each well time series. Therefore, neither a unique set of calibrated model parameters (such as estimated values for field capacity) nor a unique set of estimated model output (ET and runoff rates) could be determined at this time. At this point, the only available calibration data are the groundwater level time series data. Clearly, the selected model is over-specified (too many parameters) to uniquely calibrate to the available (457 day) time series data alone. However, it seems highly likely that this problem could be resolved with the addition of more time series data and with a complementary data set such as gauged stream discharge, both of which should be available after the next data freeze in July 2005.

Recommended future work

Based on these results, the following recommendations are given:

- It is recommended that this modelling effort be revisited again after the next data freeze. With the addition of stream flow measurements, it should be possible to remove considerable uncertainty in the calibration process and identify unique, meaningful solutions that still provide excellent fit to the data. Furthermore, the additional year of time series data could be used to extend the calibration time series or used as a validation dataset.
- Once the model is more accurately calibrated and validated, this could be a very useful predictive tool for extending groundwater level time series.

References

Carlsson B, Bergström S, Brandt M, Lindström G, 1987. PULS-modellen: Struktur och tillämpningar. SMHI Rapporter Hydrologi Nr 8. (In Swedish.)

Gustafsson D, Gärdenäs A, Jansson P-E, Eckersten H, 2005. Simulated carbon and water processes of forest ecosystems in Forsmark and Simpevarp during a 100-year period. SKB report in progress.

Heneryd N, 2004. Forsmark site investigation. Snow depth, ground frost and ice cover during the winter 2003/2004. SKB P-04-137. Svensk Kärnbränslehantering AB.

Lindström G, Gardelin M, Johansson B, Persson, M, Bergström S, 1996. HBV-96: En areellt fördelad modell för vattenkrafthydrologin. SMHI Rapporter Hydrologi Nr 12. (In Swedish.)

Johnson J, 1993. Utveckling av metodik för simulering och prognos av grundvattennivåer. Delrapport av SGU finansierat internt FoU-projekt 1992/93. (In Swedish.)

Sandberg, G, 1982. Utvärdering och modellsimulering av grundvattenmätningarna i Ångermanälvens övre tillrinningsområde. SMHI Hydrologiska/oceanografiska avdelningen. (In Swedish.)

Appendix 4

Terrain characteristics for groundwater monitoring well sites

Lars Brydsten, Umeå University, February 2005

Introduction

In order to investigate whether correlations could be found between terrain characteristics and depth to groundwater, a number of geomorphometrical and hydrological parameters were calculated for the areas around groundwater wells. These parameters were then statistically analysed against groundwater level measurements. In addition, the representativity of the locations of the existing groundwater wells, in terms of terrain characteristics, was checked based on the same geomorphological and hydrological parameters.

A subset of the existing groundwater wells was selected for the analysis. When wells were located in the immediate vicinity of each other, only one of the wells was used. Furthermore, wells below open water and wells with very short time series were not included in the study. Basic data for the selected 28 groundwater wells are presented in Table A4-1. For the location of the wells, see Figure 3-27 in the main report.

Table A4-1. Basic data for groundwater wells: Elevation = Ground elevation in m a s l in the RH70 elevation system, Rock surface = Rock surface in metres below ground, Count = Time series length in days, Avg = Mean groundwater level in metres below ground, Q50 = Median groundwater level in metres below ground, Max = Maximum level in metres below ground, Min = Minimum level in metres below ground, Ampl = Maximum groundwater amplitude in metres, Soil = Soil type at the well location based on the digital soil map /Sohlenius et al. 2004/.

Well	Elevation	Rock surface	Count	Avg	Q50	Max	Min	Ampl	Soil
SFM 30	1.67	–3.6	457	–0.57	–0.29	0.10	–2.61	2.72	Till, sandy
SFM 26	0.70	–16.1	347	0.22	0.32	1.09	–1.04	2.13	Glacial clay
SFM 21	1.43	–2.1	423	–0.43	–0.35	0.02	–1.76	1.78	Till, sandy
SFM 08	3.37	–5.5	345	–2.87	–2.93	–1.95	–3.62	1.67	Till, clay
SFM 10	12.90	–1.6	412	–0.22	–0.01	0.29	–1.36	1.65	Till, sandy
SFM 36	0.61	–1.8	457	–0.24	–0.06	0.23	–1.41	1.64	Till, sandy
SFM 19	3.67	–4.8	457	–0.50	–0.38	–0.08	–1.59	1.51	Till, sandy
SFM 33	0.53	–2.6	391	–0.07	–0.03	0.26	–1.17	1.43	Till, sandy
SFM 02	1.62	–4.8	457	–0.38	–0.29	–0.06	–1.46	1.41	Till, sandy
SFM 01	0.95	–4.8	457	–0.44	–0.35	–0.08	–1.43	1.34	Till, sandy
SFM 03	1.54	–10.2	457	–0.23	–0.16	0.01	–1.31	1.33	Till, sandy
SFM 04	3.54	–5.1	457	–0.50	–0.52	–0.07	–1.38	1.31	Till, sandy
SFM 28	0.22	–7.1	450	–0.01	0.04	0.45	–0.83	1.27	Clay gyttja
SFM 09	4.33	–2.5	448	–0.32	–0.19	0.07	–1.12	1.19	Glacial clay
SFM 57	4.27	–3.9	232	–0.60	–0.57	0.06	–1.12	1.18	Till, sandy
SFM 05	6.00	–2.1	364	–1.04	–1.04	–0.59	–1.70	1.11	Till, sandy
SFM 20	1.67	–3.2	457	–0.28	–0.22	0.13	–0.92	1.04	Glacial clay
SFM 06	5.88	–3.4	154	–0.93	–0.93	–0.56	–1.40	0.83	Till, clay sandy–silt

Well	Elevation	Rock surface	Count	Avg	Q50	Max	Min	Ampl	Soil
SFM 58	3.55	–3.9	65	–2.39	–2.44	–1.80	–2.60	0.80	Till, sandy
SFM 49	2.93	–3.9	421	–0.62	–0.52	–0.35	–1.14	0.79	Till, sandy
SFM 34	0.67	–2.0	457	–0.18	–0.14	0.05	–0.73	0.79	Till, sandy
SFM 13	3.68	–4.6	457	–0.01	0.02	0.28	–0.48	0.76	Till, sandy
SFM 11	5.79	–3.9	457	–0.06	–0.03	0.18	–0.54	0.72	Till, sandy
SFM 14	5.59	–2.0	404	–0.29	–0.26	–0.04	–0.73	0.69	Till, sandy
SFM 17	5.65	–4.0	457	–0.11	–0.06	0.08	–0.51	0.58	Marsh
SFM 18	5.77	–4.5	398	–0.52	–0.48	–0.31	–0.86	0.55	Marsh
SFM 16	5.22	–7.2	457	–0.01	0.01	0.17	–0.28	0.45	Till, sandy
SFM 59	4.03	–5.3	166	–3.96	–3.96	–3.85	–4.05	0.20	Glaciofluvium

Methods

General

The parameters were evaluated using three GIS-functions:

(i) Geomorphometrical classification – Using the 1st and 2nd order differentials of the DEM (Digital Elevation Model), a number of curvature parameters were calculated. These parameters were used to classify six geomorphological features: peak, ridge, pass, plane, channel, and pit.

(ii) Flow accumulation function – This function calculates the accumulated flow or number of up-slope cells based on a flow direction grid. A high flow accumulation value indicates a probability for a groundwater discharge area.

(iii) Topographical wetness index (TWI) – This calculation is based on flow accumulation values and slopes; a high TWI-value indicates a discharge area.

Calculations of geomorphometrical parameters

For the geomorphological classification, the GIS program LandSerf was used /Wood, 1996/ (http://www.soi.city.ac.uk/~jwo/landserf). The program uses a DEM as input data and calculates eight curvature values for each cell in the DEM. Based on these eight values, the DEM is classified into six geomorphological features. The curvature calculations are as follows:

(i) slope – the rate of maximum change for locations on grid (degrees),

(ii) profile convexity (prof, for short) – intersecting with the plane of the Z-axis and aspect direction,

(iii) plan convexity (plan) – intersecting with the XY plane,

(iv) cross-sectional curvature (cross) – intersecting with the plane of slope, normal and perpendicular aspect direction,

(v) longitudinal curvature (long) – intersecting with the plane of the slope normal and aspect direction,

(vi) maximum curvature (maxi) – in any plane,

(vii) minimum curvature (mini) – in any plane,

(viii) mean curvature (mean) – in any plane.

The curvature values are calculated for a rectangular window where the user chooses the size of the window. The smallest window is 3×3 cells, and the size must be an odd value (5, 7, 9, etc). The program uses a bivariate quadratic function for calculation of the curvature values:

$Z = ax^2 + by^2 + cxy + dx + ey + f$

The DEM is classified into six geometrical features using the classification scheme presented in Table A4-2. For example, for a cell to be classified as a peak the maxi and mini values should be positive and the slope zero.

Table A4-2. Geometrical features classification scheme.

Feature	slope	cross	maxi	mini
Peak	0	#	+	+
Ridge	0	#	+	0
	+	+	#	#
Pass	0	#	+	–
Plane	0	#	0	0
	+	0	#	#
Channel	0	#	0	–
	+	–	#	#
Pit	0	#	–	–

The user sets the slope tolerance value. The tolerance value is the highest slope value allowed while still being classified as a plane. The user can change two parameters: the size of the local window (the scale) and the slope tolerance value.

Calculation of hydrological parameters

The flow accumulation values (number of up-slope cells based on a flow direction grid) were calculated in ArcGis 8.3 Hydrological Modelling Extension, using the regional DEM for the Forsmark area /Brydsten, 2004/.

The topographical wetness index (TWI) is used to calculate the likelihood for soil saturation /Beven and Kirkby, 1979/. The wetness index is defined as follows:

$$TWI = \ln\left(\frac{Flowacc}{\tan\beta}\right)$$

where *TWI* is the topographical wetness index, *Flowacc* is a specific catchments area, and β is the local slope in degrees. It can be seen that high *TWI* values occur in places with high flow accumulation values and flat slopes.

Results

Geomorphometrical parameters

A large number of calculations were performed with the LandSerf program using different window sizes (3, 7 and 11 cells), a slope tolerance value of 1 degree, and a curvature tolerance value of > 0.1 (dimensionless). The calculated geomorphometrical values are presented in Appendix A4-1. Negative curvature values are concave lines. Generally, the curvature values are extremely low due to the flat topography in the Forsmark area. This implies that small errors in the DEM can lead to changes in curvature values from a small negative value (concave line) to a small positive value.

Geomorphological feature classification

The results of the geomorphological feature classification are presented in Appendix A4-2. The classifications were performed with different windows sizes and two tolerance levels. Most of the groundwater well sites have been classified to the same feature type, independent of the window size or tolerance level. For a few sites there have been different classifications for different parameter settings, settings that were often classified to two feature types. For example, the well SFM0001 is classified to either a ridge or a plane. This means there is a ridge at the site, but this ridge is low and indistinct.

Hydrological parameters

As mentioned above, both the flow accumulation values and the topographical wetness index are calculated using the ArcGis 8.3 GIS program. Both calculations were performed at the pixel level (i.e. not with different window sizes). Instead, the groundwater well sites were buffered with different radius length, and the maximum values within each buffer were recorded. The results of the hydrological parameters calculations are presented in Appendix A4-3.

Statistical analysis of groundwater level measurements

Data from Table A4-1 and from Appendix A4-1 and A4-3 were merged into one single database. In order to minimize the effects of differences in soil properties, the analysis was performed for wells situated in till only. The statistical analyses were performed with stepwise multiple linear regression using the statistical program SPSS. The dependent variables are

- mean groundwater level below ground surface in metres (Avg),
- median groundwater level below ground surface in metres (Q50),
- maximum groundwater level below ground surface in metres (Max),
- minimum groundwater level below ground surface in metres (Min),
- maximum amplitude in groundwater level in metres (Ampl).

Independent variables are all curvature calculations in Appendix A4-1 and A4-3. The stepping method criteria in the multiple linear regressions were chosen to probability of F = 0.05 to enter and 0.10 to remove. The results of the statistical analysis are presented in Table A4-3.

Table A4-3. Results from the stepwise multiple linear regression.

Dependent var	1st Indep var	2nd Indep var	3rd Indep var	R^2	Sig
Avg	Mean11	Slope7	Maxi7	0.674	0.000
Q50	Mean11	Slope11	Maxi7	0.658	0.000
Max	Mean11	Slope11	–	0.566	0.002
Min	Slope7	–	–	0.266	0.017
Ampl	Mini3	–	–	0.433	0.001

Although all five statistical models are significant to 0.05, the degrees of explanation (R^2) are low, particularly for the Min and Ampl models. The best model is the Avg-model with a R^2-value of 0.674. Coefficients for the linear equation for the Avg-model are shown in Table A4-4.

Table A4-4. Coefficients for the linear equation for the Avg-model.

	Unstandardised Coeff		Standardised Coeff	t	Sig
	B	Std Error	Beta		
(Constant)	–0.523	0.180		–2.896	0.010
Mean11	–9.763	2.367	–0.847	–4.124	0.001
Slope7	–0.360	0.115	–0.455	–3.130	0.006
Maxi7	3.965	1.798	0.452	2.206	0.041

The results are logical. As the average groundwater levels are negative, values increasing downwards and negative curvature values imply concave curvature, low average groundwater levels are occurring at steep convex slopes – i.e. on ridges – that probably are groundwater recharge areas. High groundwater levels, however, occur on flat concave slopes, typical geometry for groundwater discharge areas.

Analysis of the groundwater well locations in the terrain

The analysis was performed with two techniques: by comparing the curvature and hydrological parameters for groundwater well sites with the same number of sites around randomly placed points, and by comparing the distribution of classified geomorphometrical features for groundwater well sites with the distribution of classified geomorphometrical features for the whole area.

The data set with randomly placed points was created with the GIS program ArcView 3.3 and the extension Random_sites.avx. The placement rules were set to the shortest distance between two points 10 metres apart, and no points were placed on lakes. Geomorphometrical and hydrological parameters were calculated for these points using the same method as for the groundwater well sites (Table A4-5).

Table A4-5. Average values for different geomorphometrical and hydrological parameters for the areas around groundwater wells, and the areas around 31 random points.

	GW_wells	Random points
TWI_Pix	9.02	8.58
TWI_10	9.80	8.93
TWI_25	11.66	10.77
Flow_Pix	62	184
Flow_10	3,441	1,194
Flow_25	11,667	3,944
Slope3	1.09	1.43
Slope7	0.91	1.18
Slope11	0.80	0.92
Prof3	0.0030	–0.0102
Prof7	–0.0044	–0.0154
Prof11	–0.0105	–0.0081
Plan3	0.0657	–0.0243
Plan7	0.5626	1.0159
Plan11	0.2643	1.4193
Cross3	–0.0072	–0.0048
Cross7	–0.0069	–0.0138
Cross11	–0.0022	–0.0104
Long3	0.0030	–0.0102
Long7	–0.0044	–0.0154
Long11	–0.0105	–0.0081
Mini3	–0.0626	–0.0733
Mini7	–0.0700	–0.0866
Mini11	–0.0666	–0.0727
Maxi3	0.0543	0.0432
Maxi7	0.0475	0.0282
Maxi11	0.0411	0.0358
Mean3	–0.0041	–0.0150
Mean7	–0.0112	–0.0292
Mean11	–0.0128	–0.0185

The table shows very similar values for curvature calculations (Prof3 – Mean11), but somewhat wetter environments (TWI_Pix – Flow25) and also somewhat flatter slopes (Slope3 – Slope11) for groundwater well sites compared with randomly placed points.

The geomorphometrical feature classification was done with a 11×11 cell calculation window (based on the linear regression results) and a slope tolerance value of > 1 degree and curvature tolerance value of > 0.1 (dimensionless). The results of the classification are presented in Table A4-6.

Table A4-6. Comparison of the distribution of classified geomorphometrical features for groundwater well sites with the distribution of classified geomorphometrical features for the whole area.

Feature	Area (km^2)	Area (%)	No Features	%	Difference (%)
Pit	0.11	0.17	0	0.00	0.17
Channel	7.37	11.27	5	16.13	–4.86
Pass	0.87	1.33	1	3.23	–1.90
Ridge	8.76	13.40	2	6.45	6.95
Peak	0.35	0.53	0	0.00	0.53
Plane	47.92	73.30	23	74.19	–0.90

The table shows that the distribution of groundwater wells over different geomorphometrical features agrees well with the distribution for the whole area; possibly, the channel feature is somewhat overrepresented and the ridge feature is somewhat underrepresented. This is in accordance with the results in Table A4-5: the groundwater wells are placed on somewhat wetter environments (Plane and Channel) compared to the whole area.

Discussion

The statistical analysis shows that in addition to soil properties and position in the terrain there are other factors that affect the groundwater levels and in particular the groundwater level amplitudes. Perhaps variations in vegetation density and vegetation types could explain the variations in groundwater level amplitudes.

References

Beven K J, Kirkby M, 1979. A physically based variable contributing area model of basin hydrology. Hydrological Science Bulletins, 24(1), 43–69.

Brydsten L, 2004. A method for constriction of digital elevation models for site investigation program in Forsmark and Simpevarp. SKB P-04-03. Svensk Kärnbränslehantering AB.

Sohlenius G, Rudmark L, Hedenström A, 2004. Mapping of unconsolidated Quaternary deposits 2002–2003. Map description. SKB R-04-39. Svensk Kärnbränslehantering AB.

Wood J D, 1996. The geomorphological characterisation of digital elevation models. Ph.D. thesis, University of Leicester, U.K.

Appendix A4-1. Calculated geomorphometrical parameters for areas around groundwater wells. The numbers in the file names indicate the size of the window. Negative curvature values are concave lines looking down slope.

GW Well	SLOPE3	SLOPE7	SLOPE11	PROF3	PROF7	PROF11	PLAN3	PLAN7	PLAN11	CROSS3	CROSS7	CROSS11
SFM0001	1.0129	0.7294	0.3136	–0.0076	0.0731	0.0298	–10.0000	–2.8665	–1.2573	0.1799	0.0365	0.0069
SFM0002	2.8115	1.3832	1.1508	0.1363	0.0437	–0.0036	0.8481	0.9710	2.4236	–0.0304	–0.0234	–0.0487
SFM0003	1.1682	0.9814	0.9509	–0.0547	–0.0670	–0.0464	–0.6990	0.8041	0.5850	0.0137	–0.0138	–0.0097
SFM0004	1.5618	0.7624	0.4179	0.0147	–0.0045	–0.0727	1.0232	4.8149	–4.0536	–0.0363	–0.0641	0.0296
SFM0005	0.3147	0.0680	0.0249	0.0139	–0.0095	–0.0004	–10.0000	0.6211	–3.3139	0.0481	–0.0007	0.0014
SFM0006	2.3121	1.9182	1.7224	0.0008	0.0227	0.0129	–0.6618	–0.6517	–1.2697	0.0266	0.0218	0.0382
SFM0007	0.5251	0.5973	0.6384	0.0134	–0.0012	0.0070	–0.0009	0.5454	–0.3433	0.0000	–0.0057	0.0038
SFM0008	3.3909	3.3580	2.5746	–0.0060	–0.0045	–0.0074	0.2680	0.3937	–0.4320	–0.0244	–0.0231	0.0194
SFM0009	0.0960	0.3229	0.2531	0.0038	0.0213	0.0031	–0.0652	–1.2807	–4.6229	0.0003	0.0072	0.0204
SFM0010	2.5060	1.1732	0.8977	–0.0253	0.0016	0.0253	2.5044	2.5157	0.4166	–0.0605	–0.0515	–0.0065
SFM0011	0.0000	0.0000	0.0000	0.0000	0.0000	0.0000	0.0000	0.0000	0.0000	0.0000	0.0000	0.0000
SFM0013	0.0000	0.0000	0.1204	0.0000	0.0000	–0.0109	0.0000	0.0000	10.0000	0.0000	0.0000	–0.0242
SFM0014	1.4648	1.9410	1.5599	0.0007	0.0867	0.0109	0.0128	–0.0926	–0.0796	–0.0002	0.0031	0.0022
SFM0016	0.0000	0.1013	0.5019	0.0000	–0.0107	–0.0491	0.0000	2.7905	1.4492	0.0000	–0.0049	–0.0127
SFM0017	0.2639	0.3878	0.7013	0.0032	–0.0235	–0.0393	0.7582	2.3922	5.6860	–0.0030	–0.0162	–0.0696
SFM0018	2.3936	0.5926	0.3392	0.0410	–0.0025	0.0017	1.4236	5.5531	10.0000	–0.0256	–0.0574	–0.1200
SFM0019	0.0000	0.0000	0.0074	0.0000	0.0000	–0.0011	0.0000	0.0000	–4.2490	0.0000	0.0000	0.0005
SFM0020	0.6328	1.0425	0.7564	–0.0137	–0.0530	–0.0441	0.6004	0.4308	0.2325	–0.0173	–0.0078	–0.0031
SFM0021	0.4501	0.4803	0.5929	–0.0013	–0.0260	–0.0328	–0.7217	–0.4774	–0.4087	0.0061	0.0040	0.0042
SFM0026	0.1313	0.3306	0.3345	–0.0175	–0.0248	–0.0288	3.1165	–0.4592	0.4656	–0.0150	0.0026	–0.0027
SFM0027	0.4114	0.4932	0.4416	0.0031	–0.0195	–0.0216	–0.2600	–0.0739	0.4206	0.0026	0.0006	–0.0032
SFM0028	0.0000	0.0181	0.1595	0.0000	–0.0024	–0.0178	0.0000	–5.2813	–0.8622	0.0000	0.0017	0.0024
SFM0030	1.2052	0.8039	0.6550	0.0505	–0.0128	–0.0255	10.0000	1.9020	–0.2599	–0.1802	–0.0267	0.0030
SFM0033	1.0059	0.3642	0.9026	0.0000	–0.0333	–0.0735	0.0000	5.4419	1.6512	0.0000	–0.0346	–0.0260
SFM0034	0.3686	0.5631	0.6380	–0.0774	–0.1049	–0.0807	1.0610	–3.1793	–3.0831	–0.0111	0.0312	0.0343
SFM0036	2.3423	2.2173	1.8557	–0.1451	–0.1598	–0.0754	1.5858	–1.0362	–1.4001	–0.0619	0.0401	0.0454
SFM0049	0.3204	0.3570	0.3694	0.0000	–0.0359	–0.0287	0.0000	3.3378	2.2542	0.0000	–0.0208	–0.0145
SFM0057	3.3462	2.3295	1.7774	–0.0423	–0.0629	–0.0197	–0.3289	0.7915	0.2851	0.0203	–0.0322	–0.0088
SFM0058	0.1952	1.5297	2.1486	0.0539	0.1398	0.1635	0.4373	–1.9159	–1.4718	–0.0042	0.0512	0.0552
SFM0059	2.0500	2.7905	1.3780	0.1211	0.1053	0.1005	0.5577	0.3215	–0.5351	–0.0377	–0.0157	0.0129
SFM0060	1.6566	0.6997	0.7596	0.0275	0.0278	–0.0017	0.5776	1.1285	–0.0333	–0.0117	–0.0138	0.0004

Appendix A4-1. Continued.

GW Well	LONG3	LONG7	LONG11	MINI3	MINI7	MINI11	MAXI3	MAXI7	MAXI11	MEAN3	MEAN7	MEAN11
SFM0001	–0.0076	0.0731	0.0298	–0.0217	0.0319	–0.0116	0.3663	0.1873	0.0851	0.1723	0.1096	0.0367
SFM0002	0.1366	0.0437	–0.0036	–0.0621	–0.0538	–0.1146	0.2745	0.0944	0.0100	0.1062	0.0203	–0.0523
SFM0003	–0.0548	–0.0670	–0.0465	–0.1659	–0.2049	–0.1592	0.0837	0.0433	0.0468	–0.0411	–0.0808	–0.0562
SFM0004	0.0147	–0.0045	–0.0727	–0.1015	–0.1905	–0.1458	0.0583	0.0534	0.0596	–0.0216	–0.0685	–0.0431
SFM0005	0.0139	–0.0095	–0.0004	0.0278	–0.0212	–0.0008	0.0962	0.0008	0.0029	0.0620	–0.0102	0.0011
SFM0006	0.0008	0.0227	0.0129	0.0002	0.0244	0.0145	0.0546	0.0647	0.0877	0.0274	0.0446	0.0511
SFM0007	0.0134	–0.0012	0.0070	–0.0007	–0.0225	0.0063	0.0276	0.0087	0.0154	0.0135	–0.0069	0.0109
SFM0008	–0.0060	–0.0045	–0.0074	–0.0614	–0.0609	–0.0186	0.0005	0.0058	0.0427	–0.0304	–0.0276	0.0120
SFM0009	0.0038	0.0213	0.0031	–0.0180	0.0030	–0.0026	0.0262	0.0541	0.0497	0.0041	0.0285	0.0235
SFM0010	–0.0253	0.0016	0.0253	–0.1608	–0.1647	–0.0404	–0.0108	0.0648	0.0780	–0.0858	–0.0499	0.0188
SFM0011	0.0000	0.0000	0.0000	0.0000	0.0000	0.0001	0.0000	0.0000	0.0001	0.0000	0.0000	0.0001
SFM0013	0.0000	0.0000	–0.0109	0.0000	0.0000	–0.0567	0.0000	0.0000	–0.0134	0.0000	0.0000	–0.0351
SFM0014	0.0007	0.0869	0.0110	–0.0036	0.0038	0.0027	0.0046	0.1762	0.0236	0.0005	0.0900	0.0131
SFM0016	0.0000	–0.0107	–0.0491	0.0000	–0.0215	–0.0995	0.0000	–0.0098	–0.0241	0.0000	–0.0156	–0.0618
SFM0017	0.0032	–0.0235	–0.0393	–0.0063	–0.0691	–0.1679	0.0067	–0.0103	–0.0500	0.0002	–0.0397	–0.1089
SFM0018	0.0411	–0.0025	0.0017	–0.1656	–0.1491	–0.2524	0.1965	0.0293	0.0159	0.0155	–0.0599	–0.1182
SFM0019	0.0000	0.0000	–0.0011	0.0000	0.0000	–0.0022	0.0000	0.0000	0.0011	0.0000	0.0000	–0.0005
SFM0020	–0.0137	–0.0531	–0.0441	–0.0379	–0.1220	–0.1123	–0.0243	0.0002	0.0179	–0.0311	–0.0609	–0.0472
SFM0021	–0.0013	–0.0260	–0.0329	–0.0076	–0.0541	–0.0675	0.0172	0.0100	0.0103	0.0048	–0.0220	–0.0286
SFM0026	–0.0175	–0.0248	–0.0288	–0.0575	–0.0507	–0.0577	–0.0076	0.0064	–0.0053	–0.0325	–0.0222	–0.0315
SFM0027	0.0031	–0.0195	–0.0216	–0.0042	–0.0391	–0.0440	0.0157	0.0015	–0.0057	0.0057	–0.0188	–0.0249
SFM0028	0.0000	–0.0024	–0.0178	0.0000	–0.0048	–0.0366	0.0000	0.0034	0.0059	0.0000	–0.0007	–0.0154
SFM0030	0.0505	–0.0129	–0.0255	–0.3731	–0.1255	–0.0922	0.1139	0.0465	0.0471	–0.1296	–0.0395	–0.0226
SFM0033	0.0000	–0.0333	–0.0736	0.0000	–0.0831	–0.1491	0.0000	–0.0527	–0.0501	0.0000	–0.0679	–0.0996
SFM0034	–0.0774	–0.1049	–0.0807	–0.1549	–0.2099	–0.1648	–0.0221	0.0626	0.0721	–0.0885	–0.0737	–0.0464
SFM0036	–0.1454	–0.1602	–0.0755	–0.3110	–0.3277	–0.1554	–0.1036	0.0877	0.0952	–0.2073	–0.1200	–0.0301
SFM0049	0.0000	–0.0359	–0.0287	0.0000	–0.0752	–0.0606	0.0000	–0.0382	–0.0259	0.0000	–0.0567	–0.0433
SFM0057	–0.0425	–0.0630	–0.0197	–0.0969	–0.1350	–0.0752	0.0525	–0.0555	0.0181	–0.0222	–0.0952	–0.0285
SFM0058	0.0539	0.1400	0.1638	–0.0107	0.1006	0.1035	0.1102	0.2817	0.3346	0.0498	0.1911	0.2191
SFM0059	0.1219	0.1056	0.1006	–0.0969	–0.1144	–0.0570	0.2653	0.2943	0.2839	0.0842	0.0900	0.1135
SFM0060	0.0275	0.0278	–0.0017	–0.0492	–0.0337	–0.0477	0.0809	0.0618	0.0451	0.0159	0.0141	–0.0013

Appendix A4-2. Geomorphological feature classification of areas around groundwater wells.

1 = Pit, 2 = Channel, 3 = Pass, 4 = □
(Slope > 1 degree and Curva□
(Slope > 0.5 degree and Curvature > 0.05 (dimensionless)).

GW Well	FEAT3H	FEAT5H	FEAT7H	FEAT9H	FEAT11H	FEAT3L	FEAT5L	FEAT7L	FEAT9L	FEAT11L
SFM0001	4	4	4	4	6	4	4	6	6	4
SFM0002	6	6	6	6	6	6	6	6	6	6
SFM0003	6	6	2	2	2	6	6	6	6	6
SFM0004	6	6	2	2	2	6	6	2	3	3
SFM0005	6	6	6	6	6	4	6	6	6	6
SFM0006	6	6	6	6	6	6	6	6	6	6
SFM0007	6	6	6	6	6	6	6	6	6	6
SFM0008	6	6	6	6	6	6	6	6	6	6
SFM0009	6	6	6	6	6	6	6	4	4	6
SFM0010	6	6	6	6	6	2	2	2	6	6
SFM0011	6	6	6	6	6	6	6	6	6	6
SFM0013	6	6	6	6	6	6	6	6	6	2
SFM0014	6	6	6	6	6	6	6	6	6	6
SFM0016	6	6	6	6	6	6	6	6	2	6
SFM0017	6	6	6	2	2	6	6	2	6	2
SFM0018	6	2	2	2	2	6	2	2	2	2
SFM0019	6	6	6	6	6	6	6	6	6	6
SFM0020	6	6	6	2	2	6	6	6	6	6
SFM0021	6	6	6	6	6	6	6	2	6	6
SFM0026	6	6	6	6	6	2	6	2	2	2
SFM0027	6	6	6	6	6	6	6	6	6	6
SFM0028	6	6	6	6	6	6	6	6	6	6
SFM0030	3	2	2	2	6	2	2	6	6	6
SFM0033	6	6	6	2	2	6	2	1	6	6
SFM0034	2	2	2	2	2	6	2	6	6	6
SFM0036	6	6	6	6	6	2	6	6	6	6
SFM0049	6	6	6	6	6	6	2	2	2	2
SFM0057	6	6	6	6	6	6	6	6	6	6
SFM0058	4	6	6	6	6	6	6	4	4	4
SFM0059	6	6	6	6	6	6	6	6	6	6
SFM0060	6	6	6	6	6	6	6	6	6	6

Appendix A4-3. Calculated hydrological parameters at groundwater well areas.

TWI_PIX = topographical wetness inde
point (1 to 4 cells), TWI_25 = the highe
accumulation values.

GW Well	TWI_PIX	TWI_10	TWI_25	FLOW_PIX	FLOW_10	FLOW_25
SFM0001	8.64	8.64	9.37	0	1	7
SFM0002	7.76	8.01	10.77	15	15	204
SFM0003	8.50	11.18	11.87	0	1,016	1,017
SFM0004	8.83	9.08	9.82	87	87	93
SFM0005	9.85	11.42	12.80	4	78	134
SFM0006	7.94	7.94	8.27	13	13	14
SFM0007	9.32	9.32	10.15	2	2	12
SFM0008	7.54	8.17	9.16	11	61	98
SFM0009	11.00	11.22	11.49	0	1	5
SFM0010	7.74	8.24	8.93	1	7	33
SFM0011	n.a.	n.a.	n.a.	8	9	244
SFM0013	n.a.	n.a.	n.a.	67	73	88
SFM0014	8.31	8.78	9.25	4	4	5
SFM0016	n.a.	n.a.	14.76	42	971	3,543
SFM0017	10.25	10.51	13.67	30	30	665
SFM0018	7.78	8.28	12.50	0	0	1,691
SFM0019	n.a.	n.a.	n.a.	26	27	14,078
SFM0020	11.80	11.80	13.89	1,375	1,375	1,529
SFM0021	9.47	9.58	10.42	2	5	13
SFM0026	10.68	10.68	13.98	0	836	955
SFM0027	9.54	10.73	13.98	0	235	818
SFM0028	n.a.	11.21	11.88	23	23	273
SFM0030	8.51	15.58	16.51	4	101,556	101,570
SFM0033	8.65	9.68	10.13	0	25	103,808
SFM0034	9.74	9.74	16.72	9	9	127,746
SFM0036	7.85	7.92	11.46	5	5	95
SFM0049	10.85	11.89	15.12	189	189	3,165
SFM0057	7.46	7.73	8.63	2	2	64
SFM0058	10.29	10.77	11.63	0	0	3
SFM0059	7.94	7.95	9.27	0	1	4
SFM0060	8.20	8.70	10.17	5	5	17